Functionality-Enhanced Antibodies for Precision Cancer Therapy

TECHNISCHE UNIVERSITÄT DARMSTADT

Vom Fachbereich Chemie
der Technischen Universität Darmstadt

zur Erlangung des Grades
Doctor rerum naturalium
(Dr. rer. nat.)

Dissertation
von
Katrin Schoenfeld, M.Sc.
aus Mainz

Erstgutachter: Prof. Dr. Harald Kolmar

Zweitgutachterin: Prof. Dr. Evelyn Ullrich

Darmstadt 2024

Schoenfeld, Katrin: Functionality-Enhanced Antibodies for Precision Cancer Therapy

Darmstadt, Technische Universität Darmstadt

Jahr der Veröffentlichung der Dissertation auf TUprints: 2024

URN: urn:nbn:de:tuda-tuprints-285692

URI: https://tuprints.ulb.tu-darmstadt.de/id/eprint/28569

Tag der Einreichung: 27. August 2024

Tag der mündlichen Prüfung: 11. Oktober 2024

Die vorliegende Arbeit wurde unter der Leitung von Herrn Prof. Dr. Harald Kolmar am Clemens-Schöpf-Institut für Organische Chemie und Biochemie der Technischen Universität Darmstadt im Zeitraum von Januar 2021 bis Juni 2024 angefertigt.

Publications derived from this work

Publications

Schoenfeld K, Harwardt J, Habermann J, Elter A and Kolmar H (2023) Conditional activation of an anti-IgM antibody-drug conjugate for precise B cell lymphoma targeting. *Frontiers in Immunology* doi: 10.3389/fimmu.2023.1258700

Schoenfeld K*, Harwardt J*, Kolmar H (2024) Better safe than sorry: dual targeting antibodies for cancer immunotherapy. *Biological Chemistry* doi: 10.1515/hsz-2023-0329

Schoenfeld K, Habermann J, Wendel P, Harwardt J, Ullrich E, Kolmar H (2024) T cell receptor-directed antibody-drug conjugates for the treatment of T cell-derived cancers. *Molecular Therapy Oncology* doi: 10.1016/j.omton.2024.200850

Pfeifer Serrahima J*, **Schoenfeld K***, Kühnel I, Harwardt J, Macarrón Palacios A, Prüfer M, Kolaric M, Oberoi P, Kolmar H, Wels WS (2024) Bispecific killer cell engagers employing species cross-reactive NKG2D binders redirect human and murine lymphocytes to ErbB2/HER2-positive malignancies. *Frontiers in Immunology* doi: 10.3389/fimmu.2024.1457887

Ali A, Happel D, Habermann J, **Schoenfeld K**, Macarrón Palacios A, Bitsch S, Englert S, Schneider H, Avrutina O, Fabritz S, Kolmar H (2022) Sactipeptide engineering by probing the substrate tolerance of a thioether-bond-forming sactisynthase. *Angewandte Chemie (International ed. in English)* doi: 10.1002/anie.202210883

Harwardt J, Carrara SC, Bogen JP, **Schoenfeld K**, Grzeschik J, Hock B, Kolmar H (2023) Generation of a symmetrical trispecific NK cell engager based on a two-in-one antibody. *Frontiers in Immunology* doi: 10.3389/fimmu.2023.1170042

Harwardt J, Geyer FK, **Schoenfeld K**, Baumstark D, Molkenthin V, Kolmar H (2024) Balancing the affinity and tumor cell binding of a two-in-one antibody simultaneously targeting EGFR and PD-L1. *Antibodies* doi: 10.3390/antib13020036

*shared first authorship

Patents

Ullrich E, Wendel P, Wels WS, Oberoi P, Kolmar H, Macarrón Palacios A, Habermann J, **Schoenfeld K** (2021) Personalized vNAR-based chimeric antigen receptors (vNAR-CAR) for the treatment of clonal B-and T-cell malignancies, and methods for producing vNAR-CARs. EP4141028A1 (Pending)

Contributions to conferences

Posters

Schoenfeld K, Macarrón Palacios A, Habermann J, Elter A and Kolmar H (2022) Generation of IgM-directed antibodies for the treatment of B cell cancers. *Protein Engineering Summit Europe*, Barcelona, Spain

Schoenfeld K, Macarrón Palacios A, Habermann J, Elter A and Kolmar H (2023) Generation of IgM-directed antibodies for the treatment of B cell cancers. *74th Mosbacher Kolloquium*, Mosbach, Germany

Schoenfeld K, Harwardt J, Habermann J, Elter A and Kolmar H (2023) Precise targeting of B cell lymphoma by a conditionally activated anti-IgM antibody-drug conjugate. *Protein Engineering Summit Europe*, Lisbon, Portugal

Harwardt J, **Schoenfeld K**, Carrara SC, Bogen JP, Kolmar H (2023) The potential of 2in1 antibodies: affinity maturation & trifunctionalization. *Protein Engineering Summit Europe*, Lisbon, Portugal

Table of Contents

Zusammenfassung und wissenschaftlicher Erkenntnisgewinn

In den vergangenen Jahrzehnten haben sich monoklonale Antikörper als leistungsstarke Biologika erwiesen, die die Behandlung verschiedener Krankheiten, darunter Krebs, revolutioniert haben. Dennoch werden weiterhin Forschungsanstrengungen unternommen, um die Funktionalität von Antikörpern zu steigern und damit die Generierung präziserer und wirksamerer Antikörpertherapeutika zu ermöglichen.

Die erste Studie im Rahmen dieser kumulativen Dissertation konzentrierte sich auf die Entwicklung eines konditional aktivierten anti-IgM Antikörper-Wirkstoff-Konjugats zur präzisen Bekämpfung von B-Zell-Lymphomen. Zu diesem Zweck wurde ein vom Huhn stammender IgM-spezifischer Antikörper (aIgM) isoliert und mit der epitoptragenden IgM-Domäne CH2 als affinitätsbasierte Maskierungseinheit über einen tumorproteaseempfindlichen Linker fusioniert. Der entwickelte CH2-maskierte aIgM Antikörper zeigte keine Wechselwirkungen mit IgM aus Humanserum, während die Proteasebehandlung des CH2-aIgM die Antigenbindungsfunktionalität wiederherstellte. Auf zellulärer Ebene war CH2-aIgM auch inert gegenüber Wechselwirkungen mit IgM-positiven Lymphom-B-Zellen, wohingegen die Protease-gespaltene Variante ausgezeichnete Zellbindungsaffinitäten im einstelligen nanomolaren Bereich aufwies, vergleichbar mit dem unmaskierten parentalen Antikörper. Die aIgM Antikörpervarianten wurden anschließend mit dem zytotoxischen Wirkstoff Monomethylauristatin E (MMAE) zur Generierung von Antikörper-Wirkstoff-Konjugaten gekoppelt. Die spezifische und effektive rezeptorvermittelte zelluläre Aufnahme des aIgM Antikörpers stand in engem Zusammenhang mit der Induktion des apoptotischen Lymphomzelltodes. Demzufolge war die Zytotoxizität des inaktiven CH2-aIgM Antikörper-Wirkstoff-Konjugats auf ein Minimum reduziert. Da Off-Target-Effekte die therapeutische Wirksamkeit von Antikörpern beschränken, gewährleistet das Design des maskierten aIgM Antikörper-Wirkstoff-Konjugats die Diffusion im systemischen Blutkreislauf, ohne von sekretierten, pentameren IgM Molekülen abgefangen zu werden oder nicht-maligne IgM-positive B-Zellen zu beeinträchtigen. Bei Erreichen des Tumors führt die Protease-vermittelte Linker-Hydrolyse zur Antikörper-Wirkstoff-Konjugat-Aktivierung und zum anschließenden Tod der Krebszelle, wodurch der therapeutische Index, der durch die Toxizität des Medikaments im Verhältnis zu seiner Wirksamkeit bestimmt wird, erweitert wird.

Das Ziel des zweiten Projekts bestand in der Entwicklung von T-Zell-Rezeptor-direktionierten Antikörper-Wirkstoff-Konjugaten zur Behandlung von Krebserkrankungen, die von T-Zellen ausgehen. Da es nicht möglich ist, Pan-T-Zell-Antigene zu adressieren, weil dieses mit dem Risiko einer lebensbedrohlichen T-Zell-Aplasie verbunden ist, wurde ein tumorspezifischer Antikörper entworfen, der auf den klonspezifischen T-Zell-Rezeptor (*T cell receptor*, TCR) einer malignen T-Zellpopulation abzielt. Nach der Isolierung eines anti-TCR (aTCR) Idiotyp Antikörpers aus einer Huhn-Immunbibliothek erfolgte die Konjugation mit dem zytotoxischen Mikrotubuli-Inhibitor MMAE über einer spaltbaren Linker, was zur Generierung von Antikörper-Wirkstoff-Konjugaten mit einem durchschnittlichen Verhältnis von Wirkstoff zu Antikörper von zwei beziehungsweise fünf führte. Der unkonjugierte Antikörper wies eine ausgezeichnete Spezifität und Affinität im einstelligen nanomolaren Bereich zu dem Target-TCR auf molekularer und zellulärer Ebene auf. Die aTCR Antikörper-Wirkstoff-Konjugate, deren Wirkung in erster Linie auf der Induktion des apoptotischen Zelltods beruht, zeigten *in vitro* eine

starke anti-Tumor-Aktivität. Nach der zellulären Freisetzung des Zytotoxins wurden proliferationshemmende *Bystander*-Effekte auf Nicht-Tumor-Zellen beobachtet, die möglicherweise zusätzlich zu den tumoriziden Eigenschaften der aTCR Antikörper-Wirkstoff-Konjugate beitragen. Dieser neuartige, maßgeschneiderte Ansatz ermöglicht eine effiziente Eliminierung von Lymphom-/Leukämie-T-Zellen, während das für eine intakte zelluläre Immunität verantwortliche T-Zell-Repertoire erhalten bleibt.

Der dritte Teil dieser Arbeit befasste sich mit der Entwicklung bispezifischer Killerzell-*Engager* (BiKE) die Spezies-kreuzreaktive NKG2D-Binder nutzen, um menschliche und murine Lymphozyten auf ErbB2/HER2-positive Erkrankungen auszurichten. Die Rekrutierung von natürlichen Killerzellen (NK-Zellen) über den aktivierenden Rezeptor der natürlichen Killergruppe 2, Mitglied D (NKG2D) stellt eine neue Strategie für die Krebstherapie dar, die sich die zytotoxische Immuneffektorfunktion von NK-Zellen zunutze macht. Die Generierung kreuzreaktiver Antikörper für Mensch- und Maus-NKG2D wurde durch eine Reihe aufeinanderfolgender Immunisierungen eines Huhns mit den Rezeptoren beider Spezies und anschließender Durchmusterung der Antikörperbibliothek erreicht. Nachfolgend wurden bispezifische tetravalente Antikörper aus einer Reihe von vier isolierten anti-NKG2D *single-chain variable fragments* (scFvs) in Kombination mit einer zuvor beschriebenen anti-ErbB2/HER2-targetierenden Einheit hergestellt. Die vier entwickelten BiKE-Moleküle (bezeichnet als scNKAB-ErbB2) zeigten Bindungsspezifität und -affinität gegenüber HER2/ErbB2-exprimierenden Krebszellen sowie NK-92-Zellen, die mit von humanem und murinem NKG2D abgeleiteten chimären Antigenrezeptoren modifiziert wurden, und NKG2D-positiven primären humanen und murinen Lymphozyten. Die Konkurrenz zwischen scNKAB-ErbB2 und dem natürlichen NKG2D-Liganden MICA wurde untersucht, wobei sich herausstellte, dass zwei der Entitäten mit MICA konkurrieren und dadurch Immun-*Escape*-Mechanismen von Tumoren verhindern können. Schließlich erwiesen sich alle vier BiKEs als effektiv in der spezifischen Redirektionierung der zytotoxischen Aktivität von menschlichen und murinen NKG2D-CAR-modifizierten NK-92-Zellen und primären menschlichen und murinen Lymphozyten auf ErbB2-positive Krebszellen. Diese neu entwickelten BiKEs haben das Potential, die NKG2D-abhängige NK-Zell-Zytotoxizität auf Tumorzellen zu vermitteln und mit der implementierten Immunrezeptor-Spezies-Kreuzreaktivität die präklinische Entwicklung in immunkompetenten Maus-Tumormodellen zu erleichtern.

Zusammengefasst zielen die im Rahmen dieser Arbeit vorgestellten Projekte darauf ab, funktional erweiterte Antikörper für eine präzise Krebstherapie zu entwickeln. Der Einsatz neuartiger, fortschrittlicher Modifikationen in Antikörpern, wie beispielsweise konditional freigesetzte Maskierungseinheiten, hochwirksame zytotoxische Wirkstoffe, maßgeschneiderte Spezifitäten sowie zusätzliche Spezifitäten, die Immun-Effektorzellen effektiv rekrutieren, könnte den Grundstein für eine neue Generation von Antikörper-basierten Krebstherapien legen.

Scientific novelty and significance

In recent decades, monoclonal antibodies have emerged as powerful biologics that have revolutionized the treatment of various diseases, including cancer. Nevertheless, ongoing research efforts are being made to enhance antibody functionality, enabling the generation of more precise and effective antibody therapeutics.

The first study within this cumulative thesis focused on the development of a conditionally activated anti-IgM antibody-drug conjugate for precise targeting of B cell lymphoma. To this end, a chicken-derived IgM-specific antibody (aIgM) was isolated and fused to the epitope-bearing IgM domain CH2 as an affinity-based masking unit through a tumor protease-sensitive linker. The designed CH2-masked aIgM antibody displayed no interaction with IgM from human serum, while protease treatment of the CH2-aIgM restored the antigen binding functionality. On the cellular level, CH2-aIgM was also inert to interactions with IgM-positive lymphoma B cells, whereas the protease-cleaved variant demonstrated excellent on-cell affinities in the single-digit nanomolar range, comparable to the parental unmasked antibody. The aIgM antibody variants were subsequently coupled to the cytotoxic drug monomethyl auristatin E (MMAE) under generation of antibody-drug conjugates. Specific and effective receptor-mediated cellular uptake of the aIgM antibody was closely associated with the induction of apoptotic lymphoma cell death. Hence, cytotoxicity of the inactive CH2-aIgM antibody-drug conjugate was reduced to a minimum. As off-target effects limit the therapeutic potency of antibodies, the masked aIgM antibody-drug conjugate design ensures diffusion in the systemic blood circulation without being captured by secreted, pentameric IgM molecules or affecting non-malignant IgM-positive B cells. Upon reaching the tumor site, protease-mediated linker hydrolysis results in antibody-drug conjugate activation followed by cancer cell death, thereby expanding the therapeutic index determined by drug toxicity relative to drug effectivity.

The objective of the second project involved the generation of T cell receptor-directed antibody-drug conjugates for the treatment of T cell-derived cancers. Given the unfeasibility of targeting pan-T cell antigens as this is associated with the risk of life-threatening T cell aplasia, a tumor-specific antibody was devised by addressing the clonally rearranged T cell receptor (TCR) of a malignant T cell population. The isolation of an anti-TCR (aTCR) idiotype antibody from a chicken immune library, was followed by conjugation to the cytotoxic microtubule-inhibitor MMAE *via* a cleavable linker, resulting in the generation of antibody-drug conjugates with drug-to-antibody ratios of two and five on average, respectively. The unconjugated antibody exhibited exceptional specificity and affinity in the single digit nanomolar range for the target TCR on molecular and cellular level. Primarily based on the induction of apoptotic cell death, the aTCR antibody-drug conjugates revealed potent *in vitro* anti-tumor activity. Following the cellular release of cytotoxin, anti-proliferative bystander effects were observed on non-tumor cells, which may further contribute to aTCR antibody-drug conjugates' tumoricidal properties. This novel, tailored approach facilitates efficient elimination of lymphoma/leukemia T cells, while preserving the T cell repertoire responsible for an intact cellular immunity.

The third part of this thesis explored the development of bispecific killer cell engagers (BiKEs), which employ species cross-reactive NKG2D binders to redirect human and murine lymphocytes to ErbB2/HER2-positive malignancies. Recruitment of natural killer (NK) cells *via* the activating natural-killer group 2, member D (NKG2D) receptor represents an emerging strategy for cancer therapy, harnessing the cytotoxic immune effector function of NK cells. The generation of cross-reactive antibodies to human and murine NKG2D was achieved through a series of consecutive chicken immunizations with the receptors derived from both species, followed by antibody library screening. Subsequently, bispecific tetravalent antibodies were assembled from a panel of four isolated anti-NKG2D single-chain variable fragments (scFvs) combined with a previously described tumor-targeting anti-ErbB2/HER2 moiety. The four devised BiKE molecules (termed scNKAB-ErbB2) demonstrated binding specificity and affinity to HER2/ErbB2-expressing cancer cells as well as NK-92 cells engineered with chimeric antigen receptors derived from human and murine NKG2D, and NKG2D-positive primary human and murine lymphocytes. Competition of the scNKAB-ErbB2 with the natural NKG2D ligand MICA was investigated, and two of the entities were found to behave competitively to MICA, thereby preventing immune escape mechanisms of tumors. Ultimately, all four BiKEs proved effective in specifically redirecting the cytotoxic activity of human and murine NKG2D CAR-engineered NK-92 cells and primary human and murine lymphocytes to ErbB2-positive cancer cells. The designed BiKEs represent novel molecules with the potential to effectively mediate NKG2D-dependent NK cell cytotoxicity against tumor cells, and with implemented immune receptor species cross-reactivity facilitating the preclinical development in immunocompetent mouse tumor models.

In summary, the projects presented within this thesis intended to devise functionality-enhanced antibodies for precision cancer therapy. The incorporation of novel, advanced modifications into antibodies, such as conditionally released masking units, highly potent cytotoxic drugs, custom-made specificities as well as additional specificities effectively recruiting immune effector cell mechanisms, may pave the way for the next generation of antibody-based cancer therapeutics.

Individuelle Beiträge von K. Schoenfeld zum kumulativen Teil der Dissertation

1) **Schoenfeld K**, Harwardt J, Habermann J, Elter A and Kolmar H (2023) Conditional activation of an anti-IgM antibody-drug conjugate for precise B cell lymphoma targeting. *Frontiers in Immunology* doi: 10.3389/fimmu.2023.1258700

Beiträge von K. Schoenfeld:

- Initiale Idee und Planung des Projekts
- Generierung und Screening der scFv Bibliothek
- Design, Produktion und Charakterisierung der maskierten Antikörper
- Herstellen von Antikörper-Wirkstoff-Konjugaten
- Testen der maskierten Antikörper-Wirkstoff-Konjugate auf Zellen
- Schreiben des Manuskripts und Erstellung der Abbildungen

Der Beitrag von K. Schoenfeld beläuft sich auf insgesamt 80%. Die restlichen 20% verteilen sich auf J. Harwardt, J. Habermann, A. Elter und H. Kolmar für die Unterstützung bei dem Screening der Bibliothek, der Antikörpercharakterisierung und das Korrigieren des Manuskripts.

2) **Schoenfeld K***, Harwardt J*, Kolmar H (2024) Better safe than sorry: dual targeting antibodies for cancer immunotherapy. *Biological Chemistry* doi: 10.1515/hsz-2023-0329.
*geteilte Erstautorenschaft

Beiträge von K. Schoenfeld:

- Literaturrecherche mit J. Harwardt
- Zusammenfassung der Literaturdaten und Planung des Reviewartikels mit J. Harwardt
- Schreiben des Manuskripts und Erstellung der Abbildungen mit J. Harwardt

Der Beitrag von K. Schoenfeld beläuft sich auf insgesamt 45%. Der Anteil von J. Harwardt beläuft sich als Co-Erstautorin ebenfalls auf 45%. Die verbleibenden 10% liegen bei H. Kolmar für und das kritische Korrigieren des Manuskripts.

3) **Schoenfeld K**, Habermann J, Wendel P, Harwardt J, Ullrich E, Kolmar H (2024) T cell receptor-directed antibody-drug conjugates for the treatment of T cell-derived cancers. *Molecular Therapy Oncology* doi: 10.1016/j.omton.2024.200850

Beiträge von K. Schoenfeld:

- Planung des Projekts
- Generierung und Screening der scFv Bibliothek
- Produktion und Charakterisierung der Antikörper und der Antikörper-Wirkstoff-Konjugate
- Testen der Antikörper-Wirkstoff-Konjugate auf Zellen
- Schreiben des Manuskripts und Erstellung der Abbildungen

Der Beitrag von K. Schoenfeld beläuft sich auf insgesamt 80%. Die restlichen 20% verteilen sich auf J. Habermann, P. Wendel, J. Harwardt, E. Ullrich und H. Kolmar für die Unterstützung bei dem Screening der Bibliothek, der Generierung von Zelllinien und das Korrigieren des Manuskripts.

4) Pfeifer Serrahima J*, **Schoenfeld K***, Kühnel I, Harwardt J, Macarrón Palacios A, Prüfer M, Kolaric M, Oberoi P, Kolmar H, Wels WS (2024) Bispecific killer cell engagers employing species cross-reactive NKG2D binders redirect human and murine lymphocytes to ErbB2/HER2-positive malignancies. *Frontiers in Immunology* doi: 10.3389/fimmu.2024.1457887
*geteilte Erstautorenschaft

Beiträge von K. Schoenfeld:

- Planung des Projekts mit J. Pfeifer Serrahima
- Generierung und Screening der scFv Bibliothek nach human/murin cross-reaktiven NKG2D Bindern
- Produktion und Charakterisierung der scFv und scFv-Fc Antikörper
- Schreiben des Manuskripts und Erstellung von Abbildungen mit J. Pfeifer Serrahima

Der Beitrag von K. Schoenfeld beläuft sich auf insgesamt 40%. Der Anteil von J. Pfeifer Serrahima beläuft sich als Co-Erstautor ebenfalls auf 40%. Die verbleibenden 20% verteilen sich auf I. Kühnel, J. Harwardt, A. Macarrón Palacios, M. Prüfer, M. Kolaric, P. Oberoi, H. Kolmar und W. S. Wels für die experimentelle Beteiligung an funktionalen Assays und das Korrigieren des Manuskripts.

1 Introduction

1.1 Immune System

Higher organisms like vertebrates are protected from pathogens by a diverse array of molecules and cells that together make up the immune system. The individual components are attributed to two main entities: the innate and the adaptive immune system. The innate immune system serves as the body's non-specific first line of defense, intervening rapidly upon pathogen encounter. On the other hand, responses by the adaptive immune system are antigen-specific, require a longer period of time to develop and impart long-term protection against reinfection (1, 2).

When exposed to foreign substances, initial resistance to invading organisms is provided by anatomical hurdles such as skin, mucous membranes, and blood-brain barrier, as well as and chemical barriers, e.g. antimicrobial proteins, regions of lowered pH and complement proteins (3, 4). Once pathogens enter host tissues, cells of the innate immunity are activated by pathogen-associated molecular patterns (PAMPs), which are evolutionary conserved molecular structures shared by a broad group of pathogens, such as mannose-rich oligosaccharides, lipopolysaccharides, lipoproteins, peptidoglycans and unmethylated CpG DNA (5). Invariant germline-encoded pattern-recognition receptors (PRRs) including Toll-like receptors (TLRs), retinoic acid-inducible gene 1-like receptors (RLRs), nucleotide-binding oligomerization domain-like receptors (NLRs), C-type lectin receptors (CLRs), and absent in melanoma-2-like receptors (ALRs), enable recognition of PAMPs (6). PRRs are expressed by sensor cells of the innate immunity such as dendritic cells (DCs), macrophages and neutrophils allowing rapid detection of foreign substances. Triggered sensor cells directly react *via* phagocytosis and degradation of the pathogens, besides the secretion of inflammatory mediators including cytokines (e.g. IL-1β, IL-6, TNFα and IL-12) and chemokines (e.g. CXCL8) that recruit natural killer (NK) cells and other innate lymphoid cells (7, 8). Into inflammatory tissue migrated NK cells recognize altered expression of different surface antigens on target cells through a variety of invariant inhibitory and activating receptors (9). Downregulation of major histocompatibility complex (MHC) class I expression ("missing self") on nucleated cells is indirectly detected by inhibitory NK cell receptors: the killing immunoglobulin-like receptors (KIRs), belonging to the immunoglobulin family, and CD94/natural-killer group 2, member A (NKG2A) heterodimers, belonging to the C-type lectin-like family (10). Presentation of activating ligands, such as MHC class I chain-related proteins A/B (MICA/MICB), serving as "kill-me" signal, interact with the activating natural-killer group 2, member D (NKG2D) NK cell receptor (11, 12). The germline-encoded natural cytotoxicity receptors (NCRs) NKp46, NKp44, NKp30 of the immunoglobulin family complete the set of activating NK cell receptors (13). The absence of inhibitory signals or the predominance of activating signals received through NK cell receptors leads to the exertion of immune effector activities, such as cell killing *via* release of cytotoxic granules, production of cytokines with direct antiviral activity, or immune cell activating effects (8, 14).

Translation from innate to adaptive immunity is based on the presentation of pathogen-derived peptides by antigen-presenting cells (APCs). Thereby, DCs patrol in peripheric tissues where they take up foreign substances *via* receptor-mediated endocytosis or receptor-independent micropinocytosis, and subsequently process the antigens as peptides for surface presentation on MHC molecules (15).

Migration of the activated antigen-displaying DCs to secondary lymphoid organs triggers initial activation of naïve T cells, which are adaptive immune cells maturing in the thymus, by T cell receptor (TCR) interaction with the peptide-MHC structure (16). Co-stimulatory molecules expressed on the cell surface of activated APCs, such as B7 molecules, deliver a second signal promoting T cell survival and proliferation (17). Thirdly, APC-secreted cytokines mediate T cell differentiation into one of several subsets of effector T cells, belonging to the major groups of cluster of differentiation (CD) 4-positive helper T cells that interact with MHC class II, or CD8-positive cytotoxic T cells that interact with MHC class I and are capable of directly killing transformed and infected cells by the secretion of cytotoxic granules (18). The second key cell type of adaptive immunity is represented by B cells, arising and maturing in the bone marrow (2). B cells express diverse B cell receptors (BCRs) specifically recognizing antigens, which are subsequently internalized, processed and displayed on MHC class II molecules (19). When a helper T cell primed with the same cognate antigen encounters the B cell, stimulating surface ligands and cytokines induce B cell proliferation, migration to germinal centers, and differentiation into plasma cells or resting memory cells (20). Plasma cells secret a soluble form of the BCR, referred to as antibody, mediating the humoral immune response by neutralization, opsonization, and complement activation (2, 20, 21).

1.1.1 Lymphocyte antigen receptors

Recognition of millions of different antigens during the immune response is mediated by antigen receptors, surface membrane-bound immunoglobulins (Igs), termed BCRs on B lymphocytes and TCRs on T lymphocytes. The extensive diversity of antigen receptors enables interaction with various distinct structures and is generated by V(D)J gene recombination processes of the Ig/TCR loci (22–24). BCRs consist of two disulfide-linked immunoglobulin heavy chains (HCs) associated with two light chains (LCs) of either κ or λ type, forming two antigen-binding sites and Igs can be secreted as antibodies (**Figure 1**) (25). However, TCRs consist of two disulfide-bonded chains, a TCRα and a TCRβ chain or a TCRγ and a TCRδ chain, representing one antigen-binding site per receptor and exist exclusively as membrane-anchored molecules (26, 27). Most mature T lymphocytes express the TCRαβ (85-98%), while a minority bears the structurally similar TCRγδ (2-15%) (28). In both, BCRs and TCRs, the antigen-binding sites are composed of two variable domains, contributed by either HC and LC or TCRα and TCRβ chain. The variable domains are encoded by V(D)J genes, which arise during early B and T cell development by somatic recombination from multiple copies of V (variable), D (diversity), and J (joining) segments in the germline DNA (**Figure 1**) (29). While the genes encoding the variable domains of Ig LC and TCRα chain are rearranged from V and J segments, the genes encoding the variable domains of Ig HC and TCRβ are generated by additional rearrangement of D and J segments prior to recombination to V-DJ joined DNA. This mechanism of rejoining is catalyzed by a recombinase enzyme system including protein products of the recombinase-activating genes RAG1 and RAG2, which introduce double-strand breaks at conserved DNA sequences flanking the individual gene segments, and enzymes that are involved in general DNA double-strand break repair (30). The resulting combinatorial diversity derived from V(D)J joining and pairing of the two protein chains (BCR: HC and LC; TCR: TCRα and TCRβ chain) amounts to approximately 10^6 different variants for a BCR and TCRαβ, respectively (28).

Random deletion and addition of nucleotides at the joints between rearranged gene segments can occur, leading to imprecise coupling. The V(D)J-recombination junctions in the BCR and TCR genes encode the complementarity-determining region 3, which is essential for binding (31). The resulting variable regions of BCRs and TCRs carry unique antigenic determinants, termed idiotypes (Ids). Junctional diversification raises the total diversity to up to 10^{14} BCR and 10^{18} TCR specificities (2, 28, 32). The constant domains of the antigen receptors are encoded by constant (C) gene segments, which are combined to the V(D)J arrangements by splicing of the primary transcript RNA. For Ig HCs an array of C regions corresponds to different immunoglobulin isotypes. Initially, the first two C segments of the isotypes μ and δ were exclusively combined resulting in expression of transmembrane IgM and IgD on naïve B cells (33).

B cells in the germinal center further undergo somatic hypermutation (SHM) in response to antigen stimulation by introduction of several single nucleotide substitutions into the rearranged V(D)J gene product *via* activation-induced cytidine deaminase (AID) (34, 35). Arising point mutations diversify the primary repertoire, generating BCRs with altered antigen-binding properties. Negative impact of antigen interaction leads to eradication of the B cell clone by apoptosis, while mutations improving affinity are expanded through an increased survival rate of the B cell clone (35). In parallel with its activity in SHM, AID is involved in Ig class switching, thereby expanding the functional diversity of the Igs (36).

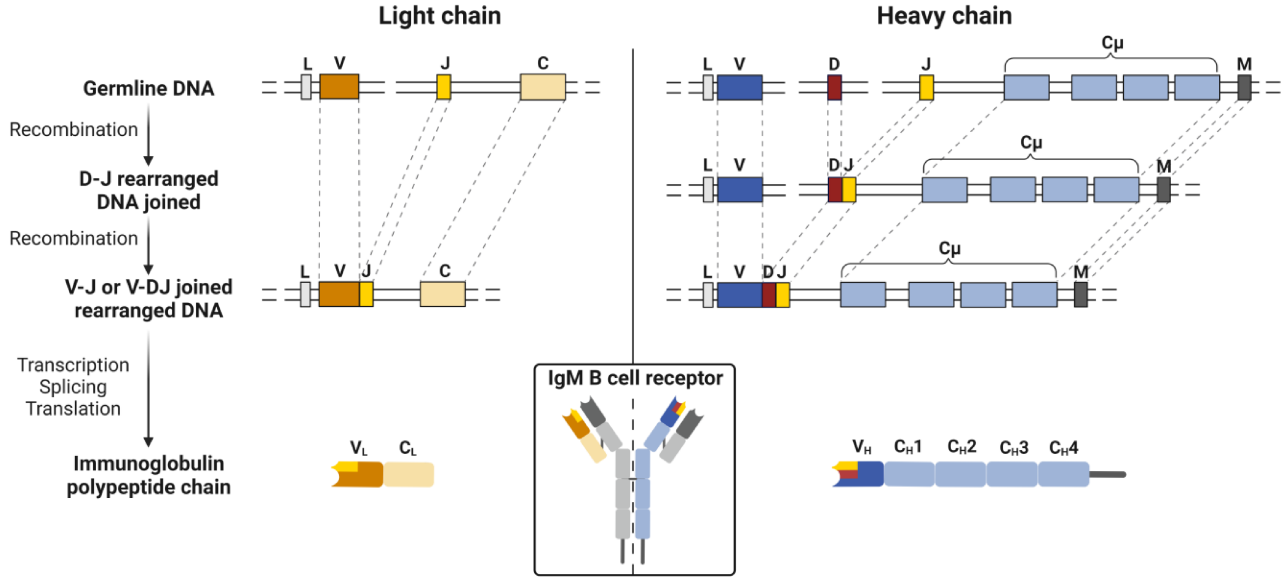

Figure 1: Somatic recombination in human immunoglobulin loci. The human immunoglobulin loci are organized in variable (V), diversity (D), joining (J) and constant (C) germline gene segments. The leader sequence (L) precedes each of the V gene segments and the exons labeled with M encode the transmembrane region and cytoplasmic tail of the membrane-bound Ig form. V(D)J recombination of gene segments results in formation of the heavy and light chain genes. Gene expression leads to BCR assembly consisting of two heavy and two light chains, exemplarily shown for an IgM B cell receptor. Created with BioRender.com.

Despite structural similarities, BCRs and TCRs display different functional capabilities (2). B cell-derived immunoglobulins bind to a wide variety of chemically different antigens and exist as membrane-bound receptors as well as secreted molecules. This allows Igs to detect and clear pathogens by distinct (Ig-dependent) effector mechanisms in extracellular spaces of the body (20). In contrast, T cell receptors are exclusively expressed as cell surface receptors responsible for the recognition of peptide-MHC structures presented by abnormal cells or immune cells. Thus, TCRs elicit cellular effector functions for the surveillance of pathogens (37).

1.2 Antibodies

Antibodies are glycoproteins of the immunoglobulin superfamily that play a central role in the adaptive immune response. The molecules exhibit the unique ability to bind antigens with high affinity and specificity, thereby directly neutralizing pathogens or acting as adapter molecules to recruit immune cells for effector functions.

1.2.1 Antibody structure and function

Mammalian antibodies are divided into five classes based on their heavy chain constant domains: IgA, IgD, IgE, IgG and IgM (**Figure 2A**). The Ig isotype determines its functional activity as well as its distribution to tissues and organs of the body. The first antigen receptors expressed by mature B cells are of IgM and IgD isotype, and the first soluble antibody produced in an immune response is of IgM isotype (38, 39). IgM is secreted as a pentamer, resulting in predominant presence in the blood and avidity effects that compensate for its relatively low affinity (40). Antibodies of IgA isotype exist as monomers and dimers, responsible for immune defense related to mucosal surfaces (41, 42). IgE mainly protects from multi-cellular parasites and is involved in common allergic diseases (43). IgGs account for 70-85% of the serum immunoglobulin repertoire and are found in the bloodstream and extracellular spaces in tissues (44, 45). The class of IgG is further divided into four subclasses: IgG1, IgG2, IgG3, and IgG4, with IgG1 being the predominant subclass (46). In general, antibodies represent secreted BCRs and share the assembly of two identical HCs and two identical LCs consisting of Ig domains of approximately 12.5 kDa and 110 amino acids arranged in a disulfide-stabilized β-sandwich structure, also termed Ig fold (**Figure 2**) (47). While the HC is constituted of one variable domain (V_H) and three to four constant domains (C_H1-C_H3/C_H4), the LC comprises one variable domain (V_L) and one constant domain (C_L) of either kappa (κ) or lambda (λ) type (**Figure 2B**). In IgG antibodies, two disulfide bonds located in the flexible hinge region link the heavy chains, and each heavy chain is connected to a light chain by a disulfide bond (45, 46). IgG1 antibodies contain a single N-linked glycan located in the C_H2 domain at asparagine 297, whereas other isotypes exhibit multiple glycosylation sites distributed throughout the constant domains (48–50).

Functionally, the two variable domains, also referred to as fragment variable (Fv), together with the C_L and C_H1 of an antibody form the fragment antigen-binding (Fab), whereas the constant domains C_H2-C_H3/C_H4 build the fragment crystallizable (Fc) (**Figure 2B**). The Fab carries the antigen-binding site or paratope at the N-terminus with three hypervariable regions, termed complementarity-determining regions (CDRs), per V_H and V_L, respectively (**Figure 2C**). The six CDRs - CDR-H1, CDR-H2, and CDR-H3 for V_H, and CDR-L1, CDR-L2, and CDR-L3 for V_L - form loops and are located between relatively conserved framework regions (Fr) representing β sheets that provide the overall scaffold of the Ig domain (47). Particularly CDR-H3 displays a high degree of sequence diversity and significantly contributes to antigen binding (51).

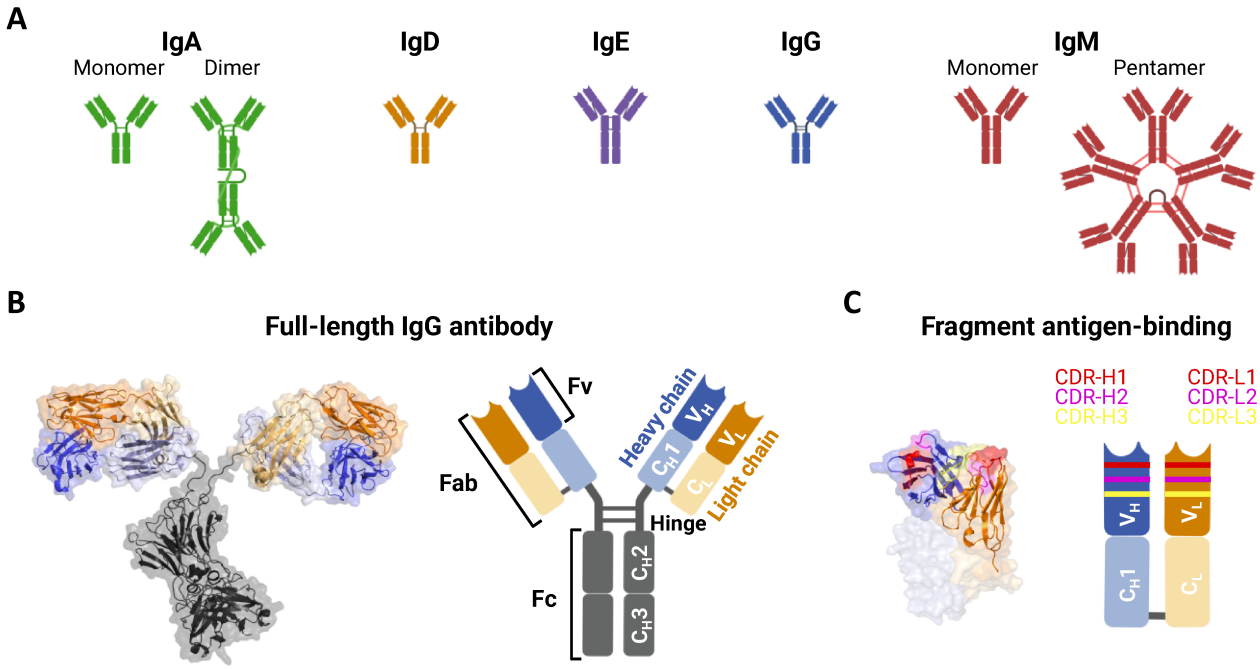

Figure 2: Structures of human antibodies. A Schematic representation of the five human immunoglobulin (Ig) isotypes with respective multimeric forms. **B** Structural and schematic depiction of a full-length IgG antibody. **C** Structural and schematic illustration of an IgG-derived fragment antigen-binding (Fab) with highlighted complementarity-determining regions (CDRs). Structure models are rendered with PyMol from PDB: 1IGT. Created with BioRender.com.

The glycosylated Fc part is key for the interaction with effector molecules and cells during immune defense. Complement-dependent cytotoxicity (CDC) is triggered by binding of the first complement component, the C1 recognition subunit (C1q), to the Fc of IgG and IgM antibodies clustered on a pathogen surface (52, 53). Further functions rely on antibody binding to Fc receptors (FcR) expressed by effector cells mediating antibody-dependent cellular phagocytosis (ADCP) and antibody-dependent cellular cytotoxicity (ADCC) (54). Engagement of Fcγ or Fcα receptors displayed on macrophages and neutrophils triggers ADCP by uptake and degradation of the pathogens in cytoplasmic vesicles, while cross-linking of the low-affinity FcγRIII (CD16) on NK cells initiates ADCC by the release of perforins and granzymes (55, 56). In addition to the constant region mediating effector functions, the C_H2-C_H3 interface of IgG antibodies interacts with the neonatal Fc receptor (FcRn) expressed by endothelial cells, which is responsible for antibody recycling and thereby prolongs serum half-life up to 21 days (57–60).

1.2.2 Antibodies as therapeutic agents

In the early 1890s, Emil von Behring developed the concept of antiserum and initiated serum therapy against diphtheria (61, 62). Over time, it became apparent that animal sera had significant limitations due to constraints on production quantities, batch variabilities, and the immunological challenges associated with repeated administration of exogenous protein (63). About a century later, in 1975, Georges Köhler and César Milstein described a novel method for the *in vitro* production of monoclonal antibodies (mAbs) from hybridomas (64). This groundbreaking technology paved the way for the development of mAbs as therapeutics. In the late 1980s, predominantly murine mAbs were explored putting forth the first mAb muromonab-CD3 (OKT3) approved for treatment of acute rejection in solid

organ transplants by the US Food and Drug Administration (FDA) (65). However, rodent-derived mAbs frequently induced allergic reactions associated with the appearance of anti-drug antibodies (ADAs) in clinical settings (66). Further drawbacks included the rapid clearance which results in a relatively short half-life in the human body, as well as diminished recruitment of host effector functions such as CDC and ADCC (66–68). In order to mitigate these limitations, chimeric mAbs build from rodent variable domains fused to human constant domains, were developed (69). As a result, the first chimeric mAb, rituximab (Rituxan), was approved for therapeutic use in non-Hodgkin lymphoma in 1997 (70). To further reduce immunogenicity and ADA formation, antibody humanization was introduced, mostly implemented by grafting the murine CDRs onto framework regions of human heavy and light chain variable domains, respectively (71, 72). Humanized mAbs consist of up to 90% human residues and account for a high proportion of approved antibodies each year, overall representing the largest group of approved antibody therapeutics (**Figure 3**) (73). Technological progress in the phage display system and the development of transgenic mouse strains expressing human antibody variable domains facilitated the discovery of fully human mAbs (66, 74, 75). In 2002, the human anti-tumor necrosis factor (TNF) alpha antibody adalimumab (Humira) was approved for the treatment of rheumatoid arthritis and achieved blockbuster status in sales (76, 77).

Besides advances made in reducing immunogenicity, antibody engineering offers the opportunity to specifically modify antibody functions. The therapeutic effect of most antibody drugs relies on Fc-mediated effector functions directed by distinct key amino acids and glycosylation patterns interacting with FcγRs and C1q (78, 79). On protein level it has been reported that the exchange of three residues (S239D/A330L/I332E) results in higher affinity to FcγRIIIa boosting ADCC activity, while elimination of fucose in the core glycosylation in IgGs contributing to the interaction with FcγRs has a similar effect (80–82). Conversely, effector functions are detrimental in some settings eliciting off-target effects, e.g. in immune cell targeting, and can be prevented by introduction of mutations, such as the LALA-PG mutation (L234A/L235A/P239G) or N297A/Q amino acid exchange producing aglycosylated antibody variants (79, 83–86). Beyond that, so-called next-generation antibodies including antibody-drug conjugates, masked antibodies and bispecific antibodies have been developed which will be introduced in detail in chapters 1.2.4.1 - 1.2.4.3.

In terms of antibody format, most approved antibodies are of full-length IgG nature (**Figure 3**). However, the limited transport across biological barriers and tissue penetration, e.g. in solid tumors, represent major challenges for canonical antibodies due to their large molecular size (~150 kDa). Therefore, smaller antibody derivatives have been exploited, including Fabs, single-chain variable fragments (scFvs), and single-domain antibodies (sdAbs), such as camelid-derived nanobodies (V_HHs) or shark-derived vNARs (87–89). These antibody fragments are emerging therapeutics with advantages in terms of size, tissue penetration and ease of manufacture, albeit they are rapidly cleared from the body due to the lack of an Fc portion (88). Abciximab (Reopro), a Fab fragment derived from a chimeric mAb for the treatment of platelet aggregation, was the first antibody fragment to reach the market in 1994 (87). Combinations of antibody entities, e.g. by joining two scFvs, result in bispecific molecules offering the possibility to implement diverse functions. Following this strategy, the bispecific T cell

engager (BiTE) blinatumomab (Blincyto) targeting CD19 and CD3 was FDA-approved in 2014 for the treatment of B cell acute lymphoblastic leukemia.

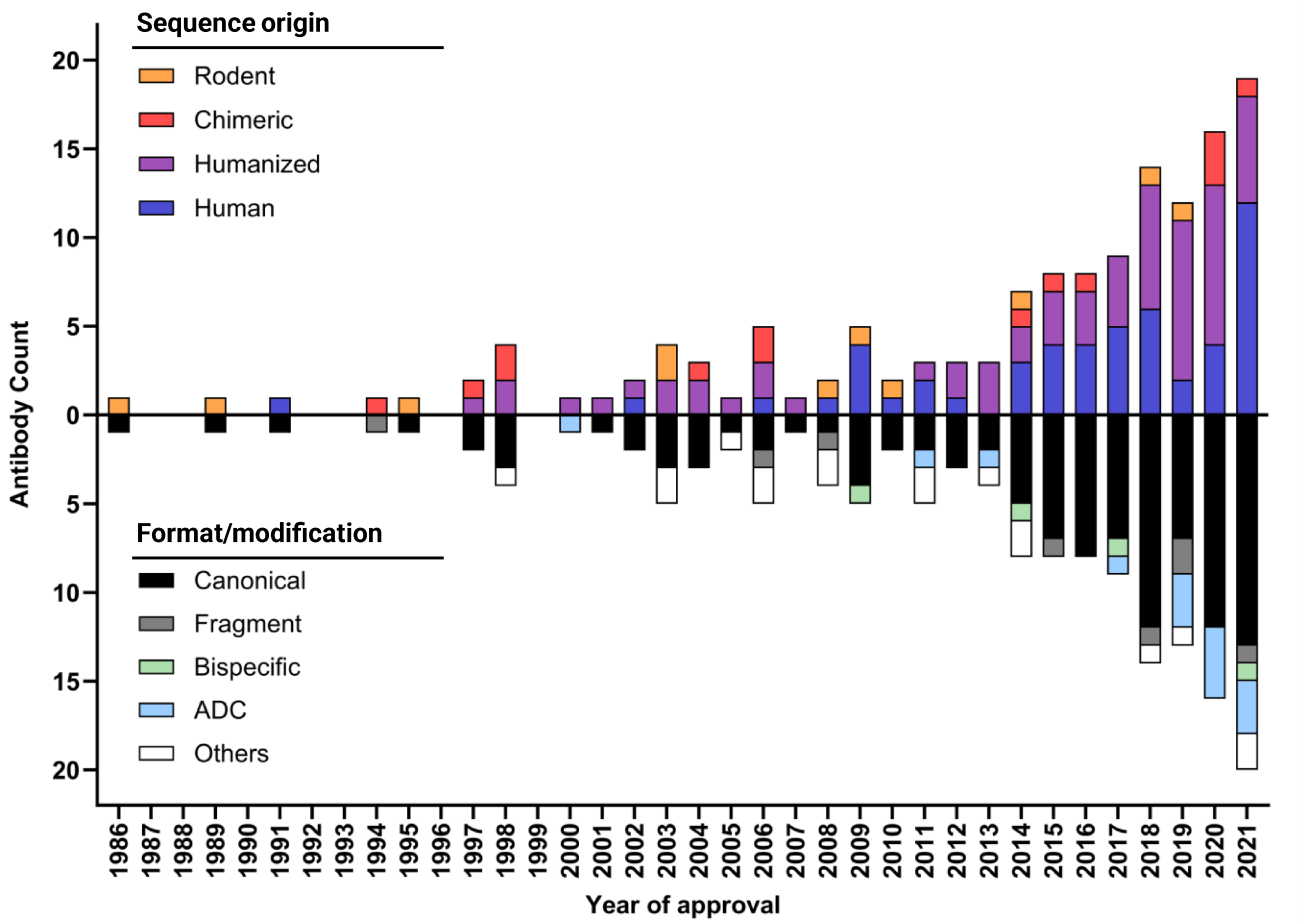

Figure 3: Number of antibody-based therapeutics globally approved over the years. Sequence origin of the antibodies is depicted in the upper half, while the respective antibody format/modification is shown in the lower part. Generated with GraphPad Software, according to (87).

In 2021, the 100th antibody-based product has been approved by the FDA (90). By the end of 2023, nearly 200 antibodies have been granted a marketing approval or are undergoing regulatory review in at least one country (91). Over the past 35 years, antibodies have become the predominant treatment modality for various diseases, particularly cancer, but also for immune-related disorders, infectious diseases, cardiovascular or hemostasis indications, and neurological disorders (91).

1.2.3 Antibody discovery

Over the past four decades, antibody discovery has evolved tremendously, producing monoclonal antibodies as powerful therapeutics. With the advent of the hybridoma technology mAbs became accessible for therapeutic use. The method involves immunization of mice with a specific antigen, subsequent isolation of antibody-producing B cells and fusion with immortal myeloma cell lines to form hybrid cell lines, that produce antibodies without amount restriction (92). Besides, antibody display systems have been developed to isolate antigen-specific antibodies with prescribed characteristics, allowing a wide variety of antigens to be addressed and the conditions of the selection process to be

tailored to the requirements (93). The display technologies enable *in vitro* selection of favorable candidates from several billion variants based on linkage of the protein variant to its genetic information, referred to as genotype phenotype coupling (94, 95).

For the construction of antibody libraries, different sources of sequence diversity and scaffolds of antibody fragments are utilized. While naïve and immune libraries rely on naturally occurring sequence diversity, synthetic libraries are shaped by design. Naïve antibody libraries are constructed by amplification of the variable antibody domains from primary B cells of non-immunized donors (96). Therefore, these libraries are limited by the size of the human antibody repertoire ($\sim 10^{11}$) and the affinity of the antibodies due to lack of *in vivo* affinity maturation (93, 97). Immune antibody libraries derive from immunized donors and are therefore pre-selected and biased towards high affinity binders against a distinct antigen (98). The first described immune library was acquired from mouse immunization, although rats, rabbits and chickens also serve as immunization hosts and provide antibodies of rodent or avian origin (99–101). Fully human antibodies are accessible *via* immunization of transgenic animals with genetically engineered Ig loci carrying the human variable region gene repertoire (75, 102, 103). Alternatively, human immune libraries can be obtained from humans that were infected or suffered from cancer resulting in either virus-neutralizing or tumor-specific antibodies (104–106). For the generation of immune libraries, blood or tissue samples are collected from the respective animals, followed by the amplification of the variable antibody domain-coding regions. Semi-synthetic and synthetic libraries are constructed utilizing random oligonucleotide synthesis which generates diversity based on *in silico* design, independent of natural maturation processes (107, 108).

Various *in vitro* selection technologies have been established, all based on the antibody display on the surface of either prokaryotes, phages, eukaryotes, or ribosomes (94). The first display technology invented for antibody discovery is phage display, which relies on filamentous bacteriophages expressing the respective protein of interest fused to a phage coat protein on the surface (109, 110). Phage panning selection and subsequent enrichment of phages by infection of *Escherichia coli* over several rounds enables the identification of antigen-specific binders. While phage display represents the most commonly utilized method for antibody discovery, other platforms include bacterial display, yeast surface display, mammalian surface display, ribosome display and mRNA display (111–117).

Upon completion of the screening process, antibody hits are deeply investigated with respect to their biochemical, biophysical, and functional properties. Further optimization of antibody candidates may entail the generation of another antibody library for humanization or affinity maturation purposes by introduction of targeted mutations (73, 94, 118). Computational advances in recent years open novel opportunities allowing for *de novo* antibody design, e.g. by epitope-driven engineering approaches, or *in silico* developability assessments and lead optimization (119, 120).

The following subsections describe in detail the antibody discovery strategy utilized for this work, comprising chicken-derived antibody immune libraries (chapter 1.2.3.1), screened by yeast surface display in combination with fluorescence-activated cell soring (chapter 1.2.3.2).

1.2.3.1 Chicken-derived antibodies

In addition to the conventional antibody isotypes IgA and IgM, avians express significant amounts of IgY isotype Igs. The term IgY, refers to its high presence in egg yolk. The avian IgY antibody shares structural and functional homology to both the mammalian IgE and IgG isotype (121, 122). As mammalian IgE, IgY exhibits a less flexible hinge region and three constant domains (C_H2-C_H4) constituting the Fc part, with the C_H2 domain forming two interchain disulfide bridges (123, 124). The light chains exclusively exist in λ type in chickens, while mammalians predominantly express κ light chains. In general, the variable regions reveal the canonical constitution of four framework regions intersected with three CDRs displaying hypervariability. In comparison to human CDR-H3, the CDR-H3 of chickens tends to be significantly longer and exhibits additional non-canonical cysteine residues that form intrachain disulfide bonds providing structural stability. The intra- and inter-CDR disulfide bond patterns provide the basis for the categorization into six types of chicken V_H domains (125). Antibody diversification in chickens is generated differently than in most mammalian species, by somatic gene hyperconversion followed by somatic hypermutation since chickens possess only one single germline gene encoding for heavy and light chain (126). The chicken Ig loci harbor single functional V and J segments, with the heavy chain locus containing approximately 15 additional D elements in between (126, 127). Following V(D)J recombination, gene conversion processes involve multiple overlapping unidirectional transfers of upstream located V region pseudogenes into the recipient germline gene, resulting in approximately $3x10^9$ antibody variants considering the combinatorial diversity of HC and LC (127–129).

As an immunization host for antibody development, chickens offer an attractive combination of phylogenetic distance from humans (*Gallus gallus*; 310 million years) while possessing an advanced immune system able to produce high-affinity canonical antibodies that closely resemble those found in humans (130). This enables the generation of to the human immune system orthogonal antibodies that recognize conserved epitopes on mammalian proteins for diagnostic and therapeutic application (131–133). Besides the utilization of chicken egg yolk-derived polyclonal IgYs, a variety of chicken-derived (monoclonal) scFvs have been developed for different applications using either phage display or yeast surface display (132–136). Due to the presence of conserved framework sequences in chickens, antibody library generation is possible by amplification of the variable domain gene repertoire using a single pair of primers for the heavy and light chain, respectively (137, 138). In addition, humanization of chicken antibodies is conveniently achieved by CDR grafting with minimal framework fine-tuning, as the orthologous IgG antibody in chickens, IgY, is highly conserved with human IgG (139, 140). In the last decade, transgenic chicken carrying humanized Ig genes were developed enabling production of in chicken diversified human sequence antibody repertoires (141, 142). The first chicken-derived, humanized antibody directed against programmed death protein-1 (Sym021), developed by Symphogen, entered clinical trials in 2019 (143).

1.2.3.2 Yeast surface display

Heterologous expression of proteins immobilized on the cell wall of *Saccharomyces cerevisiae*, termed yeast surface display (YSD), combines the benefits of the eukaryotic expression apparatus such as post-translational modifications and correct protein folding with low technical requirements and the opportunity for real-time flow cytometric analysis. The most prominent and extensively used system to target recombinant proteins to the outermost surface of the cell wall glycoprotein layer represents the a-agglutinin system developed by Boder and Wittrup (57, 144). In nature, the cell adhesion protein a-agglutinin interacts with α-agglutinin to mediate cell-cell contact of haploid yeast cells of opposite mating types during the yeast mating process (145). The display method is based on fusion of the protein of interest (POI) to the a-agglutinin II subunit (Aga2p; **Figure 4**). The Aga2p-fusion protein is secreted and forms two disulfide bonds with the a-agglutinin I subunit (Aga1p), which is anchored through glycosylphosphatidylinositol (GPI) to β-1,6-glucans of the cell wall (146). While the Aga2p fusion protein sequence, consisting of Aga2p, a hemagglutinin (HA) tag, the POI and a C-terminal cMyc tag, is provided on a synthetic yeast plasmid, Aga1p is encoded in the yeast genome. The expression of both proteins is under the control of regulatory sequences, e.g. galactose-inducible promotors are commonly utilized (146–149). Upon induction of protein expression, yeast cells display up to 10^5 copies of the respective POI on their surface (112). Besides enzymes, human growth factors, receptors and cytokines being successfully presented on yeast cells, various antibody fragments such as scFvs, Fabs and V_HH/vNAR domains, were displayed on yeast cells for antibody isolation and engineering purposes (150–152). The size of YSD libraries generated by golden gate assembly or gap repair-driven homologous recombination in yeast is typically limited to a maximum of 10^{10} transformants (153, 154). Quantification of surface presentation is achieved by immunofluorescence staining of the epitope tags. In case of antibody screening, antigen binding is detected simultaneously, using either directly fluorescent-labeled antigen or tagged-antigen which is stained by a secondary fluorophore-labeled agent (**Figure 4**).

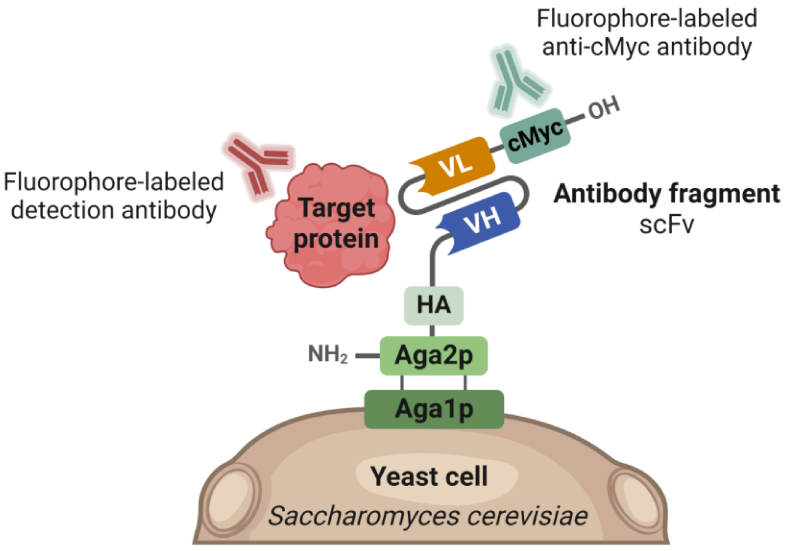

Figure 4: Schematic illustration of a yeast surface-displayed antibody fragment with respective detection antibodies. The scFv-Aga2p fusion protein is attached to Aga1p *via* two disulfide bonds. Aga1p is covalently linked to the yeast cell wall *via* a GPI anchor. Fluorophore-labeled detection antibodies against the C-terminal cMyc tag and the target protein allow the detection of yeast cells that display a functional scFv and simultaneously bind to the antigen. Created with BioRender.com.

A major advantage of the yeast display technology represents its compatibility with fluorescence-activated cell sorting (FACS), enabling real-time quantitative analysis and high-throughput screening of libraries. A two-dimensional sorting strategy allows for the isolation of clones with structural integrity and binding affinity towards the target protein. Over several consecutive sorting rounds, it is possible to effectively enrich binders and to discriminate the selected clones by affinity due to the high sensitivity of the method (154, 155). In addition, multi-parameter screening protocols for the selection of antibody variants from yeast libraries facilitate, e.g. the investigation of species cross-reactivity or epitope coverage during the screening procedure (156, 157).

1.2.4 Antibody engineering

The field of antibody engineering is primarily shaped by directed evolution to optimize binding and humanization to reduce immunogenicity. Beyond that, targeting cytotoxic molecules to cancer cells, conditional activation of antibodies and redirection of immune cells to cancer cells has been exploited. These recently developed approaches are driven by the ambition of precise targeting and efficient eradication of cancer, challenged by the heterogeneity of tumors and their microenvironment.

1.2.4.1 Antibody-drug conjugates

More than one hundred years ago, Paul Ehrlich coined the term ‘magic bullet’ to envision a therapeutic substance that fights pathogens with toxic agents without harming the body itself (158). Based on this concept, a large number of antibody-drug conjugates (ADCs) have been devised to date. ADCs consist of a tumor-targeting mAb conjugated to a cytotoxic payload through a chemical linker, providing both specific targeting and potent toxic activity (159, 160). The primary mechanism of action of ADCs commences with mAb binding to a tumor-associated antigen, receptor-mediated endocytosis which results in internalization and formation of an endosome that subsequently fuses with a lysosome (**Figure 5**). The cytotoxic payload is effectively released in the acidified, protease-rich lysosomal environment. Upon diffusion and interaction with its intracellular target molecule, the drug triggers cell death (161). Depending on the hydrophobicity of the free drug determining membrane permeability, the active substance can leave the cell and subsequently cause bystander killing effects on surrounding cells (162). Additionally, antibody Fc-mediated mechanisms such as CDC, ADCC and ADCP may contribute to the therapeutic effect of ADCs (160).

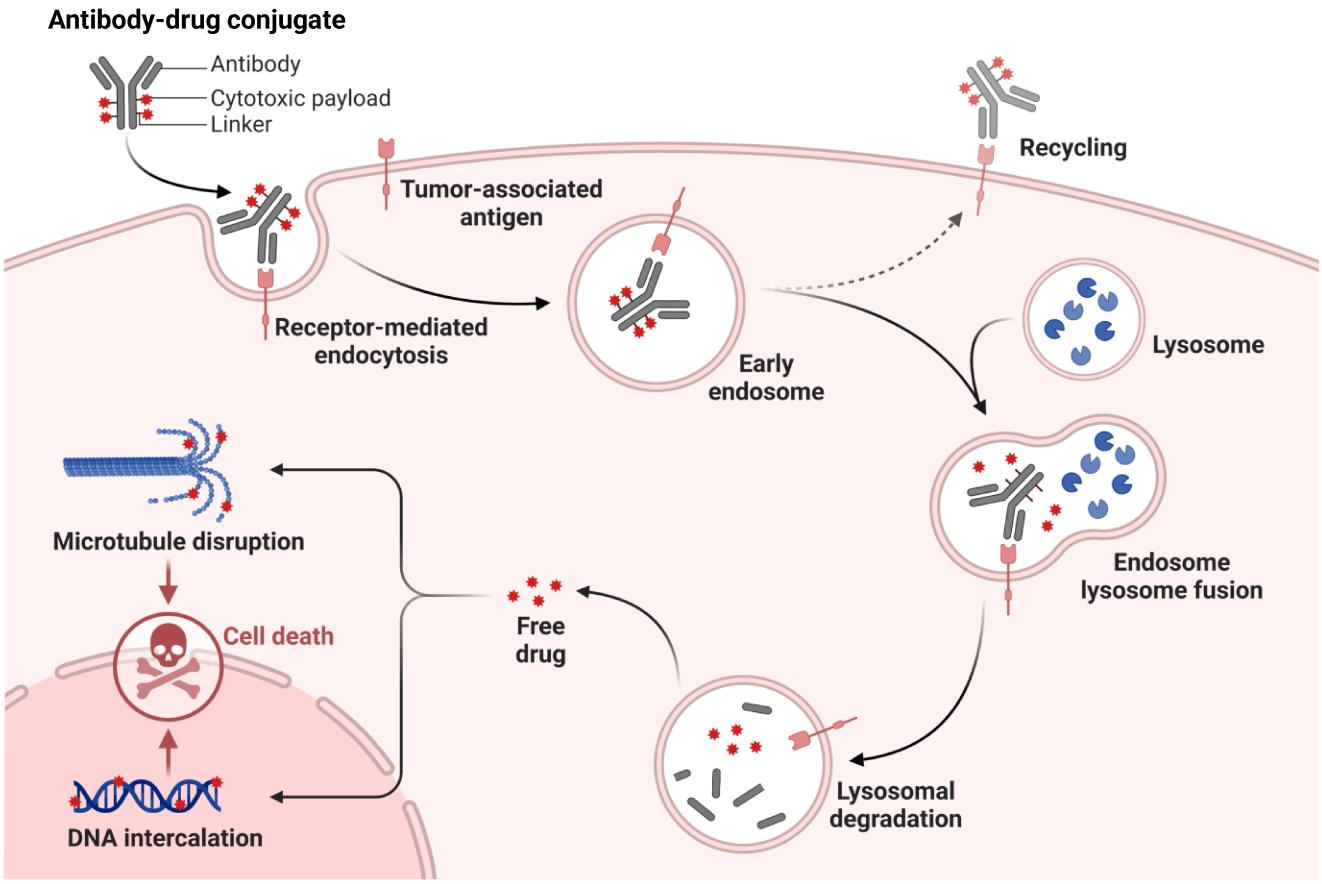

Figure 5: Schematic depiction of the structure and mechanism of action of an antibody-drug conjugate. ADCs consist of an antibody coupled to a cytotoxic payload by a synthetic linker. The mechanism of action includes ADC binding to the tumor-associated antigen and subsequent internalization by receptor-mediated endocytosis. The ADC is degraded upon endosome lysosome fusion, which results in drug release and cell death by drug-dependent mechanisms such as microtubule disruption or DNA intercalation. Created with BioRender.com.

The design of an ADC involves the selection of a target antigen, antibody moiety, chemical linker, and cytotoxic payload, which collectively determine efficacy and safety of the molecule. The target antigen marks the destination for the ADC drug, and has to fulfil criteria such as overexpression on malignant cells compared to healthy cells, presence on the cell surface, not inside the cell or in secreted forms, and capability to internalize upon antibody binding (161). As a targeting vehicle, the antibody is critical to the properties of the ADC. First, the Ig has to exhibit low immunogenicity and a long serum half-life to avoid rapid clearance and reduced efficacy (163). The most frequently utilized antibody type in ADC drugs is a humanized antibody of the IgG1 isotype, ensuring minimal immunogenicity-related side effects, maximal serum half-life of approximately 21 days, as well as immune effector functions. In terms of the binding fragment, high specificity and affinity towards the target antigen is desired (164). Besides binding kinetics, the internalization rate of the antibody-antigen complex may be influenced by the binding mode, e.g. receptor cross-linking, alteration of the internalization mechanism of the antibody-bound antigen (164). The linker connects the antibody to the chemotherapeutic drug and is crucial for the stability of the ADC. An ideal linker should combine features such as low aggregate formation and limited premature payload release in the blood circulation to mitigate off-target effects and ensure delivery to target sites. Two types of linkers including cleavable and non-cleavable linkers have been

employed in ADCs, although most of the approved ADCs have cleavable linkers allowing bystander killing effects. While non-cleavable linkers (e.g. thioether or maleimidocaproyl) rely on complete lysosomal enzymatic degradation for warhead delivery, cleavable linkers are sensitive to environmental conditions allowing regulated intracellular drug detachment (165). Cleavable linkers include chemical cleavage linkers containing pH-sensitive hydrazone bonds that are hydrolyzed upon ADC internalization in the endosome (pH 5-6) or lysosome (pH 4.8), or containing disulfide bonds that are reactive with reductive glutathione, which is present in high levels in cancer cells (165–168). In addition, enzyme cleavage linkers, activated by enzymes which are overexpressed in cancer cells, comprising glucuronide that can be cleaved by β-glucuronidase, or comprising peptide bonds sensitive to lysosomal proteases such as valine-citrulline or valine-alanine recognized by the cysteine protease cathepsin B (169–171). The cleavable dipeptide is commonly used in combination with a p-aminobenzoyloxycarbonyl (PABC) self-immolative spacer ensuring extracellular stability and efficient intracellular payload release (170, 172). The cytotoxic payload imparts toxic activity to the ADC molecule. Since only 1-2% of the total ADC administered intravenously reaches the target cells, high potency drugs are required to achieve beneficial effects (173). Currently, payloads utilized in therapeutic ADCs are potent tubulin inhibitors (60%), DNA-damaging agents (25%), and topoisomerase I inhibitors (15%) (174, 175). The auristatin derivates monomethyl auristatin E (MMAE) and monomethyl auristatin F (MMAF), represent the most commonly used microtubule inhibitors, which exert their biologic activity by perturbing microtubule growth at the β-subunits of the tubulin dimer. In comparison to the potency in the nanomolar range of half-maximal inhibitory concentrations (IC_{50}) observed with microtubule inhibitors, DNA-damaging agents are more effective with the IC_{50} values reaching the picomolar range. DNA-damaging agents mediate anti-proliferative effects through diverse mechanisms depending on the drug class, including induction of DNA double strand breaks, alkylation of DNA bases, intercalation between DNA bases, or formation of DNA crosslinks (176, 177).

The strategy applied for covalent coupling of the small molecule drug to the antibody moiety affects drug loading stoichiometry and heterogeneity. In general, ADCs are generated using either stochastic conjugation or site-specific conjugation. Stochastic conjugation involves reactions on chemically accessible sites such as endogenous lysine or cysteine residues through appropriate coupling methods (178, 179). For amide coupling, an activated carboxylic acid ester is introduced to the linker to attach the payload to lysine residues in the antibody. Cysteine coupling requires reduction of the disulfide bonds, which makes the interchain disulfides accessible for subsequent chemoselective reaction of the mercaptan groups with appropriate linker-payload complexes containing functionalities such as maleimide or haloacetamide (180). While there are up to 100 lysines distributed throughout an IgG molecule, cysteines are limited to eight at certain sites (159, 181, 182). Therefore, cysteine conjugates provide a higher degree of uniformity than lysine-based conjugates, although both strategies yield heterogeneous conjugation products with varying drug-to-antibody ratios (DARs) of 0-8 (181–183). To overcome this, site-specific conjugation methods have been developed that generate homogeneous ADC products conjugated at defined sites with consistent DARs. Site-specific approaches include conjugation to specific amino acids, unnatural amino acids, glycans, and peptide tags (184). Firstly, the introduction of reactive cysteine residues for directed antibody conjugation, developed by Junutula and co-workers,

resulted in homogenous ADC products, termed THIOMABs (185, 186). The ADCs based on cysteine engineering revealed 92% DAR 2 species and significant improvements in pharmacokinetics and safety aspects (185, 187). Introduction of unnatural amino acids, such as N-acetyl-L-phenylalanine, azidomethyl-L-phenylalanine, azido-L-lysine, or selenocysteine, further allows site-specific attachment by positioning of functional groups into the antibody and subsequent selective reaction with functionalized cargo (188–191). Besides addressing amino acids for conjugation, antibodies provide glycans at N297 allowing for unique modifications (192). Glycoconjugation is based on the placement of chemically reactive groups into the N-linked glycan, while glycan remodeling involves enzymes such as glycosyltransferases to introduce modified sugar residues to the non-reducing terminus of glycans under mild conditions, followed by coupling to an adequately equipped payload (193–195). Enzyme-assisted ligation of payload usually requires genetic modification of the antibody sequence, which involves the addition of peptide tags. The enzymes specifically recognize respective tags and catalyze bond-forming reactions on amino acid residues within the tag with provided functionalized substrates. At present, formyl glycine-generating enzyme, microbial transglutaminase and sortase A variants are frequently exploited enzymes (172, 196–201). The approach pursued in publications derived from this work utilizes the enzyme lipoate-protein ligase A (LplA) from *Escherichia coli* in combination with a respective lipoic acid ligase acceptor peptide (LAP) for antibody conjugation purposes (202, 203). LplA naturally catalyzes ATP-dependent transfer of lipoic acid to the ε-amino group of a certain lysine within a lipoate acceptor protein involved in oxidative metabolism. For biotechnological applications, the ligase has been engineered (W37V) towards a broader acceptance of substrates besides lipoic acid such as more bulky functionalized lipoate derivates (aryl azide), which allow for subsequent coupling reactions (202). In addition, an *in vitro* evolution approach enabled identification of a kinetically efficient 13-amino acid acceptor peptide for LplA (203). Following the modification of antibodies pursuing various aforementioned strategies to introduce certain functional groups, click chemistry enables convenient biorthogonal attachment of complementary modified linker-payload complexes (204, 205). Two main reactions are practiced for the use in biological systems: The strain-promoted azide-alkyne cycloaddition (SPAAC), where an azide reacts with a strained cyclic alkyne, such as bicyclononyne (BCN) or dibenzocyclooctyne (DBCO), to form an aromatic triazole, and the strain-promoted inverse electron demand Diels-Alder cycloaddition (SPIEDAC), where 1,2,4,5-tetrazines react with various dienophiles, such as BCN or norbornene, resulting in a pyridazine compound (206, 207).

The first ADC, gemtuzumab ozogamicin (Mylotarg), was approved by the FDA in 2000 for the treatment of CD33-positive acute myeloid leukemia (AML). Since then, 15 ADCs received worldwide market authorization and more than 200 ADC candidates have been investigated in clinical trials (174). While early ADC development focused on applications in hematologic malignancies, ADCs fighting solid tumors have emerged over time, overall resulting in half of the approved ADCs being used to treat hematologic malignancies and the others being prescribed for solid tumors. Human epidermal growth factor receptor (HER2) represents the most targeted receptor with three ADCs (trastuzumab emtansine (Kadcyla), trastuzumab deruxtecan (Enhertu), disitamab vedotin (Aidixi)) currently approved for clinical use in four tumor types (174).

1.2.4.2 Masked antibodies

Although mAbs have tremendously improved cancer patient outcomes, they can trigger side effects due to on-target, off-tumor toxicity (208). In the last decade, attempts have been made to direct antibodies towards the site of disease to exert their therapeutic effects, while remaining inert in circulation and healthy tissues (209). To this end, innovative antibody masking strategies have emerged bringing forth inactive, masked antibody drugs that become unmasked under specific environmental conditions associated with the disease target, such as the acidic tumor microenvironment or cancer-related enzymatic activity (**Figure 6**) (210–213). Two main concepts have been pursued for engineering of antibody masks, relying on steric hindrance or affinity toward the paratope. Steric hindrance-based masking consists of blocking the antigen binding site, e.g. by N-terminal fusion of leucin-zipper coiled-coil domains, hinge regions, antibody fragments, proteins or (poly-)peptides that either block themselves or associate with additional bulky molecules (214–220). Masks with affinity for the antigen binding region of the antibody require custom design and are derived from affinity peptides, anti-idiotypic antibody fragments, or versions of the antigen itself (221–224). The vast majority of masked antibodies are designed to be activated by specific proteases, which involves the incorporation of an appropriate protease-sensitive peptide linker (**Figure 6**). Depending on the type of cancer, different proteases are overexpressed or active for the purpose of invasion and metastasis compared to healthy tissue, such as serine proteases (e.g. matriptase, urokinase plasminogen activator), matrix metalloproteinases (MMPs; e.g. MMP-2, MMP-9), and cysteine proteases (e.g. cathepsins) (225–227).

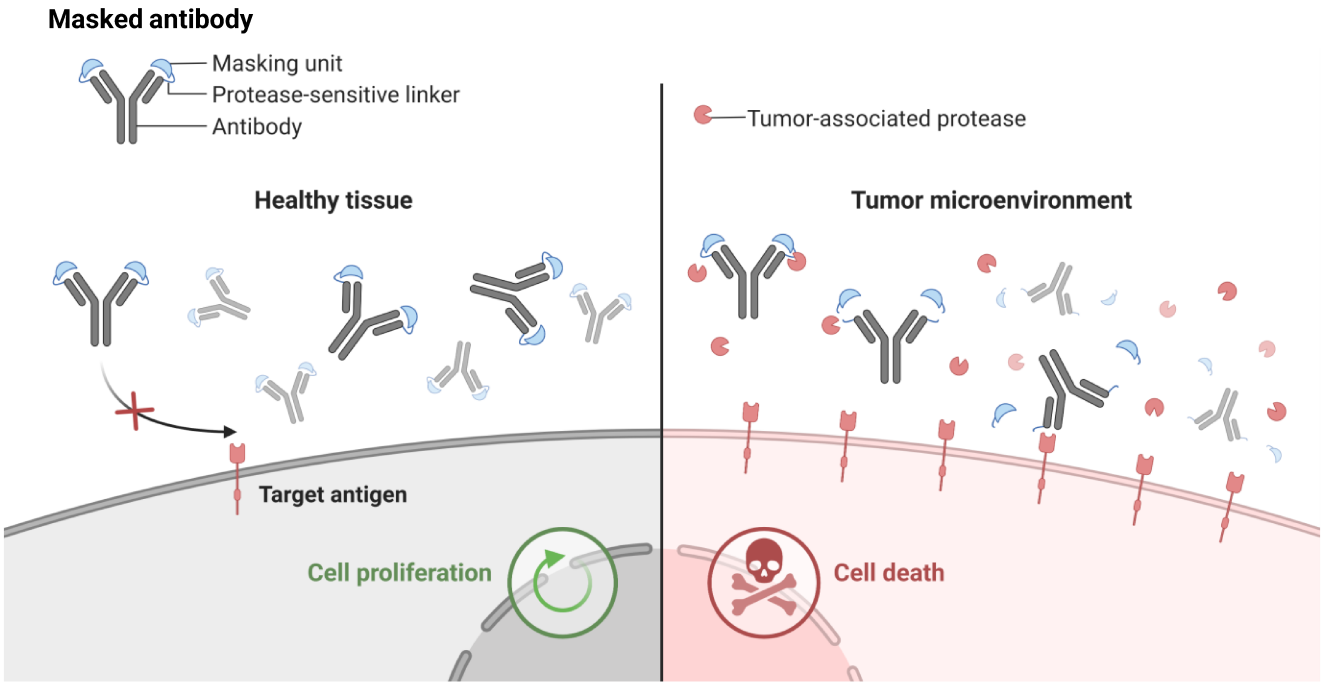

Figure 6: Schematic depiction of the structure and mode of action of a masked antibody. Masked antibodies are composed of a masking unit fused to the antibody by a protease-sensitive linker. In healthy tissue, the masked antibody is not able to bind to its target antigen. In the tumor microenvironment, tumor-associated proteases hydrolyze the linker connecting the antibody and the masking unit. The activated antibody regains binding ability, which leads to antibody-dependent mechanisms triggering cell death. Created with BioRender.com.

Designing masked antibodies requires consideration of several factors, including applicability, immunogenicity, masking and demasking efficiency, as well as overall reduction of side effects (228).

Steric hindrance-based masking, as opposed to affinity-based masking, represents a generic approach allowing application to a wide range of antibodies. However, the masking efficiency of the same blocking unit may vary from antibody to antibody (214, 218, 229). While masking units derived from human molecules have a higher probability to be tolerated, fragments from foreign or synthetic sources are predisposed to trigger immune reactions, especially during long-term systemic administration (209, 228). Nevertheless, immunogenicity needs to be extensively assessed in clinical trials, as the assembly of mask, linker and antibody may provoke neoantigens bearing the risk of ADA formation (230, 231). Effective masking and reactivation of antibodies depends on favorable competition between the target antigen and the masking moiety, which is set by the kinetic parameters of the mask (232). Ultimately, a conditionally activatable antibody should retain a high therapeutic potency comparable to that of the parental mAb, while exhibiting reduced systemic on-target toxicity, resulting in an improved therapeutic index (e.g. maximum tolerated to therapeutic dose ratio).

The field of masked antibodies has yielded diverse potential therapeutics enabling precise disease targeting and access to receptors previously considered as undruggable with conventional antibodies (209, 223). One of the most advanced platforms is the innovative universal, tunable XTEN® masking technology developed by Amunix Pharmaceuticals/Sanofi. The XTEN® mask acts by sterically blocking target binding and consists of a large unstructured, hydrophilic polypeptide, assembled from six different amino acids. The masking unit is anchored to the protein by three tandem recognition sequences addressable by three different classes of proteases frequently dysregulated in the tumor microenvironment. In addition to effective masking and conditional demasking, the attached polymer implies half-life extension and low immunogenicity (233, 234). Antibody derivatives, such as an HER2xCD3 scFv-based bispecific T cell engager (AMX-818), utilizing this masking approach demonstrated promising results and entered clinical trials in 2022 (NCT05356741) (219). The versatile Probody® platform devised by CytomX Therapeutics has been successfully applied to antibodies directed against a variety of difficult-to-target receptors. The technology involves fusion of an albumin-binding peptide to the N-terminus of the antibody light chain *via* a protease-cleavable linker (220). Upon systemic administration of the modified antibody, albumin, which is present in high amounts in the blood, associates with the attached peptide resulting in steric blocking of the binding site. Greatest achievements were reported for an anti-epithelial cell adhesion molecule (EpCAM) ADC (CX-2051) and a bispecific T cell engager (CX-904) targeting epithelial growth factor receptor (EGFR) and CD3, which are both currently under clinical investigation (NCT06265688; NCT05387265). Janux Therapeutics utilizes its platform masking technology to engineer tumor-activated T cell engagers (TRACTrs) as novel drug candidates overcoming T cell engager-related toxicity and efficacy limitations (235, 236). TRACTrs are composed of a tumor antigen-binding domain and a T cell-binding domain against CD3, which is fused to a masking affinity peptide and an appended albumin binding domain. A protease-labile linker allows tumor microenvironment-dependent demasking which results in CD3 interaction, while diffusion from the tumor site entails rapid clearance due to the lack of a half-life extending molecule. Two conditionally activated T cell engagers directed against prostate-specific membrane antigen (PSMA; JANX007) and EGFR (JANX008) revealed promising preclinical activity and safety profiles and entered clinical trials within the last two years (NCT05519449; NCT05783622) (235, 236).

1.2.4.3 Bispecific antibodies

In recent years, bispecific antibodies (bsAbs) have gained momentum and transformed from early-stage research to clinical applications approved for the treatment of patients. By combining two specificities in one molecule, bsAbs unlock novel mechanisms of action for targeting complex diseases such as cancer, which involve multiple factors and signaling pathways. Bifunctionality allows cross-linking of two receptors, modulation of two functional pathways, or recruitment of immune effector cells to diseased cells (237). Compared to conventional mAbs, engineered bsAbs offer superior therapeutic effects in terms of specificity, efficacy, toxicity and drug resistance (238). For the generation of bsAbs various platforms have been established ensuring heterologous recombination of heavy chains and respective light chains (237). In general, bsAb formats are categorized in IgG-like and non-IgG-like. Although non-IgG-like bsAbs are producible as single polypeptide chain and exhibit beneficial tissue penetration properties, function solely relies on antigen binding due to the absent Fc region, which imparts effector functions and half-life extension (237, 239, 240). Classical IgG-like bsAbs assemble from two different heavy and light chains requiring protein engineering techniques, which ensure correct heavy chain heterodimerization and light chain pairing. Developed heavy chain heterodimerization approaches include the Knobs-into-Holes (KiH) technology, based on steric hindrance introduced by mutation of amino acids in the C_H3 domain, the DEKK method, relying on mutations of amino acids in the C_H3 domain engendering electrostatic steering and the strand-exchange engineered domain (SEED) technology, based on alternating segments derived from human IgG and IgA C_H3 sequences promoting heterodimerization through steric complementary contact surfaces (241–244). Providing cognate light chain pairing, the CrossMab technology was developed by the introduction of a domain crossover of the heavy chain C_H1 and the light chain C_L in one of the two Fabs (245). Moreover, Fab interface engineering enables correct assembly through a set of complementary mutations in one of the two Fab fragments (246). The common light chain (cLC) approach produces antibodies comprising two identical light chains paired with two different heavy chains, since in many cases the heavy chain variable regions contribute predominantly to antigen binding, while the light chain mediates stability (247, 248). Additionally, IgG-like bsAbs are devised by the fusion of Fabs, scFvs or V_HHs to either the N- or C-terminus of the antibody heavy or light chain resulting in appended IgG formats (249–252). Technically, symmetrical or asymmetrical bispecific IgG antibody scaffolds can be employed for introduction of additional antibody fragments, which are commonly linked through flexible G4S repeats (249).

BsAbs were initially invented to retarget T cells to tumors, giving rise to the group of immune cell engagers (ICEs), with the first bsAb approved in 2009 (catumaxomab, withdrawn in 2017) (253). ICEs represent cell-bridging molecules, that simultaneously bind target antigens on cancer cells and immune-related molecules on endogenous effector cells, resulting in the formation of an immunological synapse followed by tumor cell death (**Figure 7**) (254, 255). The majority of T cell engagers (TCEs) function through a domain directed against CD3, which is associated with the T cell receptor complex. Engagement leads to activation of T cells, independent of MHC specificity and co-stimulatory signals, release of perforins and granzymes and ultimately cancer cell lysis (256). In addition to the BiTE blinatumomab, a CD3xCD19 tandem scFv, approved in 2014 for therapy of B cell acute lymphoblastic leukemia, the class of TCEs holds great potential to treat many types of cancer, with a total of nine TCEs

being approved for therapeutic application by the end of 2023 (257). However, a limitation emerging with TCEs is the occurrence of side effects, especially cytokine release syndrome (CRS) and immune effector cell-associated neurotoxicity syndrome (ICANS) (258). Alternative ICEs have been explored which redirect immune cells such as NK cells by CD16, NKG2D, NKp46 or NKp30, or myeloid linage cells including monocytes/macrophages and neutrophiles by CD47 or CD89 (259–262). Beyond ICEs, non-cell-bridging dual tumor targeting bsAbs exist, which bind to two different epitopes on a single target or to two distinct antigens, both expressed on tumor cells (**Figure 7**). The antibody concept leverages the unique antigenic landscape of tumors, thereby increasing tumor selectivity, allowing simultaneous modulation of two functional pathways and overcoming tumor immune escape mechanisms and drug resistance (263, 264). The first-in-class dual tumor-associated antigen-targeting antibody amivantamab, approved in 2021 for the treatment of non-small cell lung cancer with EGFR exon 20 insertion mutations, inhibits EGFR and mesenchymal epithelial transition factor (cMet) receptor tyrosine kinases simultaneously, modulating shared proliferation-promoting downstream signaling pathways and leading to improved cancer outcomes (265, 266).

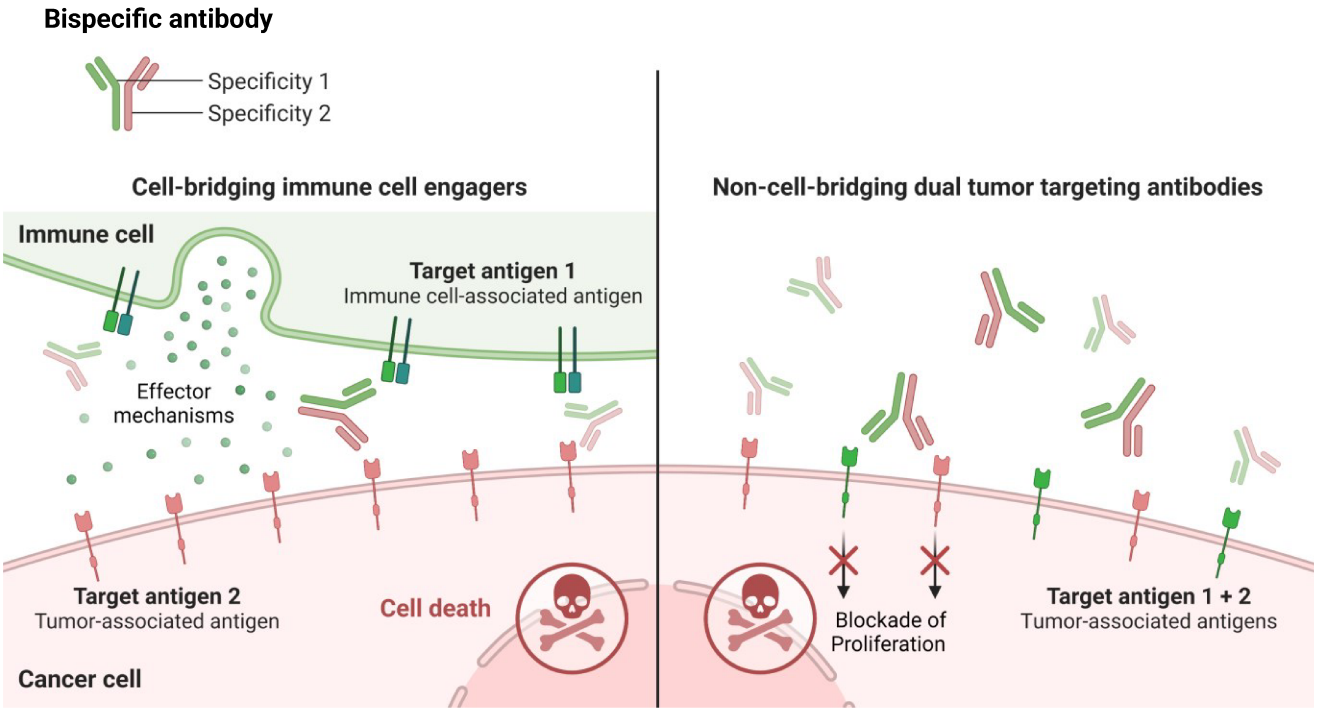

Figure 7: Schematic illustration of the structure and mechanisms of action of bispecific antibodies. Bispecific antibodies comprise two specificities. Cell-bridging immune cell engagers simultaneously bind to immune cells and cancer cells, which leads to the formation of an immunologic synapse and execution of effector mechanisms, ultimately causing tumor cell death. Non-cell-bridging dual tumor targeting antibodies simultaneously bind to two antigens on the cancer cell, which may result in blockade of proliferation and cell survival, ultimately leading to tumor cell death. Created with BioRender.com.

By the end of 2023, 14 bsAbs have received market approval, of which eleven are intended for the use in cancer patients, and three for non-oncology indications (257). From more than 200 bsAb candidates in various stages of clinical development for immuno-oncology applications, approximately 27% are devised for hematological malignancies and 73% for solid tumors (257). While TCEs dominate the field of bsAbs designed for hematologic cancers, dual immune checkpoint inhibitors and immunomodulators represent the largest group of bsAbs for solid tumors (257, 267).

1.3 Cancer

With an estimated 20 million new cancer cases and nearly 10 million deaths worldwide in 2022, cancer is one of the leading causes of death (268). About 1 in 5 people develop cancer during their lifetime, while approximately 1 in 10 individuals die from the disease. Lung cancer accounts for the most commonly occurring cancer, followed by female breast cancer, colorectal cancer, prostate cancer, stomach cancer and liver cancer (**Figure 8**) (268). In general, cancer originates from the abnormal and dysregulated proliferation of malignant cells resulting in uncontrolled growth invading healthy tissues and eventually spreading throughout the body. However, cancers exhibit diverse and complex phenotypes which are compiled into the hallmarks of cancer. Today, ten cancer hallmarks have been established, including the acquired capabilities for sustaining proliferative signaling, evading growth suppressors, avoiding immune destruction, enabling replicative immortality, tumor-promoting inflammation, activating invasion and metastasis, inducing or accessing vasculature, genome instability and mutation, resisting cell death and deregulating cellular metabolism (269).

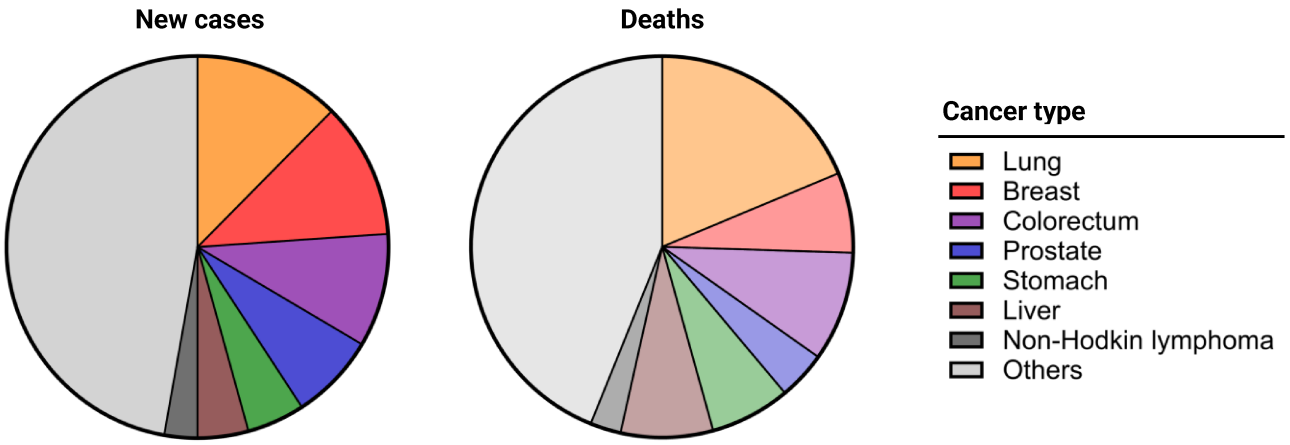

Figure 8: Distribution of new cancer cases and deaths in 2022. Data represent new cancer cases (left) and deaths (right) for different cancer types, worldwide in people of both sexes and all ages. Generated with GraphPad Software, according to (270).

Cancers are divided into two main types: solid tumor cancers and hematologic cancers. Solid tumors are heterotypic masses of cancer cells, cancer stem cells, connective tissue cells as well as immune cells, forming abnormal tissue in various organ systems. Hematologic cancer, also known as blood cancer, begins in blood-forming tissue, such as the bone marrow, or in the cells of the immune system. This cancer type represents heterogeneous group of malignancies, which is further categorized into the three groups of leukemias, lymphomas and multiple myeloma (271). Multiple myeloma derives from differentiated clonal plasma cells that proliferate and accumulate in the bone marrow in an uncontrolled manner, in most cases accompanied by increased production of monoclonal immunoglobulins (272, 273). Leukemias develop from precursors of leukocytes of myeloid or lymphoid linage arrested at a certain stage of differentiation and are further classified according to their velocity of progression in acute, fast developing, or chronic, slowly progressing (274, 275). Lymphomas arise from lymphocytes during development and affect the lymphatic system, especially secondary lymphoid organs such as lymph nodes, thymus or spleen (276). They are traditionally divided into Hodgkin lymphoma and

non-Hodgkin lymphoma (NHL), which accounts for about 3% of new cancer cases and 90% of lymphomas (270, 277). NHL is the most frequently diagnosed adult hematological cancer, is subdivided into B cell-derived (90%) and NK/T cell-derived (10%) neoplasms (278). The diversity and variability of cancer and the ability to distinguish diseased cells from healthy cells are at the root of the difficulty in curing cancer.

1.3.1 Antibody-based cancer therapy

Over many decades cancer treatment options were limited to surgery, chemotherapy or radiation therapy. While chemotherapy employs cytotoxic drugs to stop fast-growing tumor cells by interfering with cellular functions required for cell growth and survival, radiation therapy utilizes ionizing radiation to damage cancer cells' DNA (279). Despite both methods succeeded in eradicating tumors or, at least, reducing tumor burden, the non-specific nature means also damage to healthy tissues, potentially leading to serve side effects. Moreover, drug resistance frequently emerges in chemotherapeutic approaches whereby cells initially responding to the drug develop resistance mechanisms such as decreased drug uptake, alterations in particular cellular processes, or increased drug efflux (280).

The advent of targeted therapies has revolutionized the landscape of cancer treatment due to their efficacy against tumor cells and reduced off-target toxicities. Targeted therapy aims at delivering drugs to distinct molecules specific for cancer cells or the growth-promoting tissue environment. Small molecule inhibitors administered orally represent one class which improved lives of numerous cancer patients. Prominent targets for such molecules are kinases involved in cancer cell signaling. Consequently, kinase inhibitors have been developed, e.g. imatinib, inhibitor of the proliferation-promoting tyrosine kinase Bcr-Abl, for chronic myeloid leukemia; gefitinib, EGFR kinase inhibitor; and sorafenib, inhibitor of vascular epidermal growth factor receptor (VEGFR) kinase, in renal cancer (281). Antibodies, inherently featuring high specificity, Fc-mediated effector functions and the ability to modulate biological pathways, further appeared as promising targeted therapeutic for cancer treatment. The authorization of the CD20-targeting mAb rituximab for NHL treatment in 1997 marked the first clinical application of an anti-cancer antibody (70, 282). Successes were also achieved by antibodies directed against growth factor receptors, involved in cancer initiation and progression, such as EGFR and HER2 (283, 284). Anti-growth factor receptor antibodies generally function by blockade of growth factor binding and subsequent signaling and recruitment of cellular cytotoxicity (ADCC). After the launch of the anti-HER2 antibody trastuzumab for breast and stomach cancer treatment in 1998, and the anti-EGFR antibody cetuximab for colorectal and head and neck cancer treatment in 2004, two HER2 (pertuzumab and margetuximab) and three EGFR (panitumumab, nimotuzumab and necitumumab) mAbs further received FDA-approval. Another antibody-based treatment approach applicable for diverse cancer types involves blockade of immune checkpoint proteins (285, 286). Such receptors of co-inhibitory nature, normally expressed by T cells negatively regulating immune responses to maintain self-tolerance and limit collateral tissue damage during immune reactions, allow tumor cell tolerance and cause T cell exhaustion (286, 287). Hence, antibodies acting as immune checkpoint inhibitors (ICIs)

enable reactivation of immune responses against cancer cells, among them the anti-cytotoxic T lymphocyte-associated protein-4 (CTLA-4) mAb ipilimumab, and ten anti-programmed death protein-1 (PD-1)/ anti-programmed death protein-ligand 1 (PD-L1) mAbs, including pembrolizumab, nivolumab, cemiplimab, dostarlimab, retifanlimab, toripalimab and tislelizumab targeting PD-1 and atezolizumab, avelumab and durvalumab directed against the tumor-associated ligand PD-L1 (286). Beyond that, lymphocyte activation gene-3 (LAG-3) has been considered as target, the co-inhibitory receptor competitively binds to MHC class II and thereby inhibits effector T cell activation (288, 289). In 2022, a combination of the anti-LAG-3 mAb relatlimab-rmbw with the anti-PD-1 mAb nivolumab was FDA-approved (290). Besides targeting of (tumor) cell-anchored molecules, soluble factors in the tumor microenvironment (TME) that are released by cancer cells to induce angiogenesis, cancer cell proliferation, or immune tolerance, serve as targets for therapy (291). Bevacizumab, an anti-vascular endothelial growth factor (VEGF) mAb which neutralizes the ligand thereby prohibiting angiogenesis and tumor growth, reached market approval in 2004 (291, 292).

Technological advances have enabled the development of next-generation antibodies, including bispecific antibodies and antibody-drug conjugates, as well as cell-based immunotherapies, all of which have proven valuable in cancer management. The invention of bispecific antibodies has opened novel mechanisms of action for tumor eradication not available with conventional mAbs. Immune cell engagers redirect cytotoxic effects of endogenous immune cells, such as T cells, towards cancer cells. Blinatumomab, a TCE specific for the B lymphocyte antigen CD19 and T cell co-receptor CD3 led to improved outcomes in treatment of patients with B cell acute lymphoblastic leukemia (293). In addition to nine TCEs being approved for various cancer indications, dual signaling inhibitors of two different receptor tyrosine kinases (EGFRxcMet; amivantamab), and dual ICIs (PD-1xCTLA-4; cadonilimab) complete the bsAb panel for oncology (257). Furthermore, antibody-drug conjugates combine targeted therapy and chemotherapy by antibody-directed delivery of cytotoxic agents to cancerous cells without harming nearby healthy cells. Currently, three HER2-targeting ADCs are in clinical use together with twelve other ADCs approved for hematological cancers as well as solid tumors (174). An alternative method producing remarkably effective and durable clinical responses is based on adoptive T cell transfer of reprogrammed patient-derived T cells that are equipped with chimeric antigen receptors (CARs) (294). Lymphocytes are redirected to cancer cells by the specificity of their synthetic receptors and effectively eliminate tumors independent of MHC receptor interaction (295). The unparallelled success of anti-CD19 CAR-T cell therapy in B cell malignancies led to the FDA approval of tisagenlecleucel (Kymriah) and axicabtagene ciloleucel (Yescarta) in 2017, and was followed by launches of further CD19- and B cell maturation antigen (BCMA)-targeting CAR-T cell therapies (296–298). In many cancers more than one pathway is dysregulated. Hence, drug combinations may lead to additive or synergistic tumoricidal effects. For instance, it is well established that the combination of chemotherapy with rituximab provides a significant clinical benefit in the treatment of CD20-positive B cell lymphoma (299). Combination immunotherapies targeting multiple molecular alterations, such as two ICIs, ICI and anti-angiogenic mAbs, or ICI and anti-tumor antigen mAbs, demonstrated superior patient survival compared to the respective monotherapies (300).

By the end of 2023, nearly 70% of companies' therapeutic antibody pipelines in clinical trials were determined for cancer indications (91). At present, conventional mAbs continue to represent the major class of therapeutic antibodies for oncology applications (91, 257). However, engineered antibodies, such as ADCs, bsAbs and multispecific antibodies, will continue to be a part of drug discovery making an increasingly important contribution to the range of antibodies for cancer treatment (91).

2 Objective

The advent of targeted therapy marks a pivotal transition in cancer treatment, from traditional, non-specific approaches toward more precise and effective strategies. Central to this shift is the development of monoclonal antibodies that enable specific tumor targeting and recruitment of effector functions. However, cancers inherently exhibit a high degree of diversity, and the modes of action of mAbs are limited. Consequently, additional functionalities that enhance specificity and anti-tumor efficacy may be incorporated into antibodies.

Firstly, this thesis aimed at devising a conditionally activated anti-IgM antibody-drug conjugate for precise B cell lymphoma targeting. The standard frontline treatment for B cell lymphoma is based on mAbs targeting pan-B lymphocyte-associated antigens, such as CD20 by rituximab, which facilitates opsonization and subsequent elimination of cancer cells. Although rituximab in combination with chemotherapy has proven successful in clinical applications, it may lead to an overall immunosuppression since it affects the entire B cell population and effectiveness is ultimately limited by the development of treatment resistance. Therefore, this project intended to generate antibodies directed against the B cell receptor of IgM isotype, frequently expressed by malignant B cells, to eliminate the cancerous subpopulation while preserving the majority of healthy B lymphocytes that maintain adaptive immunity. Anti-human IgM antibodies were obtained from screening of a chicken-derived immune library. The selected anti-IgM antibody was equipped with the epitope-bearing human IgM domain, serving as antigenic affinity-based mask, to reduce off-target effects regarding healthy IgM-positive B cells as well as capture by soluble pentameric IgM in systemic circulation. Conditional reactivation of the masked antibody was achieved through implementation of a linker sensitive to specific proteases that are present in the tumor microenvironment, providing augmented cancer specificity. With respect to efficacy, the antibody was conjugated with the chemotherapeutic agent MMAE, imparting cytotoxic properties to the antibody. Effective blockade by the masking unit and protease-mediated restoration of IgM binding was assessed on molecular and cellular level. Ultimately, the masked and demasked anti-IgM antibody-drug conjugates were evaluated towards their potential to internalize, and subsequently induce cell death in lymphoma B cells.

Another research aspect of the thesis included T cell receptor-directed antibody-drug conjugates for the treatment of T cell-derived cancers. T cell malignancies occur less frequently compared to B cell malignancies. However, T cell cancers represent a clinically heterogeneous group associated with poor clinical outcomes. In most cases, treatment exclusively relies on chemotherapy, as discrimination of diseased cells from healthy cells is virtually impossible and total eradication of T cells is fatal for the patient. This part of the thesis aimed at exploring a novel strategy for specific recognition and elimination of malignant T cells through targeting the clonally rearranged T cell receptor displayed by the cancerous T cell population, while preserving overall T cell repertoire integrity and cellular immunity. Antibodies were raised against a specific TCR by chicken immunization and subsequent antibody library screening. The selected TCR binders were investigated for their anti-idiotypic properties using engineered target T cells as well as polyclonal T lymphocytes isolated from healthy human donor blood. Two distinct antibody-drug conjugates were derived from the selected anti-TCR antibody, differing in their amounts

of MMAE loading. The ADCs were finally subjected to cytotoxicity studies, as well as bystander killing assays to determine the capability to overcome drug resistance in case of TCR downregulation or rearrangement by cancer T cells.

A third project intended the design of bispecific killer cell engagers employing species cross-reactive NKG2D binders that redirect human and murine lymphocytes to ErbB2/HER2-positive malignancies. Compared to monoclonal antibodies, bispecific antibodies broaden the spectrum of possible mechanisms of action. The most commonly adopted approach utilizes immune cell engagers to mediate redirection of cytotoxic lymphocytes to cancer cells, resulting in the formation of an immunological synapse and subsequent tumor cell killing. Exploiting this concept, IgG4-based bispecific killer cell engagers (termed scNKAB-ErbB2) were developed, that simultaneously target the tumor-associated antigen ErbB2/HER2 and the human and murine activating NK cell receptor NKG2D for the ligand-independent recruitment of immune effector cells. To decouple effectiveness of the devised engagers from cytotoxic functionality of the endogenous lymphocytes, *ex vivo* expanded NK cells from healthy donors or cells derived from the human NK cell line NK-92, which may additionally be modified with chimeric antigen receptors, are commonly utilized for adoptive NK cell therapies. Cross-reactive antibodies to human and murine molecules were generated by chicken immunization with NKG2D proteins of both origins, followed by library screening for binding of human and murine receptor derivatives to facilitate preclinical development using immunocompetent mouse tumor models. A panel of the selected anti-NKG2D antibodies were subsequently explored in ErbB2/HER2-directed bispecific tetravalent antibodies. Specificities of the different generated scNKAB-ErbB2 molecules were investigated *via* binding to HER2/ErbB2-expressing cancer cells as well as NK-92 cells engineered with chimeric antigen receptors derived from human and murine NKG2D, and NKG2D-positive primary human and murine lymphocytes. In addition to the competition of the bispecific engagers with the natural NKG2D ligand MICA, the ability to redirect the cytotoxicity of human and murine NKG2D CAR-engineered NK-92 cells and primary human and murine lymphocytes to ErbB2-positive cancer cells was assessed.

In summary, the projects undertaken as part of this thesis sought to develop functionality-enhanced antibodies for precision cancer therapy. The integration of sophisticated modifications into antibodies, enabling controlled activation in the tumor microenvironment, custom-tailored specificity, delivery of highly potent cytotoxic drugs, and augmented immune effector cell recruitment, will be evaluated with respect to precise and effective cancer eradication.

3 References

1. lngale A. *Basic Immunology*. La Vergne: New Central Book Agency (2020). 305 p.
2. Murphy K, Janeway CA. *Janeway's immunobiology*. New York, N.Y.: Garland Science, Taylor & Francis Group (2016).
3. Thaiss CA, Zmora N, Levy M, Elinav E. The microbiome and innate immunity. *Nature* (2016) **535**:65–74. doi:10.1038/nature18847
4. Riera Romo M, Pérez-Martínez D, Castillo Ferrer C. Innate immunity in vertebrates: an overview. *Immunology* (2016) **148**:125–39. doi:10.1111/imm.12597
5. Wagner H. Interactions between bacterial CpG-DNA and TLR9 bridge innate and adaptive immunity. *Curr Opin Microbiol* (2002) **5**:62–9. doi:10.1016/S1369-5274(02)00287-4
6. Li D, Wu M. Pattern recognition receptors in health and diseases. *Signal Transduct Target Ther* (2021) **6**:291. doi:10.1038/s41392-021-00687-0
7. Lee MS, Kim Y-J. Signaling pathways downstream of pattern-recognition receptors and their cross talk. *Annu Rev Biochem* (2007) **76**:447–80. doi:10.1146/annurev.biochem.76.060605.122847
8. Zhou J, Tian Z, Peng H. Tissue-resident NK cells and other innate lymphoid cells. *Adv Immunol* (2020) **145**:37–53. doi:10.1016/bs.ai.2019.11.002
9. Sivori S, Vacca P, Del Zotto G, Munari E, Mingari MC, Moretta L. Human NK cells: surface receptors, inhibitory checkpoints, and translational applications. *Cell Mol Immunol* (2019) **16**:430–41. doi:10.1038/s41423-019-0206-4
10. Ljunggren HG, Kärre K. In search of the 'missing self': MHC molecules and NK cell recognition. *Immunol Today* (1990) **11**:237–44. doi:10.1016/0167-5699(90)90097-S
11. Wensveen FM, Jelenčić V, Polić B. NKG2D: A Master Regulator of Immune Cell Responsiveness. *Front Immunol* (2018) **9**:441. doi:10.3389/fimmu.2018.00441
12. Bauer S, Groh V, Wu J, Steinle A, Phillips JH, Lanier LL, et al. Activation of NK cells and T cells by NKG2D, a receptor for stress-inducible MICA. *Science* (1999) **285**:727–9. doi:10.1126/science.285.5428.727
13. Abel AM, Yang C, Thakar MS, Malarkannan S. Natural Killer Cells: Development, Maturation, and Clinical Utilization. *Front Immunol* (2018) **9**:1869. doi:10.3389/fimmu.2018.01869
14. Shifrin N, Raulet DH, Ardolino M. NK cell self tolerance, responsiveness and missing self recognition. *Semin Immunol* (2014) **26**:138–44. doi:10.1016/j.smim.2014.02.007
15. Clark GJ, Angel N, Kato M, López JA, MacDonald K, Vuckovic S, et al. The role of dendritic cells in the innate immune system. *Microbes Infect* (2000) **2**:257–72. doi:10.1016/S1286-4579(00)00302-6
16. Moll H. Antigen delivery by dendritic cells. *Int J Med Microbiol* (2004) **294**:337–44. doi:10.1016/j.ijmm.2004.03.003
17. Smith-Garvin JE, Koretzky GA, Jordan MS. T cell activation. *Annu Rev Immunol* (2009) **27**:591–619. doi:10.1146/annurev.immunol.021908.132706
18. Pennock ND, White JT, Cross EW, Cheney EE, Tamburini BA, Kedl RM. T cell responses: naive to memory and everything in between. *Adv Physiol Educ* (2013) **37**:273–83. doi:10.1152/advan.00066.2013
19. Sproul TW, Cheng PC, Dykstra ML, Pierce SK. A role for MHC class II antigen processing in B cell development. *Int Rev Immunol* (2000) **19**:139–55. doi:10.3109/08830180009088502
20. Cyster JG, Allen CD. B Cell Responses: Cell Interaction Dynamics and Decisions. *Cell* (2019) **177**:524–40. doi:10.1016/j.cell.2019.03.016
21. Goldberg BS, Ackerman ME. Antibody-mediated complement activation in pathology and protection. *Immunol Cell Biol* (2020) **98**:305–17. doi:10.1111/imcb.12324

22. Wu Y-C, Kipling D, Dunn-Walters D. Assessment of B Cell Repertoire in Humans. *Methods Mol Biol* (2015) **1343**:199–218. doi:10.1007/978-1-4939-2963-4_16
23. Jackson KJ, Kidd MJ, Wang Y, Collins AM. The shape of the lymphocyte receptor repertoire: lessons from the B cell receptor. *Front Immunol* (2013) **4**:263. doi:10.3389/fimmu.2013.00263
24. Hata S, Clabby M, Devlin P, Spits H, Vries JE de, Krangel MS. Diversity and organization of human T cell receptor delta variable gene segments. *J Exp Med* (1989) **169**:41–57. doi:10.1084/jem.169.1.41
25. Tonegawa S. Somatic generation of antibody diversity. *Nature* (1983) **302**:575–81. doi:10.1038/302575a0
26. Davis MM, Bjorkman PJ. T-cell antigen receptor genes and T-cell recognition. *Nature* (1988) **334**:395–402. doi:10.1038/334395a0
27. Takihara Y, Tkachuk D, Michalopoulos E, Champagne E, Reimann J, Minden M, et al. Sequence and organization of the diversity, joining, and constant region genes of the human T-cell delta-chain locus. *Proc Natl Acad Sci U S A* (1988) **85**:6097–101. doi:10.1073/pnas.85.16.6097
28. van Dongen JM, Langerak AW, Szczepanski T. *Laboratory hematology practice: Immunoglobulin and T-cell receptor gene rearrangement analysis for diagnosis of hematological malignancies*. Chichester, West Sussex, UK, Hoboken, NJ: Blackwell Pub (2012). 199-219.
29. Hozumi N, Tonegawa S. Evidence for somatic rearrangement of immunoglobulin genes coding for variable and constant regions. *Proc Natl Acad Sci U S A* (1976) **73**:3628–32. doi:10.1073/pnas.73.10.3628
30. Oettinger MA, Schatz DG, Gorka C, Baltimore D. RAG-1 and RAG-2, adjacent genes that synergistically activate V(D)J recombination. *Science* (1990) **248**:1517–23. doi:10.1126/science.2360047
31. Rock EP, Sibbald PR, Davis MM, Chien YH. CDR3 length in antigen-specific immune receptors. *J Exp Med* (1994) **179**:323–8. doi:10.1084/jem.179.1.323
32. Cabaniols JP, Fazilleau N, Casrouge A, Kourilsky P, Kanellopoulos JM. Most alpha/beta T cell receptor diversity is due to terminal deoxynucleotidyl transferase. *J Exp Med* (2001) **194**:1385–90. doi:10.1084/jem.194.9.1385
33. Pieper K, Grimbacher B, Eibel H. B-cell biology and development. *J Allergy Clin Immunol* (2013) **131**:959–71. doi:10.1016/j.jaci.2013.01.046
34. Di Noia JM, Neuberger MS. Molecular mechanisms of antibody somatic hypermutation. *Annu Rev Biochem* (2007) **76**:1–22. doi:10.1146/annurev.biochem.76.061705.090740
35. Maul RW, Gearhart PJ. AID and somatic hypermutation. *Adv Immunol* (2010) **105**:159–91. doi:10.1016/S0065-2776(10)05006-6
36. Muramatsu M, Kinoshita K, Fagarasan S, Yamada S, Shinkai Y, Honjo T. Class switch recombination and hypermutation require activation-induced cytidine deaminase (AID), a potential RNA editing enzyme. *Cell* (2000) **102**:553–63. doi:10.1016/S0092-8674(00)00078-7
37. Hennecke J, Wiley DC. T cell receptor-MHC interactions up close. *Cell* (2001) **104**:1–4. doi:10.1016/s0092-8674(01)00185-4
38. Nguyen TG. The therapeutic implications of activated immune responses via the enigmatic immunoglobulin D. *Int Rev Immunol* (2022) **41**:107–22. doi:10.1080/08830185.2020.1861265
39. Geisberger R, Lamers M, Achatz G. The riddle of the dual expression of IgM and IgD. *Immunology* (2006) **118**:429–37. doi:10.1111/j.1365-2567.2006.02386.x
40. Keyt BA, Baliga R, Sinclair AM, Carroll SF, Peterson MS. Structure, Function, and Therapeutic Use of IgM Antibodies. *Antibodies (Basel)* (2020) **9**. doi:10.3390/antib9040053
41. Otten MA, van Egmond M. The Fc receptor for IgA (FcalphaRI, CD89). *Immunol Lett* (2004) **92**:23–31. doi:10.1016/j.imlet.2003.11.018

42. Kumar Bharathkar S, Parker BW, Malyutin AG, Haloi N, Huey-Tubman KE, Tajkhorshid E, et al. The structures of secretory and dimeric immunoglobulin A. *Elife* (2020) **9**. doi:10.7554/eLife.56098
43. Sutton BJ, Davies AM, Bax HJ, Karagiannis SN. IgE Antibodies: From Structure to Function and Clinical Translation. *Antibodies (Basel)* (2019) **8**. doi:10.3390/antib8010019
44. Tiller KE, Tessier PM. Advances in Antibody Design. *Annu Rev Biomed Eng* (2015) **17**:191–216. doi:10.1146/annurev-bioeng-071114-040733
45. Damelang T, Brinkhaus M, van Osch TL, Schuurman J, Labrijn AF, Rispens T, et al. Impact of structural modifications of IgG antibodies on effector functions. *Front Immunol* (2023) **14**:1304365. doi:10.3389/fimmu.2023.1304365
46. Vidarsson G, Dekkers G, Rispens T. IgG Subclasses and Allotypes: From Structure to Effector Functions. *Front Immunol* (2014) **5**. doi:10.3389/fimmu.2014.00520
47. Amzel LM, Poljak RJ. Three-dimensional structure of immunoglobulins. *Annu Rev Biochem* (1979) **48**:961–97. doi:10.1146/annurev.bi.48.070179.004525
48. Sitia R, Rubartelli A, Hämmerling U. The role of glycosylation in secretion and membrane expression of immunoglobulins M and A. *Mol Immunol* (1984) **21**:709–19. doi:10.1016/0161-5890(84)90023-3
49. Arnold JN, Radcliffe CM, Wormald MR, Royle L, Harvey DJ, Crispin M, et al. The glycosylation of human serum IgD and IgE and the accessibility of identified oligomannose structures for interaction with mannan-binding lectin. *J Immunol* (2004) **173**:6831–40. doi:10.4049/jimmunol.173.11.6831
50. Zheng K, Bantog C, Bayer R. The impact of glycosylation on monoclonal antibody conformation and stability. *mAbs* (2011) **3**:568–76. doi:10.4161/mabs.3.6.17922
51. Weitzner BD, Dunbrack RL, Gray JJ. The origin of CDR H3 structural diversity. *Structure* (2015) **23**:302–11. doi:10.1016/j.str.2014.11.010
52. Hughes-Jones NC, Gardner B. The reaction between the complement subcomponent C1q, IgG complexes and polyionic molecules. *Immunology* (1978) **34**:459–63.
53. Cooper NR. The classical complement pathway: activation and regulation of the first complement component. *Adv Immunol* (1985) **37**:151–216. doi:10.1016/S0065-2776(08)60340-5
54. Raghavan M, Bjorkman PJ. Fc receptors and their interactions with immunoglobulins. *Annu Rev Cell Dev Biol* (1996) **12**:181–220. doi:10.1146/annurev.cellbio.12.1.181
55. Gómez Román VR, Murray JC, Weiner LM. "Antibody-Dependent Cellular Cytotoxicity (ADCC),". In: *Antibody Fc*. Elsevier (2014). p. 1–27.
56. Tay MZ, Wiehe K, Pollara J. Antibody-Dependent Cellular Phagocytosis in Antiviral Immune Responses. *Front Immunol* (2019) **10**:332. doi:10.3389/fimmu.2019.00332
57. Lencer WI, Blumberg RS. A passionate kiss, then run: exocytosis and recycling of IgG by FcRn. *Trends Cell Biol* (2005) **15**:5–9. doi:10.1016/j.tcb.2004.11.004
58. Roopenian DC, Akilesh S. FcRn: the neonatal Fc receptor comes of age. *Nat Rev Immunol* (2007) **7**:715–25. doi:10.1038/nri2155
59. Kacskovics I, Cervenak J, Erdei A, Goldsby RA, Butler JE. Recent advances using FcRn overexpression in transgenic animals to overcome impediments of standard antibody technologies to improve the generation of specific antibodies. *mAbs* (2011) **3**:431–9. doi:10.4161/mabs.3.5.17023
60. Rodewald R. pH-dependent binding of immunoglobulins to intestinal cells of the neonatal rat. *J Cell Biol* (1976) **71**:666–9. doi:10.1083/jcb.71.2.666
61. Winau F, Winau R. Emil von Behring and serum therapy. *Microbes Infect* (2002) **4**:185–8. doi:10.1016/S1286-4579(01)01526-X
62. Kaufmann SH. Immunology's Coming of Age. *Front Immunol* (2019) **10**:684. doi:10.3389/fimmu.2019.00684

63. Stockwin LH, Holmes S. Antibodies as therapeutic agents: vive la renaissance! *Expert Opin Biol Ther* (2003) **3**:1133–52. doi:10.1517/14712598.3.7.1133

64. Leavy O. The birth of monoclonal antibodies. *Nat Immunol* (2016) **17**:S13-S13. doi:10.1038/ni.3608

65. Hooks MA, Wade CS, Millikan WJ. Muromonab CD-3: a review of its pharmacology, pharmacokinetics, and clinical use in transplantation. *Pharmacotherapy* (1991) **11**:26–37.

66. Vaisman-Mentesh A, Gutierrez-Gonzalez M, DeKosky BJ, Wine Y. The Molecular Mechanisms That Underlie the Immune Biology of Anti-drug Antibody Formation Following Treatment With Monoclonal Antibodies. *Front Immunol* (2020) **11**:1951. doi:10.3389/fimmu.2020.01951

67. Ober RJ, Radu CG, Ghetie V, Ward ES. Differences in promiscuity for antibody-FcRn interactions across species: implications for therapeutic antibodies. *Int Immunol* (2001) **13**:1551–9. doi:10.1093/intimm/13.12.1551

68. Stern M, Herrmann R. Overview of monoclonal antibodies in cancer therapy: present and promise. *Crit Rev Oncol Hematol* (2005) **54**:11–29. doi:10.1016/j.critrevonc.2004.10.011

69. Morrison SL, Johnson MJ, Herzenberg LA, Oi VT. Chimeric human antibody molecules: mouse antigen-binding domains with human constant region domains. *Proc Natl Acad Sci U S A* (1984) **81**:6851–5. doi:10.1073/pnas.81.21.6851

70. Grillo-López AJ, White CA, Dallaire BK, Varns CL, Shen CD, Wei A, et al. Rituximab: the first monoclonal antibody approved for the treatment of lymphoma. *Curr Pharm Biotechnol* (2000) **1**:1–9. doi:10.2174/1389201003379059

71. Jones PT, Dear PH, Foote J, Neuberger MS, Winter G. Replacing the complementarity-determining regions in a human antibody with those from a mouse. *Nature* (1986) **321**:522–5. doi:10.1038/321522a0

72. Riechmann L, Clark M, Waldmann H, Winter G. Reshaping human antibodies for therapy. *Nature* (1988) **332**:323–7. doi:10.1038/332323a0

73. Safdari Y, Farajnia S, Asgharzadeh M, Khalili M. Antibody humanization methods - a review and update. *Biotechnology and Genetic Engineering Reviews* (2013) **29**:175–86. doi:10.1080/02648725.2013.801235

74. Winter G, Griffiths AD, Hawkins RE, Hoogenboom HR. Making antibodies by phage display technology. *Annu Rev Immunol* (1994) **12**:433–55. doi:10.1146/annurev.iy.12.040194.002245

75. Green LL, Hardy MC, Maynard-Currie CE, Tsuda H, Louie DM, Mendez MJ, et al. Antigen-specific human monoclonal antibodies from mice engineered with human Ig heavy and light chain YACs. *Nat Genet* (1994) **7**:13–21. doi:10.1038/ng0594-13

76. Rau R. Adalimumab (a fully human anti-tumour necrosis factor alpha monoclonal antibody) in the treatment of active rheumatoid arthritis: the initial results of five trials. *Ann Rheum Dis* (2002) **61 Suppl 2**:ii70-3. doi:10.1136/ard.61.suppl_2.ii70

77. Coghlan J, He H, Schwendeman AS. Overview of Humira® Biosimilars: Current European Landscape and Future Implications. *J Pharm Sci* (2021) **110**:1572–82. doi:10.1016/j.xphs.2021.02.003

78. Buss NA, Henderson SJ, McFarlane M, Shenton JM, Haan L de. Monoclonal antibody therapeutics: history and future. *Curr Opin Pharmacol* (2012) **12**:615–22. doi:10.1016/j.coph.2012.08.001

79. Wang X, Mathieu M, Brezski RJ. IgG Fc engineering to modulate antibody effector functions. *Protein Cell* (2018) **9**:63–73. doi:10.1007/s13238-017-0473-8

80. Strohl WR. Optimization of Fc-mediated effector functions of monoclonal antibodies. *Curr Opin Biotechnol* (2009) **20**:685–91. doi:10.1016/j.copbio.2009.10.011

81. Lazar GA, Dang W, Karki S, Vafa O, Peng JS, Hyun L, et al. Engineered antibody Fc variants with enhanced effector function. *Proc Natl Acad Sci U S A* (2006) **103**:4005–10. doi:10.1073/pnas.0508123103

82. Niwa R, Hatanaka S, Shoji-Hosaka E, Sakurada M, Kobayashi Y, Uehara A, et al. Enhancement of the antibody-dependent cellular cytotoxicity of low-fucose IgG1 Is independent of FcgammaRIIIa functional polymorphism. *Clin Cancer Res* (2004) **10**:6248–55. doi:10.1158/1078-0432.CCR-04-0850

83. Bolt S, Routledge E, Lloyd I, Chatenoud L, Pope H, Gorman SD, et al. The generation of a humanized, non-mitogenic CD3 monoclonal antibody which retains in vitro immunosuppressive properties. *Eur J Immunol* (1993) **23**:403–11. doi:10.1002/eji.1830230216

84. Schlothauer T, Herter S, Koller CF, Grau-Richards S, Steinhart V, Spick C, et al. Novel human IgG1 and IgG4 Fc-engineered antibodies with completely abolished immune effector functions. *Protein Eng Des Sel* (2016) **29**:457–66. doi:10.1093/protein/gzw040

85. Tao MH, Morrison SL. Studies of aglycosylated chimeric mouse-human IgG. Role of carbohydrate in the structure and effector functions mediated by the human IgG constant region. *J Immunol* (1989) **143**:2595–601. doi:10.4049/jimmunol.143.8.2595

86. Xu D, Alegre ML, Varga SS, Rothermel AL, Collins AM, Pulito VL, et al. In vitro characterization of five humanized OKT3 effector function variant antibodies. *Cell Immunol* (2000) **200**:16–26. doi:10.1006/cimm.2000.1617

87. Lyu X, Zhao Q, Hui J, Wang T, Lin M, Wang K, et al. The global landscape of approved antibody therapies. *Antib Ther* (2022) **5**:233–57. doi:10.1093/abt/tbac021

88. Pirkalkhoran S, Grabowska WR, Kashkoli HH, Mirhassani R, Guiliano D, Dolphin C, et al. Bioengineering of Antibody Fragments: Challenges and Opportunities. *Bioengineering (Basel)* (2023) **10**. doi:10.3390/bioengineering10020122

89. Cheong WS, Leow CY, Abdul Majeed AB, Leow CH. Diagnostic and therapeutic potential of shark variable new antigen receptor (VNAR) single domain antibody. *Int J Biol Macromol* (2020) **147**:369–75. doi:10.1016/j.ijbiomac.2020.01.039

90. Mullard A. FDA approves 100th monoclonal antibody product. *Nat Rev Drug Discov* (2021) **20**:491–5. doi:10.1038/d41573-021-00079-7

91. Crescioli S, Kaplon H, Chenoweth A, Wang L, Visweswaraiah J, Reichert JM. Antibodies to watch in 2024. *mAbs* (2024) **16**:2297450. doi:10.1080/19420862.2023.2297450

92. Mitra S, Tomar PC. Hybridoma technology; advancements, clinical significance, and future aspects. *J Genet Eng Biotechnol* (2021) **19**:159. doi:10.1186/s43141-021-00264-6

93. Ponsel D, Neugebauer J, Ladetzki-Baehs K, Tissot K. High affinity, developability and functional size: the holy grail of combinatorial antibody library generation. *Molecules* (2011) **16**:3675–700. doi:10.3390/molecules16053675

94. Valldorf B, Hinz SC, Russo G, Pekar L, Mohr L, Klemm J, et al. Antibody display technologies: selecting the cream of the crop. *Biol Chem* (2022) **403**:455–77. doi:10.1515/hsz-2020-0377

95. Zielonka S, Krah S, editors. *Genotype Phenotype Coupling: Methods and Protocols*. New York, NY: Springer New York (2020). Online-Ressource.

96. Lim BN, Chin CF, Choong YS, Ismail A, Lim TS. Generation of a naïve human single chain variable fragment (scFv) library for the identification of monoclonal scFv against Salmonella Typhi Hemolysin E antigen. *Toxicon* (2016) **117**:94–101. doi:10.1016/j.toxicon.2016.04.032

97. Moon SA, Ki MK, Lee S, Hong M-L, Kim M, Kim S, et al. Antibodies against non-immunizing antigens derived from a large immune scFv library. *Mol Cells* (2011) **31**:509–13. doi:10.1007/s10059-011-2268-8

98. Zhou H, Zhang Y-L, Lu G, Ji H, Rodi CP. Recombinant antibody libraries and selection technologies. *N Biotechnol* (2011) **28**:448–52. doi:10.1016/j.nbt.2011.03.013

99. Huse WD, Sastry L, Iverson SA, Kang AS, Alting-Mees M, Burton DR, et al. Generation of a large combinatorial library of the immunoglobulin repertoire in phage lambda. *Science* (1989) **246**:1275–81. doi:10.1126/science.2531466

100. Rader C, Ritter G, Nathan S, Elia M, Gout I, Jungbluth AA, et al. The rabbit antibody repertoire as a novel source for the generation of therapeutic human antibodies. *J Biol Chem* (2000) **275**:13668–76. doi:10.1074/jbc.275.18.13668

101. Tsai K-C, Chang C-D, Cheng M-H, Lin T-Y, Lo Y-N, Yang T-W, et al. Chicken-Derived Humanized Antibody Targeting a Novel Epitope F2pep of Fibroblast Growth Factor Receptor 2: Potential Cancer Therapeutic Agent. *ACS Omega* (2019) **4**:2387–97. doi:10.1021/acsomega.8b03072

102. Lonberg N. Human antibodies from transgenic animals. *Nat Biotechnol* (2005) **23**:1117–25. doi:10.1038/nbt1135

103. Brüggemann M, Osborn MJ, Ma B, Hayre J, Avis S, Lundstrom B, et al. Human antibody production in transgenic animals. *Arch Immunol Ther Exp (Warsz)* (2015) **63**:101–8. doi:10.1007/s00005-014-0322-x

104. Kramer RA, Marissen WE, Goudsmit J, Visser TJ, Clijsters-Van der Horst M, Bakker AQ, et al. The human antibody repertoire specific for rabies virus glycoprotein as selected from immune libraries. *Eur J Immunol* (2005) **35**:2131–45. doi:10.1002/eji.200526134

105. Carvalho Nicacio C de, Williamson RA, Parren PW, Lundkvist A, Burton DR, Björling E. Neutralizing human Fab fragments against measles virus recovered by phage display. *J Virol* (2002) **76**:251–8. doi:10.1128/jvi.76.1.251-258.2002

106. Cai X, Garen A. Anti-melanoma antibodies from melanoma patients immunized with genetically modified autologous tumor cells: selection of specific antibodies from single-chain Fv fusion phage libraries. *Proc Natl Acad Sci U S A* (1995) **92**:6537–41. doi:10.1073/pnas.92.14.6537

107. Barbas CF, Bain JD, Hoekstra DM, Lerner RA. Semisynthetic combinatorial antibody libraries: a chemical solution to the diversity problem. *Proc Natl Acad Sci U S A* (1992) **89**:4457–61. doi:10.1073/pnas.89.10.4457

108. Knappik A, Ge L, Honegger A, Pack P, Fischer M, Wellnhofer G, et al. Fully synthetic human combinatorial antibody libraries (HuCAL) based on modular consensus frameworks and CDRs randomized with trinucleotides. *J Mol Biol* (2000) **296**:57–86. doi:10.1006/jmbi.1999.3444

109. Smith GP. Filamentous fusion phage: novel expression vectors that display cloned antigens on the virion surface. *Science* (1985) **228**:1315–7. doi:10.1126/science.4001944

110. McCafferty J, Griffiths AD, Winter G, Chiswell DJ. Phage antibodies: filamentous phage displaying antibody variable domains. *Nature* (1990) **348**:552–4. doi:10.1038/348552a0

111. Francisco JA, Campbell R, Iverson BL, Georgiou G. Production and fluorescence-activated cell sorting of Escherichia coli expressing a functional antibody fragment on the external surface. *Proc Natl Acad Sci U S A* (1993) **90**:10444–8. doi:10.1073/pnas.90.22.10444

112. Boder ET, Wittrup KD. Yeast surface display for screening combinatorial polypeptide libraries. *Nat Biotechnol* (1997) **15**:553–7. doi:10.1038/nbt0697-553

113. Feldhaus MJ, Siegel RW, Opresko LK, Coleman JR, Feldhaus JM, Yeung YA, et al. Flow-cytometric isolation of human antibodies from a nonimmune Saccharomyces cerevisiae surface display library. *Nat Biotechnol* (2003) **21**:163–70. doi:10.1038/nbt785

114. Beerli RR, Bauer M, Buser RB, Gwerder M, Muntwiler S, Maurer P, et al. Isolation of human monoclonal antibodies by mammalian cell display. *Proc Natl Acad Sci U S A* (2008) **105**:14336–41. doi:10.1073/pnas.0805942105

115. Mattheakis LC, Bhatt RR, Dower WJ. An in vitro polysome display system for identifying ligands from very large peptide libraries. *Proc Natl Acad Sci U S A* (1994) **91**:9022–6. doi:10.1073/pnas.91.19.9022

116. Lipovsek D, Plückthun A. In-vitro protein evolution by ribosome display and mRNA display. *J Immunol Methods* (2004) **290**:51–67. doi:10.1016/j.jim.2004.04.008

117. Wilson DS, Keefe AD, Szostak JW. The use of mRNA display to select high-affinity protein-binding peptides. *Proc Natl Acad Sci U S A* (2001) **98**:3750–5. doi:10.1073/pnas.061028198

118. Gram H, Marconi LA, Barbas CF, Collet TA, Lerner RA, Kang AS. In vitro selection and affinity maturation of antibodies from a naive combinatorial immunoglobulin library. *Proc Natl Acad Sci U S A* (1992) **89**:3576–80. doi:10.1073/pnas.89.8.3576

119. Tharakaraman K, Watanabe S, Chan KR, Huan J, Subramanian V, Chionh YH, et al. Rational Engineering and Characterization of an mAb that Neutralizes Zika Virus by Targeting a Mutationally Constrained Quaternary Epitope. *Cell Host Microbe* (2018) **23**:618-627.e6. doi:10.1016/j.chom.2018.04.004

120. Bauer J, Rajagopal N, Gupta P, Gupta P, Nixon AE, Kumar S. How can we discover developable antibody-based biotherapeutics? *Front Mol Biosci* (2023) **10**:1221626. doi:10.3389/fmolb.2023.1221626

121. Zhang X, Calvert RA, Sutton BJ, Doré KA. IgY: a key isotype in antibody evolution. *Biol Rev Camb Philos Soc* (2017) **92**:2144–56. doi:10.1111/brv.12325

122. Taylor AI, Fabiane SM, Sutton BJ, Calvert RA. The crystal structure of an avian IgY-Fc fragment reveals conservation with both mammalian IgG and IgE. *Biochemistry* (2009) **48**:558–62. doi:10.1021/bi8019993

123. Müller S, Schubert A, Zajac J, Dyck T, Oelkrug C. IgY antibodies in human nutrition for disease prevention. *Nutr J* (2015) **14**:109. doi:10.1186/s12937-015-0067-3

124. Parvari R, Avivi A, Lentner F, Ziv E, Tel-Or S, Burstein Y, et al. Chicken immunoglobulin gamma-heavy chains: limited VH gene repertoire, combinatorial diversification by D gene segments and evolution of the heavy chain locus. *EMBO J* (1988) **7**:739–44. doi:10.1002/j.1460-2075.1988.tb02870.x

125. Wu L, Oficjalska K, Lambert M, Fennell BJ, Darmanin-Sheehan A, Ní Shúilleabháin D, et al. Fundamental characteristics of the immunoglobulin VH repertoire of chickens in comparison with those of humans, mice, and camelids. *J Immunol* (2012) **188**:322–33. doi:10.4049/jimmunol.1102466

126. McCormack WT, Tjoelker LW, Thompson CB. Avian B-cell development: generation of an immunoglobulin repertoire by gene conversion. *Annu Rev Immunol* (1991) **9**:219–41. doi:10.1146/annurev.iy.09.040191.001251

127. Reynaud CA, Dahan A, Anquez V, Weill JC. Somatic hyperconversion diversifies the single Vh gene of the chicken with a high incidence in the D region. *Cell* (1989) **59**:171–83. doi:10.1016/0092-8674(89)90879-9

128. Ratcliffe MJ, Härtle S. “B cells, the bursa of Fabricius, and the generation of antibody repertoires,”. In: *Avian Immunology*. Elsevier (2022). p. 71–99.

129. Reynaud CA, Anquez V, Grimal H, Weill JC. A hyperconversion mechanism generates the chicken light chain preimmune repertoire. *Cell* (1987) **48**:379–88. doi:10.1016/0092-8674(87)90189-9

130. Dodgson JB, Delany ME, Cheng HH. Poultry genome sequences: progress and outstanding challenges. *Cytogenet Genome Res* (2011) **134**:19–26. doi:10.1159/000324413

131. Abdiche YN, Harriman R, Deng X, Yeung YA, Miles A, Morishige W, et al. Assessing kinetic and epitopic diversity across orthogonal monoclonal antibody generation platforms. *mAbs* (2016) **8**:264–77. doi:10.1080/19420862.2015.1118596

132. Hinz SC, Elter A, Rammo O, Schwämmle A, Ali A, Zielonka S, et al. A Generic Procedure for the Isolation of pH- and Magnesium-Responsive Chicken scFvs for Downstream Purification of Human Antibodies. *Front Bioeng Biotechnol* (2020) **8**:688. doi:10.3389/fbioe.2020.00688

133. Elter A, Bock T, Spiehl D, Russo G, Hinz SC, Bitsch S, et al. Carbohydrate binding module-fused antibodies improve the performance of cellulose-based lateral flow immunoassays. *Sci Rep* (2021) **11**:7880. doi:10.1038/s41598-021-87072-7

134. Davies EL, Smith JS, Birkett CR, Manser JM, Anderson-Dear DV, Young JR. Selection of specific phage-display antibodies using libraries derived from chicken immunoglobulin genes. *J Immunol Methods* (1995) **186**:125–35. doi:10.1016/0022-1759(95)00143-X

135. Li J, Xu Y, Wang X, Li Y, Wang L, Li X. Construction and characterization of a highly reactive chicken-derived single-chain variable fragment (scFv) antibody against Staphylococcus aureus developed with the T7 phage display system. *Int Immunopharmacol* (2016) **35**:149–54. doi:10.1016/j.intimp.2016.02.024

136. Grzeschik J, Yanakieva D, Roth L, Krah S, Hinz SC, Elter A, et al. Yeast Surface Display in Combination with Fluorescence-activated Cell Sorting Enables the Rapid Isolation of Antibody Fragments Derived from Immunized Chickens. *Biotechnol J* (2019) **14**:e1800466. doi:10.1002/biot.201800466

137. Andris-Widhopf J, Rader C, Steinberger P, Fuller R, Barbas CF. Methods for the generation of chicken monoclonal antibody fragments by phage display. *J Immunol Methods* (2000) **242**:159–81. doi:10.1016/s0022-1759(00)00221-0

138. Hof D, Hoeke MO, Raats JM. Multiple-antigen immunization of chickens facilitates the generation of recombinant antibodies to autoantigens. *Clin Exp Immunol* (2008) **151**:367–77. doi:10.1111/j.1365-2249.2007.03569.x

139. Nishibori N, Horiuchi H, Furusawa S, Matsuda H. Humanization of chicken monoclonal antibody using phage-display system. *Mol Immunol* (2006) **43**:634–42. doi:10.1016/j.molimm.2005.04.002

140. Elter A, Bogen JP, Hinz SC, Fiebig D, Macarrón Palacios A, Grzeschik J, et al. Humanization of Chicken-Derived scFv Using Yeast Surface Display and NGS Data Mining. *Biotechnol J* (2021) **16**:e2000231. doi:10.1002/biot.202000231

141. Schusser B, Yi H, Collarini EJ, Izquierdo SM, Harriman WD, Etches RJ, et al. Harnessing gene conversion in chicken B cells to create a human antibody sequence repertoire. *PLoS One* (2013) **8**:e80108. doi:10.1371/journal.pone.0080108

142. Ching KH, Collarini EJ, Abdiche YN, Bedinger D, Pedersen D, Izquierdo S, et al. Chickens with humanized immunoglobulin genes generate antibodies with high affinity and broad epitope coverage to conserved targets. *mAbs* (2018) **10**:71–80. doi:10.1080/19420862.2017.1386825

143. Gjetting T, Gad M, Fröhlich C, Lindsted T, Melander MC, Bhatia VK, et al. Sym021, a promising anti-PD1 clinical candidate antibody derived from a new chicken antibody discovery platform. *mAbs* (2019) **11**:666–80. doi:10.1080/19420862.2019.1596514

144. Boder ET, Wittrup KD. Yeast surface display for directed evolution of protein expression, affinity, and stability. *Methods Enzymol* (2000) **328**:430–44. doi:10.1016/s0076-6879(00)28410-3

145. Lipke PN, Kurjan J. Sexual agglutination in budding yeasts: structure, function, and regulation of adhesion glycoproteins. *Microbiol Rev* (1992) **56**:180–94. doi:10.1128/mr.56.1.180-194.1992

146. Teymennet-Ramírez KV, Martínez-Morales F, Trejo-Hernández MR. Yeast Surface Display System: Strategies for Improvement and Biotechnological Applications. *Front Bioeng Biotechnol* (2021) **9**:794742. doi:10.3389/fbioe.2021.794742

147. Könning D, Kolmar H. Beyond antibody engineering: directed evolution of alternative binding scaffolds and enzymes using yeast surface display. *Microb Cell Fact* (2018) **17**:32. doi:10.1186/s12934-018-0881-3

148. Schröter C, Krah S, Beck J, Könning D, Grzeschik J, Valldorf B, et al. Isolation of pH-Sensitive Antibody Fragments by Fluorescence-Activated Cell Sorting and Yeast Surface Display. *Methods Mol Biol* (2018) **1685**:311–31. doi:10.1007/978-1-4939-7366-8_19

149. Zhao S, Guo D, Zhu Q, Dou W, Guan W. Display of Microbial Glucose Dehydrogenase and Cholesterol Oxidase on the Yeast Cell Surface for the Detection of Blood Biochemical Parameters. *Biosensors (Basel)* (2020) **11**. doi:10.3390/bios11010013

150. Pepper LR, Cho YK, Boder ET, Shusta EV. A decade of yeast surface display technology: where are we now? *Comb Chem High Throughput Screen* (2008) **11**:127–34. doi:10.2174/138620708783744516

151. Boder ET, Raeeszadeh-Sarmazdeh M, Price JV. Engineering antibodies by yeast display. *Arch Biochem Biophys* (2012) **526**:99–106. doi:10.1016/j.abb.2012.03.009

152. Kolmar H, Grzeschik J, Könning D, Krah S, Zielonka S. Construction of Semisynthetic Shark vNAR Yeast Surface Display Antibody Libraries. *Methods Mol Biol* (2023) **2702**:227–43. doi:10.1007/978-1-0716-3381-6_11
153. Rosowski S, Becker S, Toleikis L, Valldorf B, Grzeschik J, Demir D, et al. A novel one-step approach for the construction of yeast surface display Fab antibody libraries. *Microb Cell Fact* (2018) **17**:3. doi:10.1186/s12934-017-0853-z
154. Benatuil L, Perez JM, Belk J, Hsieh C-M. An improved yeast transformation method for the generation of very large human antibody libraries. *Protein Eng Des Sel* (2010) **23**:155–9. doi:10.1093/protein/gzq002
155. Doerner A, Rhiel L, Zielonka S, Kolmar H. Therapeutic antibody engineering by high efficiency cell screening. *FEBS Lett* (2014) **588**:278–87. doi:10.1016/j.febslet.2013.11.025
156. Schröter C, Beck J, Krah S, Zielonka S, Doerner A, Rhiel L, et al. Selection of Antibodies with Tailored Properties by Application of High-Throughput Multiparameter Fluorescence-Activated Cell Sorting of Yeast-Displayed Immune Libraries. *Mol Biotechnol* (2018) **60**:727–35. doi:10.1007/s12033-018-0109-0
157. Kaempffe A, Jäger S, Könning D, Kolmar H, Schröter C. Isolation of Tailor-Made Antibody Fragments from Yeast-Displayed B-Cell Receptor Repertoires by Multiparameter Fluorescence-Activated Cell Sorting. *Methods Mol Biol* (2020) **2070**:249–66. doi:10.1007/978-1-4939-9853-1_14
158. Strebhardt K, Ullrich A. Paul Ehrlich's magic bullet concept: 100 years of progress. *Nat Rev Cancer* (2008) **8**:473–80. doi:10.1038/nrc2394
159. Alley SC, Okeley NM, Senter PD. Antibody-drug conjugates: targeted drug delivery for cancer. *Curr Opin Chem Biol* (2010) **14**:529–37. doi:10.1016/j.cbpa.2010.06.170
160. Fu Z, Li S, Han S, Shi C, Zhang Y. Antibody drug conjugate: the "biological missile" for targeted cancer therapy. *Signal Transduct Target Ther* (2022) **7**:93. doi:10.1038/s41392-022-00947-7
161. Zhao P, Zhang Y, Li W, Jeanty C, Xiang G, Dong Y. Recent advances of antibody drug conjugates for clinical applications. *Acta Pharm Sin B* (2020) **10**:1589–600. doi:10.1016/j.apsb.2020.04.012
162. Giugliano F, Corti C, Tarantino P, Michelini F, Curigliano G. Bystander effect of antibody-drug conjugates: fact or fiction? *Curr Oncol Rep* (2022) **24**:809–17. doi:10.1007/s11912-022-01266-4
163. Ritchie M, Bloom L, Carven G, Sapra P. “Selecting an Optimal Antibody for Antibody- Drug Conjugate Therapy,”. In: Wang J, Shen W-C, Zaro JL, editors. *Antibody-Drug Conjugates*. Cham: Springer International Publishing (2015). p. 23–48.
164. Xu S. Internalization, Trafficking, Intracellular Processing and Actions of Antibody-Drug Conjugates. *Pharm Res* (2015) **32**:3577–83. doi:10.1007/s11095-015-1729-8
165. Sheyi R, La Torre BG de, Albericio F. Linkers: An Assurance for Controlled Delivery of Antibody-Drug Conjugate. *Pharmaceutics* (2022) **14**. doi:10.3390/pharmaceutics14020396
166. Senter PD. Potent antibody drug conjugates for cancer therapy. *Curr Opin Chem Biol* (2009) **13**:235–44. doi:10.1016/j.cbpa.2009.03.023
167. Firestone RA, Willner D, Hofstead SJ, King HD, Kaneko T, Braslawsky GR, et al. Synthesis and antitumor activity of the immunoconjugate BR96-Dox. *Journal of Controlled Release* (1996) **39**:251–9. doi:10.1016/0168-3659(95)00160-3
168. Hamann PR, Hinman LM, Hollander I, Beyer CF, Lindh D, Holcomb R, et al. Gemtuzumab ozogamicin, a potent and selective anti-CD33 antibody-calicheamicin conjugate for treatment of acute myeloid leukemia. *Bioconjug Chem* (2002) **13**:47–58. doi:10.1021/bc010021y
169. Jeffrey SC, Andreyka JB, Bernhardt SX, Kissler KM, Kline T, Lenox JS, et al. Development and properties of beta-glucuronide linkers for monoclonal antibody-drug conjugates. *Bioconjug Chem* (2006) **17**:831–40. doi:10.1021/bc0600214

170. Dubowchik GM, Firestone RA, Padilla L, Willner D, Hofstead SJ, Mosure K, et al. Cathepsin B-labile dipeptide linkers for lysosomal release of doxorubicin from internalizing immunoconjugates: model studies of enzymatic drug release and antigen-specific in vitro anticancer activity. *Bioconjug Chem* (2002) **13**:855–69. doi:10.1021/bc025536j

171. Katz J, Janik JE, Younes A. Brentuximab Vedotin (SGN-35). *Clin Cancer Res* (2011) **17**:6428–36. doi:10.1158/1078-0432.CCR-11-0488

172. Schneider H, Deweid L, Avrutina O, Kolmar H. Recent progress in transglutaminase-mediated assembly of antibody-drug conjugates. *Anal Biochem* (2020) **595**:113615. doi:10.1016/j.ab.2020.113615

173. Teicher BA, Chari RV. Antibody conjugate therapeutics: challenges and potential. *Clin Cancer Res* (2011) **17**:6389–97. doi:10.1158/1078-0432.CCR-11-1417

174. Ruan D-Y, Wu H-X, Meng Q, Xu R-H. Development of antibody-drug conjugates in cancer: Overview and prospects. *Cancer Commun (Lond)* (2024) **44**:3–22. doi:10.1002/cac2.12517

175. Dumontet C, Reichert JM, Senter PD, Lambert JM, Beck A. Antibody-drug conjugates come of age in oncology. *Nat Rev Drug Discov* (2023) **22**:641–61. doi:10.1038/s41573-023-00709-2

176. Cheung-Ong K, Giaever G, Nislow C. DNA-damaging agents in cancer chemotherapy: serendipity and chemical biology. *Chem Biol* (2013) **20**:648–59. doi:10.1016/j.chembiol.2013.04.007

177. Fu Y, Ho M. DNA damaging agent-based antibody-drug conjugates for cancer therapy. *Antib Ther* (2018) **1**:33–43. doi:10.1093/abt/tby007

178. Wang L, Amphlett G, Blättler WA, Lambert JM, Zhang W. Structural characterization of the maytansinoid-monoclonal antibody immunoconjugate, huN901-DM1, by mass spectrometry. *Protein Sci* (2005) **14**:2436–46. doi:10.1110/ps.051478705

179. Sun MM, Beam KS, Cerveny CG, Hamblett KJ, Blackmore RS, Torgov MY, et al. Reduction-alkylation strategies for the modification of specific monoclonal antibody disulfides. *Bioconjug Chem* (2005) **16**:1282–90. doi:10.1021/bc050201y

180. Nadkarni DV. Conjugations to Endogenous Cysteine Residues. *Methods Mol Biol* (2020) **2078**:37–49. doi:10.1007/978-1-4939-9929-3_3

181. Lyon RP, Meyer DL, Setter JR, Senter PD. Conjugation of anticancer drugs through endogenous monoclonal antibody cysteine residues. *Methods Enzymol* (2012) **502**:123–38. doi:10.1016/B978-0-12-416039-2.00006-9

182. Jain N, Smith SW, Ghone S, Tomczuk B. Current ADC Linker Chemistry. *Pharm Res* (2015) **32**:3526–40. doi:10.1007/s11095-015-1657-7

183. Kim MT, Chen Y, Marhoul J, Jacobson F. Statistical modeling of the drug load distribution on trastuzumab emtansine (Kadcyla), a lysine-linked antibody drug conjugate. *Bioconjug Chem* (2014) **25**:1223–32. doi:10.1021/bc5000109

184. Zhou Q. Site-Specific Antibody Conjugation for ADC and Beyond. *Biomedicines* (2017) **5**. doi:10.3390/biomedicines5040064

185. Junutula JR, Raab H, Clark S, Bhakta S, Leipold DD, Weir S, et al. Site-specific conjugation of a cytotoxic drug to an antibody improves the therapeutic index. *Nat Biotechnol* (2008) **26**:925–32. doi:10.1038/nbt.1480

186. Junutula JR, Flagella KM, Graham RA, Parsons KL, Ha E, Raab H, et al. Engineered thio-trastuzumab-DM1 conjugate with an improved therapeutic index to target human epidermal growth factor receptor 2-positive breast cancer. *Clin Cancer Res* (2010) **16**:4769–78. doi:10.1158/1078-0432.CCR-10-0987

187. Shen B-Q, Xu K, Liu L, Raab H, Bhakta S, Kenrick M, et al. Conjugation site modulates the in vivo stability and therapeutic activity of antibody-drug conjugates. *Nat Biotechnol* (2012) **30**:184–9. doi:10.1038/nbt.2108

188. Tian F, Lu Y, Manibusan A, Sellers A, Tran H, Sun Y, et al. A general approach to site-specific antibody drug conjugates. *Proc Natl Acad Sci U S A* (2014) **111**:1766–71. doi:10.1073/pnas.1321237111
189. Zimmerman ES, Heibeck TH, Gill A, Li X, Murray CJ, Madlansacay MR, et al. Production of site-specific antibody-drug conjugates using optimized non-natural amino acids in a cell-free expression system. *Bioconjug Chem* (2014) **25**:351–61. doi:10.1021/bc400490z
190. VanBrunt MP, Shanebeck K, Caldwell Z, Johnson J, Thompson P, Martin T, et al. Genetically Encoded Azide Containing Amino Acid in Mammalian Cells Enables Site-Specific Antibody-Drug Conjugates Using Click Cycloaddition Chemistry. *Bioconjug Chem* (2015) **26**:2249–60. doi:10.1021/acs.bioconjchem.5b00359
191. Li X, Nelson CG, Nair RR, Hazlehurst L, Moroni T, Martinez-Acedo P, et al. Stable and Potent Selenomab-Drug Conjugates. *Cell Chem Biol* (2017) **24**:433-442.e6. doi:10.1016/j.chembiol.2017.02.012
192. Jaramillo ML, Sulea T, Durocher Y, Acchione M, Schur MJ, Robotham A, et al. A glyco-engineering approach for site-specific conjugation to Fab glycans. *mAbs* (2023) **15**:2149057. doi:10.1080/19420862.2022.2149057
193. Wu K-L, Yu C, Lee C, Zuo C, Ball ZT, Xiao H. Precision Modification of Native Antibodies. *Bioconjug Chem* (2021) **32**:1947–59. doi:10.1021/acs.bioconjchem.1c00342
194. Okeley NM, Toki BE, Zhang X, Jeffrey SC, Burke PJ, Alley SC, et al. Metabolic engineering of monoclonal antibody carbohydrates for antibody-drug conjugation. *Bioconjug Chem* (2013) **24**:1650–5. doi:10.1021/bc4002695
195. Ramakrishnan B, Qasba PK. Structure-based design of beta 1,4-galactosyltransferase I (beta 4Gal-T1) with equally efficient N-acetylgalactosaminyltransferase activity: point mutation broadens beta 4Gal-T1 donor specificity. *J Biol Chem* (2002) **277**:20833–9. doi:10.1074/jbc.M111183200
196. Boeggeman E, Ramakrishnan B, Kilgore C, Khidekel N, Hsieh-Wilson LC, Simpson JT, et al. Direct identification of nonreducing GlcNAc residues on N-glycans of glycoproteins using a novel chemoenzymatic method. *Bioconjug Chem* (2007) **18**:806–14. doi:10.1021/bc060341n
197. Rabuka D, Rush JS, deHart GW, Wu P, Bertozzi CR. Site-specific chemical protein conjugation using genetically encoded aldehyde tags. *Nat Protoc* (2012) **7**:1052–67. doi:10.1038/nprot.2012.045
198. Jeger S, Zimmermann K, Blanc A, Grünberg J, Honer M, Hunziker P, et al. Site-specific and stoichiometric modification of antibodies by bacterial transglutaminase. *Angew Chem Int Ed Engl* (2010) **49**:9995–7. doi:10.1002/anie.201004243
199. Strop P, Liu S-H, Dorywalska M, Delaria K, Dushin RG, Tran T-T, et al. Location matters: site of conjugation modulates stability and pharmacokinetics of antibody drug conjugates. *Chem Biol* (2013) **20**:161–7. doi:10.1016/j.chembiol.2013.01.010
200. Chen I, Dorr BM, Liu DR. A general strategy for the evolution of bond-forming enzymes using yeast display. *Proc Natl Acad Sci U S A* (2011) **108**:11399–404. doi:10.1073/pnas.1101046108
201. Beerli RR, Hell T, Merkel AS, Grawunder U. Sortase Enzyme-Mediated Generation of Site-Specifically Conjugated Antibody Drug Conjugates with High In Vitro and In Vivo Potency. *PLoS One* (2015) **10**:e0131177. doi:10.1371/journal.pone.0131177
202. Baruah H, Puthenveetil S, Choi Y-A, Shah S, Ting AY. An engineered aryl azide ligase for site-specific mapping of protein-protein interactions through photo-cross-linking. *Angew Chem Int Ed Engl* (2008) **47**:7018–21. doi:10.1002/anie.200802088
203. Puthenveetil S, Liu DS, White KA, Thompson S, Ting AY. Yeast display evolution of a kinetically efficient 13-amino acid substrate for lipoic acid ligase. *J Am Chem Soc* (2009) **131**:16430–8. doi:10.1021/ja904596f

204. Kolb HC, Finn MG, Sharpless KB. Click Chemistry: Diverse Chemical Function from a Few Good Reactions. *Angew. Chem. Int. Ed.* (2001) **40**:2004–21. doi:10.1002/1521-3773(20010601)40:11<2004:AID-ANIE2004>3.0.CO;2-5

205. Baskin JM, Prescher JA, Laughlin ST, Agard NJ, Chang PV, Miller IA, et al. Copper-free click chemistry for dynamic in vivo imaging. *Proc Natl Acad Sci U S A* (2007) **104**:16793–7. doi:10.1073/pnas.0707090104

206. Dommerholt J, Rutjes FP, van Delft FL. Strain-Promoted 1,3-Dipolar Cycloaddition of Cycloalkynes and Organic Azides. *Top Curr Chem (Cham)* (2016) **374**:16. doi:10.1007/s41061-016-0016-4

207. Horner KA, Valette NM, Webb ME. Strain-promoted reaction of 1,2,4-triazines with bicyclononynes. *Chemistry* (2015) **21**:14376–81. doi:10.1002/chem.201502397

208. Hansel TT, Kropshofer H, Singer T, Mitchell JA, George AJ. The safety and side effects of monoclonal antibodies. *Nat Rev Drug Discov* (2010) **9**:325–38. doi:10.1038/nrd3003

209. Lucchi R, Bentanachs J, Oller-Salvia B. The Masking Game: Design of Activatable Antibodies and Mimetics for Selective Therapeutics and Cell Control. *ACS Cent Sci* (2021) **7**:724–38. doi:10.1021/acscentsci.0c01448

210. Engelen W, Zhu K, Subedi N, Idili A, Ricci F, Tel J, et al. Programmable Bivalent Peptide-DNA Locks for pH-Based Control of Antibody Activity. *ACS Cent Sci* (2020) **6**:22–31. doi:10.1021/acscentsci.9b00964

211. Vasiljeva O, Menendez E, Nguyen M, Craik CS, Michael Kavanaugh W. Monitoring protease activity in biological tissues using antibody prodrugs as sensing probes. *Sci Rep* (2020) **10**:5894. doi:10.1038/s41598-020-62339-7

212. Liu B, Shen J, Yu W, Jing C, Saha S, Rangan V, et al. CX-2043, an EpCAM-targeting probody drug conjugate, demonstrates anti-tumor activity with a favorable safety profile in preclinical models. *European Journal of Cancer* (2020) **138**:S15. doi:10.1016/S0959-8049(20)31104-7

213. Biewenga L, Vermathen R, Rosier BJ, Merkx M. A Generic Antibody-Blocking Protein That Enables pH-Switchable Activation of Antibody Activity. *ACS Chem Biol* (2024) **19**:48–57. doi:10.1021/acschembio.3c00449

214. Trang VH, Zhang X, Yumul RC, Zeng W, Stone IJ, Wo SW, et al. A coiled-coil masking domain for selective activation of therapeutic antibodies. *Nat Biotechnol* (2019) **37**:761–5. doi:10.1038/s41587-019-0135-x

215. Lu Y-C, Chuang C-H, Chuang K-H, Chen I-J, Huang B-C, Lee W-H, et al. Specific activation of pro-Infliximab enhances selectivity and safety of rheumatoid arthritis therapy. *PLoS Biol* (2019) **17**:e3000286. doi:10.1371/journal.pbio.3000286

216. Metz S, Panke C, Haas AK, Schanzer J, Lau W, Croasdale R, et al. Bispecific antibody derivatives with restricted binding functionalities that are activated by proteolytic processing. *Protein Eng Des Sel* (2012) **25**:571–80. doi:10.1093/protein/gzs064

217. Pai C-CS, Simons DM, Lu X, Evans M, Wei J, Wang Y-H, et al. Tumor-conditional anti-CTLA4 uncouples antitumor efficacy from immunotherapy-related toxicity. *J Clin Invest* (2019) **129**:349–63. doi:10.1172/JCI123391

218. Chen I-J, Chuang C-H, Hsieh Y-C, Lu Y-C, Lin W-W, Huang C-C, et al. Selective antibody activation through protease-activated pro-antibodies that mask binding sites with inhibitory domains. *Sci Rep* (2017) **7**:11587. doi:10.1038/s41598-017-11886-7

219. Cattaruzza F, Nazeer A, To M, Hammond M, Koski C, Liu LY, et al. Precision-activated T-cell engagers targeting HER2 or EGFR and CD3 mitigate on-target, off-tumor toxicity for immunotherapy in solid tumors. *Nat Cancer* (2023) **4**:485–501. doi:10.1038/s43018-023-00536-9

220. Lowman HB, Liu S. ACTIVATABLE ANTIBODIES HAVING NON-BINDING STERIC MOIETIES AND MEHTODS OF USING THE SAME. US201261663151P **C07K16/00;C12P19/34**(WO2013192546 (A1)) (2013).

221. Desnoyers LR, Vasiljeva O, Richardson JH, Yang A, Menendez EE, Liang TW, et al. Tumor-specific activation of an EGFR-targeting probody enhances therapeutic index. *Sci Transl Med* (2013) **5**:207ra144. doi:10.1126/scitranslmed.3006682
222. Yang Y, Guo Q, Xia M, Li Y, Peng X, Liu T, et al. Generation and characterization of a target-selectively activated antibody against epidermal growth factor receptor with enhanced anti-tumor potency. *mAbs* (2015) **7**:440–50. doi:10.1080/19420862.2015.1008352
223. Geiger M, Stubenrauch K-G, Sam J, Richter WF, Jordan G, Eckmann J, et al. Protease-activation using anti-idiotypic masks enables tumor specificity of a folate receptor 1-T cell bispecific antibody. *Nat Commun* (2020) **11**:3196. doi:10.1038/s41467-020-16838-w
224. Donaldson JM, Kari C, Fragoso RC, Rodeck U, Williams JC. Design and development of masked therapeutic antibodies to limit off-target effects: application to anti-EGFR antibodies. *Cancer Biol Ther* (2009) **8**:2147–52. doi:10.4161/cbt.8.22.9765
225. Duffy MJ. Proteases as prognostic markers in cancer. *Clin Cancer Res* (1996) **2**:613–8.
226. Pulz LH, Strefezzi RF. Proteases as prognostic markers in human and canine cancers. *Vet Comp Oncol* (2017) **15**:669–83. doi:10.1111/vco.12223
227. Martin CE, List K. Cell surface-anchored serine proteases in cancer progression and metastasis. *Cancer metastasis reviews* (2019) **38**:357–87. doi:10.1007/s10555-019-09811-7
228. Lin W-W, Lu Y-C, Chuang C-H, Cheng T-L. Ab locks for improving the selectivity and safety of antibody drugs. *J Biomed Sci* (2020) **27**:76. doi:10.1186/s12929-020-00652-z
229. Onuoha SC, Ferrari M, Sblattero D, Pitzalis C. Rational design of antirheumatic prodrugs specific for sites of inflammation. *Arthritis Rheumatol* (2015) **67**:2661–72. doi:10.1002/art.39232
230. Lin J, Lee SL, Russell AM, Huang RF, Batt MA, Chang SS, et al. A structure-based engineering approach to abrogate pre-existing antibody binding to biotherapeutics. *PLoS One* (2021) **16**:e0254944. doi:10.1371/journal.pone.0254944
231. Jawa V, Cousens LP, Awwad M, Wakshull E, Kropshofer H, Groot AS de. T-cell dependent immunogenicity of protein therapeutics: Preclinical assessment and mitigation. *Clin Immunol* (2013) **149**:534–55. doi:10.1016/j.clim.2013.09.006
232. Orozco CT, Bersellini M, Irving LM, Howard WW, Hargreaves D, Devine PW, et al. Mechanistic insights into the rational design of masked antibodies. *mAbs* (2022) **14**:2095701. doi:10.1080/19420862.2022.2095701
233. Schellenberger V, Wang C-W, Geething NC, Spink BJ, Campbell A, To W, et al. A recombinant polypeptide extends the in vivo half-life of peptides and proteins in a tunable manner. *Nat Biotechnol* (2009) **27**:1186–90. doi:10.1038/nbt.1588
234. Podust VN, Balan S, Sim B-C, Coyle MP, Ernst U, Peters RT, et al. Extension of in vivo half-life of biologically active molecules by XTEN protein polymers. *J Control Release* (2016) **240**:52–66. doi:10.1016/j.jconrel.2015.10.038
235. Salek-Ardakani S, DiRaimondo T, Budimir N, Ma L, Shenhav S, Cicchini V, et al. “1123 Preclinical activity and safety profile or JANX008, a novel EGFR-targeting tumor-activated T cell engager for treatment of solid tumors,”. In: *Regular and Young Investigator Award Abstracts*. BMJ Publishing Group Ltd (2022). A1167-A1167.
236. DiRaimondo T, Budimir N, Shenhav S, Wu H, Cicchini V, Jocic R, et al. “1325 Preclinical activity and safety profile of JANX007, a novel PSMA-targeting tumor-activated T Cell engager for treatment of metastatic castration-resistant prostate cancer,”. In: *Regular and Young Investigator Award Abstracts*. BMJ Publishing Group Ltd (2022). A1376-A1376.
237. Ma J, Mo Y, Tang M, Shen J, Qi Y, Zhao W, et al. Bispecific Antibodies: From Research to Clinical Application. *Front Immunol* (2021) **12**:626616. doi:10.3389/fimmu.2021.626616
238. Segaliny AI, Jayaraman J, Chen X, Chong J, Luxon R, Fung A, et al. A high throughput bispecific antibody discovery pipeline. *Commun Biol* (2023) **6**:380. doi:10.1038/s42003-023-04746-w

239. Krah S, Sellmann C, Rhiel L, Schröter C, Dickgiesser S, Beck J, et al. Engineering bispecific antibodies with defined chain pairing. *N Biotechnol* (2017) **39**:167–73. doi:10.1016/j.nbt.2016.12.010

240. Kontermann RE, Brinkmann U. Bispecific antibodies. *Drug Discov Today* (2015) **20**:838–47. doi:10.1016/j.drudis.2015.02.008

241. Ridgway JB, Presta LG, Carter P. 'Knobs-into-holes' engineering of antibody CH3 domains for heavy chain heterodimerization. *Protein Eng* (1996) **9**:617–21. doi:10.1093/protein/9.7.617

242. Gunasekaran K, Pentony M, Shen M, Garrett L, Forte C, Woodward A, et al. Enhancing antibody Fc heterodimer formation through electrostatic steering effects: applications to bispecific molecules and monovalent IgG. *J Biol Chem* (2010) **285**:19637–46. doi:10.1074/jbc.M110.117382

243. Davis JH, Aperlo C, Li Y, Kurosawa E, Lan Y, Lo K-M, et al. SEEDbodies: fusion proteins based on strand-exchange engineered domain (SEED) CH3 heterodimers in an Fc analogue platform for asymmetric binders or immunofusions and bispecific antibodies. *Protein Eng Des Sel* (2010) **23**:195–202. doi:10.1093/protein/gzp094

244. Nardis C de, Hendriks LJ, Poirier E, Arvinte T, Gros P, Bakker AB, et al. A new approach for generating bispecific antibodies based on a common light chain format and the stable architecture of human immunoglobulin G1. *J Biol Chem* (2017) **292**:14706–17. doi:10.1074/jbc.M117.793497

245. Schaefer W, Regula JT, Bähner M, Schanzer J, Croasdale R, Dürr H, et al. Immunoglobulin domain crossover as a generic approach for the production of bispecific IgG antibodies. *Proc Natl Acad Sci U S A* (2011) **108**:11187–92. doi:10.1073/pnas.1019002108

246. Lewis SM, Wu X, Pustilnik A, Sereno A, Huang F, Rick HL, et al. Generation of bispecific IgG antibodies by structure-based design of an orthogonal Fab interface. *Nat Biotechnol* (2014) **32**:191–8. doi:10.1038/nbt.2797

247. Merchant AM, Zhu Z, Yuan JQ, Goddard A, Adams CW, Presta LG, et al. An efficient route to human bispecific IgG. *Nat Biotechnol* (1998) **16**:677–81. doi:10.1038/nbt0798-677

248. Xu JL, Davis MM. Diversity in the CDR3 region of V(H) is sufficient for most antibody specificities. *Immunity* (2000) **13**:37–45. doi:10.1016/s1074-7613(00)00006-6

249. Klein C, Schaefer W, Regula JT. The use of CrossMAb technology for the generation of bi- and multispecific antibodies. *mAbs* (2016) **8**:1010–20. doi:10.1080/19420862.2016.1197457#

250. Pang X, Huang Z, Zhong T, Zhang P, Wang ZM, Xia M, et al. Cadonilimab, a tetravalent PD-1/CTLA-4 bispecific antibody with trans-binding and enhanced target binding avidity. *mAbs* (2023) **15**:2180794. doi:10.1080/19420862.2023.2180794

251. Zhou X, Geyer FK, Happel D, Takimoto J, Kolmar H, Rabinovich B. Using protein geometry to optimize cytotoxicity and the cytokine window of a ROR1 specific T cell engager. *Front Immunol* (2024) **15**:1323049. doi:10.3389/fimmu.2024.1323049

252. Zhang C, Röder J, Scherer A, Bodden M, Pfeifer Serrahima J, Bhatti A, et al. Bispecific antibody-mediated redirection of NKG2D-CAR natural killer cells facilitates dual targeting and enhances antitumor activity. *J Immunother Cancer* (2021) **9**. doi:10.1136/jitc-2021-002980

253. Brinkmann U, Kontermann RE. Bispecific antibodies. *Science* (2021) **372**:916–7. doi:10.1126/science.abg1209

254. Grakoui A, Bromley SK, Sumen C, Davis MM, Shaw AS, Allen PM, et al. The immunological synapse: a molecular machine controlling T cell activation. *Science* (1999) **285**:221–7. doi:10.1126/science.285.5425.221

255. Tapia-Galisteo A, Álvarez-Vallina L, Sanz L. Bi- and trispecific immune cell engagers for immunotherapy of hematological malignancies. *J Hematol Oncol* (2023) **16**:83. doi:10.1186/s13045-023-01482-w

256. Huehls AM, Coupet TA, Sentman CL. Bispecific T-cell engagers for cancer immunotherapy. *Immunol Cell Biol* (2015) **93**:290–6. doi:10.1038/icb.2014.93

257. Klein C, Brinkmann U, Reichert JM, Kontermann RE. The present and future of bispecific antibodies for cancer therapy. *Nat Rev Drug Discov* (2024) **23**:301–19. doi:10.1038/s41573-024-00896-6

258. Shanshal M, Caimi PF, Adjei AA, Ma WW. T-Cell Engagers in Solid Cancers-Current Landscape and Future Directions. *Cancers (Basel)* (2023) **15**. doi:10.3390/cancers15102824

259. Whalen KA, Rakhra K, Mehta NK, Steinle A, Michaelson JS, Baeuerle PA. Engaging natural killer cells for cancer therapy via NKG2D, CD16A and other receptors. *mAbs* (2023) **15**:2208697. doi:10.1080/19420862.2023.2208697

260. Yang Y, Yang Z, Yang Y. Potential Role of CD47-Directed Bispecific Antibodies in Cancer Immunotherapy. *Front Immunol* (2021) **12**:686031. doi:10.3389/fimmu.2021.686031

261. Li B, Xu L, Pi C, Yin Y, Xie K, Tao F, et al. CD89-mediated recruitment of macrophages via a bispecific antibody enhances anti-tumor efficacy. *Oncoimmunology* (2017) **7**:e1380142. doi:10.1080/2162402X.2017.1380142

262. Sewnath C an, Behrens LM, van Egmond M. Targeting myeloid cells with bispecific antibodies as novel immunotherapies of cancer. *Expert Opin Biol Ther* (2022) **22**:983–95. doi:10.1080/14712598.2022.2098675

263. Huang S, van Duijnhoven SM, Sijts AJ, van Elsas A. Bispecific antibodies targeting dual tumor-associated antigens in cancer therapy. *J Cancer Res Clin Oncol* (2020) **146**:3111–22. doi:10.1007/s00432-020-03404-6

264. Schubert I, Stein C, Fey GH. Dual-Targeting for the Elimination of Cancer Cells with Increased Selectivity. *Antibodies* (2012) **1**:2–18. doi:10.3390/antib1010002

265. Moores SL, Chiu ML, Bushey BS, Chevalier K, Luistro L, Dorn K, et al. A Novel Bispecific Antibody Targeting EGFR and cMet Is Effective against EGFR Inhibitor-Resistant Lung Tumors. *Cancer Res* (2016) **76**:3942–53. doi:10.1158/0008-5472.CAN-15-2833

266. Syed YY. Amivantamab: First Approval. *Drugs* (2021) **81**:1349–53. doi:10.1007/s40265-021-01561-7

267. Wang S, Chen K, Lei Q, Ma P, Yuan AQ, Zhao Y, et al. The state of the art of bispecific antibodies for treating human malignancies. *EMBO Mol Med* (2021) **13**:e14291. doi:10.15252/emmm.202114291

268. Ferlay J, Ervik M, Lam F, Laversanne M, Colombet M, Mery L, Piñeros M, Znaor A, Soerjomataram I, Bray F. *Global Cancer Observatory: Cancer Today: Lyon, France: International Agency for Research on Cancer.* (2024) [cited 2024 Jun 01]. Available from: https://gco.iarc.who.int/today

269. Hanahan D. Hallmarks of Cancer: New Dimensions. *Cancer Discov* (2022) **12**:31–46. doi:10.1158/2159-8290.CD-21-1059

270. Sung H, Ferlay J, Siegel RL, Laversanne M, Soerjomataram I, Jemal A, et al. Global Cancer Statistics: GLOBOCAN Estimates of Incidence and Mortality Worldwide for 36 Cancers in 185 Countries. *CA Cancer J Clin* (2022).

271. Nakamura-García AK, Espinal-Enríquez J. The network structure of hematopoietic cancers. *Sci Rep* (2023) **13**:19837. doi:10.1038/s41598-023-46655-2

272. Rajkumar SV, Kumar S. Multiple Myeloma: Diagnosis and Treatment. *Mayo Clin Proc* (2016) **91**:101–19. doi:10.1016/j.mayocp.2015.11.007

273. Gerecke C, Fuhrmann S, Strifler S, Schmidt-Hieber M, Einsele H, Knop S. The Diagnosis and Treatment of Multiple Myeloma. *Dtsch Arztebl Int* (2016) **113**:470–6. doi:10.3238/arztebl.2016.0470

274. Patel N, Mishra A. Automated Leukaemia Detection Using Microscopic Images. *Procedia Computer Science* (2015) **58**:635–42. doi:10.1016/j.procs.2015.08.082

275. Szczepański T, van der Velden VH, van Dongen JJ. Classification systems for acute and chronic leukaemias. *Best Pract Res Clin Haematol* (2003) **16**:561–82. doi:10.1016/S1521-6926(03)00086-0

276. “Hematopoietic Cancers,”. In: *Primer to the Immune Response*. Elsevier (2014). p. 553–85.
277. Armitage JO, Gascoyne RD, Lunning MA, Cavalli F. Non-Hodgkin lymphoma. *Lancet* (2017) **390**:298–310. doi:10.1016/S0140-6736(16)32407-2
278. Siegel RL, Miller KD, Wagle NS, Jemal A. Cancer statistics, 2023. *CA Cancer J Clin* (2023) **73**:17–48. doi:10.3322/caac.21763
279. Nygren P. What is cancer chemotherapy? *Acta Oncol* (2001) **40**:166–74. doi:10.1080/02841860151116204
280. Szakács G, Paterson JK, Ludwig JA, Booth-Genthe C, Gottesman MM. Targeting multidrug resistance in cancer. *Nat Rev Drug Discov* (2006) **5**:219–34. doi:10.1038/nrd1984
281. Padma VV. An overview of targeted cancer therapy. *Biomedicine (Taipei)* (2015) **5**:19. doi:10.7603/s40681-015-0019-4
282. Maloney DG, Grillo-López AJ, White CA, Bodkin D, Schilder RJ, Neidhart JA, et al. IDEC-C2B8 (Rituximab) Anti-CD20 Monoclonal Antibody Therapy in Patients With Relapsed Low-Grade Non-Hodgkin's Lymphoma. *Blood* (1997) **90**:2188–95. doi:10.1182/blood.V90.6.2188
283. Press MF, Lenz H-J. EGFR, HER2 and VEGF pathways: validated targets for cancer treatment. *Drugs* (2007) **67**:2045–75. doi:10.2165/00003495-200767140-00006
284. Tiash S, Chowdhury E. Growth factor receptors: promising drug targets in cancer. *J Cancer Metastasis Treat* (2015) **1**:190. doi:10.4103/2394-4722.163151
285. Sun Q, Hong Z, Zhang C, Wang L, Han Z, Ma D. Immune checkpoint therapy for solid tumours: clinical dilemmas and future trends. *Signal Transduct Target Ther* (2023) **8**:320. doi:10.1038/s41392-023-01522-4
286. Pardoll DM. The blockade of immune checkpoints in cancer immunotherapy. *Nat Rev Cancer* (2012) **12**:252–64. doi:10.1038/nrc3239
287. Sadeghi Rad H, Monkman J, Warkiani ME, Ladwa R, O'Byrne K, Rezaei N, et al. Understanding the tumor microenvironment for effective immunotherapy. *Med Res Rev* (2021) **41**:1474–98. doi:10.1002/med.21765
288. Shi X, Li C-W, Tan L-C, Wen S-S, Liao T, Zhang Y, et al. Immune Co-inhibitory Receptors PD-1, CTLA-4, TIM-3, LAG-3, and TIGIT in Medullary Thyroid Cancers: A Large Cohort Study. *J Clin Endocrinol Metab* (2021) **106**:120–32. doi:10.1210/clinem/dgaa701
289. Chocarro L, Blanco E, Arasanz H, Fernández-Rubio L, Bocanegra A, Echaide M, et al. Clinical landscape of LAG-3-targeted therapy. *Immunooncol Technol* (2022) **14**:100079. doi:10.1016/j.iotech.2022.100079
290. Tawbi HA, Schadendorf D, Lipson EJ, Ascierto PA, Matamala L, Castillo Gutiérrez E, et al. Relatlimab and Nivolumab versus Nivolumab in Untreated Advanced Melanoma. *N Engl J Med* (2022) **386**:24–34. doi:10.1056/NEJMoa2109970
291. Garcia J, Hurwitz HI, Sandler AB, Miles D, Coleman RL, Deurloo R, et al. Bevacizumab (Avastin®) in cancer treatment: A review of 15 years of clinical experience and future outlook. *Cancer Treat Rev* (2020) **86**:102017. doi:10.1016/j.ctrv.2020.102017
292. Ellis LM, Hicklin DJ. VEGF-targeted therapy: mechanisms of anti-tumour activity. *Nat Rev Cancer* (2008) **8**:579–91. doi:10.1038/nrc2403
293. Jen EY, Xu Q, Schetter A, Przepiorka D, Shen YL, Roscoe D, et al. FDA Approval: Blinatumomab for Patients with B-cell Precursor Acute Lymphoblastic Leukemia in Morphologic Remission with Minimal Residual Disease. *Clin Cancer Res* (2019) **25**:473–7. doi:10.1158/1078-0432.CCR-18-2337
294. June CH, O'Connor RS, Kawalekar OU, Ghassemi S, Milone MC. CAR T cell immunotherapy for human cancer. *Science* (2018) **359**:1361–5. doi:10.1126/science.aar6711
295. Sadelain M, Brentjens R, Rivière I. The basic principles of chimeric antigen receptor design. *Cancer Discov* (2013) **3**:388–98. doi:10.1158/2159-8290.CD-12-0548

296. Awasthi R, Maier HJ, Zhang J, Lim S. Kymriah® (tisagenlecleucel) - An overview of the clinical development journey of the first approved CAR-T therapy. *Hum Vaccin Immunother* (2023) **19**:2210046. doi:10.1080/21645515.2023.2210046

297. Chen Y-J, Abila B, Mostafa Kamel Y. CAR-T: What Is Next? *Cancers (Basel)* (2023) **15**. doi:10.3390/cancers15030663

298. AlDallal SM. Yescarta: A New Era for Non-Hodgkin Lymphoma Patients. *Cureus* (2020) **12**:e11504. doi:10.7759/cureus.11504

299. Kahl B. Chemotherapy Combinations With Monoclonal Antibodies in Non-Hodgkin's Lymphoma. *Semin Hematol* (2008) **45**:90–4. doi:10.1053/j.seminhematol.2008.02.003

300. Lu L, Zhan M, Li X-Y, Zhang H, Dauphars DJ, Jiang J, et al. Clinically approved combination immunotherapy: Current status, limitations, and future perspective. *Curr Res Immunol* (2022) **3**:118–27. doi:10.1016/j.crimmu.2022.05.003

4 Cumulative section

4.1 Conditional activation of an anti-IgM antibody-drug conjugate for precise B cell lymphoma targeting

Title:

Conditional activation of an anti-IgM antibody-drug conjugate for precise B cell lymphoma targeting

Authors:

Katrin Schoenfeld, Julia Harwardt, Jan Habermann, Adrian Elter and Harald Kolmar

Bibliographic data:

Frontiers in Immunology

Volume 14 - 2023, Section Cancer Immunity and Immunotherapy

Article first published: 28th September 2023

DOI: 10.3389/fimmu.2023.1258700

Contributions by Katrin Schoenfeld:

- Initial idea and planning of the project
- Generation and screening of the scFv library
- Design, production and characterization of masked antibodies
- Generation of antibody-drug conjugates
- Testing of masked antibody-drug conjugates on cells
- Writing of manuscript and generation of figures

frontiers | Frontiers in Immunology

TYPE Original Research
PUBLISHED 28 September 2023
DOI 10.3389/fimmu.2023.1258700

OPEN ACCESS

EDITED BY
Robert Ohgami,
The University of Utah, United States

REVIEWED BY
Oliver Seifert,
University of Stuttgart, Germany
Michael R. Green,
University of Texas MD Anderson Cancer Center, United States
Benjamí Oller Salvia,
Institut Químic de Sarrià, Spain

*CORRESPONDENCE
Harald Kolmar
Harald.Kolmar@TU-Darmstadt.de

RECEIVED 14 July 2023
ACCEPTED 07 September 2023
PUBLISHED 28 September 2023

CITATION
Schoenfeld K, Harwardt J, Habermann J, Elter A and Kolmar H (2023) Conditional activation of an anti-IgM antibody-drug conjugate for precise B cell lymphoma targeting.
Front. Immunol. 14:1258700.
doi: 10.3389/fimmu.2023.1258700

Conditional activation of an anti-IgM antibody-drug conjugate for precise B cell lymphoma targeting

Katrin Schoenfeld[1], Julia Harwardt[1], Jan Habermann[1], Adrian Elter[1] and Harald Kolmar[1,2]*

[1]Institute for Organic Chemistry and Biochemistry, Technical University of Darmstadt, Darmstadt, Germany, [2]Centre for Synthetic Biology, Technical University of Darmstadt, Darmstadt, Germany

Cancerous B cells are almost indistinguishable from their non-malignant counterparts regarding their surface antigen expression. Accordingly, the challenge to be faced consists in elimination of the malignant B cell population while maintaining a functional adaptive immune system. Here, we present an IgM-specific antibody-drug conjugate masked by fusion of the epitope-bearing IgM constant domain. Antibody masking impaired interaction with soluble pentameric as well as cell surface-expressed IgM molecules rendering the antibody cytotoxically inactive. Binding capacity of the anti-IgM antibody drug conjugate was restored upon conditional protease-mediated demasking which consequently enabled target-dependent antibody internalization and subsequent induction of apoptosis in malignant B cells. This easily adaptable approach potentially provides a novel mechanism of clonal B cell lymphoma eradication to the arsenal available for non-Hodgkin's lymphoma treatment.

KEYWORDS

B cell receptor, antibody-drug conjugate, masked antibody, conditional activated antibody, MMP-9, matriptase, B cell lymphoma

Introduction

Immunotherapies represent a broad and rapidly growing type of therapies having a substantial impact on cancer outcomes. Monoclonal antibodies (mAbs) are among the first groups of immunotherapies approved for anti-tumor treatment and are still of exceptional relevance in current treatment regimens (1). Rituximab, the first US Food and Drug Administration (FDA)-approved mAb implemented in oncology, has widely been administered in patients suffering from B cell non-Hodgkin's lymphoma (NHL). NHL is a heterogeneous group of neoplasms and the most frequently diagnosed adult hematological cancer, accounting for the seventh most common cancer and the ninth leading cause of cancer deaths in the US (2). Targeting the pan-B cell antigen CD20, rituximab exerts anti-tumor activity in four main ways, three of which rely on recruiting

effector mechanisms from the patient's immune system such as complement-dependent cytotoxicity (CDC), antibody-dependent cell-mediated cytotoxicity (ADCC) and antibody-dependent phagocytosis (ADP) (3). A fourth proposed mechanism of action is the induction of apoptosis through both caspase-dependent and -independent mechanisms (3, 4). Although rituximab in combination with chemotherapy has tremendously improved the chance of cure for NHL patients, the clinical effectiveness of rituximab is ultimately limited by the development of treatment resistance. Notably, only 40% of the patients initially responding to rituximab have the ability to respond again after relapse (5, 6).

The B cell receptor (BCR) complex plays a pivotal role in the adaptive immune response. Comprising a membrane-bound immunoglobulin (Ig) and a non-covalently linked heterodimer composed of Igα and Igβ it is expressed on the surface of B lymphocytes with each B cell clone possessing a unique BCR of Ig isotype IgA, IgD, IgE, IgG, or IgM (7, 8). Previous reports have demonstrated that malignant B cells frequently express IgM BCRs (9–12). A subtype of the diffuse large B cell lymphoma (DLBCL) is activated B cell-like DLBCL, where it has been reported that IgM-positivity of tumor correlates with a poor prognosis and a shorter overall survival for patients (10–12). Harnessing the fact that clonal B cell cancers in most cases express BCRs of one Ig isotype, it might be possible to selectively deplete malignant B cells of the IgM isotype while sparing the majority of B lymphocytes expressing other isotype or no BCRs. However, therapeutic antibodies directed against IgM may not fully function in the body due to the presence of soluble IgM molecules in large amounts. In order to address the problem of selectivity and potential target-mediated drug disposition, an IgMxHLA-DR bispecific antibody targeting two B cell antigens has recently been engineered which demonstrated significant *in vitro* anti-tumor activity as well as efficacy and tolerability in non-human primate studies (13).

Besides improving specificity via multispecific cancer targeting, masking strategies have been developed allowing for conditional activation of antibodies in tumor tissue (14–16). The approach requires the generation of a suitable masking unit which prevents antibody-antigen interaction either by steric hindrance, e.g. by fusion of a bulky mask, or by specific binding to the antibody paratope, such as an epitope-mimetic or anti-idiotypic antibody fragment (14, 16). Antibody activation through demasking is typically mediated by proteases, such as serine proteases (e.g. matriptase), matrix metalloproteinases (e.g. MMP-2/MMP-9) and cysteine proteases (e.g. cathepsin S) frequently overexpressed in tumor tissues (17–19). Previous masking attempts put forth antibody therapeutics with improved safety profiles, while retaining anti-disease activity (20–24). The versatile probody therapeutic technology platform developed by CytomX Therapeutics has been applied to target a variety of receptors including CTLA-4, EGFR, as well as molecules considered undruggable because of their broad tissue expression, such as CD71 and EpCAM (25–27). The conditionally activated probody-drug conjugate CX-2029 (anti-CD71) demonstrated tumor regression and was well tolerated in patients with advanced solid tumors (28).

To combat resistance of current mAb-based therapies and improve the potency of biomolecules, antibody-drug conjugates (ADC) feature ideal properties for precise and efficient tumor targeting (29, 30). The first-in-class ADC to be FDA-approved for therapy was gemtuzumab ozogamicin (Mylotarg), in 2000 for the treatment of CD33-positive acute myeloid leukemia (AML) (31). Since then, 14 ADCs received worldwide market approval, besides over 100 ADC candidates being investigated in clinical stages at present (32). ADCs are typically composed of mAbs covalently bound to potent cytotoxic payload through synthetic (cleavable) linkers. However, there is ongoing optimization of certain parameters, including mAb specificity, linker technology, drug potency as well as stoichiometry and placement of warheads (30, 32). The mechanism leading to ADC's anti-tumor effect includes binding of the ADC to its target antigen that triggers ADC internalization and intracellular release of the payload which eventually mediates cytotoxic effects. Hence, candidate ADCs must be carefully selected regarding numerous properties influencing safety and efficacy. Particularly, the antigen to be targeted by the ADC must fulfill certain characteristics such as overexpression on the surface of cancer cells with minimal expression in normal tissue and the potency to rapidly internalize upon ADC binding (32). Since B cell NHL is currently treated with either chemotherapy or immunotherapy or a combination of both, it is anticipated that ADCs can be rational for NHL control.

In this study, we developed a proteolytically activatable IgM-directed antibody-drug conjugate for precise targeting of IgM-positive B cell lymphoma (Figure 1). Starting with the immunization of a chicken with IgM from human serum, we isolated IgM binders by single-chain variable fragment (scFv) immune library screening using yeast surface display (YSD) in combination with fluorescence-activated cell sorting (FACS). After expression and characterization of isolated binders in scFv format, full-length antibodies in Fab-Fc format were generated. With respect to potential off-target effects on healthy IgM-expressing B cells and capturing of antibodies by soluble IgM in the blood stream, we identified the antigenic constant Ig domain, derived from the IgM antigen, for antibody masking. The masking unit was genetically fused to the N-terminus of the anti-IgM light chain (LC) via a dual-protease cleavable linker addressable by matrix metalloproteinase-9 (MMP-9) and matriptase since these proteases are described to be overexpressed in B cell lymphoma (33, 34). The IgM-targeting antibody was further conjugated with the highly toxic and clinically proven chemotherapeutic agent monomethyl auristatin E (MMAE) imparting cytotoxic properties to the molecule (32). The resulting masked anti-IgM ADC demonstrated no significant interactions with different types of B cells. However, unmasking resulted in specific targeting and efficient killing of IgM-positive lymphoma cells while largely sparing other lymphocytes from chemotherapeutic damage.

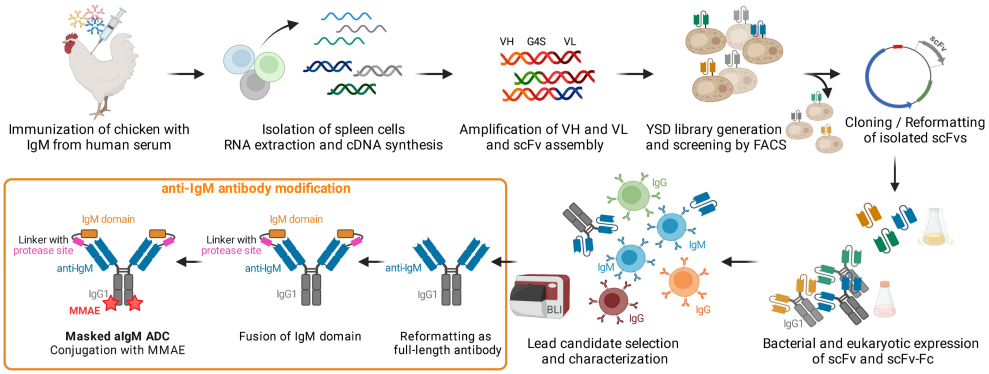

FIGURE 1
Concept Overview. Chicken immunization with IgM from human serum was followed by splenic RNA isolation and cDNA synthesis. Variable antibody domains were amplified and assembled as scFvs for yeast surface display and FACS. IgM binding scFvs were reformatted and cloned into bacterial and mammalian vectors for scFv/scFv-Fc expression. After selection and characterization of a lead candidate, the IgM binder was reformatted as full-length antibody, fused with the masking IgM domain and ultimately conjugated with MMAE resulting in a masked anti-IgM (aIgM) ADC. Created with BioRender.com.

Results

Design of protease-activated masked anti-IgM antibody-drug conjugates

Based on a chicken-derived anti-IgM (aIgM) antibody, we designed an antibody-drug conjugate that is masked to overcome potential off-target effects towards circulating IgM$^+$ B cells and interactions with soluble IgM in the blood stream (Figure 2). In our approach, the human IgM domain targeted by the antibody served as masking unit attached to the aIgM light chain. We assumed that the heavy chain CDRs are mainly responsible for antigen recognition as this was discovered in previous chicken-derived antibodies including common light chain approaches and is reinforced by the fact that chicken CDR3 of the VH tend to be longer and have much higher cysteine content leading to increased stability and complexity (36–39). Fusion of the masking unit was achieved via a synthetic linker (33 amino acids) comprising a dual-protease site (MMP site and MatA site) recognized by MMP-2/9 and matriptase (Figure 2A). Linker sequence and applicability to protease-activated antibodies in tumor context have been recently described by *Geiger et al.*, demonstrating a synergistic effect for the

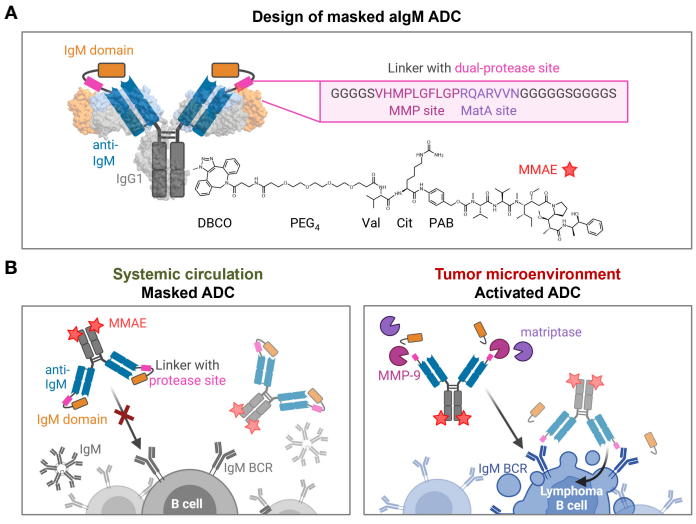

FIGURE 2
Design and mode of action of masked aIgM ADC. **(A)** Schematic representation of the masked aIgM ADC. The anti-IgM LC is (N-terminally) fused to an IgM domain via a linker with dual-protease site, the HC is (C-terminally) modified with DBCO-PEG$_4$-Val-Cit-PAB-MMAE. DBCO, Dibenzocyclooctyne; PEG, polyethylene glycol; Val, valine, Cit: citrulline; PAB, p-aminobenzyl alcohol; MMAE, monomethyl auristatin E. Surface representation rendered with UCSF ChimeraX (35) from PDB: 1IGT/7XQ8. **(B)** Conceptional mode of action of the masked anti-IgM ADC. In systemic circulation the masked aIgM ADC is not able to bind to either soluble pentameric IgM nor membrane-bound IgM. Once reaching the tumor microenvironment, tumor-specific proteases such as MMP-9 or matriptase hydrolyze the linker connecting the aIgM antibody and the masking IgM domain. The activated aIgM ADC regains binding ability leading to specific ADC uptake and killing of IgM$^+$ lymphoma B cells. Created with BioRender.com.

combination of the cleavage sites for MMP-2/9-matriptase compared to MatA site or MMP site linkers alone (21). For the generation of an ADC the mAb component was further provided with MMAE, since NHL is known to be sensitive to microtubule inhibitors (40, 41). The payload consists of DBCO, PEG_4 linker, Val-Cit dipeptide sequence as cathepsin substrate, p-aminobenzyl alcohol (PAB) self-immolative spacer and the cytotoxic payload MMAE. Site-specific coupling of DBCO-PEG_4-Val-Cit-PAB-MMAE was accomplished via a chemoenzymatic conjugation approach, resulting in a theoretical drug-to-antibody ratio (DAR) of two (detailed conjugation strategy described in section 'Cytotoxicity of masked and protease-activated CH2-aIgM ADC'). The aIgM ADC should remain masked in systemic circulation, but upon reaching the tumor microenvironment, upregulated protease activity promotes cleavage of the substrate linker and subsequent release of the blocking IgM domain (Figure 2B). Following antibody-directed binding to tumor target IgM isotype BCRs, the ADC is expected to be effectively internalized, followed by lysosomal degradation resulting in cleavage of the drug linker and intracellular release of the cytotoxic agent. Finally, MMAE binds to tubulin which inhibits its polymerization and ultimately triggers tumor cell death (42).

Generation of chicken-derived anti-IgM antibodies

In order to generate protease-activated anti-human IgM antibodies, we screened for IgM binders which are in a second step equipped with the epitope-bearing human IgM domain serving as antigenic affinity-based mask. Antibodies of IgM isotype play important roles in non-immune as well as antigen-induced immune reactions and constant domains of Ig heavy chain are broadly conserved in mammals (43–45). Hence, immunization of popularly chosen mammalian species such as mouse, rabbit or goat might not result in the desired immune response. Accordingly, chickens were considered for immunization as they are phylogenetic distant from humans and previous attempts succeeded in accessing antibodies against conserved epitopes on mammalian molecules (46, 47). Recently, we described the isolation of highly affine antibody fragments derived from immunized chickens using yeast surface display in combination with FACS (48–50). Applying this approach, we obtained high chicken antibody titers against human IgM and were able to enrich binders within two consecutive sorting rounds using 500 nM or 10 nM IgM from human serum, respectively (Supplementary Figures 1A, B). Sequence analysis of four yeast single clones emerging from the screening revealed four distinct scFv candidates (S5, S6, S8, S9). The four scFvs were heterologously expressed in *Escherichia coli* and were subjected to B cell binding assays. Antibody clone aIgM S8 was selected as lead candidate since it demonstrated affine binding to IgM^+ lymphocytes while IgM^- cells were not targeted indicating isotypic specificity (Supplementary Figure 2).

Generation and characterization of conditionally activated aIgM

The aIgM scFv S8 was reformatted as scFv-Fc fusion and as Fab-Fc full-length antibody. To investigate which of the four constant IgM domains aIgM S8 targets, biolayer interferometry (BLI) epitope binning was performed. To this end, His-tagged CH1-CH4 IgM domains were expressed separately in Expi293F™ cells and cell culture supernatants were immobilized on Ni-NTA biosensors. Association with aIgMscFv-Fc revealed specific and exclusive binding to IgM CH2 domain (Figure 3A). Consequently, simultaneous binding of full-length IgM and IgM CH2 domain should not be possible. This was confirmed by loading of biotinylated aIgMscFv-Fc onto SAX biosensors and stepwise association with equimolar concentrations of CH2 in antigens using 1,000 nM single IgM CH2 domain and 100 nM (pentameric) IgM from human serum (Figure 3B). The slightly increased binding signal detected when incubating with CH2, following the first IgM association can be ascribed to the small size of IgM CH2 (13 kDa) in comparison to the pentameric IgM molecule (970 kDa) allowing the single Ig domain to bind unoccupied paratopes which are sterically unavailable for pentameric IgM. Attempts to determine the affinity of aIgMscFv-Fc towards IgM CH2 failed as the off-rate turned out to be very low, nevertheless, implying high-affinity binding (Supplementary Figure 3A) . In a similar setup, a competition assay with B cells was performed using IgM^+ SUP-B8 and Ramos cells incubated with 100 nM aIgMscFv-Fc and varying concentrations of IgM CH2 (39-10,000 nM) (Figure 3C). In accordance with the BLI measurements, B cell binding decreased with increasing IgM CH2 concentration amounting to IC_{50} values of 143 nM and 135 nM for SUP-B8 and Ramos cells, respectively. Hence, BCRs of IgM isotype on the cell surface compete with the soluble IgM CH2 domain for scFv binding corroborating the notion that CH2 is the epitope-bearing IgM domain.

Taken together, these results indicate that human IgM CH2 domain suits as masking unit for the previously identified aIgM S8 antibody since pre-incubation of antibody with IgM CH2 efficiently impairs IgM binding in biolayer interferometric studies as well as on a cellular level with membrane-bound IgM.

For masking of aIgM S8 antibody the IgM CH2 domain was fused to the light chain by a linker with dual-protease site. The unmasked aIgM and masked aIgM antibody variant, referred to as CH2-aIgM, were expressed in Expi293F™ cells and purified via Protein A affinity chromatography. Integrity, size and purity of the proteins including stability of the linker during production and purification process were confirmed using reducing SDS-PAGE analysis (Figure 4A). Thermal stability investigated by SYPRO Orange revealed melting temperatures of 72.5°C and 71.5°C for the aIgM and CH2-aIgM, respectively (Supplementary Figure 4). Thus, no significant change in thermal stability was observed by attachment of the additional Ig domain. The functionality of the parental full-length aIgM concerning binding of IgM from human serum and IgM-derived CH2 domain was confirmed by BLI (Supplementary Figure 3B). In order to prove feasibility of

10.3389/fimmu.2023.1258700

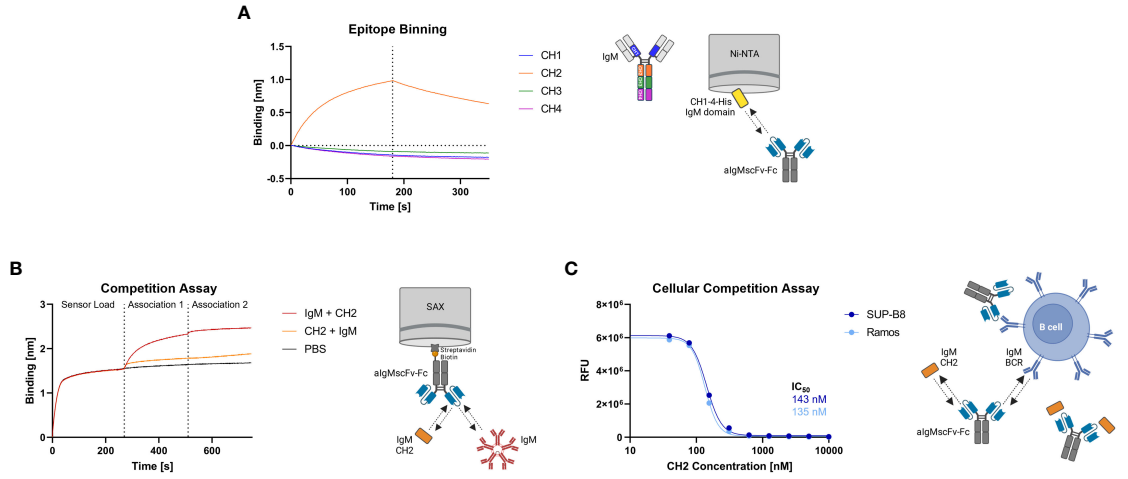

FIGURE 3
Epitope binning of aIgMscFv-Fc and CH2/IgM competition. **(A)** BLI-assisted epitope binning. The four His-tagged constant IgM domains of the HC (CH1, CH2, CH3 and CH4) were loaded onto Ni-NTA biosensor tips and associated with 150 nM aIgMscFv-Fc, followed by dissociation. **(B)** BLI-assisted competition assay. Biotinylated aIgMscFv-Fc was loaded onto SAX tips and IgM CH2/IgM from human serum were associated in sequence. **(C)** Cellular competition assay. IgM$^+$ SUP-B8 and Ramos B cells were incubated with 100 nM aIgMscFv-Fc and varying concentrations of IgM CH2 domain (39-10,000 nM). Detection was performed using anti-human IgG Fc-PE staining and flow cytometry.

reactivation of the aIgM binding capability in the masked antibody, CH2-aIgM was treated with either MMP-9 or matriptase. Linker proteolysis was analyzed by SDS-PAGE demonstrating successful and complete linker cleavage of the CH2-aIgM LC by both proteases which resulted in the aIgM LC migrating slightly higher in SDS gel electrophoresis than the unmasked aIgM LC due to residual linker amino acids, and the solitary CH2 domain (Figure 4A). Biolayer interferometry measurements were conducted to investigate, whether the binding capacity of CH2-aIgM is diminished and can in a next step be restored by protease cleavage. Therefore, aIgM, CH2-aIgM, protease treated CH2-aIgM and rituximab as an unrelated control were immobilized onto AHC biosensors and subsequently incubated with IgM from human serum. With CH2-aIgM loaded, association of IgM is completely impaired since the binding signal is comparable to rituximab control (Figure 4B). As previous experiments have shown that the dissociation rate of soluble IgM CH2 from the antibody is low, a Protein A purification step was systematically introduced after protease-mediated linker hydrolysis in subsequent assays in order to remove a large fraction of cleaved CH2 domain. MMP-9-cleaved, purified CH2-aIgM allows IgM association, although maximum binding capacity of aIgM may not fully be restored. This effect of reduced interaction might be traced back to remaining cleaved masking units blocking the aIgM paratope due to slow dissociation. Similar results were obtained in BLI experiments associating with different IgM concentrations (3.9-125 nM) for competition with cleaved CH2 masking moiety as well as in a reverse experimental setup immobilizing IgM to the biosensor and incubating with the respective antibody variants (Supplementary Figures 3C, D).

On-cell binding of masked and protease-activated CH2-aIgM

To investigate, whether the masked CH2-aIgM remains innate to IgM interaction when membrane-bound in a high copy number on cells and whether protease-activation of CH2-aIgM restores binding functionality, cell binding experiments were performed

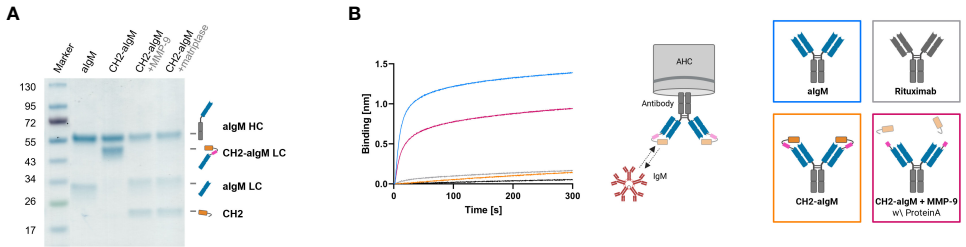

FIGURE 4
Protease-activation of CH2-masked aIgM. **(A)** Reducing SDS-PAGE of depicted antibodies with schematic representations of heavy and (masked) light chains. **(B)** BLI measurement. The four antibody constructs (Rituximab, aIgM, CH2-aIgM, Protein A purified CH2-aIgM+MMP-9) were loaded onto AHC biosensor tips and associated with 100 nM IgM from human serum.

using flow cytometry. SUP-B8 and Ramos B lymphoid cell lines derived from Burkitt lymphoma were used as IgM^+ cells while IgM^-/IgG^+ IM-9 B cells served as control (51–53). Cells were stained with 100 nM of respective antibody and PE-conjugated secondary antibody for detection. While aIgM represents maximum binding on IgM^+ SUP-B8 and Ramos cells, the masked variant CH2-aIgM shows 61-fold and 102-fold reduced cell binding, respectively (Figure 5A). Upon MMP-9 cleavage and Protein A purification of CH2-aIgM cell binding capacity is fully restored to a maximum binding comparable to the unmasked aIgM version. None of the antibodies showed unspecific interactions with IgM^-/IgG^+ IM-9 off-target cells. Furthermore, cell titration was conducted for determination of on-cell affinities for the masked and the proteolytically activated CH2-aIgM. Antibodies were applied to the cells in a serial dilution with concentrations ranging from 0.125 to 200 nM. Apparent binding affinities for aIgM amounted to 0.9 nM for SUP-B8 cells and 2.4 nM for Ramos cells, while titration of cleaved CH2-aIgM resulted in similar values of 1.5 nM and 2.6 nM for SUP-B8 and Ramos, respectively (Figure 5B). Besides comparable on-cell K_Ds of aIgM and protease treated CH2-aIgM, maximal binding levels are also restored. The masked CH2-aIgM displayed significantly reduced cell binding indicated by multiple-fold increased on-cell affinity values and decreased saturation binding levels (Figure 5B; Supplementary Figure 5A). Furthermore, interactions of aIgM and CH2-aIgM with PBMCs isolated from healthy human donor blood were scrutinized revealing binding of aIgM likely to the B cell subpopulation while the blocked aIgM antibody largely spares PBMCs (Supplementary Figure 5B). These results suggest that masking the aIgM antibody using a covalently linked blocking domain increases the likelihood of the mask remaining on the antibody due to loss of conformational degrees of freedom and high affinity, and thus significantly reduces binding of IgM. However, the MMP-9 treated CH2-aIgM revealed recovery in binding which indicates dissociation of the linker-cleaved CH2 domain from the antibody by reasons of competition with a high number of IgM BCRs in a cellular context (Figure 5). While covalent linkage of the CH2 domain shows efficient masking, presence of the cleaved masking unit reduces cell binding of the unmasked antibody to some extent (Supplementary Figure 6). This may be attributed to the relatively high concentration of masked antibody used (100 nM) and the slow dissociation kinetics of the masking CH2 domain.

Overall, transferring the features of the masked IgM antibody in a physiological setting, the blocked antibody is expected to be inert to interactions and interceptions related to IgM in systemic circulation while linker hydrolysis in the tumor microenvironment might result in localized unrestricted binding capacity and robust tumor targeting.

Cytotoxicity of masked and protease-activated CH2-aIgM ADC

For investigation of cytotoxicity mediated by an aIgM ADC and its masked variant CH2-aIgM ADC, both antibody versions were armed with MMAE generating ADCs with an expected DAR of two. Attachment of DBCO-PEG_4-Val-Cit-PAB-MMAE to the antibodies was accomplished site-specifically by a two-step approach of enzyme-assisted azide modification of the heavy chain's C-terminus which was endowed with a recognition sequence for lipoate-protein ligase A and click chemistry with DBCO-conjugated payload. Prior to cytotoxicity studies aIgM and CH2-masked aIgM were investigated towards internalization properties using our antibodies labeled with pH-dependent dye and flow cytometric analysis (54–56). In IgM^+ cell lines, the

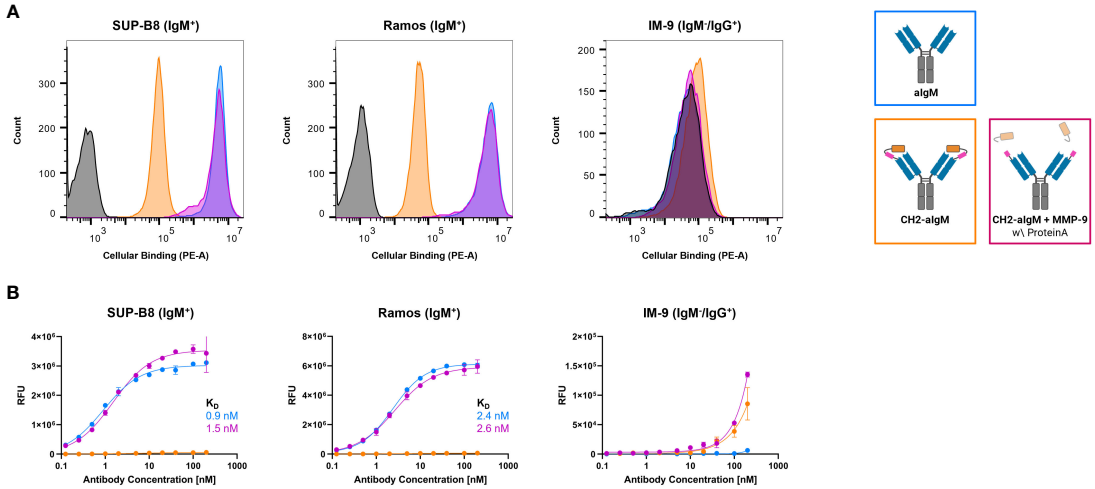

FIGURE 5
Cellular binding of unmasked and CH2-masked aIgM variants. Flow cytometry analysis of IgM^+ (SUP-B8, Ramos) and IgM^- (IM-9) B cells incubated with aIgM, CH2-aIgM and Protein A purified CH2-aIgM+MMP-9 antibodies and stained via anti-human IgG Fc-PE secondary detection antibody. **(A)** B cells were incubated with 100 nM of respective antibodies. Negative control samples (0 nM, black) represent cells stained with secondary detection antibody only. Histograms were created using FlowJoTM v10 Software (BD Life Sciences). **(B)** Cell titration of respective antibodies (0.125-200 nM) on B cells. On-cell K_Ds were determined using variable slope four-parameter fit. Results are shown as mean RFU, error bars represent standard deviation derived from experimental duplicates. Data is representative of three independent experiments.

proportion of endocytosed aIgM increased concentration-dependently reaching saturation in the single-digit nanomolar range while significantly less internalization was detected for CH2-aIgM (Figure 6). Internalization of aIgM and CH2-aIgM was barely measurable in IgM$^-$ B cells. Data points of internalization measurement were removed for clarity but are available in the Supplementary Material for all investigated molecules (Supplementary Figure 7).

First, *in vitro* cytotoxicity studies were conducted with aIgM-MMAE, its masked variant CH2-aIgM-MMAE as well as a pre-cleaved, Protein A purified CH2-aIgM-MMAE version using on-target SUP-B8 and Ramos cells while IM-9 served as off-target cells. Consistent with the internalization properties of aIgM in target cells, IgM$^+$ cells were sensitive to aIgM ADC-induced cell death (Figure 6). The aIgM ADC displayed potent dose-dependent cell killing with EC_{50} values amounting to 0.43 nM and 0.66 nM for SUP-B8 and Ramos cells, respectively. No significant reduction in cell proliferation was observed by application of the aIgM-MMAE molecule to IM-9 B cells not expressing IgM. Paratope-masked aIgM ADC was unable to mediate cell death in any cell line, which we expected since no endogenous proteolytic activity was observed in cell culture supernatants supplemented with CH2-aIgM during 72 h of incubation (data not shown). Notably, MMP-9 and matriptase activity was detected in B cell lymphoma tumor tissue warranting the concept of protease-mediated antibody activation (33, 34). The activity of aIgM was mostly restored after linker hydrolysis since CH2-aIgM pre-treated with MMP-9 resulted in significantly decreased survival of IgM$^+$ cells. Comparing potencies of the parental unmasked ADC to the pre-cleaved CH2-aIgM, an approximately 5-fold reduced cytotoxic effect was observed on SUP-B8 cells, whilst on Ramos cells efficacy was fully recovered (Figure 6). Besides comparable induction of lymphoma cell killing in EC_{50} values, similar levels in maximal cell lysis were observed. MMP-9 treated unpurified CH2-aIgM ADC, revealed 8-9-fold increased half maximal effective doses compared to the parental unmasked ADC in target lymphoma cells (Supplementary Figure 8).

Next, we investigated whether apoptosis was triggered by aIgM-MMAE and CH2-aIgM-MMAE. To this end, cells expressing BCRs of IgM and IgG isotype were treated with the respective ADCs for 72 h and analyzed by Annexin V-FITC and propidium iodide (PI) staining using flow cytometry. Application of 50 nM aIgM-MMAE resulted in increased fractions of Annexin V-FITC-positive IgM$^+$ cells, indicating that apoptosis was induced by antibody-guided chemotherapeutic damage (Figure 7). SUP-B8 and Ramos cells being exposed to aIgM-MMAE showed approximately 4-fold and 26-fold increase in Annexin V-FITC positivity, respectively, compared to untreated control cells (0 nM). Previous investigations have postulated that MMAE induces cell death through a rarely studied mechanism termed mitotic catastrophe possibly being a prelude mechanism to apoptotic or necrotic cell death and further includes signs of autophagy (57–60). In contrast, CH2 masked aIgM ADC did not induce any killing detectable by Annexin V-FITC or PI staining. Likewise, IM-9 IgM$^-$/IgG$^+$ off-target cells remained unaffected during aIgM ADC treatment.

Discussion

Overcoming the limitations of treatment paradigms for B cell NHL, novel approaches of highly potent immunotherapies that work in concert with the host immune system such as bispecific T cell engaging antibodies and chimeric antigen receptor (CAR) T cells have been introduced (61–64). Great efforts have further been made in probing antibody-drug conjugates for lymphoma therapies. Brentuximab vedotin, Polatozumab vedotin and Loncastuximab tesirine represent FDA-approved ADCs to treat different types of B cell lymphoma, targeting antigens such as CD30, which is expressed by activated B cells, CD79b, and CD19, present on all B cell types apart from pre-proB cells and mature plasma cells (32, 65–67).

Besides selection of an appropriate antibody ensuring to reach the tumor target site without affecting healthy cells in the periphery, linker and cytotoxic payload are key design parameters in ADCs.

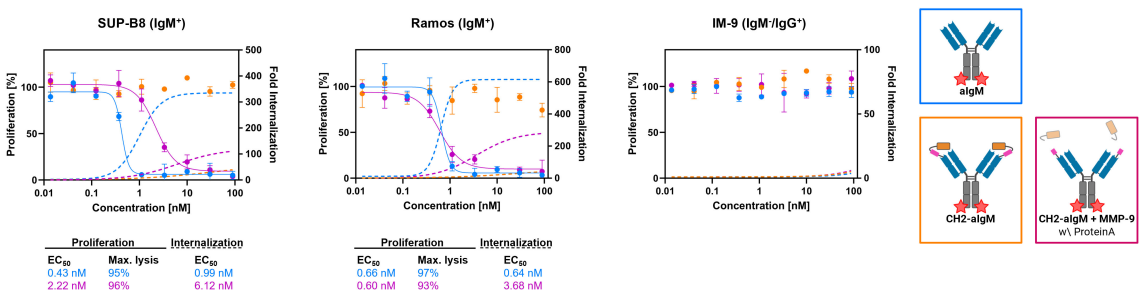

FIGURE 6
Internalization and cytotoxicity of unmasked and CH2-masked aIgM ADC variants towards B cells. For cytotoxicity studies IgM$^+$ (SUP-B8, Ramos) and IgM$^-$ (IM-9) B cells were exposed to varying concentrations (0.014-90 nM) of aIgM, CH2-aIgM and Protein A purified CH2-aIgM+MMP-9 MMAE-conjugated antibodies for 72 h. Cell proliferation was normalized to untreated control cells (0 nM). For internalization studies pHAb-conjugated aIgM, CH2-aIgM and Protein A purified CH2-aIgM+MMP-9 (0.014-90 nM) were applied to B cells and incubated overnight. Fold internalization was defined by the ratio of relative fluorescence units (RFU) of the respective antibody sample and the untreated sample without antibody (0 nM). EC_{50}s were determined using variable slope four-parameter fit. Results are shown as mean, error bars represent standard deviation derived from experimental duplicates.

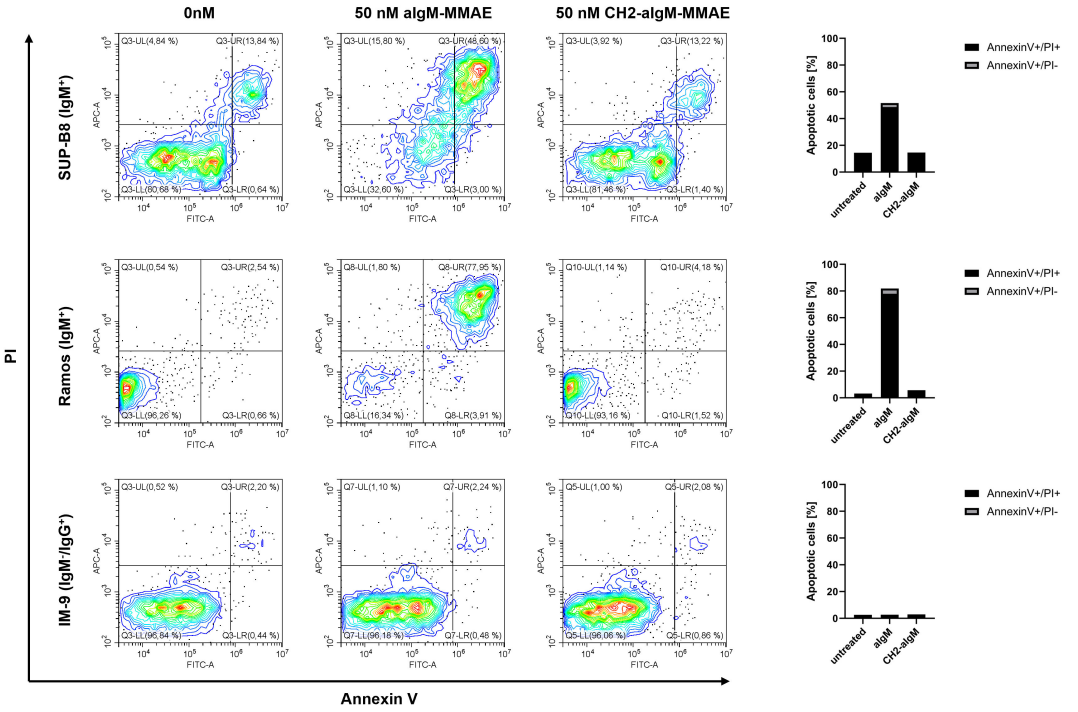

FIGURE 7
Apoptosis induction of aIgM and CH2-masked aIgM ADC in B cells. IgM$^+$ (SUP-B8, Ramos) and IgM$^-$ (IM-9) B cells were exposed to 0 nM, 50 nM of aIgM-MMAE and 50 nM CH2-aIgM-MMAE for 72 h. Cells were stained with Annexin V-FITC and propidium iodide (PI) and analyzed by flow cytometry. Percentage of Annexin V-FITC+/PI+ and Annexin V-FITC+/PI- (apoptotic cells) is depicted in right bar chart. Data is representative of two independent experiments.

Related to those criterions is the DAR which plays a pivotal role determining ADC's potency, safety, and pharmacokinetics. In general, higher drug loading comes along with increased anti-tumor activity. However, improvement in efficacy is limited and excessive cytotoxic payload may cause instabilities and aggregation and further lead to inferior pharmacokinetics such as in plasma clearance and tumor exposure (68, 69). *Bryant et al.* demonstrated that a DAR of 4 in a (trastuzumab) conjugate revealed highest potency *in vitro* and a significantly increased *in vivo* efficacy compared to the lower DAR conjugates (70). Referred to as the first approved mAb for cancer patients, auristatin-based rituximab ADCs have been developed with DARs of 7-7.5 and 4.2, respectively, both demonstrating potent therapeutic efficacy *in vitro* and *in vivo* (60, 71). Hence, further improvements may be reached for the CH2-masked aIgM ADC by examination of optimal drug loading but were out-of-scope for this proof-of-concept study.

To further promote safety and efficacy of ADCs several innovative approaches have been developed in the last decades. One of them includes the generation of a bispecific ADC that targets HER2 as tumor-associated antigen and CD63 rendering enhanced lysosomal delivery (72). Another appealing tool is introduced by CytomX Therapeutics with the probody platform expanding the availability of new targets for ADCs by antibody paratope masking and tumor-specific protease-activation. Probody-drug conjugates are supplied with a protease cleavable linker connected to a peptide mask limiting target engagement in normal tissue and circulation (73). CX-2029 targeting transferrin receptor 1 (CD71) attached to MMAE is currently being investigated in phase II clinical trials displaying translational and clinical activity at tolerable doses in patients (27, 73).

In this study, we present a novel conditionally activated anti-IgM antibody-drug conjugate for precise B cell lymphoma elimination. To this end, we isolated a chicken-derived IgM-specific antibody (aIgM), which was further fused to the epitope-holding IgM domain CH2 by a tumor-protease cleavable linker ultimately equipped with the cytotoxic payload MMAE. Efficient blockage of the tumor targeting moiety in CH2-aIgM was confirmed by biolayer interferometry. The masked antibody regained activity upon protease treatment, displaying affine binding to IgM from human serum. On a cellular level CH2-aIgM was inert to interact with IgM$^+$ B cells while the cleaved variant revealed excellent on-cell affinities comparable to the parental unmasked antibody regarding on-cell affinity constants in the low single-digit nanomolar range as well as maximum binding capacities. This allows penetration into the tumor microenvironment without being captured by soluble IgM or non-malignant IgM$^+$ B cells ultimately improving pharmacokinetic properties. Reaching the tumor target site, tumor-protease-mediated linker hydrolysis engenders high affinity targeting. The aIgM ADC demonstrated specific and effective receptor-mediated cellular uptake which was closely linked to killing of lymphoma cells exhibiting strong signs of apoptotic cell death. Cytotoxicity of the inactive ADC version was shown to be reduced since no cell killing was observed in the investigated concentration range, thus potentially preventing systemic side effects. CH2-aIgM is rendered active by proteases leading to regained toxicity towards malignant IgM$^+$ B

lymphocytes. Further animal studies are required to reveal whether the restrictive and potent *in vitro* anti-tumor efficacy of the antibody introduced in this study can be confirmed *in vivo*.

Our results further show that it is feasible to generate proteolytically activated antibody-drug conjugates against immunoglobulins of isotype (Ig)M for B cell lymphoma treatment. This novel strategy of Ig targeting in B cell-derived malignancies may be superior to conventional approaches in several respects. By addressing only a fraction of B cells, unwanted on-target off-tumor effects are reduced which is further enhanced through the masking functionality while conventional pan-B cell targeting results in patients suffering from B cell-aplasia induced immunosuppression (74). In case of the anti-CD20 antibody rituximab, various resistance mechanisms are existing such as tumor-dependent alterations e.g., antigen downregulation and antigenic modulation or host-dependent immunologic factors e.g., Fc receptor polymorphisms (75–79). Alternative attempts addressing the BCR include patient-specific anti-idiotypic peptides or antibodies against variable regions, however, laborious and time-consuming manufacturing may limit developability (80–83). We propose an alternative mechanism of tumor clearance providing the possibility to therapy relapsed or refractory NHL in the second- or third-line setting solely implying BCR sequencing to identify the disease-causing B cell clone. This concept would be effortlessly applicable to different kinds of B cell-derived malignancies as there are only four human Ig isotypes (IgM, IgG, IgD, IgA) expressed as BCRs, against which antibodies are already available and can in a next step be masked by the respective epitope-bearing Ig domains. As for the CH2-masked aIgM antibody, further protein or antibody engineering may be required to fine-tune the affinity, particularly concerning the off-rate of the blocking moiety to the antibody. In this *in vitro* study, the cleaved IgM CH2 masking unit not being removed from the assay sample associates to the aIgM paratope and thus hampers full functionality of the antibody in terms of (cell) binding and cytotoxicity requiring further purification to decrease the molar ratio of CH2 to corresponding aIgM antibody. In the body, demasking is mediated by proteases such as MMP-9 and matriptase described to be prognostic factors for B cell lymphoma when overexpressed (33, 34). The mechanisms of masking domain release may be shaped by multiple variables *in vivo*. Each individual binding event is a one-step reversible biomolecular process obeying the law of mass action. While interaction to cut CH2 is of monovalent nature, binding to IgM on B cells involves both antibody valences showing avidity effects. Moreover, unrestricted diffusion of the soluble masking domain in blood is opposed to spatial clustered B cell surface receptors effecting rebinding of aIgM which likely leads to local dilution of the masking domain ultimately resulting in preferred cell binding (84, 85). Contrary to synthetic peptide masks, the Ig domain used for paratope-blocking is of human origin reducing the risk of immunogenicity. However, aIgM is a chimeric antibody constituted of chicken-derived variable domains fused to human IgG1 constant domains. Hence, humanization is required to minimize immunogenicity in therapeutic applications. Our group recently developed a straightforward method to humanize avian-derived antibodies by CDR grafting onto a human germline framework based on Vernier residue randomization that could be applied for this purpose but is beyond the scope of this study (86, 87).

Taken together, our approach demonstrates a novel mechanism to specifically eradicate NHL B cells while preserving healthy human B lymphocytes that do not display IgM isotype BCRs. Constituting an inactive anti-IgM antibody-drug conjugate which is actuated in the proteolytic tumor environment, the molecule unites an enhanced safety profile due to tumor-proximity restricted activation and potent anti-tumor efficacy relying on a highly cytotoxic payload. Furthermore, our study provides a basis for the development of protease-activated anti-Ig ADCs for the treatment of B cell-driven pathologies.

Materials and methods

Chicken immunization and yeast library construction

Chicken immunization and scFv yeast surface display library generation were performed as described previously (48). In brief, an adult chicken (*Gallus gallus domesticus*) was immunized with IgM from human serum (Sigma Aldrich) on days 1, 14, 28, 35, and 56. The animal was sacrificed on day 63, followed by isolation of the spleen and total RNA extraction. The immunization process as well as splenic RNA isolation were executed by Davids Biotechnologie GmbH (Regensburg, Germany). For library construction, RNA was reverse transcribed to cDNA. Subsequently, genes encoding VH and VL were amplified and transferred into a YSD vector (pCT) via homologous recombination in yeast (*Saccharomyces cerevisiae* strain EBY100). Library generation in EBY100 cells was conducted according to Benatuil and colleagues (88). Cultivation and general handling of yeast cells are described elsewhere (48, 83).

Yeast library screening

Induction of gene expression and scFv surface presentation was achieved by inoculation of yeast cells in Synthetic Galactose minimal medium with Casein Amino Acids (SG-CAA) at an OD_{600} of 1.0 and incubation overnight at 30°C and 180 rpm. For library sorting, cells were harvested by centrifugation and washed with PBS+0.1% (w/v) BSA (PBS-B). Antigen staining was conducted with DyLight650™-labelled IgM from human serum (Sigma Aldrich) conjugated beforehand using 5-fold excess of DyLight650™ NHS Ester (Thermo Fisher Scientific). Simultaneously, staining for surface presentation using anti-cMyc antibody FITC-conjugated (Miltenyi Biotec; diluted 1:50) was performed for 30 min on ice. After another PBS-B washing step, the yeast library was screened using BD Influx cell sorter with corresponding BD FACS Sortware v1.0.

Expression and purification of scFv, scFv-Fc and Fab-Fc variants

Reformatting, expression and purification of scFvs was performed as described previously (89). Briefly, isolated yeast vectors were sequenced and scFv encoding genes were reformatted into a pET30 plasmid using golden gate assembly,

followed by recombinant expression in *E. coli* SHuffle® T7 Express (New England Biolabs). A two-step affinity purification was performed including IMAC and Strep-Tactin®XT purification, followed by buffer exchange against PBS. Production of Fc-fused scFvs and full-length antibodies (Fab-Fc) was conducted with pTT5-derived golden gate assembly vectors in Expi293F™ cells (Thermo Fisher Scientific). Expi293F™ cells were transiently transfected using ExpiFectamine™ 293 Transfection Kit (Thermo Fisher Scientific) following the manufacturer's protocol. For purification of Fc-containing antibody constructs, cell culture supernatants were collected five days post transfection, sterile filtered and applied to a HiTrap™ Protein A HP column (GE Healthcare) using an ÄKTA pure™ chromatography system (GE Healthcare). Buffer exchange against PBS or TBS was performed using a HiTrap™ Desalting column (GE Healthcare).

Cell lines

B cells including SUP-B8, IM-9 and Ramos cells were cultured at 37°C and 5% CO_2. All B cell lines were maintained in RPMI-1640 supplemented with 15% FBS and 1% Penicillin-Streptomycin and sub-cultured every 2-3 days. Expi293F™ cells were cultured in Expi293™ Expression Medium (Thermo Fisher Scientific), sub-cultured every 3-4 days and incubated at 37°C and 8% CO_2.

Protease-mediated protein hydrolysis

Recombinant human MMP-9 (Acro Biosystems) or recombinant human matriptase/ST14 catalytic domain (Bio-Techne) were used to cleave the dual-protease cleavable linker of CH2-aIgM. Prior to the protein hydrolysis reaction, MMP-9 was pre-activated with 1 mM 4-aminophenylmercuric acetate (APMA) overnight at 37°C. Proteins were dissolved in TBS pH 7.4, if necessary, by buffer exchange, ensuring suitable conditions for the MMP-9 and matriptase hydrolysis reaction. 0.25 mg of the respective antibody variant was mixed with 0.25 µg (0.1 mg/ml) of activated human MMP-9 or matriptase. Protein cleavage was performed at 37°C for 48 h. Complete linker hydrolysis was confirmed using SDS-PAGE under reducing conditions. Cleaved CH2-aIgM protein was further purified using Protein A spin columns (Protein A HP SpinTrap, Cytiva) in order to remove fractions of the masking IgM CH2 domain.

Thermal shift assay

Experiments to determine thermal stability were performed using a CFX Connect Real-Time PCR Detection System (BioRad) with a temperature gradient from 20°C to 95°C and 0.5°C/10 s. The derivatives of the melt curves were calculated with the corresponding BioRad CFX Maestro software to determine the melt temperature (Tm). All reactions were performed in PBS in presence of 0.1 mg/ml protein and SYPRO Orange (Thermo Fisher Scientific, diluted 1:100).

Biolayer interferometry

For biolayer interferometric measurements the Octet RED96 system (ForteBio, Sartorius) was used. Therefore, respective biosensor tips were soaked in PBS pH 7.4 for at least 10 min before assay start.

For epitope binning, Ni-NTA Biosensors (NTA, Sartorius) were loaded with cell culture supernatants of single His-tagged IgM domains expressed in Expi293F™ cells. All following steps were performed using kinetics buffer (KB, Sartorius). Association was measured for 180 s with 150 nM aIgMscFv-Fc followed by dissociation for 180 s.

For the CH2/IgM competition assay, High Precision Streptavidin biosensors (SAX, Sartorius) were loaded biotinylated aIgMscFv-Fc. After quenching in KB, two association steps of 250 s were conducted in sequence, a first association step using either 100 nM IgM from human serum (Sigma Aldrich) or 1,000 nM IgM CH2 was followed by a second association using 1,000 nM IgM CH2 or 100 nM serum, respectively.

For affinity determination of aIgMscFv-Fc and aIgMFab-Fc anti-human IgG Fc capture biosensors (AHC, Sartorius) were used to immobilize the aIgM antibodies. After a quenching step in KB, an association step using CH2-His with concentrations ranging from 31.25 to 500 nM or IgM from human serum (Sigma Aldrich) was performed followed by a dissociation step in KB. Association in KB served as reference and was subtracted prior to evaluation steps. Data analysis was performed using ForteBio data analysis software 9.0. Binding kinetics including the equilibrium constant K_D were determined using Savitzky-Golay filtering and 1:1 Langmuir model.

To confirm that the parental full-length aIgM antibody binds to IgM and IgM-derived CH2, aIgM antibody was loaded onto AHC biosensor tips, followed by quenching in KB, association with 50 nM IgM from human serum or 250 nM IgM CH2 and dissociation in PBS. In the same experimental setup, binding of aIgM, CH2-aIgM, non-purified and Protein A purified CH2-aIgM+MMP-9 and rituximab (control) were evaluated for IgM binding by association of 100 nM or 3.9-125 nM IgM from human serum. In a reverse experimental setup, biotinylated IgM from human serum was loaded onto SAX biosensor tips. After a quenching step in KB, 100 nM of the respective antibody variants were associated.

PBMC isolation

Peripheral blood mononuclear cells (PBMCs) were isolated from buffy coats from healthy human donors supplied by the Deutsche Rotes Kreuz (Frankfurt). To this end, 25 ml blood was mixed 1:1 with PBS +2% (w/v) FBS and PBMCs were purified using SepMate-50 tubes following the manufacturer's instructions (StemCell Technologies).

Cellular binding

Cellular binding of the antibodies was determined by affinity titration using IgM^+ SUP-B8 and Ramos cells. IgM^- (IgG^+) IM-9 cells were used to analyze unspecific cell binding. To this end, cells ($1.5x10^5$ cells/well) were washed with PBS-B and subsequently incubated with the respective antibody constructs in varying concentrations (for cell titration: 0.125-200 nM, serial dilution) for 30 min on ice. Followed by another PBS-B washing step, anti-human IgG Fc PE-conjugated secondary antibody (Thermo Fisher Scientific, diluted 1:50), anti-his AF647-conjugated secondary antibody (Thermo Fisher Scientific, diluted 1:50) or Streptavidin-APC conjugate (Thermo Fisher Scientific, diluted 1:50) was applied for 20 min on ice. After final washing with PBS-B, flow cytometry was performed using CytoFLEX S System (Beckman Coulter). The relative fluorescence units (RFU) were plotted against the respective logarithmic antibody concentration. The resulting curves were fitted with a variable slope four-parameter fit using GraphPad Prism.

Internalization assays

Investigations towards receptor-mediated antibody internalization were performed using pHAb Amine Reactive dye (Promega) according to the manufacturer's instructions. In brief, aIgM, CH2-aIgM, non-purified and Protein A purified CH2-aIgM +MMP-9 were conjugated with pHAb dyes and applied to B cells ($2x10^4$ cells/well) in different concentrations (0.014-90 nM) in a 96-well plate. After incubation overnight, cells were washed once with PBS and internalization was measured using flow cytometry. Fold internalization was determined by the ratio of relative fluorescence units (RFU) of the respective antibody sample and the untreated sample without antibody (0 nM). The resulting curves were fitted with a variable slope four-parameter fit and EC_{50}s were calculated using GraphPad Prism.

Generation of antibody-drug conjugates

Antibody-drug conjugates were generated via a two-step approach of enzymatic modification and click chemistry for conjugation of monomethyl auristatin E (MMAE) to the Fc fragment. Therefore, the C-terminus of the antibody heavy chain was genetically fused with a lipoic acid ligase acceptor peptide (LAP) serving as recognition sequence for lipoate-protein ligase A (LplA) from *Escherichia coli* (90). Lipoic acid ligase reaction was conducted with 0.1 equivalents (eq.) of a mutant lipoic acid ligase A ($LplA^{W37V}$) (91) accepting various carboxylic acid derivatives in the presence of 5 mM ATP, 5 mM Mg $(Ac)_2$ and 10-20 eq. azide-bearing lipoic acid derivative (synthesized in-house) in PBS pH 7.4 for 1h at 37°C. Covalent protein azide-functionalization was confirmed by hydrophobic interaction chromatography followed by click reaction with 5 eq. DBCO-PEG_4-Val-Cit-PAB-MMAE on Protein A resin (Protein A HP SpinTrap, Cytiva) overnight at 4°C. After acidic elution of ADC from Protein A column the buffer was exchanged to PBS pH 7.4.

Cytotoxicity assays

Cytotoxic effects of aIgM ADCs were evaluated by exposing IgM^+ lymphoma B cells or off-target (IgM^-) cells to different ADC concentrations. Cell viability was analyzed 72 h post ADC addition by a colorimetric method using CellTiter 96® AQ_{ueous} One Solution Cell Proliferation Assay (Promega). Briefly, cells were seeded ($1x10^4$ cells/well) in a 96-well plate with the desired antibody concentrations ranging from 0.014-90 nM in a serial dilution. After 72 h, MTS solution was added to the cells and plate was incubated for 2 h. Absorption was measured at 490 nm using CLARIOstar plus microplate reader (BMG LABTECH). Cell proliferation was normalized to untreated control cell absorption values. The resulting curves were fitted with a variable slope four-parameter fit and EC_{50}s were calculated using GraphPad Prism.

Apoptosis assays

For AnnexinV-FITC/PI staining ROTITEST® Annexin V (Carl Roth GmbH + Co. KG) was applied for apoptosis detection of B cells according to the manufacturer's instructions. The analysis was performed using CytoFLEX S System (Beckman Coulter).

Data availability statement

The raw data supporting the conclusions of this article will be made available by the authors, without undue reservation.

Ethics statement

Ethical approval was not required for the studies on animals because animal (chicken) immunization was performed by Davids Biotechnologie GmbH. Experimental procedures and animal care were in accordance with EU animal welfare protection laws and regulations.

Author contributions

KS: Conceptualization, Investigation, Data curation, Writing - original draft. JuH: Investigation, Writing - review & editing. JaH: Investigation, Writing - review & editing. AE: Conceptualization, Writing - review & editing. HK: Conceptualization, Project administration, Writing - original draft.

Funding

The authors declare financial support was received for the research, authorship, and/or publication of this article. Funding for this work was provided in part by the Ministry of Higher Education, Research and Arts of the State of Hesse under the LOEWE project "TRABITA".

Acknowledgments

The authors would like to thank Peter Bitsch for synthesis of azide-modified lipoic acid and Sebastian Harald Bitsch for the provision of LplA enzyme. We acknowledge support by the Deutsche Forschungsgemeinschaft (DFG – German Research Foundation) and the Open Access Publishing Fund of Technical University of Darmstadt.

Conflict of interest

The authors declare that the research was conducted in the absence of any commercial or financial relationships that could be construed as a potential conflict of interest.

Publisher's note

Supplementary material

The Supplementary Material for this article can be found online at: https://www.frontiersin.org/articles/10.3389/fimmu.2023.1258700/full#supplementary-material

References

1. Lu R-M, Hwang Y-C, Liu I-J, Lee C-C, Tsai H-Z, Li H-J, et al. Development of therapeutic antibodies for the treatment of diseases. *J BioMed Sci* (2020) 27:1. doi: 10.1186/s12929-019-0592-z

2. Siegel RL, Miller KD, Wagle NS, Jemal A. Cancer statistics, 2023. *CA Cancer J Clin* (2023) 73:17–48. doi: 10.3322/caac.21763

3. Pierpont TM, Limper CB, Richards KL. Past, present, and future of rituximab-the world's first oncology monoclonal antibody therapy. *Front Oncol* (2018) 8:163. doi: 10.3389/fonc.2018.00163

4. Hofmeister JK, Cooney D, Coggeshall KM. Clustered CD20 induced apoptosis: src-family kinase, the proximal regulator of tyrosine phosphorylation, calcium influx, and caspase 3-dependent apoptosis. *Blood Cells Molecules Dis* (2000) 26:133–43. doi: 10.1006/bcmd.2000.0287

5. Rezvani AR, Maloney DG. Rituximab resistance. *Best Pract Res Clin Haematol* (2011) 24:203–16. doi: 10.1016/j.beha.2011.02.009

6. Jazirehi AR, Vega MI, Bonavida B. Development of rituximab-resistant lymphoma clones with altered cell signaling and cross-resistance to chemotherapy. *Cancer Res* (2007) 67:1270–81. doi: 10.1158/0008-5472.CAN-06-2184

7. Su Q, Chen M, Shi Y, Zhang X, Huang G, Huang B, et al. Cryo-EM structure of the human IgM B cell receptor. *Science* (2022) 377:875–80. doi: 10.1126/science.abo3923

8. Kwak K, Akkaya M, Pierce SK. B cell signaling in context. *Nat Immunol* (2019) 20:963–9. doi: 10.1038/s41590-019-0427-9

9. D'Avola A, Drennan S, Tracy I, Henderson I, Chiecchio L, Larrayoz M, et al. Surface IgM expression and function are associated with clinical behavior, genetic abnormalities, and DNA methylation in CLL. *Blood* (2016) 128:816–26. doi: 10.1182/blood-2016-03-707786

10. Ruminy P, Etancelin P, Couronné L, Parmentier F, Rainville V, Mareschal S, et al. The isotype of the BCR as a surrogate for the GCB and ABC molecular subtypes in diffuse large B-cell lymphoma. *Leukemia* (2011) 25:681–8. doi: 10.1038/leu.2010.302

11. Cox MC, Di Napoli A, Scarpino S, Salerno G, Tatarelli C, Talerico C, et al. Clinicopathologic characterization of diffuse-large-B-cell lymphoma with an associated serum monoclonal IgM component. *PloS One* (2014) 9:e93903. doi: 10.1371/journal.pone.0093903

12. Cox MC, Marcheselli L, Scafetta G, Visco C, Hohaus S, Annibali O, et al. IgM-secreting diffuse large B-cell lymphoma: results of a multicentre clinicopathological and molecular study. *Leukemia* (2022) 36:2719–23. doi: 10.1038/s41375-022-01706-x

13. Ohashi T, Miyashita H, Nagata Y, Otsuka H, Suzuki H, et al. A Novel Anti-IgM/HLA-DR Bispecific Antibody for Treatment of Refractory B Cell Malignancies. *Blood* (2018) 132:1670. doi: 10.1182/blood-2018-99-117552

14. Lucchi R, Bentanachs J, Oller-Salvia B. The masking game: design of activatable antibodies and mimetics for selective therapeutics and cell control. *ACS Cent Sci* (2021) 7:724–38. doi: 10.1021/acscentsci.0c01448

15. Polu KR, Lowman HB. Probody therapeutics for targeting antibodies to diseased tissue. *Expert Opin Biol Ther* (2014) 14:1049–53. doi: 10.1517/14712598.2014.920814

16. Lin W-W, Lu Y-C, Chuang C-H, Cheng T-L. Ab locks for improving the selectivity and safety of antibody drugs. *J BioMed Sci* (2020) 27:76. doi: 10.1186/s12929-020-00652-z

17. Duffy MJ. Proteases as prognostic markers in cancer. *Clin Cancer Res* (1996) 2:613–8.

18. Rakash S. Role of proteases in cancer: A review. *Biotechnol Mol Biol Rev* (2012) 7:90–101. doi: 10.5897/BMBR11.027

19. Duffy MJ. The role of proteolytic enzymes in cancer invasion and metastasis. *Clin Exp Metastasis* (1992) 10:145–55. doi: 10.1007/BF00132746

20. Elter A, Yanakieva D, Fiebig D, Hallstein K, Becker S, Betz U, et al. Protease-activation of fc-masked therapeutic antibodies to alleviate off-tumor cytotoxicity. *Front Immunol* (2021) 12:715719. doi: 10.3389/fimmu.2021.715719

21. Geiger M, Stubenrauch K-G, Sam J, Richter WF, Jordan G, Eckmann J, et al. Protease-activation using anti-idiotypic masks enables tumor specificity of a folate receptor 1-T cell bispecific antibody. *Nat Commun* (2020) 11:3196. doi: 10.1038/s41467-020-16838-w

22. Naing A, Thistlethwaite F, de VEG, FA E, Uboha N, Ott PA, et al. CX-072 (pacmilimab), a Probody ® PD-L1 inhibitor, in advanced or recurrent solid tumors (PROCLAIM-CX-072): an open-label dose-finding and first-in-human study. *J Immunother Cancer* (2021) 9:e002447. doi: 10.1136/jitc-2021-002447

23. Etxeberria I, Bolaños E, Teijeira A, Garasa S, Yanguas A, Azpilikueta A, et al. Antitumor efficacy and reduced toxicity using an anti-CD137 Probody therapeutic. *Proc Natl Acad Sci U.S.A.* (2021) 118:e2025930118. doi: 10.1073/pnas.2025930118

24. Cattaruzza F, Nazeer A, To M, Hammond M, Koski C, Liu LY, et al. Precision-activated T-cell engagers targeting HER2 or EGFR and CD3 mitigate on-target, off-tumor toxicity for immunotherapy in solid tumors. *Nat Cancer* (2023) 4:485–501. doi: 10.1038/s43018-023-00536-9

25. Boustany LM, LaPorte SL, Wong L, White C, Vinod V, Shen J, et al. A probody T cell-engaging bispecific antibody targeting EGFR and CD3 inhibits colon cancer growth with limited toxicity. *Cancer Res* (2022) 82:4288–98. doi: 10.1158/0008-5472.CAN-21-2483

26. Gutierrez M, Friedman CF, Long GV, Ascierto PA, Melero I, Richards D, et al. 740P Anti-cytotoxic T-lymphocyte antigen-4 (CTLA 4) probody BMS-986249 ± nivolumab (NIVO) in patients (pts) with advanced cancers: Updated phase I results. *Ann Oncol* (2022) 33:S882. doi: 10.1016/j.annonc.2022.07.866

27. Singh S, Serwer L, DuPage A, Elkins K, Chauhan N, Ravn M, et al. Nonclinical efficacy and safety of CX-2029, an anti-CD71 probody-drug conjugate. *Mol Cancer Ther* (2022) 21:1326–36. doi: 10.1158/1535-7163.MCT-21-0193

28. Johnson M, El-Khoueiry A, Hafez N, Lakhani N, Mamdani H, Rodon J, et al. First-in-human study of the probody therapeutic CX-2029 in adults with advanced solid tumor Malignancies. *Clin Cancer Res* (2021) 27:4521–30. doi: 10.1158/1078-0432.CCR-21-0194

29. Alley SC, Okeley NM, Senter PD. Antibody-drug conjugates: targeted drug delivery for cancer. *Curr Opin Chem Biol* (2010) 14:529–37. doi: 10.1016/j.cbpa.2010.06.170

30. Fu Z, Li S, Han S, Shi C, Zhang Y. Antibody drug conjugate: the "biological missile" for targeted cancer therapy. *Signal Transduct Target Ther* (2022) 7:93. doi: 10.1038/s41392-022-00947-7

31. Sievers EL. Efficacy and safety of gemtuzumab ozogamicin in patients with CD33-positive acute myeloid leukaemia in first relapse. *Expert Opin Biol Ther* (2001) 1:893–901. doi: 10.1517/14712598.1.5.893

32. Samantasinghar A, Sunildutt NP, Ahmed F, Soomro AM, Salih AR, Parihar P, et al. A comprehensive review of key factors affecting the efficacy of antibody drug conjugate. *BioMed Pharmacother* (2023) 161:114408. doi: 10.1016/j.biopha.2023.114408

33. Sakata K, Satoh M, Someya M, Asanuma H, Nagakura H, Oouchi A, et al. Expression of matrix metalloproteinase 9 is a prognostic factor in patients with non-Hodgkin lymphoma. *Cancer* (2004) 100:356–65. doi: 10.1002/cncr.11905

34. Chou F-P, Chen Y-W, Zhao XF, Xu-Monette ZY, Young KH, Gartenhaus RB, et al. Imbalanced matriptase pericellular proteolysis contributes to the pathogenesis of Malignant B-cell lymphomas. *Am J Pathol* (2013) 183:1306–17. doi: 10.1016/j.ajpath.2013.06.024

35. Pettersen EF, Goddard TD, Huang CC, Meng EC, Couch GS, Croll TI, et al. UCSF ChimeraX: Structure visualization for researchers, educators, and developers. *Protein Sci* (2021) 30:70–82. doi: 10.1002/pro.3943

36. Wu L, Oficjalska K, Lambert M, Fennell BJ, Darmanin-Sheehan A, Ní Shúilleabháin D, et al. Fundamental characteristics of the immunoglobulin VH repertoire of chickens in comparison with those of humans, mice, and camelids. *J Immunol* (2012) 188:322–33. doi: 10.4049/jimmunol.1102466

37. Xu JL, Davis MM. Diversity in the CDR3 region of V(H) is sufficient for most antibody specificities. *Immunity* (2000) 13:37–45. doi: 10.1016/S1074-7613(00)00006-6

38. Krah S, Schröter C, Eller C, Rhiel L, Rasche N, Beck J, et al. Generation of human bispecific common light chain antibodies by combining animal immunization and yeast display. *Protein Eng Des Sel* (2017) 30:291–301. doi: 10.1093/protein/gzw077

39. Bogen JP, Carrara SC, Fiebig D, Grzeschik J, Hock B, Kolmar H. Design of a trispecific checkpoint inhibitor and natural killer cell engager based on a 2 + 1 common light chain antibody architecture. *Front Immunol* (2021) 12:669496. doi: 10.3389/fimmu.2021.669496

40. Bai R, Pettit GR, Hamel E. Dolastatin 10, a powerful cytostatic peptide derived from a marine animal. Inhibition of tubulin polymerization mediated through the vinca alkaloid binding domain. *Biochem Pharmacol* (1990) 39:1941–9. doi: 10.1016/0006-2952(90)90613-P

41. Chen H, Lin Z, Arnst KE, Miller DD, Li W. Tubulin inhibitor-based antibody-drug conjugates for cancer therapy. *Molecules* (2017) 22:1281. doi: 10.3390/molecules22081281

42. Johansson MP, Maaheimo H, Ekholm FS. New insight on the structural features of the cytotoxic auristatins MMAE and MMAF revealed by combined NMR spectroscopy and quantum chemical modelling. *Sci Rep* (2017) 7:15920. doi: 10.1038/s41598-017-15674-1

43. Han B, Yuan H, Wang T, Li B, Ma L, Yu S, et al. Multiple igH isotypes including IgD, subclasses of IgM, and IgY are expressed in the common ancestors of modern birds. *J Immunol* (2016) 196:5138–47. doi: 10.4049/jimmunol.1600307

44. Grönwall C, Vas J, Silverman GJ. Protective roles of natural IgM antibodies. *Front Immunol* (2012) 3:66. doi: 10.3389/fimmu.2012.00066

45. Díaz-Zaragoza M, Hernández-Ávila R, Viedma-Rodríguez R, Arenas-Aranda D, Ostoa-Saloma P. Natural and adaptive IgM antibodies in the recognition of tumor-associated antigens of breast cancer (Review). *Oncol Rep* (2015) 34:1106–14. doi: 10.3892/or.2015.4095

46. Larsson A, Bålöw RM, Lindahl TL, Forsberg PO. Chicken antibodies: taking advantage of evolution–a review. *Poult Sci* (1993) 72:1807–12. doi: 10.3382/ps.0721807

47. Davies EL, Smith JS, Birkett CR, Manser JM, Anderson-Dear DV, Young JR. Selection of specific phage-display antibodies using libraries derived from chicken immunoglobulin genes. *J Immunol Methods* (1995) 186:125–35. doi: 10.1016/0022-1759(95)00143-X

48. Grzeschik J, Yanakieva D, Roth L, Krah S, Hinz SC, Elter A, et al. Yeast surface display in combination with fluorescence-activated cell sorting enables the rapid isolation of antibody fragments derived from immunized chickens. *Biotechnol J* (2019) 14:e1800466. doi: 10.1002/biot.201800466

49. Bogen JP, Grzeschik J, Krah S, Zielonka S, Kolmar H. Rapid generation of chicken immune libraries for yeast surface display. *Methods Mol Biol* (2020) 2070:289–302. doi: 10.1007/978-1-4939-9853-1_16

50. Roth L, Grzeschik J, Hinz SC, Becker S, Toleikis L, Busch M, et al. Facile generation of antibody heavy and light chain diversities for yeast surface display by Golden Gate Cloning. *Biol Chem* (2019) 400:383–93. doi: 10.1515/hsz-2018-0347

51. Dussault N, Ducas E, Racine C, Jacques A, Paré I, Côté S, et al. Immunomodulation of human B cells following treatment with intravenous immunoglobulins involves increased phosphorylation of extracellular signal-regulated kinases 1 and 2. *Int Immunol* (2008) 20:1369–79. doi: 10.1093/intimm/dxn090

52. Carroll WL, Link MP, Cleary ML, Bologna S, Carswell C, Amylon MD, et al. Idiotype as a tumor-specific marker in childhood B cell acute lymphoblastic leukemia. *Blood* (1988) 71:1068–73. doi: 10.1182/blood.V71.4.1068.1068

53. Fahey JL, Buell DN, Sox HC. Proliferation and differentiation of lymphoid cells: studies with human lymphoid cell lines and immunoglobulin synthesis. *Ann N Y Acad Sci* (1971) 190:221–34. doi: 10.1111/j.1749-6632.1971.tb13537.x

54. Li Z, Wang M, Yao X, Li H, Li S, Liu L, et al. Development of novel anti-CD19 antibody-drug conjugates for B-cell lymphoma treatment. *Int Immunopharmacol* (2018) 62:299–308. doi: 10.1016/j.intimp.2018.06.034

55. Li Z, Wang M, Yao X, Luo W, Qu Y, Yu D, et al. Development of a novel EGFR-targeting antibody-drug conjugate for pancreatic cancer therapy. *Target Oncol* (2019) 14:93–105. doi: 10.1007/s11523-018-0616-8

56. Parameswaran N, Luo L, Zhang L, Chen J, DiFilippo FP, Androjna C, et al. CD6-targeted antibody-drug conjugate as a new therapeutic agent for T cell lymphoma. *Leukemia* (2023). doi: 10.1038/s41375-023-01997-8

57. Cunningham D, Parajuli KR, Zhang C, Wang G, Mei J, Zhang Q, et al. Monomethyl auristatin E phosphate inhibits human prostate cancer growth. *Prostate* (2016) 76:1420–30. doi: 10.1002/pros.23226

58. Portugal J, Mansilla S, Bataller M. Mechanisms of drug-induced mitotic catastrophe in cancer cells. *Curr Pharm Des* (2010) 16:69–78. doi: 10.2174/138161210789941801

59. Vakifahmetoglu H, Olsson M, Zhivotovsky B. Death through a tragedy: mitotic catastrophe. *Cell Death Differ* (2008) 15:1153–62. doi: 10.1038/cdd.2008.47

60. Wang Y, Zhang X, Fan J, Chen W, Luan J, Nan Y, et al. Activating autophagy enhanced the antitumor effect of antibody drug conjugates rituximab-monomethyl auristatin E. *Front Immunol* (2018) 9:1799. doi: 10.3389/fimmu.2018.01799

61. June CH, Sadelain M. Chimeric antigen receptor therapy. *N Engl J Med* (2018) 379:64–73. doi: 10.1056/NEJMra1706169

62. Schuster SJ, Svoboda J, Chong EA, Nasta SD, Mato AR, Anak Ö, et al. Chimeric antigen receptor T cells in refractory B-cell lymphomas. *N Engl J Med* (2017) 377:2545–54. doi: 10.1056/NEJMoa1708566

63. Jen EY, Xu Q, Schetter A, Przepiorka D, Shen YL, Roscoe D, et al. FDA approval: blinatumomab for patients with B-cell precursor acute lymphoblastic leukemia in morphologic remission with minimal residual disease. *Clin Cancer Res* (2019) 25:473–7. doi: 10.1158/1078-0432.CCR-18-2337

64. Falchi L, Vardhana SA, Salles GA. Bispecific antibodies for the treatment of B-cell lymphoma: promises, unknowns, and opportunities. *Blood* (2023) 141:467–80. doi: 10.1182/blood.2021011994

65. Chu Y, Zhou X, Wang X. Antibody-drug conjugates for the treatment of lymphoma: clinical advances and latest progress. *J Hematol Oncol* (2021) 14:88. doi: 10.1186/s13045-021-01097-z

66. Barreca M, Lang N, Tarantelli C, Spriano F, Barraja P, Bertoni F. Antibody-drug conjugates for lymphoma patients: preclinical and clinical evidences. *Explor Target Antitumor Ther* (2022) 3:763–94. doi: 10.37349/etat.2022.00112

67. Ku M, Chong G, Hawkes EA. Tumour cell surface antigen targeted therapies in B-cell lymphomas: Beyond rituximab. *Blood Rev* (2017) 31:23–35. doi: 10.1016/j.blre.2016.08.001

68. Hamblett KJ, Senter PD, Chace DF, Sun MM, Lenox J, Cerveny CG, et al. Effects of drug loading on the antitumor activity of a monoclonal antibody drug conjugate. *Clin Cancer Res* (2004) 10:7063–70. doi: 10.1158/1078-0432.CCR-04-0789

69. Adem YT, Schwarz KA, Duenas E, Patapoff TW, Galush WJ, Esue O. Auristatin antibody drug conjugate physical instability and the role of drug payload. *Bioconjug Chem* (2014) 25:656–64. doi: 10.1021/bc400439x

70. Bryant P, Pabst M, Badescu G, Bird M, McDowell W, Jamieson E, et al. *In vitro* and *in vivo* evaluation of cysteine rebridged trastuzumab-MMAE antibody drug conjugates with defined drug-to-antibody ratios. *Mol Pharm* (2015) 12:1872–9. doi: 10.1021/acs.molpharmaceut.5b00116

71. Law C-L, Cerveny CG, Gordon KA, Klussman K, Mixan BJ, Chace DF, et al. Efficient elimination of B-lineage lymphomas by anti-CD20-auristatin conjugates. *Clin Cancer Res* (2004) 10:7842–51. doi: 10.1158/1078-0432.CCR-04-1028

72. de Goeij BE, Vink T, ten Napel H, Breij EC, Satijn D, Wubbolts R, et al. Efficient payload delivery by a bispecific antibody-drug conjugate targeting HER2 and CD63. *Mol Cancer Ther* (2016) 15:2688–97. doi: 10.1158/1535-7163.MCT-16-0364

73. Boni V, Fidler MJ, Arkenau H-T, Spira A, Meric-Bernstam F, Uboha N, et al. Praluzatamab ravtansine, a CD166-targeting antibody-drug conjugate, in patients with advanced solid tumors: an open-label phase I/II trial. *Clin Cancer Res* (2022) 28:2020–9. doi: 10.1158/1078-0432.CCR-21-3656

74. Morrison VA. Immunosuppression associated with novel chemotherapy agents and monoclonal antibodies. *Clin Infect Dis* (2014) 59 Suppl 5:S360–4. doi: 10.1093/cid/ciu592

75. Beers SA, French RR, Chan HT, Lim SH, Jarrett TC, Vidal RM, et al. Antigenic modulation limits the efficacy of anti-CD20 antibodies: implications for antibody selection. *Blood* (2010) 115:5191–201. doi: 10.1182/blood-2010-01-263533

76. Czuczman MS, Olejniczak S, Gowda A, Kotowski A, Binder A, Kaur H, et al. Acquirement of rituximab resistance in lymphoma cell lines is associated with both global CD20 gene and protein down-regulation regulated at the pretranscriptional and posttranscriptional levels. *Clin Cancer Res* (2008) 14:1561–70. doi: 10.1158/1078-0432.CCR-07-1254

77. Beum PV, Kennedy AD, Williams ME, Lindorfer MA, Taylor RP. The shaving reaction: rituximab/CD20 complexes are removed from mantle cell lymphoma and chronic lymphocytic leukemia cells by THP-1 monocytes. *J Immunol* (2006) 176:2600–9. doi: 10.4049/jimmunol.176.4.2600

78. Dornan D, Spleiss O, Yeh R-F, Duchateau-Nguyen G, Dufour A, Zhi J, et al. Effect of FCGR2A and FCGR3A variants on CLL outcome. *Blood* (2010) 116:4212–22. doi: 10.1182/blood-2010–03–272765

79. Maeshima AM, Taniguchi H, Nomoto J, Maruyama D, Kim S-W, Watanabe T, et al. Histological and immunophenotypic changes in 59 cases of B-cell non-Hodgkin's lymphoma after rituximab therapy. *Cancer Sci* (2009) 100:54–61. doi: 10.1111/j.1349-7006.2008.01005.x

80. Torchia J, Weiskopf K, Levy R. Targeting lymphoma with precision using semisynthetic anti-idiotype peptibodies. *Proc Natl Acad Sci U.S.A.* (2016) 113:5376–81. doi: 10.1073/pnas.1603335113

81. Miller RA, Maloney DG, Warnke R, Levy R. Treatment of B-cell lymphoma with monoclonal anti-idiotype antibody. *N Engl J Med* (1982) 306:517–22. doi: 10.1056/NEJM198203043060906

82. Hamblin TJ, Cattan AR, Glennie MJ, MacKenzie MR, Stevenson FK, Watts HF, et al. Initial experience in treating human lymphoma with a chimeric univalent derivative of monoclonal anti-idiotype antibody. *Blood* (1987) 69:790–7. doi: 10.1182/blood.V69.3.790.790

83. Macarrón Palacios A, Grzeschik J, Deweid L, Krah S, Zielonka S, Rösner T, et al. Specific targeting of lymphoma cells using semisynthetic anti-idiotype shark antibodies. *Front Immunol* (2020) 11:560244. doi: 10.3389/fimmu.2020.560244

84. Goldstein B, Dembo M. Approximating the effects of diffusion on reversible reactions at the cell surface: ligand-receptor kinetics. *Biophys J* (1995) 68:1222–30. doi: 10.1016/S0006-3495(95)80298-5

85. Goldstein B, Posner RG, Torney DC, Erickson J, Holowka D, Baird B. Competition between solution and cell surface receptors for ligand. Dissociation of hapten bound to surface antibody in the presence of solution antibody. *Biophys J* (1989) 56:955–66. doi: 10.1016/S0006-3495(89)82741-9

86. Elter A, Bogen JP, Hinz SC, Fiebig D, Macarrón Palacios A, Grzeschik J, et al. Humanization of chicken-derived scFv using yeast surface display and NGS data mining. *Biotechnol J* (2021) 16:e2000231. doi: 10.1002/biot.202000231

87. Bogen JP, Elter A, Grzeschik J, Hock B, Kolmar H. Humanization of chicken-derived antibodies by yeast surface display. *Methods Mol Biol* (2022) 2491:335–60. doi: 10.1007/978-1-0716-2285-8_18

88. Benatuil L, Perez JM, Belk J, Hsieh C-M. An improved yeast transformation method for the generation of very large human antibody libraries. *Protein Eng Des Sel* (2010) 23:155–9. doi: 10.1093/protein/gzq002

89. Hinz SC, Elter A, Rammo O, Schwämmle A, Ali A, Zielonka S, et al. A Generic Procedure for the Isolation of pH- and Magnesium-Responsive Chicken scFvs for Downstream Purification of Human Antibodies. *Front Bioeng Biotechnol* (2020) 8:688. doi: 10.3389/fbioe.2020.00688

90. Puthenveetil S, Liu DS, White KA, Thompson S, Ting AY. Yeast display evolution of a kinetically efficient 13-amino acid substrate for lipoic acid ligase. *J Am Chem Soc* (2009) 131:16430–8. doi: 10.1021/ja904596f

91. Baruah H, Puthenveetil S, Choi Y-A, Shah S, Ting AY. An engineered aryl azide ligase for site-specific mapping of protein-protein interactions through photo-cross-linking. *Angew Chem Int Ed Engl* (2008) 47:7018–21. doi: 10.1002/anie.200802088

Supplementary Material

Conditional activation of an anti-IgM antibody-drug conjugate for precise B cell lymphoma targeting

Katrin Schoenfeld, Julia Harwardt, Jan Habermann, Adrian Elter and Harald Kolmar*

***Correspondence:** Harald Kolmar: harald.kolmar@tu-darmstadt.de

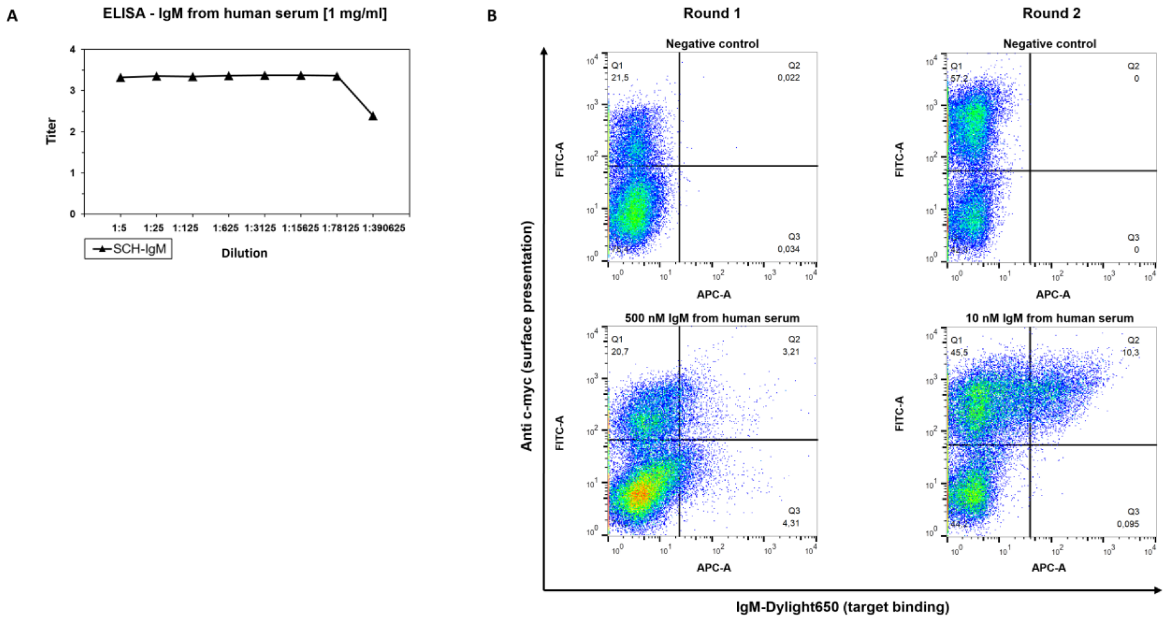

Supplementary Figure 1. Chicken immune response and screening of IgM immune library. (A) Enzyme-linked immunosorbent assay (ELISA) for determination of antibody titer in serum of immunized chickens against IgM from human serum. Experiment was conducted by Davids Biotechnologie GmbH. (B) Sorting of the chicken-derived yeast surface-displayed scFv library. Surface presentation was analyzed using anti c-myc FITC-conjugated antibodies and antigen binding was detected by directly Dylight650-labelled IgM from human serum. Dot plots were created using FlowJoTM v10 Software (BD Life Sciences).

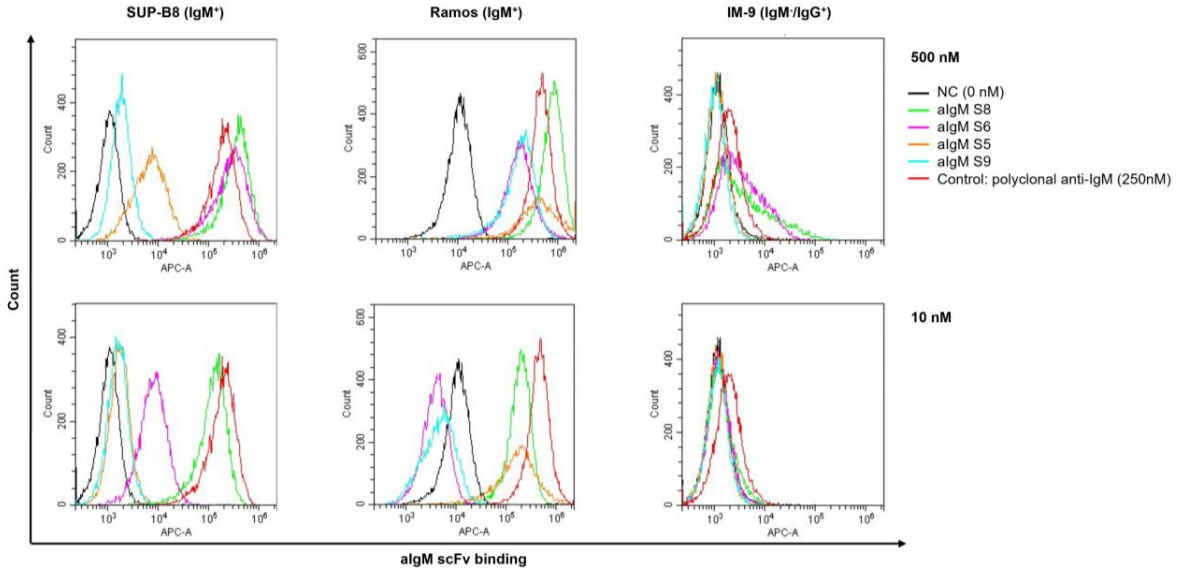

Supplementary Figure 2. Cellular binding of aIgM scFv candidates. Flow cytometry analysis of IgM^+ (SUP-B8, Ramos) and IgM^- (IM-9) B cells incubated with 500 nM and 10 nM of aIgM scFv candidates S8, S6, S5, S9 as well as with 250 nM polyclonal anti-IgM antibody serving as positive control. Negative control samples (0nM, black) represent cells stained with secondary detection antibody only. Staining was conducted via anti-his AF647-conjugated secondary antibody.

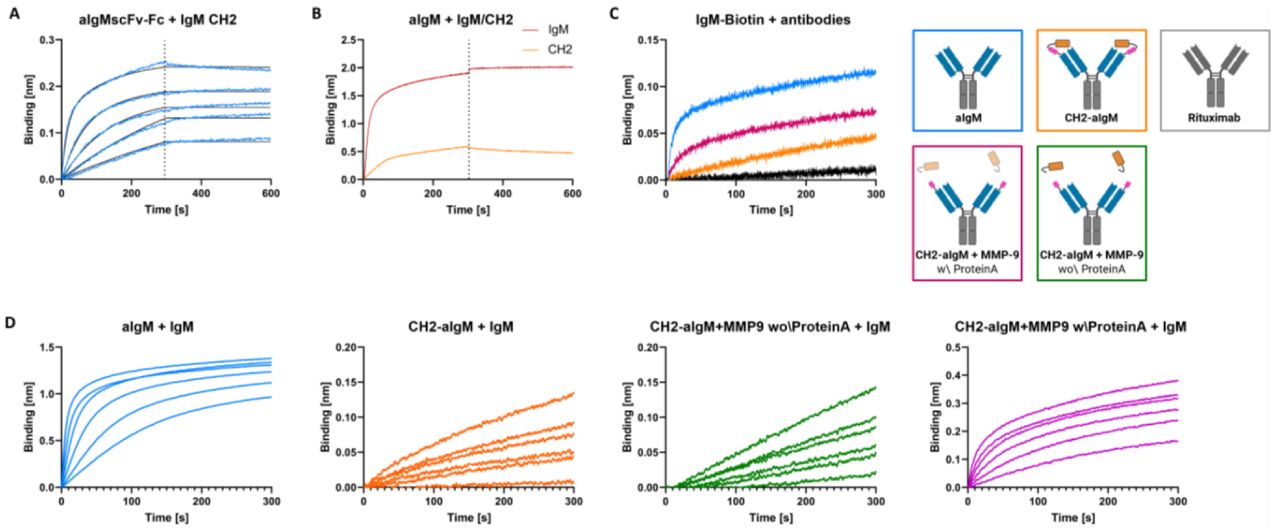

Supplementary Figure 3. Characterization of antigen binding of the aIgM antibody by BLI measurements. (A) Binding kinetics. aIgMscFv-Fc was loaded onto AHC biosensor tips and associated with 31.25 to 500 nM IgM CH2 domain, followed by dissociation in KB. (B) BLI measurement of parental full-length aIgMFab-Fc. aIgM was immobilized to AHC biosensors and associated with 50 nM IgM from human serum or 250 nM IgM CH2, followed by dissociation in PBS. (C) BLI measurement in reverse experimental setup. Biotinylated IgM from human serum was loaded onto SAX biosensor tips and associated with 100 nM of the four antibody constructs (Rituximab, aIgM, CH2-aIgM, Protein A purified CH2-aIgM+MMP-9). (D) BLI measurement using different IgM concentrations. The four antibody constructs (aIgM, CH2-aIgM, non-purified and Protein A purified CH2-aIgM+MMP-9) were loaded onto AHC biosensor tips and associated with 3.9 nM - 125 nM IgM from human serum.

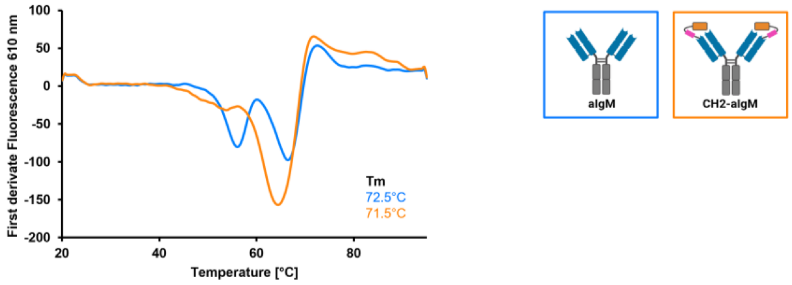

Supplementary Figure 4. Thermal shift assay. Thermal stability was analyzed by means of a temperature gradient from 20°C to 95°C and 0.5°C/10 s. Derivatives of melt curves and melting temperatures (Tm) were determined using the BioRad CFX Maestro software.

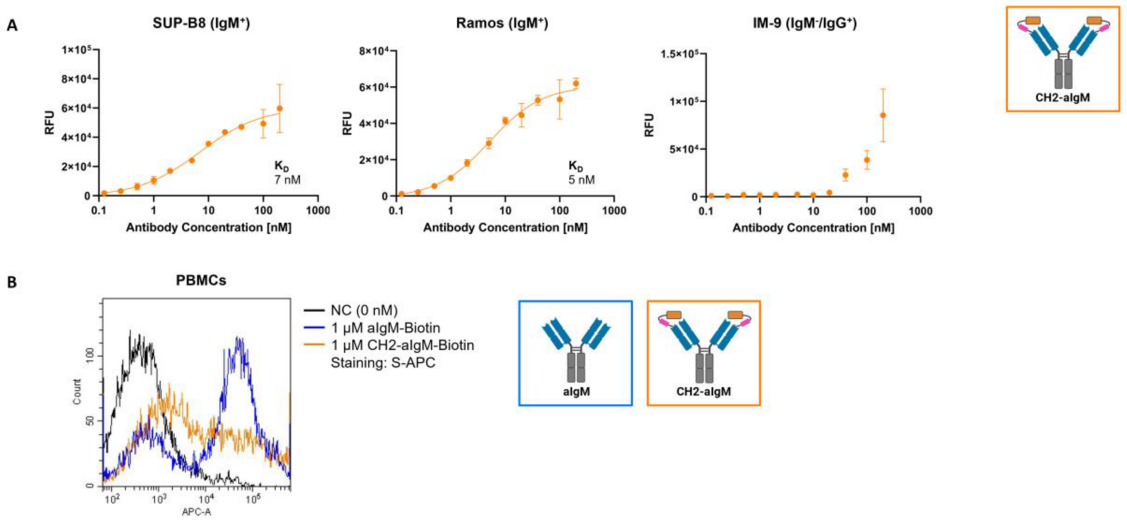

Supplementary Figure 5. Cellular binding of CH2-masked aIgM. (A) Flow cytometry analysis by cell titration of 0.125-200 nM CH2-aIgM on IgM^+ (SUP-B8, Ramos) and IgM^- (IM-9) B cells. Staining was conducted via anti-human IgG Fc-PE secondary detection antibody. On-cell K_Ds were determined using variable slope four-parameter fit. Results are shown as mean RFU, error bars represent standard deviation derived from experimental duplicates. (B) Flow cytometry analysis of PBMCs incubated with biotinylated aIgM and CH2-aIgM (1µM) and stained by Streptavidin-APC. Negative control samples (0nM, black) represent cells stained with secondary detection reagent only.

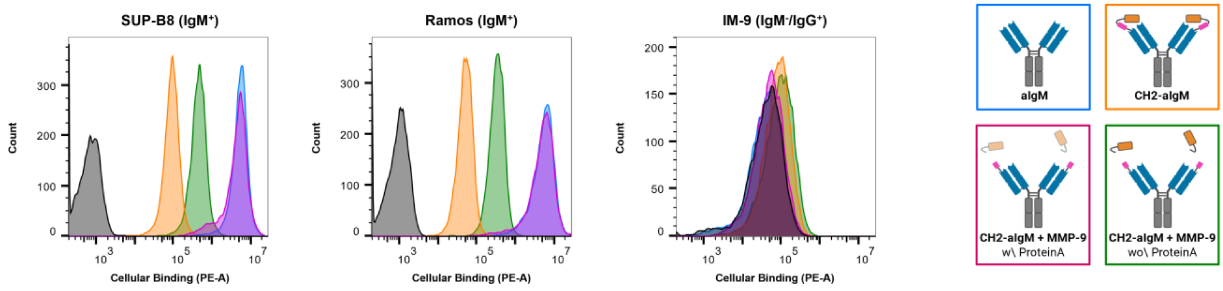

Supplementary Figure 6. Cellular binding of unmasked and CH2-masked aIgM variants to B cells. Flow cytometry analysis of IgM^+ (SUP-B8, Ramos) and IgM^- (IM-9) B cells incubated with aIgM, CH2-aIgM, Protein A purified and non-purified CH2-aIgM+MMP-9 antibodies and stained via anti-human IgG Fc-PE secondary detection antibody. B cells were incubated with 100 nM of respective antibodies. Negative control samples (0nM, black) represent cells stained with secondary detection antibody only.

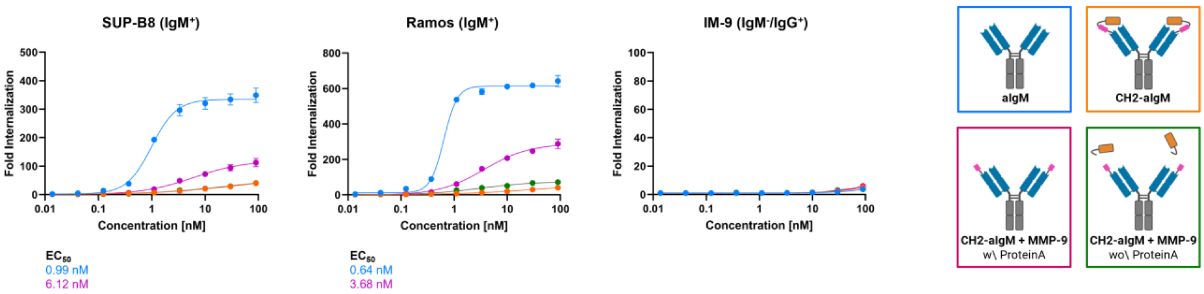

Supplementary Figure 7. Internalization assays of unmasked and CH2-masked aIgM antibody variants in B cells. Internalization of pHab-conjugated aIgM, CH2-aIgM, Protein A purified and non-purified CH2-aIgM+MMP-9 (0.014-90 nM) via endocytosis was analyzed overnight using IgM^+ (SUP-B8, Ramos) and IgM^- (IM-9) B cells. Fluorescence of pH-sensitive dye indicating internalization was measured by flow cytometry. Fold internalization was defined by the ratio of relative fluorescence units (RFU) of the respective antibody sample and the untreated sample without antibody (0 nM). EC_{50}s were determined using variable slope four-parameter fit. Results are shown as mean, error bars represent standard deviation derived from experimental duplicates.

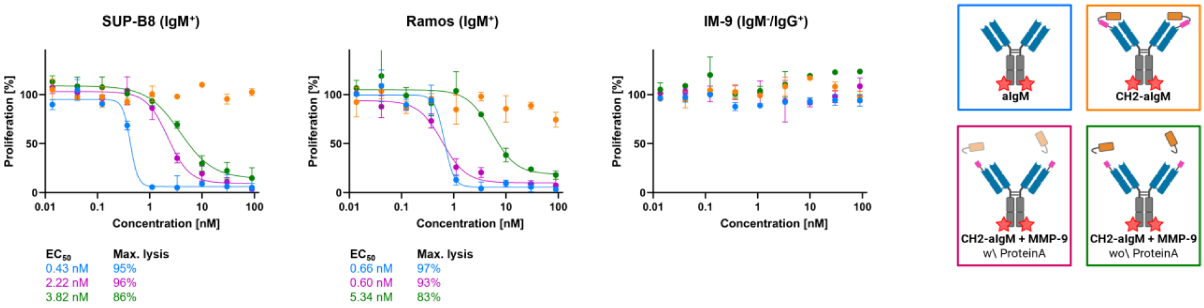

Supplementary Figure 8. Cytotoxicity of unmasked and CH2-masked aIgM ADC variants towards B cells. IgM^+ (SUP-B8, Ramos) and IgM^- (IM-9) B cells were exposed to varying concentrations (0.14-90 nM) of aIgM, CH2-aIgM, Protein A purified and non-purified CH2-aIgM+MMP-9 MMAE-conjugated antibodies for 72 h. EC_{50}s were determined using variable slope four-parameter fit. Results are shown as mean, error bars represent standard deviation derived from experimental duplicates.

4.2 Better safe than sorry: dual targeting antibodies for cancer immunotherapy

Title:

Better safe than sorry: dual targeting antibodies for cancer immunotherapy

Authors:

Katrin Schoenfeld*, Julia Harwardt* and Harald Kolmar

*shared first authorship

Bibliographic data:

Biological Chemistry

Volume 405 - 2024, Issue 7-8, Highlight: New developments in immunoengineering

Article first published: 1st February 2024

DOI: 10.1515/hsz-2023-0329

Contributions by Katrin Schoenfeld:

- Literature research with Julia Harwardt
- Summarizing data from literature and planning of the review article with Julia Harwardt
- Writing of the manuscript and generation of figures with Julia Harwardt

Review

Katrin Schoenfeld, Julia Harwardt and Harald Kolmar*

Better safe than sorry: dual targeting antibodies for cancer immunotherapy

https://doi.org/10.1515/hsz-2023-0329
Received October 17, 2023; accepted January 11, 2024;
published online February 1, 2024

Abstract: Antibody-based therapies are revolutionizing cancer treatment and experience a steady increase from preclinical and clinical pipelines to market share. While the clinical success of monoclonal antibodies is frequently limited by low response rates, treatment resistance and various other factors, multispecific antibodies open up new prospects by addressing tumor complexity as well as immune response actuation potently improving safety and efficacy. Novel antibody approaches involve simultaneous binding of two antigens on one cell implying increased specificity and reduced tumor escape for dual tumor-associated antigen targeting and enhanced and durable cytotoxic effects for dual immune cell-related antigen targeting. This article reviews antibody and cell-based therapeutics for oncology with intrinsic dual targeting of either tumor cells or immune cells. As revealed in various preclinical studies and clinical trials, dual targeting molecules are promising candidates constituting the next generation of antibody drugs for fighting cancer.

Keywords: bispecific antibody; cancer immunotherapy; dual targeting; immune cell engager; multispecific antibody

1 Introduction

It took 35 years to reach an impressive milestone in therapeutic antibody discovery with the Food and Drug Administration (FDA) approval of the 100th antibody-based product in April 2021 (Mullard 2021). Since then, the number has steadily increased, demonstrating that antibodies have become a class of therapeutics of considerable value in recent years. In particular, antibodies are of great importance for cancer drug development, as about one in two antibodies is approved for the treatment of oncology patients. While the number of approved bispecific antibodies is relatively small (nine), interest in bi- and multispecific molecules as well as antibody-drug conjugated and cell-based therapeutics is growing rapidly, as evidenced by the large number of such molecules being investigated in various stages of research and clinical trials (>100) (Lyu et al. 2022).

Examples of novel and potent antibody-based molecules targeting various relevant antigens and key pathways of tumor growth include (i) bispecific antibodies simultaneously targeting two tumor-associated antigens (TAAs) demonstrating enhanced cancer cell selectivity and reduced tumor immune escape (Huang et al. 2020; Schubert et al. 2012), (ii) dual TAA-targeting antibody drug conjugates (ADCs) that efficiently deliver cytotoxic drugs to tumor cells (Huang et al. 2020), (iii) dual TAA-targeting CAR-T cells reducing the likelihood of antigen escape and increasing tumor cell killing activity (Sterner and Sterner 2021; Xie et al. 2022), and (iv) multispecific antibodies targeting tumors in combination with single or dual immune cell targeting which activate immune cells more intense and durable, thereby enhancing effector cell-mediated cytotoxicity (Tapia-Galisteo et al. 2023).

This review focuses on antibody and cell-based therapeutics for oncology clinical development with intrinsic dual targeting of different antigens on the same cell, thereby overcoming bottlenecks of single mode cell targeting. In this context, dual TAA-targeting bispecific antibodies, as well as dual TAA-targeting ADCs and CAR-T cells are described in chapter 2 (Table 1). Furthermore, trispecific immune cell engagers are highlighted in chapter 3, which either simultaneously target two TAAs or two immune cell-related antigens.

2 Bispecific dual tumor cell-targeting antibodies

In this chapter, the current status of bispecific antibodies concurrently targeting two different TAAs or different epitopes

Katrin Schoenfeld and Julia Harwardt contributed equally to this work.

***Corresponding author: Harald Kolmar**, Institute for Organic Chemistry and Biochemistry, Technical University of Darmstadt, Peter-Grünberg-Strasse 4, D-64287 Darmstadt, Germany; and Centre for Synthetic Biology, Technical University of Darmstadt, Darmstadt, Germany,
E-mail: Harald.Kolmar@TU-Darmstadt.de. https://orcid.org/0000-0002-8210-1993
Katrin Schoenfeld and Julia Harwardt, Institute for Organic Chemistry and Biochemistry, Technical University of Darmstadt, Peter-Grünberg-Strasse 4, D-64287 Darmstadt, Germany

Table 1: Dual targeting antibodies in preclinical and clinical development.

Drug name	Specificity	Development status	Sponsor/investigator/developer
Bispecific dual tumor cell-targeting antibodies			
Amivantamab (JNJ-61186372)	EGFR × c-Met	FDA-approved	Janssen Biotech
MCLA-129	EGFR × c-Met	Clinical study phase 1/2 (NCT04868877; NCT04930432)	Merus
EMB-01	EGFR × c-Met	Clinical study phase 1/2 (NCT03797391; NCT05176665)	EpimAb Biotherapeutics
SI-B001	EGFR × HER3	Clinical study phase 2/3 (NCT05020769)	Sichuan Baili Pharmaceutical Co. Ltd.
MCLA-158	EGFR × LGR5	Clinical study phase 1/2 (NCT03526835)	Merus
MCLA-128 Zenocutuzumab	HER2 × HER3	Clinical study phase 2 (NCT02912949; NCT05588609)	Merus
ZW25	HER2 × HER2	Clinical study phase 2 (NCT04513665)	BeiGene
MBS301	HER2 × HER2	Clinical study phase 1 (NCT03842085)	Mabwork
KN026	HER2 × HER2	Clinical study phase 2 (NCT04165993)	Alphamab Oncology
RO6874813	FAP × DR5	Clinical study phase 1 (NCT02558140)	Roche
BI905711	DR5 × CDH17	Clinical study phase 1 (NCT04137289)	Boehringer Ingelheim
IMGS-001	PD-L1 × PD-L2	Clinical study phase 1 (NCT06014502)	ImmunoGenesis
PM8001	PD-L1 × TGF-β	Clinical study phase 2 (NCT05537051)	Biotheus Inc.
SHR-1701	PD-L1 × TGF-β	Clinical study phase 1 (NCT03710265; NCT03774979)	Jiangsu HengRui Medicine
TG-1801	CD47 × CD19	Clinical study phase 1 (NCT03804996)	TG Therapeutics
NI-1801	CD47 × MSLN	Clinical study phase 1 (NCT05403554)	NovImmune
IBI322	CD47 × PD-L1	Clinical study phase 1 (NCT04795128)	Innovent Biologics
IMM2902	CD47 × HER2	Clinical study phase 1 (NCT05805956)	ImmuneOnco Biopharmaceuticals
IMM0306	CD47 × CD20	Clinical study phase 1 (NCT05805943)	ImmuneOnco Biopharmaceuticals
Dual tumor-targeting antibody-drug conjugates			
bsHER2xCD63his-Duo3	HER2 × CD63	Preclinical	Goeij et al.
PRLR × HER2 BsADC	HER2 × PRLR	Preclinical	Zong et al.
ZW49	HER2 × HER2	Clinical study phase 1 (NCT03821233)	Zymeworks/BeiGene
REGN5093-M114	MET × MET	Clinical study phase 1/2 (NCT04982224)	Regeneron Pharmaceuticals
DT2219	CD19 × CD22	Clinical study phase 1/2 (NCT02370160)	Masonic Cancer Center, University of Minnesota
Dual tumor-targeting chimeric antigen receptor-T cells			
TanCARCD19/20 T cells	CD19 × CD20	Clinical study phase 1/2 (NCT03097770)	Chinese PLA General Hospital
CAR-20/19-T	CD19 × CD20	Clinical study phase 1 (NCT03019055)	Medical College of Wisconsin
CART19/20	CD19 × CD20	Clinical study phase 1 (NCT04007029)	Jonsson Comprehensive Cancer Center
CD19/CD22 Bicistronic CAR-T cells	CD19 × CD22	Clinical study phase 1/2 (NCT05442515)	National Cancer Institute (NCI)
CD19/CD22 dual targeted CAR-T cell	CD19 × CD22	Clinical study phase 1 (NCT05225831)	Hebei Senlang Biotechnology Inc., Ltd.
CD19/CD22-CAR-T cell	CD19 × CD22	Clinical study phase 1 (NCT03448393)	National Cancer Institute (NCI)
FasT CAR-T GC012F	BCMA × CD19	Clinical study phase 1/2 (NCT04935580)	Shanghai Changzheng Hospital
BM38 CAR-T	BCMA × CD38	Clinical study phase 1/2 (NCT03767751)	Chinese PLA General Hospital
BCMA/CS1 CAR-T	BCMA × CD319	Preclinical	Zah et al.
BCMA/GPRC5D CAR-T	BCMA × GPRC5D	Preclinical	De Larrea et al.
Trispecific dual targeting immune cell engager			
Dual tumor cell-targeting ICEs			
TCE	CD19 × CD20 × CD3	Preclinical	Wang et al.
TCE	CD19 × CD22 × CD3	Preclinical	Zhao et al.
TCE	CD19 × CD33 × CD3	Preclinical	Roskopf et al.
TCE	EGFR × EpCAM × CD3	Preclinical	Tapia-Galisteo et al.
TCE	HER2 × VEGFR2 × CD3	Preclinical	Liu et al.
NKCE	CD33 × CD19 × CD16	Preclinical	Schubert et al.

Table 1: (continued)

Drug name	Specificity	Development status	Sponsor/investigator/developer
NKCE	CD33 × CD123 × CD16	Preclinical	Kügler et al.
NKCE	CD22 × CD19 × CD16	Preclinical	Gleaseon et al.
NKCE	BCMA × CD2000 × CD16	Preclinical	Gantke et al.
NKCE	EGFR × PD-L1 × CD16	Preclinical	Bogen et al.
NKCE	EGFR × PD-L1 × CD16	Preclinical	Harwardt et al.
Dual immune cell-targeting ICEs			
Dual T cell-targeting ICEs			
SAR442257	CD38 × CD3 × CD28	Clinical study phase 1 (NCT04401020)	Sanofi
SAR443216	HER2 × CD3 × CD28	Clinical study phase 1 (NCT05013554)	Sanofi
Dual NK cell-targeting ICEs			
NKCEs	CD16 × NKp46 × CD19/CD20/EGFR	Preclinical	Innate Pharma
ANKET IPH62	CD16 × NKp46 × B7-H3	Preclinical	Innate Pharma/Sanofi
ANKET IPH6101 (SAR443579)	CD16 × NKp46 × CD123	Clinical study phase 1/2 (NCT05086315)	Innate Pharma/Sanofi
ANKET IPH6401	CD16 × NKp46 × BCMA	Clinical study phase 1/2 (NCT05839626)	Innate Pharma/Sanofi
TriNKETs	NKG2D × CD16 × TAA (e.g. HLA-E/CCR4/PD-L1/FLT3)	Preclinical	Dragonfly Therapeutics
TriNKET DF9001	NKG2D × CD16 × EGFR	Clinical study phase 1/2 (NCT05597839)	Dragonfly Therapeutics
TriNKET DF3001	NKG2D × CD16 × BCMA	Clinical study phase 1 (NCT04975399)	Bristol-Myers Squibb
TriNKET DF2001	NKG2D × CD16 × CD33	Clinical study phase 1 (NCT04789655)	Bristol-Myers Squibb
TriNKET DF1001	NKG2D × CD16 × HER2	Clinical study phase 1/2 (NCT04143711)	Dragonfly Therapeutics
Tetraspecific dual targeting immune cell engager			
ANKET4	NKp46 × CD16a × IL-2Rβ × CD20	Preclinical	Innate Pharma
GNC-035, GNC-038 and GNC-039	CD3 × 4-1BB × PD-L1 × ROR1/CD19/EGFRvIII	Clinical study phase 1/2 (NCT05160545; NCT04606433; NCT04794972)	Sichuan Baili/Systimmune

on the same TAA is reviewed. Dual TAA-targeting antibodies are a subclass of bispecific antibodies that offer several advantages, including increased tumor selectivity, simultaneous modulation of two functional pathways in the tumor cell and circumvention of drug resistance or immune escape mechanisms (Figure 1) (Huang et al. 2020; Schubert et al. 2012). Monospecific antibodies are frequently not able to sharply discriminate between malignant and healthy cells carrying the same target antigen which may result in on-target off-tumor toxicity (Brennan et al. 2010). The generation of bispecific dual TAA-targeting antibodies that show relatively low affinity for one or both of the antigens while binding with high affinity to tumor cells that display both targets on their cell surface, results in increased tumor selectivity (Figure 1) (Harwardt et al. 2022; Sun et al. 2021). The appropriate fine-tuning of individual affinities can result in an augmented toxic effect against the tumor while therapy-related side effects are reduced, which is associated with superior drug tolerability and safety (Bendell et al. 2018; Dheilly et al. 2017; Jiang et al. 2021). Antibodies that address two receptors expressed on tumor cells further enable simultaneous modulation of two distinct functional pathways evoking alternative cell fates (Huang et al. 2020; Temraz et al. 2016). Moreover, treatment of a multi-factorial disease like cancer with monoclonal antibodies is always at risk of causing drug resistance, particularly via tumor escape mechanisms such as antigen mutation, downregulation or shedding (Reslan et al. 2009; Vasan et al. 2019). The feature of bispecific dual TAA-targeting antibodies to target two different, individually overexpressed targets on tumor cells can contribute to risk mitigation regarding drug resistance and immune escape, e.g., via immune checkpoints such as programmed cell death protein 1 (PD-1)/PD-L1 or signal regulatory protein α (SIRPα)/CD47 (Figure 1) (Huang et al. 2020; Schubert et al. 2012). The following section outlines TAA combinations for which bispecific antibodies have been developed, focusing on those currently in clinical trials or already approved for clinical use.

2.1 EGFR × c-Met

The epithelial growth factor receptor (EGFR) and the mesenchymal epithelial transition factor (c-Met) are commonly expressed on tumor cells and are involved in the development and progression of various tumor types through their diverse

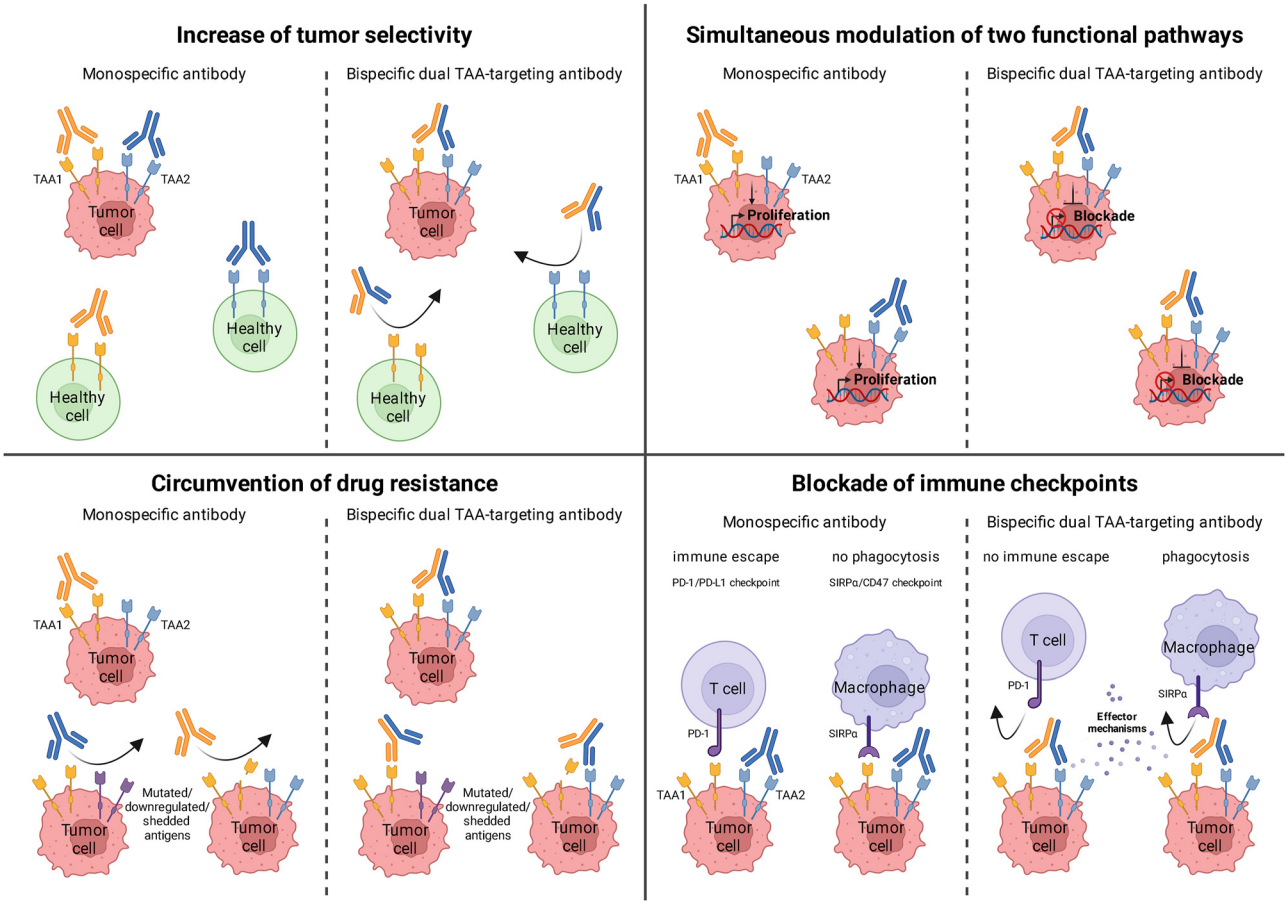

Figure 1: Mechanisms of bispecific dual tumor cell-targeting antibodies compared to monospecific antibodies. Bispecific dual TAA-targeting antibodies increase tumor specificity by binding to tumor cells expressing both antigens, but not to healthy cells expressing one of the antigens. They simultaneously modulate two functional pathways resulting in alternative signaling and cell fates, circumvent drug resistance and block immune checkpoints thereby preserving antibody-mediated effector mechanisms.

effects on the cell cycle, programmed cell death, and invasion (Sigismund et al. 2018; van Herpe and van Cutsem 2023). Notably, they utilize a highly overlapping repertoire of signaling adapters and downstream signaling pathways (Giovannetti and Leon 2014). Based on the signaling crosstalk between EGFR and c-Met, combinatorial inhibition of both receptors may restrict compensatory pathway activation and improve the overall efficacy of therapeutic antibodies (Moores et al. 2016). Amivantamab (JNJ-61186372) is a bispecific EGFR and c-Met-targeting antibody developed by Janssen Biotech utilizing Genmab's DuoBody® technology, that inhibits both, EGFR and c-Met signaling by blocking ligand-induced activation and inducing receptor degradation. Moreover, interaction of the amivantamab Fc domain with Fcγ receptors on natural killer (NK) cells leads to antibody-dependent cellular cytotoxicity (ADCC), and interaction with Fcγ receptors on monocytes and macrophages results in cytokine production and trogocytosis (Moores et al. 2016; Vijayaraghavan et al. 2020). Amivantamab is the first-in-class dual TAA-targeting antibody that received FDA approval in May 2021 in the US for the treatment of adult patients with locally advanced or metastatic non-small cell lung cancer (NSCLC) harboring EGFR Exon 20 insertion mutations with progression on or after platinum-based chemotherapy (Syed 2021). The efficacy of amivantamab is partly based on its ability to target a NSCLC mutation that has historically had a poor prognosis due to innate resistance to previously approved EGFR tyrosine kinase inhibitors (Russell et al. 2023). A phase 3 study showed that the use of amivantamab in combination with chemotherapy results in superior efficacy compared to chemotherapy alone as first-line treatment of patients with advanced NSCLC with EGFR exon 20 insertions (Zhou et al. 2023). Two other EGFR- and c-Met-targeting bispecific antibodies currently undergoing clinical trials for the treatment of advanced solid tumors are represented by the full-length, common light chain (cLC), electrostatic CH3--engineered (DEKK), ADCC enhanced antibody MCLA-129, discovered by Merus (NCT04868877; NCT04930432) (Ou et al. 2022) and the tetravalent antibody EMB-01 developed by

EpimAb Biotherapeutics based on the proprietary FIT-Ig® platform (NCT03797391; NCT05176665) (Qing et al. 2022; Ren et al. 2020). Both molecules have demonstrated efficacy in multiple preclinical cancer models highlighting the synergistic function of EGFR and c-Met signaling blockade (Ou et al. 2022; Ren et al. 2020).

2.2 EGFR × HER3

Another member of the ErbB/HER receptor tyrosine kinase (RTK) family found in various tumor types promoting cell proliferation, is the human epidermal growth factor receptor 3 (HER3). Expression and activation of HER3 has been associated with resistance to drugs targeting EGFR (Gandullo-Sánchez et al. 2022). Therefore, dual targeting of EGFR and HER3 may be an approach to overcome this resistance and increase selectivity for EGFR/HER3 double positive tumors inhibiting both signaling pathways simultaneously (Temraz et al. 2016). Sichuan Baili Pharmaceutical Co. Ltd developed the bispecific antibody SI-B001 which is built on a tetravalent platform exhibiting two highly selective binding domains for EGFR and HER3, respectively. *In vitro*, SI-B001-mediated inhibition of tumor cell growth was stronger than that of cetuximab and duligotuzumab mAb combination (Renshaw et al. 2023). The dual blockade bispecific antibody has demonstrated encouraging anti-tumor efficacy in several xenograft models of epithelium squamous cell carcinomas (Xue et al. 2020) and is now being investigated in a clinical phase 2/3 study (NCT05020769).

2.3 EGFR × LGR5

To specifically trigger EGFR degradation in leucine-rich repeat-containing G-protein-coupled receptor 5 (LGR5)-positive cancer stem cells, Merus developed the human cLC IgG1 bispecific antibody, MCLA-158, against EGFR and LGR5 with enhanced ADCC activity (Herpers et al. 2022). MCLA-158 was found to be a potent inhibitor of colorectal cancer organoid growth blocking the initiation of metastasis, as well as growth in various preclinical models of cancer, including head and neck, esophagus and stomach tumors (García et al. 2023). Currently, MCLA-158 is tested in a phase 1/2 clinical trial (NCT03526835) where it demonstrates encouraging clinical efficacy (Cohen et al. 2023). Compared to other EGFR-targeting antibodies, MCLA-158 displays superior selectivity for tumor-derived organoids and an augmented therapeutic activity (Herpers et al. 2022), which is most likely caused by dual TAA targeting.

2.4 HER2 × HER3

Neuregulin 1 (NRG1)-mediated HER3 activation promotes asymmetric dimerization of HER3 with other members of the ErbB/RTK family, of which the HER2/HER3 dimers represent the most oncogenic ones (Klapper et al. 1999; Zhang et al. 2006). Consequently, addressing HER2/HER3 signaling is a promising therapeutic approach. The bispecific humanized full-length IgG1 antibody MCLA-128 developed by Merus targeting HER2 and HER3 is designed to block the binding of NRG1 to HER3 (Geuijen et al. 2018). One arm of the antibody binds to the HER2 receptor, optimally positioning the other arm to block the NRG1/HER3 interaction. In tumor models resistant to HER2–targeting agents, MCLA-128 effectively inhibits HER3 signaling via this "dock & block" mechanism (Geuijen et al. 2018; Schram et al. 2022). MCLA-128 demonstrated therapeutic efficacy *in vitro* and *in vivo* in various tumors harboring NRG1 fusions. The potential use of MCLA-128 as a therapy for NRG1 fusion-driven cancers is being investigated in an ongoing phase 2 trial (NCT02912949; NCT05588609) (Schram et al. 2022).

2.5 HER2 × HER2

Another option to improve the efficacy of an antibody by preventing resistance via dual tumor targeting is addressing two non-overlapping epitopes of the same TAA. Three so-called biparatopic antibodies targeting extracellular domains (ECDs) II and IV of HER2, which are also bound by the mAbs trastuzumab (IV) and pertuzumab (II) (Hao et al. 2019), are currently being investigated in clinical trials (NCT04513665, NCT03842085, NCT04165993). HER2 is overexpressed in many solid tumors, leading to activation of various signaling pathways that promote cell proliferation and tumorigenesis (Rubin and Yarden 2001). Since many patients experience disease progression over time after treatment with anti-HER2 agents, intrinsic and acquired resistance to approved HER2 therapies is a clinical concern (Rexer and Arteaga 2012). Biparatopic binding of the anti-HER2 antibodies effects receptor crosslinking which promotes receptor internalization and degradation. BeiGenes' ZW25 antibody, Mabworks' MBS301 antibody and Alphamab Oncologys' KN026 antibody have the potential to be used for treating HER2-positive, trastuzumab-resistant solid tumors (Huang et al. 2018; Weisser et al. 2023; Xu et al. 2023).

2.6 DR5 × TAA

Since dysregulated cellular apoptosis and resistance to cell death are characteristics of neoplastic initiation and

progression, the development of compounds that overcome the abnormal death regulation in tumor cells is of great therapeutic value. Activation of the extrinsic apoptotic pathway is highly dependent on hyperclustering of death receptors (DRs) on the cell surface, and therefore tumor-targeted induction of apoptosis may be achieved with antibodies binding DR5 and a TAA (Brünker et al. 2016). This was confirmed by the Roche-developed tetravalent antibody RO6874813, which targets the fibroblast activation protein (FAP) on cancer-associated fibroblasts in tumor stroma with high affinity and DR5 with low affinity (Bendell et al. 2018). Bivalent binding of both FAP and DR5 results in avidity-driven hyperclustering of DR5, further leading to induction of apoptosis in tumor cells but not in normal cells (Brünker et al. 2016). The anti-tumor efficacy of RO6874813 is strictly FAP-dependent and superior to conventional DR5 antibodies. The antibody demonstrated a favorable safety profile in patients with multiple solid tumor types in a phase 1 trial (NCT02558140), indicating that tetravalent binding of FAP and DR5 is a promising approach to overcome tumor-associated resistance to apoptosis (Bendell et al. 2018). Another TAA that shows positive effects in combination with DR5 is CDH17, a cell surface molecule member of the Cadherin superfamily of adhesion molecules (Tian et al. 2023). Boehringer Ingelheim developed the tetravalent bispecific antibody BI905711, targeting both DR5 and CDH17. The molecule triggers strong and tissue-specific DR5 activation, rendering it highly effective and strictly dependent on CDH17 expression in various colorectal xenograft models (García-Martínez et al. 2021).

2.7 PD-L1 × TAA

The PD-1/PD-L1 axis, representing an immune checkpoint for T cells and NK cells, is of huge interest in clinical practice as its inhibition has tremendous impact on cancer treatment outcomes (Brahmer et al. 2012; Sun et al. 2020). To overcome immune surveillance, programmed cell death 1-ligand 1 (PD-L1 or CD274) is upregulated in many malignant cancers (Ju et al. 2020). Three FDA-approved PD-L1-targeting antibodies demonstrated durable clinical benefits and long-term remissions, however, this effect has been limited to a small proportion of patients suffering from certain cancer types (Alvarez-Argote and Dasanu 2019; Kim 2017; Markham 2016; O'Donnell et al. 2017; Pang et al. 2023). Bispecific antibodies capable of simultaneously targeting another TAA may deliver advances in cancer immunotherapy. In this particular context, high expression of programmed cell death 1-ligand 2 (PD-L2 or CD273), a second ligand for PD-1, has been shown to play an important role in tumorigenesis and immune escape (Wang et al. 2023). The antibody IMGS-001 developed by ImmunoGenesis concurrently targets PD-L1 and PD-L2, which is why the molecule could benefit patients that are resistant to existing PD-(L)1 therapy by restoring immune-driven anti-tumor activity (Gagliardi et al. 2022). IMGS-001 is currently being investigated in a clinical phase 1 study (NCT06014502). Further PD-L1 × TAA molecules, including PD-L1 × PD-L2/TGF-β, effectively providing synergistic blockade, were introduced by Biotheus (Riu Martinez et al. 2022). The transforming growth factor (TGF)-β-addressing variant, PM8001, is constituted of a humanized anti-PD-L1 VHH domain and the ECD of TGF-β receptor II fused to a human IgG1 Fc portion, and is currently under clinical investigation displaying promising anti-tumor activity in advanced solid tumors (NCT05537051) (Guo et al. 2022). In addition to this dual-targeting PD-L1 × TGF-β antibody, Jiangsu HengRui Medicine developed a similar bifunctional fusion protein composed of a mAb against PD-L1 fused with the ECD of TGF-β receptor II scrutinized as first-line therapy for PD-L1-positive advanced/metastatic NSCLC as well as for advanced solid tumors in phase 1 studies (NCT03710265; NCT03774979) (Feng et al. 2021; Liu et al. 2021). Another TAA that has been reported to be overexpressed in a variety of cancers is represented by EGFR, as described above (Sigismund et al. 2018). Co-targeting of PD-L1 and EGFR elicits immune checkpoint blockade and enhances the anti-tumor response, as demonstrated by three preclinically developed PD-L1 × EGFR bispecific antibodies. The molecules inhibit EGF-mediated proliferation, effectively block PD-1/PD-L1 interaction and induce a strong ADCC effect *in vitro* (Harwardt et al. 2022; Koopmans et al. 2018; Rubio-Pérez et al. 2023).

2.8 CD47 × TAA

Since the interaction of CD47 with thrombispondin-1 and SIRPα triggers a "don't eat me" signal on macrophages, overexpression of CD47 enables the tumor to evade immune surveillance by blocking phagocytic mechanisms (Jiang et al. 2021). However, CD47 is ubiquitously expressed on human cells which resulted in anti-CD47 antibodies causing severe anemia and thrombocytopenia. To circumvent this, bispecific antibodies were designed simultaneously targeting another tumor antigen to promote tumor-selective interaction of an affinity-optimized arm targeting CD47 (Jiang et al. 2021; Sun et al. 2021). TG-1801 is a fully humanized bispecific IgG1 κλ body developed by TG Therapeutics consisting of one arm targeting the B cell specific marker CD19, widely expressed across B cell malignancies, with high affinity, and another arm targeting CD47 with low affinity (Normant et al. 2019; Wang et al. 2012). By binding to CD19 with high affinity,

TG-1801 selectively inhibits CD47 signaling in B cells (Buatois et al. 2018) and is therefore currently undergoing a phase 1 clinical trial for B cell lymphoma patients (NCT03804996). Furthermore, the bispecific κλ body NI-1801 was developed by NovImmune targeting Mesothelin (MSLN), which is highly expressed in many solid tumors, with high affinity and blocking CD47 with an affinity-optimized arm (Hatterer et al. 2020). Also in this case, the unbalanced affinity allows selective CD47 blockade in MSLN-expressing cells. After demonstrating an inhibitory effect on tumor growth in xenograft models *in vivo*, NI-1801 is now being investigated in a first-in-human clinical trial (NCT05403554) (Romano et al. 2022).

Another antibody based on the concept of targeting CD47 with low affinity and an additional TAA with high affinity is the anti-PD-L1/CD47 antibody IBI322 developed by Innovent Biologics. Due to optimized target selectivities, IBI322 is able to selectively bind CD47/PD-L1 double positive tumor cells, even in the presence of CD47 positive erythrocytes. Consisting of a Fab anti-CD47 arm and a 2-VHH anti-PD-L1 arm, IBI322 blocks an innate and an adaptive immune checkpoint, resulting in potent tumor inhibition (Wang et al. 2021). In a phase 1 clinical study (NCT04795128), IBI322 showed encouraging anti-tumor efficacy and a manageable safety profile, exhibiting its potential to overcome immunotherapy resistance for patients with classical Hodkin lymphoma.

Two bispecific therapeutic fusion proteins developed by ImmuneOnco Biopharmaceuticals that also target the CD47 immune checkpoint are the anti-CD47/HER2 molecule IMM2902 and the anti-CD47/CD20 protein IMM0306. The fusion proteins consist of either a HER2- or CD20-targeting antibody containing a SIRPα binding domain trapped on the light chain or heavy chain, respectively (Meng et al. 2023; Yu et al. 2023; Zhang et al. 2023). The dual TAA-targeting antibodies drive several anti-tumoral killing mechanisms supporting the choice of CD47 × TAA as therapeutic targets.

2.9 Dual tumor-targeting antibody-drug conjugates

Antibody-drug conjugates (ADCs) combining the specificity of antibodies with the cytotoxic activity of a highly potent payload represent an attractive fast-growing drug class for anti-tumor therapies (Alley et al. 2010; Fu et al. 2022). Functionality of ADCs, composed of mAbs covalently bound to cytotoxic payloads through synthetic (cleavable) linkers, requires binding of the target antigen and subsequent internalization, lysosomal processing and release of the warhead mediating cytotoxic effects (Samantasinghar et al. 2023). The optimization of ADCs regarding the antibody portion, internalization capacity and specificity is currently addressed by the design of bispecific dual TAA-targeting ADCs (Figure 2). Such next-generation ADCs currently in preclinical development or clinical trials are outlined below.

Trastuzumab, targeting HER2 is used as first-line treatment for HER2-positive patients. Besides the mAb, two trastuzumab ADCs have been FDA-approved within the last decade which are trastuzumab emtansine (Kadcyla) for metastatic breast cancer and trastuzumab deruxtecan (Enhertu) for metastatic breast cancer and locally advanced or metastatic HER2-positive gastric or gastroesophageal adenocarcinoma (Matikonda et al. 2022). Despite the clinical successes of trastuzumab-based ADCs, improved internalization properties may result in more potent molecules since their internalization usually relies on crosslinking of HER2 while monomeric HER2 does not internalize efficiently (Baulida et al. 1996; Goeij et al. 2014). Goeij et al. developed a bispecific dual tumor cell-targeting ADC against HER2 and the lysosome-associated membrane protein 3 (LAMP3 or CD63) featuring enhanced lysosomal ADC delivery (Goeij et al. 2016). CD63 shuttles between the plasma membrane and intracellular compartments and has been reported to be overexpressed in various cancer types including cervical, breast and gastrointestinal cancer and is frequently associated with tumor metastasis (Mujcic et al. 2009; Nagelkerke et al. 2011; Pols and Klumperman 2009; Sun et al. 2014). The HER2 × CD63 ADC efficiently internalized, accumulated in the lysosomes, and conjugated to the microtubule disrupting agent duostatin-3 cytotoxicity in HER2-positive tumor cells was potently mediated *in vitro* and in a xenograft model *in vivo* (Goeij et al. 2016).

In a similar manner, a bispecific MMAE-conjugated antibody was generated targeting HER2, by utilizing a trastuzumab-based arm, and prolactin preceptor (PRLR) (Zong et al. 2022). Besides the two receptors displaying crosstalk signaling in breast cancer cells, PRLR has been reported to undergo rapid internalization thereby facilitating ADC uptake (Kavarthapu et al. 2021; Piazza et al. 2009). *In vitro* studies demonstrated higher internalization efficiency and augmented anti-tumor activity compared to trastuzumab ADC in human breast cancer cell lines (Zong et al. 2022).

In terms of ADCs' tumor specificity, several bispecific ADCs have been engineered featuring dual tumor targeting using either biparatopic approaches or addressing co-expressed TAAs. Zanidatamab zovodotin (ZW49), developed by Zymeworks in collaboration with BeiGene, represents a biparatopic anti-HER2 ADC targeting subdomain II and IV of the ECD of HER2 (Jhaveri et al. 2022). Multiple mechanisms of action are described to be induced by ZW49

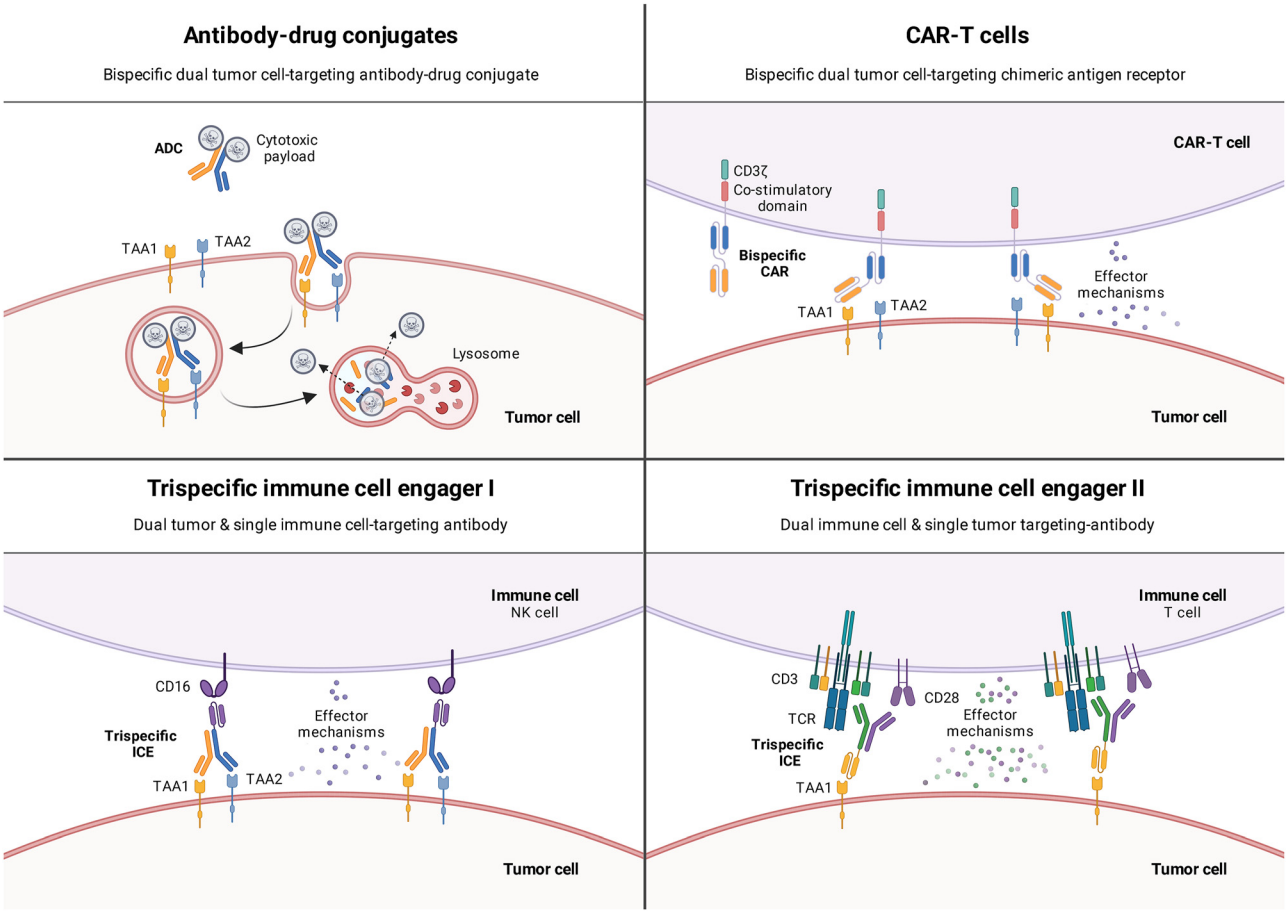

Figure 2: Antibody derivates involving dual tumor cell-targeting or dual immune cell-targeting. Dual TAA-targeting ADCs efficiently deliver cytotoxic drugs to tumor cells, dual TAA-targeting CAR-T cells and dual TAA-targeting trispecific ICEs (NKCEs) enhance tumor specificity, reduce tumor immune escape and potently trigger effector mechanisms. Trispecific dual immune cell related antigen-targeting ICEs (TCEs) activate immune cells more intense and augment effector mechanisms.

including enhanced binding and receptor clustering, dual HER2 signaling blockade as well as potent effector functions (Jhaveri et al. 2022). In a first-in-human phase 1 clinical trial the molecule demonstrated a manageable safety profile with encouraging single-agent anti-tumor activity in pretreated patients with HER2-positive cancers (NCT03821233).

Furthermore, a biparatopic MET × MET ADC (REGN5093-M114) was introduced by Regeneron Pharmaceuticals in order to achieve a functional MET pathway blockade (Drilon et al. 2022; Oh et al. 2023). Currently, the ADC is investigated in a phase 1/2 study in adult patients with MET-overexpressing NSCLC (NCT04982224).

Immunotherapies including ADC concepts involving CD19 targeting for treatment of B cell malignancies revealed encouraging results in the last years. Several anti-CD19 antibodies have recently been approved by the FDA as e.g. the Fc-engineered monoclonal antibody tafasitamab and the ADC loncastuximab tesirine (Zinzani and Minotti 2022). Additionally, CD22-addressing antibodies such as epratuzumab or ADCs moxetumomab pasudotox (Lumoxiti) or inotuzumab ozogamicin (Besponsa) proved efficacy (Shah and Sokol 2021). There is evidence that combined targeting of both receptors is superior to monospecific binding regarding internalization properties as well as overcoming of drug resistance (Bachanova et al. 2015; Schmohl et al. 2018). The bispecific CD19 × CD22 antibody diphtheria toxin-conjugate (DT2219) demonstrated potent anti-tumor cell effects and is currently being evaluated in phase 1/2 study in patients with relapsed/refractory B lineage leukemia or lymphoma (NCT02370160) (Schmohl et al. 2018).

2.10 Dual tumor-targeting chimeric antigen receptor-T cells

Dual TAA-targeting therapeutic antibodies can induce tumor cell death by both direct and indirect mechanisms. Direct mechanisms include blocking of growth factor receptor

signaling, whereas indirect mechanisms require interaction with components of the host immune system, including complement-dependent cytotoxicity, antibody-dependent cellular phagocytosis and ADCC (Zahavi et al. 2018). A plethora of current strategies in immune oncology rely on simultaneous targeting of immune cells such as T cells or NK cells and tumor cells with bispecific antibodies directing patients' immune cells against cancer (reviewed in chapter 3) (Goebeler and Bargou 2020). An alternative strategy is based on reprogrammed T cells endowed with chimeric antigen receptors (CAR). CARs are synthetic receptors engineered to drive T cells to recognize and eliminate cells expressing a specific target antigen. Binding of CAR-T cells to target antigens expressed on the cell surface occurs independently of major histocompatibility complex (MHC) presentation, resulting in potent T cell activation and a strong anti-tumor response (Sadelain et al. 2013). The best-studied and clinically validated CAR-T cells target CD19, a target expressed across most B cell malignancies (Davila and Brentjens 2016; Miller and Maus 2015). However, more than 50 % of patients treated with CD19 single-targeted CAR-T cells (Si-CART) experience relapse or refractory disease (Chavez et al. 2019; Xie et al. 2022). One of the major mechanisms contributing to the development of resistance to Si-CARTs is antigen escape, possibly caused by receptor genetic mutations or epitope masking (Lemoine et al. 2021). To reduce the likelihood of antigen escape and increase tumor cell killing activity, CAR-T cells that target two TAAs concurrently are being explored (Figure 2) (Sterner and Sterner 2021; Xie et al. 2022). The following section depicts dual tumor cell-targeting CAR-T cells that have proven to be effective in preclinical models or are investigated in clinical trials.

Like CD19, CD20 is expressed in B cell-derived malignancies but is not found on hematopoietic stem cells, making it one of the most promising targets for treatment of abnormal B cells (LeBien and Tedder 2008). CD19 × CD20 dual targeting CAR-T cells have demonstrated potent and durable anti-tumor response *in vivo*, as well as a strong clinical efficacy, low toxicity, and the ability to potentially reduce antigen escape relapse in patients with relapsed/refractory non-Hodgkin lymphoma (NCT03097770; NCT03019055; NCT04007029) (Larson et al. 2022; Shah et al. 2020; Tong et al. 2020). Another approach to overcome antigen loss following CAR-T cell therapy is the simultaneous targeting of CD19 and CD22, since anti-CD22 CAR-T cells have demonstrated clinical efficacy for B cell acute lymphoblastic leukemia (B-ALL) in patients resistant to CD19-targeted CAR-T cell immunotherapy (Fry et al. 2018). However, some tumors also show reduced surface expression of CD22, and therefore CAR-T cells targeting both CD19 and CD22 may have a broader anti-tumor activity. Administration of CD19 × CD22 dual targeting CAR-T cells to patients with relapsed/refractory B-ALL demonstrated potent anti-leukemic activity and a good safety profile (Dai et al. 2020; Jia et al. 2019; Wei et al. 2021), so these molecules are currently being studied in clinical trials (NCT05442515; NCT05225831; NCT03448393).

Although there is limited evidence from the current clinical data that relapse after anti-BCMA Si-CART therapy results from antigen loss, dual tumor cell-targeting CAR-T cells are being developed that target the B cell maturation antigen (BCMA) expressed in malignant plasma cells and CD19, CD38, CD319 or G protein-coupled receptor class C group 5 member D (GPRC5D) (Fernández de Larrea et al. 2020; Mei et al. 2021; Zah et al. 2020; Zhang et al. 2019). BCMA × CD19 or CD38 dual targeting CAR-T cells showed promising clinical results whereas BCMA × CD319 or GPRC5D targeting CAR-T cells were found to be effective in preclinical models (Garfall et al. 2023; Tang et al. 2022). These dual targeting CAR-T cells offer the potential to address the unmet medical need in 60 % of patients not remaining progression-free over 12 months post BCMA Si-CART treatment (Raje et al. 2019; Xie et al. 2022).

3 Trispecific dual targeting immune cell engager

Classical immune cell engagers (ICEs) simultaneously bind target antigens on tumor cells and immune-related molecules on endogenous effector cells, leading to the formation of an immunological synapse followed by tumor cell killing. Blinatumomab, the first US FDA-approved bispecific antibody, specific for B lymphocyte antigen CD19 and T cell co-receptor CD3 led to improved outcomes in treatment of patients with relapsed or refractory B-ALL (Jen et al. 2019). Beyond bispecific molecules, trispecific antibodies (tsAbs) have been explored by the addition of a third binding domain targeting either an additional tumor or immune cell antigen bringing forth ICEs with increased tumor specificity or enhanced immune cell responses against cancer (Figure 2) (Tapia-Galisteo et al. 2023). The following section reviews T cell engagers (TCE) and NK cell engagers (NKCE) in preclinical development or under clinical investigation binding two tumor cell targets and one immune cell target or targeting one tumor cell target and two immune cell targets.

3.1 Dual tumor cell-targeting ICEs

As already described for the bispecific dual TAA-targeting mAbs, dual TAA-targeting ICEs may also prevent tumor

escape due to antigen loss and overcome antigenic heterogeneity (Figure 2). In most trispecific dual TAA-targeting TCEs, the T cell binding arm targets CD3, a molecule associated with the T cell receptor (TCR) (Clevers et al. 1988). CD3-specific antibodies are able to activate T lymphocytes directing the cytolytic activity of T cells to tumor cells, which facilitates their elimination independent of MHC specificity (Singh et al. 2021). Targeting two surface antigens on cancerous B cells, Wang et al. developed a trispecific TCE specific for CD19, CD20 and CD3 (Wang et al. 2022). For the same reason, Zhao et al. fused an anti-CD19 scFv and an anti-CD22 nanobody to an anti-CD3 Fab fragment. The trispecific CD19 × CD22 × CD3 antibody showed improved anti-tumor efficacy in a patient-derived xenograft model of B-ALL and ability to overcome immune escape compared to the corresponding bispecific (CD19 × CD3) antibody and blinatumomab (Zhao et al. 2022). Since acute leukemias with co-expression of the B lymphoid lineage marker CD19 and the myeloid lineage marker CD33 usually have a poor prognosis, Roskopf et al. generated the dual-targeting triplebody 33-3-19, which induces specific lysis of myeloid and B lymphoid cell lines, favoring CD33 and CD19 double positives over single positive leukemia cells, highlighting the potential of dual TAA-targeting agents in leukemia patients (Roskopf et al. 2016). For the treatment of colorectal cancer, a trispecific dual TAA-targeting TCE has shown promising data *in vitro* and *in vivo*. A CD3-specific scFv flanked by anti-EGFR and anti-epithelial cell adhesion molecule (EpCAM) VHH fragments enabled specific cytolysis of EGFR- and/or EpCAM-expressing cancer cells. Here, bivalent bispecific targeting of double-positive cells improved *in vitro* potency by up to 100-fold compared to single-positive cells and significantly prolonged survival *in vivo* compared to corresponding bispecific antibodies (Tapia-Galisteo et al. 2022). A similar architecture was applied by Liu et al. to fuse a HER2 and a VEGFR2 binding nanobody to an anti-CD3 Fab. The trispecific HER2 × CD3 × VEGFR2 antibody showed improved anti-tumor efficacy *in vitro* and *in vivo* compared to the corresponding bispecific antibodies alone or in combination, overcoming tumor recurrence due to antigen escape or resistance to therapy observed with the anti-HER2 antibody trastuzumab or the anti-VEGFR2 antibody ramucirumab (Liu et al. 2022).

Another type of ICEs is represented by NKCEs, molecules developed to augment tumor cell killing by NK cell inherent toxicity (Demaria et al. 2021). A large portion of dual TAA-targeting NKCEs involve the activating NK cell receptor immunoglobulin Fcγ receptor IIIa (FcγRIIIa or CD16a), naturally targeted with low affinity by the Fc region of TAA-bound IgG antibodies (Khan et al. 2020). The developed NKCEs bind CD16 with increased affinity, resulting in an enhanced cytotoxicity and better/advanced safety profile compared to antibodies targeting CD16 with wild-type IgG1 Fc (Johnson et al. 2010; Tapia-Galisteo et al. 2023). The combination of the TAAs CD33 and CD19 with CD16 targeting also showed positive effects plugged in NKCEs as demonstrated by a single-chain triplebody generated by Schubert et al. (Schubert et al. 2011). Targeting of CD33 together with CD123 using the trispecific single-chain Fv derivative, CD33 × CD16 × CD123 induced significantly stronger NK-mediated lysis of primary leukemic cells compared to the trivalent bispecific construct CD123 × CD16 × CD123 (Kügler et al. 2010). CD22 × CD16 × CD19 trispecific tandem scFv molecule directly activated NK cells through CD16 and induced target specific cytotoxicity as well as cytokine and chemokine production resulting in the NK cell-mediated elimination of different types of leukemic cells (Gleason et al. 2012). Dual TAA-targeting trispecific NKCEs are beyond that generated for other indications such as multiple myeloma. Gantke et al. developed a monospecific anti-CD16 diabody with two scFvs at both termini, one anti-BCMA and one anti-CD200. This trispecific tetravalent aTriFlex showed increased selectivity for multiple myeloma cells and a 17-fold increase in *in vitro* potency (Gantke et al. 2017). Concurrent targeting of EGFR and PD-L1 besides CD16 with trispecific antibodies using the common light chain technology increased tumor specificity along with PD-L1/PD-1 checkpoint inhibition, resulting in a potent ADCC effect *in vitro* (Bogen et al. 2021; Harwardt et al. 2023). These data support the suggestion that trispecific antibodies involving dual tumor targeting strategies and redirection of immune cell cytotoxicity reveal augmented potencies compared to classical bispecific ICEs.

3.2 Dual immune cell-targeting ICEs

Besides dual tumor cell-targeting antibodies, trispecific dual immune cell-targeting molecules have been developed providing co-stimulatory signals to immune effector cells which further enhance responses against cancer (Figure 2).

3.3 Dual T cell-targeting ICEs

Complete activation of T lymphocytes naturally requires two signals, the first signal is derived from antigen recognition via the T cell receptor (TCR)/CD3 complex while the second signal is provided by engagement of co-stimulatory receptors (expressed on the T cell surface) (Chen and Flies 2013; Esensten et al. 2016; Mueller et al. 1989; Smith-Garvin et al. 2009). Ligation of co-stimulatory molecules such as CD28 enables T cell proliferation, differentiation and production

of cytokines necessary for adequate immune response (Boise et al. 1993; Esensten et al. 2016; Guo et al. 2008; Lindstein et al. 1989). Inhibitory receptors upregulated post T cell activation including PD-1, cytotoxic T lymphocyte-associated antigen 4 (CTLA-4) and B and T lymphocyte attenuator (BTLA) terminate T cell activation (Carreno and Collins 2003; Freeman et al. 2000; Walker and Sansom 2011). Harnessing cytotoxic properties of T cells, numerous TCEs that activate T cells *via* CD3 and redirect them to cancer cells have been developed and are currently undergoing clinical development (Zhou et al. 2021). The first CD28 superagonist TGN1412, intended to activate regulatory T cells for immune tolerance, failed in a first-in-human clinical trial inducing a dramatical cytokine release syndrome (CRS) (Suntharalingam et al. 2006; Tyrsin et al. 2016). Almost one decade later the antibody, renamed to TAB08, was forwarded to clinical studies (NCT01885624) again. Application of significantly lower CD28 superagonist doses to the patients resulted in desired T cell simulating effects (Tabares et al. 2014).

The CD3 molecule is non-covalently associated with the TCR and participates in antigen-specific signal transduction inducing initial activation of T cells (Chen and Flies 2013). Engagement of the co-stimulatory CD28 molecule triggers alternative signal transduction pathways and thereby inhibits unresponsiveness/anergy state and activation-induced cell death (Boise et al. 1993; Crespo et al. 2013). Recently, Sanofi developed a first-in-class dual T cell activation molecule comprising CD3 and CD28 binding domains besides the tumor-related moiety which demonstrated efficient and durable T cell stimulation and potent anti-tumor activity (Seung et al. 2022; Wu et al. 2020). Two tsAb constructs differing in TAA-targeting units were designed using the cross-over dual variable (CODV) bispecific antibody format and are currently investigated in phase 1 clinical studies (NCT04401020/NCT05013554) (Steinmetz et al. 2016).

The first of the two dual TCEs (SAR442257) targets TAA CD38 for treatment of multiple myeloma and non-Hodgkin's lymphoma. T cell co-stimulation by the tsAb increased the potency and survival of T cells lysing the tumor cells and further provoked amplification of antigen-specific memory T cells *in vitro*. Besides beneficial effects of dual T cell targeting monovalent interaction towards CD28 resulted in a reduced non-specific cytokine release *in vitro* compared to the bivalent parental anti-CD28 mAb. Beyond that the CD28 specificity contributed to superior recognition of different tumor antigen level-expressing myeloma cells ($CD38^+/CD28^+$) resulting in specific and enhanced tumor cell lysis. *In vivo* administration of the tsAb resulted in suppressed myeloma growth in a humanized mouse model and displayed acceptable pharmacodynamics and toxicity in non-human primates (Wu et al. 2020). The second trispecific molecule developed by Sanofi (SAR443216) is composed of HER2, CD3 and CD28 targeting units structurally based on their previously developed multispecific antibody platform. Overcoming current limitations of HER2-targeting monoclonal antibody therapies such as resistance in triple-negative breast cancer, the tsAb is intended to improve clinical outcomes for patients with varying HER2 level-expressing solid tumors e.g., breast or gastric cancer. Efficient stimulation of T cell activation and proliferation as well as potent anti-tumor effects against cells with low to high HER2 densities were effectuated *in vitro* by the dual TCE. Mechanisms contributing to tumor regression were shown to be exerted by CD8 T cells directly mediating tumor cell lysis *in vitro* and additionally by CD4 T cells blocking cancer cell cycle progression at G1/S and inducing pro-inflammatory responses *in vitro* and in humanized mouse models *in vivo* (Seung et al. 2022). The multispecific antibody approach providing two signals to stimulate T cells also triggers co-signaling which differs from signaling mediated by separate mAbs engaging the single receptors involved unrevealed mechanisms of T cell anti-tumor activity.

3.4 Dual NK cell-targeting ICEs

NK cells are key players in the innate immune system, exerting direct cytotoxic effects on infected or tumor cells and further eliciting multicellular immune responses ultimately resulting in sustained host protection (Vivier et al. 2008). The activation of NK lymphocytes is highly regulated by a set of germline-encoded stimulating and inhibitory receptors expressed on the cell membrane (Cooper et al. 2001). Equivalent to TCEs, NKCEs are bispecific molecules that bind to TAAs on tumor cells and to activating receptors on NK cells mediating potent anti-tumor immunity. The NK cell receptors to be addressed by NKCEs include CD16a, C-type lectin-like receptors natural-killer group 2, member D (NKG2D) and CD94/NKG2C, and natural cytotoxicity receptors NKp30, NKp44 and NKp46 (Demaria et al. 2021).

CD16 and NKp46 belong to the immunoglobulin superfamily, are both constituted of two extracellular Ig-like domains associated with FcRγ and CD3ζ ITAM-bearing polypeptides, therefore sharing protein-tyrosine kinase (PTK)-dependent signaling pathways responsible for effector cell functions (Demaria et al. 2021; Ravetch and Bolland 2001; Sivori et al. 1999). In 2019, Gauthier et al. (Innate Pharma) reported the generation of trifunctional CD16 × NKp46 × TAA antibody constructs composed of an engineered Fc for enhanced CD16 binding, a first-in-class agonist anti-NKp46 cross-mab and TAA-targeting Fabs against CD19, CD20 or EGFR (Gauthier et al. 2019). The trispecific NKCEs triggered potent cancer cell lysis by human primary NK cells *in vitro*

without inducing off-target effects or fratricidal NK cell killing. *In vivo* ADCC-mediated tumor clearance was promoted by the trifunctional antibody superior to effector-silenced versions in various preclinical mouse models of solid and invasive cancers (Gauthier et al. 2019). Based on this approach of dual NK cell engagement by CD16 and NKp46 and targeting of different TAAs, the antibody-based NK cell engager therapeutics (ANKET®) platform has been developed by Innate Pharma (Demaria et al. 2021). In collaboration with Sanofi three drug candidates are currently under preclinical and clinical phase 1/2 investigation which incorporate TAA-targeting units against B7-H3 (IPH62), CD123 (IPH6101; NCT05086315) or BCMA (IPH6401; NCT05839626) for treatment of different types of cancer.

The activating NKG2D homodimeric receptor lacks signaling properties and mediates intracellular signal propagation via two associated DAP10 adapter proteins (which trigger the PI-3K pathway and a Grb2-Vav1-dependent pathway) (Zingoni et al. 2018). The activating NK cell receptor is featured by the ability to interact with numerous distinct ligands expressed by abnormal cells resulting in transduction of different signals and NK cell reactions. Dragonfly Therapeutics designed and patented multispecific binding proteins, referred to as TriNKETs (Trispecific NK cell Engager Therapies), that bind to NKG2D, CD16 and various TAAs such as HLA-E, CCR4, PD-L1, FLT3, EGFR, CD33, BCMA or HER2 (Baruah et al. 2020; Chang et al. 2018a, b). In general, the combination of CD16 and NKG2D engagement caused a synergistic activation of NK cells and may counteract tumor immune escape mechanisms such as CD16 downmodulation. TriNKET molecule DF9001, specific for tumor antigen EGFR, displayed improved target cell lysis compared to the parental EGFR-targeting mAbs (necitumumab, panitumumab) and is currently investigated in clinical phase 1 studies (NCT05597839) (Chang et al. 2018a). DF1001, the TriNKET progressed furthest in clinical development, targets HER2 and is currently being evaluated in phase 1/2 studies of patients with advanced solid tumors (NCT04143711).

4 Conclusions and prospects

In the fight against cancer, there is high demand for the development of novel therapies, with multispecific antibodies gaining importance as they can induce and combine multiple mechanisms of actions. Compared to monospecific mAbs, bispecific antibodies allow immune cell involvement or high precision tumor targeting by dual TAA binding. Attachment of another functionality results in trispecific molecules addressing either immune cells or target cancer cells with two antibody moieties. Thereby a variety of different mechanisms can be executed at the same time including immune checkpoint blockade, simultaneous modulation of two signaling pathways, circumvention of drug resistance and immune escape or augmented immune cell activation engendering more intense and durable anti-tumor effects. Tetraspecific antibodies have recently been added to the arsenal of multispecific antibodies, including molecules derived from the Sanofi ANKET® (antibody-based NK cell engager therapeutics) platform (Demaria et al. 2022). Tetraspecific ANKETs target NKp46, CD16a, IL-2Rβ and a TAA via a single molecule inducing preferential activation and proliferation of NK cells and triggering NK cell cytotoxicity as well as cytokine and chemokine production by triple NK targeting. Besides NKCEs, tetraspecific TCEs were rendered by Sichuan Baili/Systimmune addressing CD3, 4-1BB, PD-L1 and a TAA and are currently being tested in clinical trials (NCT05160545; NCT04606433; NCT04794972) (Claus et al. 2023). The innovative molecules, not being described in scientific literature, deliver two T cell-stimulatory signals and concurrently dual target tumor cells including the blockade of an immune checkpoint. However, complex structural designs uniting diverse binding modalities also raise challenges with respect to manufacturability such as proteolysis, aggregation, incorrect assembly of multichain antibodies or low expression yields (Krah et al. 2018; Ma et al. 2020). Besides technical issues there may also be limitations regarding application of antibody drugs to humans including CRS by overstimulation of T cells or immunogenicity which requires careful pharmacologic risk assessment (Kroenke et al. 2021; Shah et al. 2023; Shimabukuro-Vornhagen et al. 2018).

In conclusion, bispecific and multispecific protein and cell-based therapies have the potential for broad use as highly effective treatment options for cancer patients, improving tumor eradication in early but also in later stages of tumor progression and reducing risk of tumor recurrence.

Research ethics: Not applicable.
Author contributions: The authors have accepted responsibility for the entire content of this manuscript and approved its submission.
Competing interests: The authors state no conflict of interest.
Research funding: None declared.
Data availability: Not applicable.

References

Alley, S.C., Okeley, N.M., and Senter, P.D. (2010). Antibody-drug conjugates: targeted drug delivery for cancer. *Curr. Opin. Chem. Biol.* 14: 529–537.
Alvarez-Argote, J. and Dasanu, C.A. (2019). Durvalumab in cancer medicine: a comprehensive review. *Expert. Opin. Biol. Ther.* 19: 927–935.

Bachanova, V., Frankel, A.E., Cao, Q., Lewis, D., Grzywacz, B., Verneris, M.R., Ustun, C., Lazaryan, A., McClune, B., Warlick, E.D., et al. (2015). Phase I study of a bispecific ligand-directed toxin targeting CD22 and CD19 (DT2219) for refractory B-cell malignancies. *Clin. Cancer Res.* 21: 1267–1272.

Baruah, H., Chang, G., Cheung, A., Grinberg, A., Juo, Z., and Mcquade, T. (2020). Proteins binding NKG2D, CD16 and FLT3. US201962915123P A61K39/395;A61P35/00;C07K16/28;C07K16/30;C07K16/46.

Baulida, J., Kraus, M.H., Alimandi, M., Di Fiore, P.P., and Carpenter, G. (1996). All ErbB receptors other than the epidermal growth factor receptor are endocytosis impaired. *J. Biol. Chem.* 271: 5251–5257.

Bendell, J., Blay, J.-Y., Cassier, P., Bauer, T., Terret, C., Mueller, C., Morel, A., Chesne, E., Xu, Z., Tessier, J., et al. (2018). Abstract A092: phase 1 trial of RO6874813, a novel bispecific FAP-DR5 antibody, in patients with solid tumors. *Mol. Cancer Ther.* 17: A092.

Bogen, J.P., Carrara, S.C., Fiebig, D., Grzeschik, J., Hock, B., and Kolmar, H. (2021). Design of a trispecific checkpoint inhibitor and natural killer cell engager based on a 2 + 1 common light chain antibody architecture. *Front. Immunol.* 12: 669496.

Boise, L.H., González-García, M., Postema, C.E., Ding, L., Lindsten, T., Turka, L.A., Mao, X., Nuñez, G., and Thompson, C.B. (1993). bcl-x, a bcl-2-related gene that functions as a dominant regulator of apoptotic cell death. *Cell* 74: 597–608.

Brahmer, J.R., Tykodi, S.S., Chow, L.Q.M., Hwu, W.-J., Topalian, S.L., Hwu, P., Drake, C.G., Camacho, L.H., Kauh, J., Odunsi, K., et al. (2012). Safety and activity of anti-PD-L1 antibody in patients with advanced cancer. *N. Engl. J. Med.* 366: 2455–2465.

Brennan, F.R., Morton, L.D., Spindeldreher, S., Kiessling, A., Allenspach, R., Hey, A., Muller, P.Y., Frings, W., and Sims, J. (2010). Safety and immunotoxicity assessment of immunomodulatory monoclonal antibodies. *MAbs* 2: 233–255.

Brünker, P., Wartha, K., Friess, T., Grau-Richards, S., Waldhauer, I., Koller, C.F., Weiser, B., Majety, M., Runza, V., Niu, H., et al. (2016). RG7386, a novel tetravalent FAP-DR5 antibody, effectively triggers FAP-dependent, avidity-driven DR5 hyperclustering and tumor cell apoptosis. *Mol. Cancer Ther.* 15: 946–957.

Buatois, V., Johnson, Z., Salgado-Pires, S., Papaioannou, A., Hatterer, E., Chauchet, X., Richard, F., Barba, L., Daubeuf, B., Cons, L., et al. (2018). Preclinical development of a bispecific antibody that safely and effectively targets CD19 and CD47 for the treatment of B-cell lymphoma and leukemia. *Mol. Cancer Ther.* 17: 1739–1751.

Carreno, B.M. and Collins, M. (2003). BTLA: a new inhibitory receptor with a B7-like ligand. *Trends Immunol.* 24: 524–527.

Chang, G.P., Cheung, A.F., Du, J., Grinberg, A., Haney, W., Sethi, D.K., Wagtmann, N., Lunde, B.M., and Prinz, B. (2018a). Proteins binding NKG2D, CD16, and EGFR, CCR4, or PD-L1. US201762546297P; US201762546300P;US201762552152P;US201762555114P; EP20180846836;WO2018US00212 A61K47/68;C07K14/705;C07K16/28; C07K16/30.

Chang, G.P., Cheung, A.F., Haney, W., Lunde, B.M., and Prinz, B. (2018b). Proteins binding HER2, NKG2D and CD16. US201762461146P; US201816486569;WO2018US18771 A61P35/00;C07K16/28;C07K16/32.

Chavez, J.C., Bachmeier, C., and Kharfan-Dabaja, M.A. (2019). CAR T-cell therapy for B-cell lymphomas: clinical trial results of available products. *Ther. Adv. Hematol.* 10: Article no. 2040620719841581.

Chen, L. and Flies, D.B. (2013). Molecular mechanisms of T cell co-stimulation and co-inhibition. *Nat. Rev. Immunol.* 13: 227–242.

Claus, C., Ferrara-Koller, C., and Klein, C. (2023). The emerging landscape of novel 4-1BB (CD137) agonistic drugs for cancer immunotherapy. *MAbs* 15: 2167189.

Clevers, H., Alarcon, B., Wileman, T., and Terhorst, C. (1988). The T cell receptor/CD3 complex: a dynamic protein ensemble. *Annu. Rev. Immunol.* 6: 629–662.

Cohen, E.E., Fayette, J., Daste, A., Even, C., Le Tourneau, C., Brana, I., Saada, E., Fontana, E., Iglesias, L., Kato, S., et al. (2023). Abstract CT012: clinical activity of MCLA-158 (petosemtamab), an IgG1 bispecific antibody targeting EGFR and LGR5, in advanced head and neck squamous cell cancer (HNSCC). *Cancer Res.* 83: CT012.

Cooper, M.A., Fehniger, T.A., and Caligiuri, M.A. (2001). The biology of human natural killer-cell subsets. *Trends Immunol.* 22: 633–640.

Crespo, J., Sun, H., Welling, T.H., Tian, Z., and Zou, W. (2013). T cell anergy, exhaustion, senescence, and stemness in the tumor microenvironment. *Curr. Opin. Immunol.* 25: 214–221.

Dai, H., Wu, Z., Jia, H., Tong, C., Guo, Y., Ti, D., Han, X., Liu, Y., Zhang, W., Wang, C., et al. (2020). Bispecific CAR-T cells targeting both CD19 and CD22 for therapy of adults with relapsed or refractory B cell acute lymphoblastic leukemia. *J. Hematol. Oncol.* 13: 30.

Davila, M.L. and Brentjens, R.J. (2016). CD19-Targeted CAR T cells as novel cancer immunotherapy for relapsed or refractory B-cell acute lymphoblastic leukemia. *Clin. Adv. Hematol. Oncol.* 14: 802–808.

Demaria, O., Gauthier, L., Debroas, G., and Vivier, E. (2021). Natural killer cell engagers in cancer immunotherapy: next generation of immuno-oncology treatments. *Eur. J. Immunol.* 51: 1934–1942.

Demaria, O., Gauthier, L., Vetizou, M., Blanchard Alvarez, A., Vagne, C., Habif, G., Batista, L., Baron, W., Belaïd, N., Girard-Madoux, M., et al. (2022). Antitumor immunity induced by antibody-based natural killer cell engager therapeutics armed with not-alpha IL-2 variant. *Cell Rep. Med.* 3: 100783.

Dheilly, E., Moine, V., Broyer, L., Salgado-Pires, S., Johnson, Z., Papaioannou, A., Cons, L., Calloud, S., Majocchi, S., Nelson, R., et al. (2017). Selective blockade of the ubiquitous checkpoint receptor CD47 is enabled by dual-targeting bispecific antibodies. *Mol. Ther.* 25: 523–533.

Drilon, A.E., Awad, M.M., Gadgeel, S.M., Villaruz, L.C., Sabari, J.K., Perez, J., Daly, C., Patel, S., Li, S., Seebach, F.A., et al. (2022). A phase 1/2 study of REGN5093-M114, a METxMET antibody-drug conjugate, in patients with mesenchymal epithelial transition factor (MET)-overexpressing NSCLC. *J. Clin. Oncol.* 40: TPS8593.

Esensten, J.H., Helou, Y.A., Chopra, G., Weiss, A., and Bluestone, J.A. (2016). CD28 costimulation: from mechanism to therapy. *Immunity* 44: 973–988.

Feng, J., Chen, J., Li, K., Li, X., Min, X., Li, B., Lin, L., Fang, Y., Sun, Y., Zhu, B., et al. (2021). 1278P SHR-1701, a bifunctional fusion protein targeting PD-L1 and TGF-β, as first-line therapy for PD-L1+ advanced/metastatic NSCLC: data from a clinical expansion cohort of a phase I study. *Ann. Oncol.* 32: S995.

Fernández de Larrea, C., Staehr, M., Lopez, A.V., Ng, K.Y., Chen, Y., Godfrey, W.D., Purdon, T.J., Ponomarev, V., Wendel, H.-G., Brentjens, R.J., et al. (2020). Defining an optimal dual-targeted CAR T-cell therapy approach simultaneously targeting BCMA and GPRC5D to prevent BCMA escape-driven relapse in multiple myeloma. *Blood Cancer Discov.* 1: 146–154.

Freeman, G.J., Long, A.J., Iwai, Y., Bourque, K., Chernova, T., Nishimura, H., Fitz, L.J., Malenkovich, N., Okazaki, T., Byrne, M.C., et al. (2000). Engagement of the PD-1 immunoinhibitory receptor by a novel B7 family member leads to negative regulation of lymphocyte activation. *J. Exp. Med.* 192: 1027–1034.

Fry, T.J., Shah, N.N., Orentas, R.J., Stetler-Stevenson, M., Yuan, C.M., Ramakrishna, S., Wolters, P., Martin, S., Delbrook, C., Yates, B., et al. (2018). CD22-targeted CAR T cells induce remission in B-ALL that is naive or resistant to CD19-targeted CAR immunotherapy. *Nat. Med.* 24: 20–28.

Fu, Z., Li, S., Han, S., Shi, C., and Zhang, Y. (2022). Antibody drug conjugate: the "biological missile" for targeted cancer therapy. *Signal Transduct. Target. Ther.* 7: 93.

Gagliardi, C., Pericle, F., Salameh, A., Blezinger, P., and Curran, M. (2022). 1333 Development of IMGS-001, a novel anti-PD-L1/PD-L2 dual specific, multi-functional antibody, to treat immune excluded tumors. In: Regular and young investigator award abstracts. BMJ Publishing Group Ltd, Boston, MA, p. A1382.

Gandullo-Sánchez, L., Ocaña, A., and Pandiella, A. (2022). HER3 in cancer: from the bench to the bedside. *J. Exp. Clin. Cancer Res.* 41: 310.

Gantke, T., Weichel, M., Herbrecht, C., Reusch, U., Ellwanger, K., Fucek, I., Eser, M., Müller, T., Griep, R., Molkenthin, V., et al. (2017). Trispecific antibodies for CD16A-directed NK cell engagement and dual-targeting of tumor cells. *Protein Eng. Des. Sel.* 30: 673–684.

García, M.D., Hollebecque, A., Garcia-Carbonero, R., Jungels, C., Smyth, E., Kato, S., Argilés, G., Martin, C.G., Magin, M., Shen, Y.-M., et al. (2023) Abstract CT156: MCLA-158 (petosemtamab), an IgG1 bispecific antibody targeting EGFR and LGR5, in advanced gastric/esophageal adenocarcinoma (GEA). *Cancer Res.* 83: CT156.

García-Martínez, J.M., Wang, S., Weishaeupl, C., Wernitznig, A., Chetta, P., Pinto, C., Ho, J., Dutcher, D., Gorman, P.N., Kroe-Barrett, R., et al. (2021). Selective tumor cell apoptosis and tumor regression in CDH17-positive colorectal cancer models using BI 905711, a novel liver-sparing TRAILR2 agonist. *Mol. Cancer Ther.* 20: 96–108.

Garfall, A.L., Cohen, A.D., Susanibar-Adaniya, S.P., Hwang, W.-T., Vogl, D.T., Waxman, A.J., Lacey, S.F., Gonzalez, V.E., Fraietta, J.A., Gupta, M., et al. (2023). Anti-BCMA/CD19 CAR T cells with early immunomodulatory maintenance for multiple myeloma responding to initial or later-line therapy. *Blood Cancer Discov.* 4: 118–133.

Gauthier, L., Morel, A., Anceriz, N., Rossi, B., Blanchard-Alvarez, A., Grondin, G., Trichard, S., Cesari, C., Sapet, M., Bosco, F., et al. (2019). Multifunctional natural killer cell engagers targeting NKp46 trigger protective tumor immunity. *Cell* 177: 1701–1713.e16.

Geuijen, C.A.W., de Nardis, C, Maussang, D., Rovers, E., Gallenne, T., Hendriks, L.J.A., Visser, T., Nijhuis, R., Logtenberg, T., de Kruif, J., et al. (2018). Unbiased combinatorial screening identifies a bispecific IgG1 that potently inhibits HER3 signaling via HER2-guided ligand blockade. *Cancer Cell* 33: 922–936.e10.

Giovannetti, E. and Leon, L.G. (2014). New strategies and applications for drugs targeting EGFR and c-Met. *Curr. Drug Targets* 15: 1261–1262.

Gleason, M.K., Verneris, M.R., Todhunter, D.A., Zhang, B., McCullar, V., Zhou, S.X., Panoskaltsis-Mortari, A., Weiner, L.M., Vallera, D.A., and Miller, J.S. (2012). Bispecific and trispecific killer cell engagers directly activate human NK cells through CD16 signaling and induce cytotoxicity and cytokine production. *Mol. Cancer Ther.* 11: 2674–2684.

Goebeler, M.-E. and Bargou, R.C. (2020). T cell-engaging therapies – BiTEs and beyond. *Nat. Rev. Clin. Oncol.* 17: 418–434.

Goeij, B.E.C.G., Peipp, M., Haij, S., van den Brink, E.N., Kellner, C., Riedl, T., de Jong, R., Vink, T., Strumane, K., Bleeker, W.K., et al. (2014). HER2 monoclonal antibodies that do not interfere with receptor heterodimerization-mediated signaling induce effective internalization and represent valuable components for rational antibody-drug conjugate design. *MAbs* 6: 392–402.

Goeij, B.E.C.G., Vink, T., Ten Napel, H., Breij, E.C.W., Satijn, D., Wubbolts, R., Miao, D., and Parren, P.W.H.I. (2016). Efficient payload delivery by a bispecific antibody-drug conjugate targeting HER2 and CD63. *Mol. Cancer Ther.* 15: 2688–2697.

Guo, F., Iclozan, C., Suh, W.-K., Anasetti, C., and Yu, X.-Z. (2008). CD28 controls differentiation of regulatory T cells from naive CD4 T cells. *J. Immunol.* 181: 2285–2291.

Guo, Y., Liu, B., Lv, D., Cheng, Y., Zhou, T., Zhong, Y., Hu, C., Chen, G., Wu, X., Yin, Y., et al. (2022). Phase I/IIa study of PM8001, a bifunctional fusion protein targeting PD-L1 and TGF-β, in patients with advanced tumors. *J. Clin. Oncol.* 40: 2512.

Hao, Y., Yu, X., Bai, Y., McBride, H.J., and Huang, X. (2019). Cryo-EM structure of HER2-trastuzumab-pertuzumab complex. *PLoS One* 14: e0216095.

Harwardt, J., Bogen, J.P., Carrara, S.C., Ulitzka, M., Grzeschik, J., Hock, B., and Kolmar, H. (2022). A generic strategy to generate bifunctional two-in-one antibodies by chicken immunization. *Front. Immunol.* 13: 888838.

Harwardt, J., Carrara, S.C., Bogen, J.P., Schoenfeld, K., Grzeschik, J., Hock, B., and Kolmar, H. (2023). Generation of a symmetrical trispecific NK cell engager based on a two-in-one antibody. *Front. Immunol.* 14: 1170042.

Hatterer, E., Chauchet, X., Richard, F., Barba, L., Moine, V., Chatel, L., Broyer, L., Pontini, G., Bautzova, T., Juan, F., et al. (2020). Targeting a membrane-proximal epitope on mesothelin increases the tumoricidal activity of a bispecific antibody blocking CD47 on mesothelin-positive tumors. *MAbs* 12: 1739408.

Herpers, B., Eppink, B., James, M.I., Cortina, C., Cañellas-Socias, A., Boj, S.F., Hernando-Momblona, X., Glodzik, D., Roovers, R.C., van de Wetering, M., et al. (2022). Functional patient-derived organoid screenings identify MCLA-158 as a therapeutic EGFR × LGR5 bispecific antibody with efficacy in epithelial tumors. *Nat. Cancer* 3: 418–436.

Huang, S., Li, F., Liu, H., Ye, P., Fan, X., Yuan, X., Wu, Z., Chen, J., Jin, C., Shen, B., et al. (2018). Structural and functional characterization of MBS301, an afucosylated bispecific anti-HER2 antibody. *MAbs* 10: 864–875.

Huang, S., van Duijnhoven, S.M.J., Sijts, A.J.A.M., and van Elsas, A. (2020). Bispecific antibodies targeting dual tumor-associated antigens in cancer therapy. *J. Cancer Res. Clin. Oncol.* 146: 3111–3122.

Jen, E.Y., Xu, Q., Schetter, A., Przepiorka, D., Shen, Y.L., Roscoe, D., Sridhara, R., Deisseroth, A., Philip, R., Farrell, A.T., et al. (2019). FDA approval: blinatumomab for patients with B-cell precursor acute lymphoblastic leukemia in morphologic remission with minimal residual disease. *Clin. Cancer Res.* 25: 473–477.

Jhaveri, K., Han, H., Dotan, E., Oh, D.-Y., Ferrario, C., Tolcher, A., Lee, K.-W., Liao, C.-Y., Kang, Y.-K., Kim, Y.H., et al. (2022). 460MO Preliminary results from a phase I study using the bispecific, human epidermal growth factor 2 (HER2)-targeting antibody-drug conjugate (ADC) zanidatamab zovodotin (ZW49) in solid cancers. *Ann. Oncol.* 33: S749–S750.

Jia, H., Wang, Z., Wang, Y., Liu, Y., Dai, H., Tong, C., Guo, Y., Guo, B., Ti, D., Han, X., et al. (2019). Haploidentical CD19/CD22 bispecific CAR-T cells induced MRD-negative remission in a patient with relapsed and refractory adult B-ALL after haploidentical hematopoietic stem cell transplantation. *J. Hematol. Oncol.* 12: 57.

Jiang, Z., Sun, H., Yu, J., Tian, W., and Song, Y. (2021). Targeting CD47 for cancer immunotherapy. *J. Hematol. Oncol.* 14: 180.

Johnson, S., Burke, S., Huang, L., Gorlatov, S., Li, H., Wang, W., Zhang, W., Tuaillon, N., Rainey, J., Barat, B., et al. (2010). Effector cell recruitment with novel Fv-based dual-affinity re-targeting protein leads to potent tumor cytolysis and in vivo B-cell depletion. *J. Mol. Biol.* 399: 436–449.

Ju, X., Zhang, H., Zhou, Z., and Wang, Q. (2020). Regulation of PD-L1 expression in cancer and clinical implications in immunotherapy. *Am. J. Cancer Res.* 10: 1–11.

Kavarthapu, R., Anbazhagan, R., and Dufau, M.L. (2021). Crosstalk between PRLR and EGFR/HER2 signaling pathways in breast cancer. Cancers 13: 4685.

Khan, M., Arooj, S., and Wang, H. (2020). NK cell-based immune checkpoint inhibition. *Front. Immunol.* 11: 167.

Kim, E.S. (2017). Avelumab: first global approval. *Drugs* 77: 929–937.

Klapper, L.N., Glathe, S., Vaisman, N., Hynes, N.E., Andrews, G.C., Sela, M., and Yarden, Y. (1999). The ErbB-2/HER2 oncoprotein of human carcinomas may function solely as a shared coreceptor for multiple stroma-derived growth factors. *Proc. Natl. Acad. Sci. U. S. A.* 96: 4995–5000.

Koopmans, I., Hendriks, D., Samplonius, D.F., van Ginkel, R.J., Heskamp, S., Wierstra, P.J., Bremer, E., and Helfrich, W. (2018). A novel bispecific antibody for EGFR-directed blockade of the PD-1/PD-L1 immune checkpoint. *Oncoimmunology* 7: e1466016.

Krah, S., Kolmar, H., Becker, S., and Zielonka, S. (2018). Engineering IgG-like bispecific antibodies-an overview. *Antibodies* 7: 28.

Kroenke, M.A., Milton, M.N., Kumar, S., Bame, E., and White, J.T. (2021). Immunogenicity risk assessment for multi-specific therapeutics. *AAPS J.* 23: 115.

Kügler, M., Stein, C., Kellner, C., Mentz, K., Saul, D., Schwenkert, M., Schubert, I., Singer, H., Oduncu, F., Stockmeyer, B., et al. (2010). A recombinant trispecific single-chain Fv derivative directed against CD123 and CD33 mediates effective elimination of acute myeloid leukaemia cells by dual targeting. *Br. J. Haematol.* 150: 574–586.

Larson, S.M., Walthers, C., Ji, B., Ghafouri, S.N., Naparstek, J., Trent, J., Harris, C., Khericha Gandhi, M., Schweppe, T., Auerbach, M.S., et al. (2022). CD19/CD20 bispecific chimeric antigen receptor (CAR) in naïve/memory T cells for the treatment of relapsed or refractory non-Hodgkin lymphoma. *J. Clin. Oncol.* 40: 2543.

LeBien, T.W. and Tedder, T.F. (2008). B lymphocytes: how they develop and function. *Blood* 112: 1570–1580.

Lemoine, J., Ruella, M., and Houot, R. (2021). Born to survive: how cancer cells resist CAR T cell therapy. *J. Hematol. Oncol.* 14: 199.

Lindstein, T., June, C.H., Ledbetter, J.A., Stella, G., and Thompson, C.B. (1989). Regulation of lymphokine messenger RNA stability by a surface-mediated T cell activation pathway. *Science* 244: 339–343.

Liu, D., Gong, J., Liu, T., Li, K., Yin, X., Liu, Y., Wang, Y., Wang, L., Wang, W., Zhang, Y., et al. (2021). Phase 1 study of SHR-1701, a bifunctional fusion protein targeting PD-L1 and TGF-β, in patients with advanced solid tumors. *J. Clin. Oncol.* 39: 2503.

Liu, D., Qi, X., Wei, X., Zhao, L., Wang, X., Li, S., Wang, Z., Shi, L., Xu, J., Hong, M., et al. (2022). A Novel Her2/VEGFR2/CD3 trispecific antibody with an optimal structural design showed improved T-cell-redirecting antitumor efficacy. *Theranostics* 12: 7788–7803.

Lyu, X., Zhao, Q., Hui, J., Wang, T., Lin, M., Wang, K., Zhang, J., Shentu, J., Dalby, P.A., Zhang, H., et al. (2022). The global landscape of approved antibody therapies. *Antib. Ther.* 5: 233–257.

Ma, H., Ó'Fágáin, C., and O'Kennedy, R. (2020). Antibody stability: a key to performance – analysis, influences and improvement. *Biochimie* 177: 213–225.

Markham, A. (2016). Atezolizumab: first global approval. *Drugs* 76: 1227–1232.

Matikonda, S.S., McLaughlin, R., Shrestha, P., Lipshultz, C., and Schnermann, M.J. (2022). Structure-activity relationships of antibody-drug conjugates: a systematic review of chemistry on the trastuzumab scaffold. *Bioconjug. Chem.* 33: 1241–1253.

Mei, H., Li, C., Jiang, H., Zhao, X., Huang, Z., Jin, D., Guo, T., Kou, H., Liu, L., Tang, L., et al. (2021). A bispecific CAR-T cell therapy targeting BCMA and CD38 in relapsed or refractory multiple myeloma. *J. Hematol. Oncol.* 14: 161.

Meng, Y., Zhang, J., Zhao, C., Cheng, Y., Zhu, L., Song, Z., Xu, N., Wang, Z., Wang, Y., Du, Y., et al. (2023). Preliminary results of a phase I, first-in-human, dose escalation study of IMM2902 in patients with HER2-expressing advanced solid tumors. *J. Clin. Oncol.* 41: e15185.

Miller, B.C. and Maus, M.V. (2015). CD19-Targeted CAR T cells: a new tool in the fight against B cell malignancies. *Oncol. Res. Treat.* 38: 683–690.

Moores, S.L., Chiu, M.L., Bushey, B.S., Chevalier, K., Luistro, L., Dorn, K., Brezski, R.J., Haytko, P., Kelly, T., Wu, S.-J., et al. (2016). A novel bispecific antibody targeting EGFR and cMet is effective against EGFR inhibitor-resistant lung tumors. *Cancer Res.* 76: 3942–3953.

Mueller, D.L., Jenkins, M.K., and Schwartz, R.H. (1989). An accessory cell-derived costimulatory signal acts independently of protein kinase C activation to allow T cell proliferation and prevent the induction of unresponsiveness. *J. Immunol.* 142: 2617–2628.

Mujcic, H., Rzymski, T., Rouschop, K.M.A., Koritzinsky, M., Milani, M., Harris, A.L., and Wouters, B.G. (2009). Hypoxic activation of the unfolded protein response (UPR) induces expression of the metastasis-associated gene LAMP3. *Radiother. Oncol.* 92: 450–459.

Mullard, A. (2021). FDA approves 100th monoclonal antibody product. *Nat. Rev. Drug Discovery* 20: 491–495.

Nagelkerke, A., Mujcic, H., Bussink, J., Wouters, B.G., van Laarhoven, H.W.M., Sweep, F.C.G.J., and Span, P.N. (2011). Hypoxic regulation and prognostic value of LAMP3 expression in breast cancer. *Cancer* 117: 3670–3681.

Normant, E., Ribeiro, M.L., Reyes, D., Miskin, H.P., Sportelli, P., Weiss, M.S., Bosch, F., and Roue, G. (2019). The novel bispecific CD47-CD19 antibody TG-1801 potentiates the activity of Ublituximab-Umbralisib (U2) drug combination in preclinical models of B-NHL. *Hematol. Oncol.* 37: 322–323.

O'Donnell, J.S., Long, G.V., Scolyer, R.A., Teng, M.W.L., and Smyth, M.J. (2017). Resistance to PD1/PDL1 checkpoint inhibition. *Cancer Treat. Rev.* 52: 71–81.

Oh, S.Y., Lee, Y.W., Lee, E.J., Kim, J.H., Park, Y., Heo, S.G., Yu, M.R., Hong, M.H., DaSilva, J., Daly, C., et al. (2023). Preclinical study of a biparatopic METxMET antibody-drug conjugate, REGN5093-M114, overcomes MET-driven acquired resistance to EGFR TKIs in EGFR-mutant NSCLC. *Clin. Cancer Res.* 29: 221–232.

Ou, S.H., Moreno Garcia, V., Gil Bazo, I., Prenen, H., Moreno, I., Johnson, M., Castañón Álvarez, E., Nagasaka, M., Adeyemi, S., Barasa, B., et al. (2022). MCLA-129, a human anti-EGFR and anti-c-MET bispecific antibody, in patients with advanced NSCLC and other solid tumors: an ongoing phase 1/2 study. *Eur. J. Cancer* 174: S122.

Pang, K., Shi, Z.-D., Wei, L.-Y., Dong, Y., Ma, Y.-Y., Wang, W., Wang, G.-Y., Cao, M.-Y., Dong, J.-J., Chen, Y.-A., et al. (2023). Research progress of therapeutic effects and drug resistance of immunotherapy based on PD-1/PD-L1 blockade. *Drug Resist. Updat.* 66: 100907.

Piazza, T.M., Lu, J.-C., Carver, K.C., and Schuler, L.A. (2009). SRC family kinases accelerate prolactin receptor internalization, modulating trafficking and signaling in breast cancer cells. *Mol. Endocrinol.* 23: 202–212.

Pols, M.S. and Klumperman, J. (2009). Trafficking and function of the tetraspanin CD63. *Exp. Cell Res.* 315: 1584–1592.

Qing, Z., Gabrail, N., Uprety, D., Rotow, J., Han, B., Jänne, P.A., Nagasaka, M., Zheng, M., Zhang, Y., Yang, G., et al. (2022). 22P EMB-01: an EGFR-cMET bispecific antibody, in advanced/metastatic solid tumors phase I results. *Ann. Oncol.* 33: S39–S40.

Raje, N., Berdeja, J., Lin, Y., Siegel, D., Jagannath, S., Madduri, D., Liedtke, M., Rosenblatt, J., Maus, M.V., Turka, A., et al. (2019). Anti-BCMA CAR T-cell therapy bb2121 in relapsed or refractory multiple myeloma. *N. Engl. J. Med.* 380: 1726–1737.

Ravetch, J.V. and Bolland, S. (2001). IgG Fc receptors. *Annu. Rev. Immunol.* 19: 275–290.

Ren, F., Wu, X., Yang, D., Wu, D., Gong, S., Zhang, Y., Lensky, S., and Wu, C. (2020) Abstract 528: EMB-01: an innovative bispecific antibody targeting EGFR and cMet on tumor cells mediates a novel mechanism to improve anti-tumor efficacy. *Cancer Res.* 80: 528.

Renshaw, B., Khalili, J.S., Xiao, S., and Zhu, Y. (2023) Abstract 6309: anti-tumor efficacy of SI-B001, a novel EGFR × HER3 bispecific antibody, against EGFR-driven epithelial tumors alone or in combination with paclitaxel and carboplatin. *Cancer Res.* 83: 6309.

Reslan, L., Dalle, S., and Dumontet, C. (2009). Understanding and circumventing resistance to anticancer monoclonal antibodies. *MAbs* 1: 222–229.

Rexer, B.N. and Arteaga, C.L. (2012). Intrinsic and acquired resistance to HER2-targeted therapies in HER2 gene-amplified breast cancer: mechanisms and clinical implications. *Crit. Rev. Oncog.* 17: 1–16.

Riu Martinez, X., Bandari, R., and Lalitha, A. (2022) American Society of Clinical Oncology (ASCO) – 58th annual meeting. Chicago/virtual – June 3–7, 2022. *Drugs Future* 47: 629.

Romano, E., Medioni, J., La Rouge, T.D.M., Fischer, N., Bardonneau, C., Ferlin, W., Hose, D., Seckinger, A., Simonelli, M., and Curigliano, G. (2022). A Phase 1, open-label, dose finding study of NI-1801, a bispecific mesothelin × CD47 engaging antibody, in patients with mesothelin expressing solid cancers. In: Regular and young investigator award abstracts. BMJ Publishing Group Ltd, Boston, MA, p. A739.

Roskopf, C.C., Braciak, T.A., Fenn, N.C., Kobold, S., Fey, G.H., Hopfner, K.-P., and Oduncu, F.S. (2016). Dual-targeting triplebody 33-3-19 mediates selective lysis of biphenotypic CD19+ CD33+ leukemia cells. *Oncotarget* 7: 22579–22589.

Rubin, I. and Yarden, Y. (2001). The basic biology of HER2. *Ann. Oncol.* 12: S3–S8.

Rubio-Pérez, L., Lázaro-Gorines, R., Harwood, S.L., Compte, M., Navarro, R., Tapia-Galisteo, A., Bonet, J., Blanco, B., Lykkemark, S., Ramírez-Fernández, Á., et al. (2023). A PD-L1/EGFR bispecific antibody combines immune checkpoint blockade and direct anti-cancer action for an enhanced anti-tumor response. *Oncoimmunology* 12: 2205336.

Russell, M.C., Garelli, A.M., and Reeves, D.J. (2023). Targeting EGFR exon 20 insertion mutation in non-small cell lung cancer: amivantamab and mobocertinib. *Ann. Pharmacother.* 57: 198–206.

Sadelain, M., Brentjens, R., and Rivière, I. (2013). The basic principles of chimeric antigen receptor design. *Cancer Discov.* 3: 388–398.

Samantasinghar, A., Sunildutt, N.P., Ahmed, F., Soomro, A.M., Salih, A.R.C., Parihar, P., Memon, F.H., Kim, K.H., Kang, I.S., and Choi, K.H. (2023). A comprehensive review of key factors affecting the efficacy of antibody drug conjugate. *Biomed. Pharmacother.* 161: 114408.

Schmohl, J.U., Todhunter, D., Taras, E., Bachanova, V., and Vallera, D.A. (2018). Development of a deimmunized bispecific immunotoxin dDT2219 against B-cell malignancies. Toxins 10: 32.

Schram, A.M., Odintsov, I., Espinosa-Cotton, M., Khodos, I., Sisso, W.J., Mattar, M.S., Lui, A.J.W., Vojnic, M., Shameem, S.H., Chauhan, T., et al. (2022). Zenocutuzumab, a HER2xHER3 bispecific antibody, is effective therapy for tumors driven by NRG1 gene rearrangements. *Cancer Discov.* 12: 1233–1247.

Schubert, I., Kellner, C., Stein, C., Kügler, M., Schwenkert, M., Saul, D., Mentz, K., Singer, H., Stockmeyer, B., Hillen, W., et al. (2011). A single-chain triplebody with specificity for CD19 and CD33 mediates effective lysis of mixed lineage leukemia cells by dual targeting. *MAbs* 3: 21–30.

Schubert, I., Stein, C., and Fey, G.H. (2012). Dual-targeting for the elimination of cancer cells with increased selectivity. *Antibodies* 1: 2–18.

Seung, E., Xing, Z., Wu, L., Rao, E., Cortez-Retamozo, V., Ospina, B., Chen, L., Beil, C., Song, Z., Zhang, B., et al. (2022). A trispecific antibody targeting HER2 and T cells inhibits breast cancer growth via CD4 cells. *Nature* 603: 328–334.

Shah, D., Soper, B., and Shopland, L. (2023). Cytokine release syndrome and cancer immunotherapies – historical challenges and promising futures. *Front. Immunol.* 14: 1190379.

Shah, N.N., Johnson, B.D., Schneider, D., Zhu, F., Szabo, A., Keever-Taylor, C.A., Krueger, W., Worden, A.A., Kadan, M.J., Yim, S., et al. (2020). Bispecific anti-CD20, anti-CD19 CAR T cells for relapsed B cell malignancies: a phase 1 dose escalation and expansion trial. *Nat. Med.* 26: 1569–1575.

Shah, N.N. and Sokol, L. (2021). Targeting CD22 for the treatment of B-cell malignancies. *ImmunoTargets Ther.* 10: 225–236.

Shimabukuro-Vornhagen, A., Gödel, P., Subklewe, M., Stemmler, H.J., Schlößer, H.A., Schlaak, M., Kochanek, M., Böll, B., and von Bergwelt-Baildon, M.S. (2018). Cytokine release syndrome. *J. Immunother. Cancer* 6: 56.

Sigismund, S., Avanzato, D., and Lanzetti, L. (2018). Emerging functions of the EGFR in cancer. *Mol. Oncol.* 12: 3–20.

Singh, A., Dees, S., and Grewal, I.S. (2021). Overcoming the challenges associated with CD3+ T-cell redirection in cancer. *Br. J. Cancer* 124: 1037–1048.

Sivori, S., Pende, D., Bottino, C., Marcenaro, E., Pessino, A., Biassoni, R., Moretta, L., and Moretta, A. (1999). NKp46 is the major triggering receptor involved in the natural cytotoxicity of fresh or cultured human NK cells. Correlation between surface density of NKp46 and natural cytotoxicity against autologous, allogeneic or xenogeneic target cells. *Eur. J. Immunol.* 29: 1656–1666.

Smith-Garvin, J.E., Koretzky, G.A., and Jordan, M.S. (2009). T cell activation. *Annu. Rev. Immunol.* 27: 591–619.

Steinmetz, A., Vallée, F., Beil, C., Lange, C., Baurin, N., Beninga, J., Capdevila, C., Corvey, C., Dupuy, A., Ferrari, P., et al. (2016). CODV-Ig, a universal bispecific tetravalent and multifunctional immunoglobulin format for medical applications. *MAbs* 8: 867–878.

Sterner, R.C. and Sterner, R.M. (2021). CAR-T cell therapy: current limitations and potential strategies. *Blood Cancer J.* 11: 69.

Sun, J., Chen, Y., Lubben, B., Adebayo, O., Muz, B., and Azab, A.K. (2021). CD47-targeting antibodies as a novel therapeutic strategy in hematologic malignancies. *Leuk. Res. Rep.* 16: 100268.

Sun, L., Zhang, L., Yu, J., Zhang, Y., Pang, X., Ma, C., Shen, M., Ruan, S., Wasan, H.S., and Qiu, S. (2020). Clinical efficacy and safety of anti-PD-1/PD-L1 inhibitors for the treatment of advanced or metastatic cancer: a systematic review and meta-analysis. *Sci. Rep.* 10: 2083.

Sun, R., Wang, X., Zhu, H., Mei, H., Wang, W., Zhang, S., and Huang, J. (2014). Prognostic value of LAMP3 and TP53 overexpression in benign and malignant gastrointestinal tissues. *Oncotarget* 5: 12398–12409.

Suntharalingam, G., Perry, M.R., Ward, S., Brett, S.J., Castello-Cortes, A., Brunner, M.D., and Panoskaltsis, N. (2006). Cytokine storm in a phase 1 trial of the anti-CD28 monoclonal antibody TGN1412. *N. Engl. J. Med.* 355: 1018–1028.

Syed, Y.Y. (2021). Amivantamab: first approval. *Drugs* 81: 1349–1353.

Tabares, P., Berr, S., Römer, P.S., Chuvpilo, S., Matskevich, A.A., Tyrsin, D., Fedotov, Y., Einsele, H., Tony, H.-P., and Hünig, T. (2014). Human regulatory T cells are selectively activated by low-dose application of the CD28 superagonist TGN1412/TAB08. *Eur. J. Immunol.* 44: 1225–1236.

Tang, Y., Yin, H., Zhao, X., Jin, D., Liang, Y., Xiong, T., Li, L., Tang, W., Zhang, J., Liu, M., et al. (2022). High efficacy and safety of CD38 and BCMA bispecific CAR-T in relapsed or refractory multiple myeloma. *J. Exp. Clin. Cancer Res.* 41: 2.

Tapia-Galisteo, A., Compte, M., Álvarez-Vallina, L., and Sanz, L. (2023). When three is not a crowd: trispecific antibodies for enhanced cancer immunotherapy. *Theranostics* 13: 1028–1041.

Tapia-Galisteo, A., Sánchez Rodríguez, Í., Aguilar-Sopeña, O., Harwood, S.L., Narbona, J., Ferreras Gutierrez, M., Navarro, R., Martín-García, L., Corbacho, C., Compte, M., et al. (2022). Trispecific T-cell engagers for dual tumor-targeting of colorectal cancer. *Oncoimmunology* 11: 2034355.

Temraz, S., Mukherji, D., and Shamseddine, A. (2016). Dual targeting of HER3 and EGFR in colorectal tumors might overcome anti-EGFR resistance. *Crit. Rev. Oncol. Hematol.* 101: 151–157.

Tian, W., Zhao, J., and Wang, W. (2023). Targeting CDH17 with chimeric antigen receptor-redirected T cells in small cell lung cancer. *Lung* 201: 489–497.

Tong, C., Zhang, Y., Liu, Y., Ji, X., Zhang, W., Guo, Y., Han, X., Ti, D., Dai, H., Wang, C., et al. (2020). Optimized tandem CD19/CD20 CAR-engineered T cells in refractory/relapsed B-cell lymphoma. *Blood* 136: 1632–1644.

Tyrsin, D., Chuvpilo, S., Matskevich, A., Nemenov, D., Römer, P.S., Tabares, P., and Hünig, T. (2016). From TGN1412 to TAB08: the return of CD28 superagonist therapy to clinical development for the treatment of rheumatoid arthritis. *Clin. Exp. Rheumatol.* 34: 45–48.

van Herpe, F. and van Cutsem, E. (2023). The role of cMET in gastric cancer-A review of the literature. Cancers 15: 1976.

Vasan, N., Baselga, J., and Hyman, D.M. (2019). A view on drug resistance in cancer. *Nature* 575: 299–309.

Vijayaraghavan, S., Lipfert, L., Chevalier, K., Bushey, B.S., Henley, B., Lenhart, R., Sendecki, J., Beqiri, M., Millar, H.J., Packman, K., et al. (2020). Amivantamab (JNJ-61186372), an Fc enhanced EGFR/cMet bispecific antibody, induces receptor downmodulation and antitumor activity by monocyte/macrophage trogocytosis. *Mol. Cancer Ther.* 19: 2044–2056.

Vivier, E., Tomasello, E., Baratin, M., Walzer, T., and Ugolini, S. (2008). Functions of natural killer cells. *Nat. Immunol.* 9: 503–510.

Walker, L.S.K. and Sansom, D.M. (2011). The emerging role of CTLA4 as a cell-extrinsic regulator of T cell responses. *Nat. Rev. Immunol.* 11: 852–863.

Wang, K., Wei, G., and Liu, D. (2012). CD19: a biomarker for B cell development, lymphoma diagnosis and therapy. *Exp. Hematol. Oncol.* 1: 36.

Wang, S., Peng, L., Xu, W., Zhou, Y., Zhu, Z., Kong, Y., Leung, S., Wang, J., Yan, X., and Mi, J.-Q. (2022). Preclinical characterization and comparison between CD3/CD19 bispecific and novel CD3/CD19/CD20 trispecific antibodies against B-cell acute lymphoblastic leukemia: targeted immunotherapy for acute lymphoblastic leukemia. *Front. Med.* 16: 139–149.

Wang, Y., Du, J., Gao, Z., Sun, H., Mei, M., Wang, Y., Ren, Y., and Zhou, X. (2023). Evolving landscape of PD-L2: bring new light to checkpoint immunotherapy. *Br. J. Cancer* 128: 1196–1207.

Wang, Y., Ni, H., Zhou, S., He, K., Gao, Y., Wu, W., Wu, M., Wu, Z., Qiu, X., Zhou, Y., et al. (2021). Tumor-selective blockade of CD47 signaling with a CD47/PD-L1 bispecific antibody for enhanced anti-tumor activity and limited toxicity. *Cancer Immunol. Immunother.* 70: 365–376.

Wei, G., Zhang, Y., Zhao, H., Wang, Y., Liu, Y., Liang, B., Wang, X., Xu, H., Cui, J., Wu, W., et al. (2021). CD19/CD22 dual-targeted CAR T-cell therapy for relapsed/refractory aggressive B-cell lymphoma: a safety and efficacy study. *Cancer Immunol. Res.* 9: 1061–1070.

Weisser, N.E., Sanches, M., Escobar-Cabrera, E., O'Toole, J., Whalen, E., Chan, P.W.Y., Wickman, G., Abraham, L., Choi, K., Harbourne, B., et al. (2023). An anti-HER2 biparatopic antibody that induces unique HER2 clustering and complement-dependent cytotoxicity. *Nat. Commun.* 14: 1394.

Wu, L., Seung, E., Xu, L., Rao, E., Lord, D.M., Wei, R.R., Cortez-Retamozo, V., Ospina, B., Posternak, V., Ulinski, G., et al. (2020). Trispecific antibodies enhance the therapeutic efficacy of tumor-directed T cells through T cell receptor co-stimulation. *Nat. Cancer* 1: 86–98.

Xie, B., Li, Z., Zhou, J., and Wang, W. (2022). Current status and perspectives of dual-targeting chimeric antigen receptor T-cell therapy for the treatment of hematological malignancies. Cancers 14: 3230.

Xu, J., Ying, J., Liu, R., Wu, J., Ye, F., Xu, N., Zhang, Y., Zhao, R., Xiang, X., Wang, J., et al. (2023). KN026 (anti-HER2 bispecific antibody) in patients with previously treated, advanced HER2-expressing gastric or gastroesophageal junction cancer. *Eur. J. Cancer* 178: 1–12.

Xue, J., Kong, D., Yao, Y., Yang, L., Yao, Q., Zhu, Y., Ding, Y., Yang, F., Gong, J., Shen, L., et al. (2020). Prediction of human pharmacokinetics and clinical effective dose of SI-B001, an EGFR/HER3 Bi-specific monoclonal antibody. *J. Pharm. Sci.* 109: 3172–3180.

Yu, J., Li, S., Chen, D., Liu, D., Guo, H., Yang, C., Zhang, W., Zhang, L., Zhao, G., Tu, X., et al. (2023). IMM0306, a fusion protein of CD20 mAb with the CD47 binding domain of SIRPα, exerts excellent cancer killing efficacy by activating both macrophages and NK cells via blockade of CD47-SIRPα interaction and FcγR engagement by simultaneously binding to CD47 and CD20 of B cells. *Leukemia* 37: 695–698.

Zah, E., Nam, E., Bhuvan, V., Tran, U., Ji, B.Y., Gosliner, S.B., Wang, X., Brown, C.E., and Chen, Y.Y. (2020). Systematically optimized BCMA/CS1 bispecific CAR-T cells robustly control heterogeneous multiple myeloma. *Nat. Commun.* 11: 2283.

Zahavi, D., AlDeghaither, D., O'Connell, A., and Weiner, L.M. (2018). Enhancing antibody-dependent cell-mediated cytotoxicity: a strategy for improving antibody-based immunotherapy. *Antib. Ther.* 1: 7–12.

Zhang, B., Li, S., Chen, D., Liu, D., Guo, H., Yang, C., Zhang, L., Zhang, W., Tu, X., Peng, L., et al. (2023) Abstract 2938: preclinical development of a novel bispecific mAb-Trap fusion protein, IMM2902, targeting both HER2 and CD47 as cancer immunotherapy. *Cancer Res.* 83: 2938.

Zhang, H., Gao, L., Liu, L., Wang, J., Wang, S., Gao, L., Zhang, C., Liu, Y., Kong, P., Liu, J., et al. (2019). A Bcma and CD19 bispecific CAR-T for relapsed and refractory multiple myeloma. *Blood* 134: 3147.

Zhang, X., Gureasko, J., Shen, K., Cole, P.A., and Kuriyan, J. (2006). An allosteric mechanism for activation of the kinase domain of epidermal growth factor receptor. *Cell* 125: 1137–1149.

Zhao, L., Li, S., Wei, X., Qi, X., Liu, D., Liu, L., Wen, F., Zhang, J.-S., Wang, F., Liu, Z.-L., et al. (2022). A novel CD19/CD22/CD3 trispecific antibody enhances therapeutic efficacy and overcomes immune escape against B-ALL. *Blood* 140: 1790–1802.

Zhou, C., Tang, K.-J., Cho, B.C., Liu, B., Paz-Ares, L., Cheng, S., Kitazono, S., Thiagarajan, M., Goldman, J.W., Sabari, J.K., et al. (2023). Amivantamab plus chemotherapy in NSCLC with EGFR exon 20 insertions. *N. Engl. J. Med.* 389: 2039–2051.

Zhou, S., Liu, M., Ren, F., Meng, X., and Yu, J. (2021). The landscape of bispecific T cell engager in cancer treatment. *Biomark. Res.* 9: 38.

Zingoni, A., Molfetta, R., Fionda, C., Soriani, A., Paolini, R., Cippitelli, M., Cerboni, C., and Santoni, A. (2018). NKG2D and its ligands: "one for all, all for one". *Front. Immunol.* 9: 476.

Zinzani, P.L. and Minotti, G. (2022). Anti-CD19 monoclonal antibodies for the treatment of relapsed or refractory B-cell malignancies: a narrative review with focus on diffuse large B-cell lymphoma. *J. Cancer Res. Clin. Oncol.* 148: 177–190.

Zong, H.-F., Zhang, B.-H., and Zhu, J.-W. (2022). Generating a bispecific antibody drug conjugate targeting PRLR and HER2 with improving the internalization. *Pharmaceut Fronts* 4: e113–e120.

4.3 T cell receptor-directed antibody-drug conjugates for the treatment of T cell-derived cancers

Title:

T cell receptor-directed antibody-drug conjugates for the treatment of T cell-derived cancers

Authors:

Katrin Schoenfeld, Jan Habermann, Philipp Wendel, Julia Harwardt, Evelyn Ullrich and Harald Kolmar

Bibliographic data:

Molecular Therapy Oncology

Volume 32 – 2024, Issue 3

Article first published: 19th July 2024

DOI: 10.1016/j.omton.2024.200850

Contributions by Katrin Schoenfeld:

- Planning of the project
- Generation and screening of the scFv library
- Production and characterization of antibodies and antibody-drug conjugates
- Testing of antibody-drug conjugates on cells
- Writing of manuscript and generation of figures

Molecular Therapy
Oncology
Original Article

T cell receptor-directed antibody-drug conjugates for the treatment of T cell-derived cancers

Katrin Schoenfeld,[1] Jan Habermann,[1,2,3] Philipp Wendel,[1,2,3,4,5] Julia Harwardt,[1] Evelyn Ullrich,[2,3,4] and Harald Kolmar[1,6]

[1]Institute for Organic Chemistry and Biochemistry, Technical University of Darmstadt, 64287 Darmstadt, Germany; [2]Goethe University, Department of Pediatrics, Experimental Immunology and Cell Therapy, 60590 Frankfurt am Main, Germany; [3]Frankfurt Cancer Institute, Goethe University, 60596 Frankfurt am Main, Germany; [4]German Cancer Consortium (DKTK), partner site Frankfurt/Mainz, 60590 Frankfurt am Main, Germany; [5]German Cancer Research Center (DKFZ), 69120 Heidelberg, Germany; [6]Centre for Synthetic Biology, Technical University of Darmstadt, 64283 Darmstadt, Germany

T cell-derived cancers are hallmarked by heterogeneity, aggressiveness, and poor clinical outcomes. Available targeted therapies are severely limited due to a lack of target antigens that allow discrimination of malignant from healthy T cells. Here, we report a novel approach for the treatment of T cell diseases based on targeting the clonally rearranged T cell receptor displayed by the cancerous T cell population. As a proof of concept, we identified an antibody with unique specificity toward a distinct T cell receptor (TCR) and developed antibody-drug conjugates, precisely recognizing and eliminating target T cells while preserving overall T cell repertoire integrity and cellular immunity. Our anti-TCR antibody-drug conjugates demonstrated effective receptor-mediated cell internalization, associated with induction of cancer cell death with strong signs of apoptosis. Furthermore, cell proliferation-inhibiting bystander effects observed on target-negative cells may contribute to the molecules' anti-tumor properties precluding potential tumor escape mechanisms. To our knowledge, this represents the first anti-TCR antibody-drug conjugate designed as custom-tailored immunotherapy for T cell-driven pathologies.

INTRODUCTION

T cell malignancies represent a clinically heterogeneous group of disorders that derive from clonal dysfunctional T cells arising through distinct mechanisms at different stages of development.[1–3] Lymphoid B cell neoplasms occur more frequently than cancers of T cell origin, which account for only about 10% of non-Hodgkin lymphomas and 15% of acute lymphoblastic leukemias (ALLs).[4–6] While there are several immunotherapeutic agents available for the treatment of B cell diseases such as monoclonal antibodies (mAbs), bispecific antibodies, antibody-drug conjugates (ADCs), and chimeric antigen receptor (CAR) T cells, patients suffering from T cell malignancies have limited therapeutic options, relying primarily on chemotherapy, which is associated with a poor prognosis.[7–11] A prospective cohort study on peripheral T cell lymphoma (TCL) demonstrated that 68% of patients were identified as refractory (47%) or relapsed (21%) within a median time of 8 months after receiving first-line treatment, and out of these patients, 47% died after a median follow up of 38 months.[12] In T cell ALL, response rates reach up to 85% in 5-year event-free survival with contemporary chemotherapy, but in relapsed disease, event-free and overall survival rates are less than 25%.[13] The concept of successful therapy for B cell malignancies is mainly based on targeting of pan-B cell antigens such as CD19 or CD20 entailing B cell aplasia, which is clinically tolerated and, in most cases, compensated by periodic immunoglobulin infusion.[14–17] However, applying this concept to T cell lymphoma is not feasible since it would lead to a permanent and ultimately fatal loss of healthy T cells.[18] Despite advances in understanding T cell disease biology, no antigens that discriminate malignant from healthy T cells have been identified. Recent advances include targeting of antigens with limited expression on healthy T cells and elevated presence on malignant T cells.[19] To date, two antibody-based drugs following this concept have received FDA approval for TCL: mogamulizumab, an anti-CCR4 mAb, and brentuximab vedotin, an anti-CD30 ADC; besides, there are several antibody-derived molecules currently undergoing clinical investigation.[19–21]

The αβ T cell receptor (TCR) constitutes a key element in the adaptive immune response mediating recognition and discrimination of self and foreign antigenic material. Consisting of disulfide-linked TCR α and TCR β chains imparting peptide-major histocompatibility complex recognition, the TCR is constitutively associated with cluster of differentiation 3 (CD3) dimers responsible for transduction of activation signals. During T cell development, TCR diversity is generated through somatic recombination of multiple variable (V), diversity (D; only for β chain), and joining (J) germline gene segments to the constant (C) region genes.[22] This results in distinct TCR rearrangement patterns that establish the antigen binding site with the V gene fragments encoding complementarity-determining regions (CDRs) CDR1 and CDR2 and the junctional V(D)J site coding for CDR3, which is the most varied sequence in the molecule providing the

Received 30 March 2024; accepted 16 July 2024;
https://doi.org/10.1016/j.omton.2024.200850.

Correspondence: Harald Kolmar, Institute for Organic Chemistry and Biochemistry, Technical University of Darmstadt, 64287 Darmstadt, Germany.
E-mail: harald.kolmar@tu-darmstadt.de

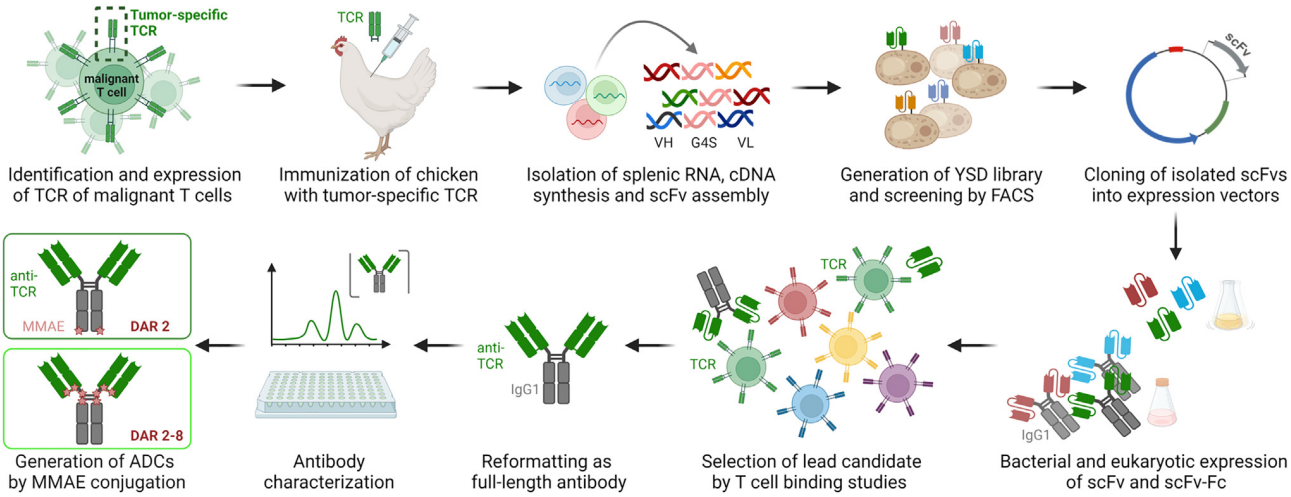

Figure 1. Concept overview

Identification and expression of tumor-specific TCR was followed by chicken immunization. Afterward, splenic RNA was isolated, and cDNA was synthesized. Genes encoding the variable antibody domains were amplified and assembled as scFv gene string for yeast surface display and subsequent screening by FACS. TCR-binding scFvs were cloned into bacterial and mammalian vectors for scFv and scFv-Fc expression, respectively. After selection of a lead candidate, the TCR idiotype-specific binder was reformatted as full-length antibody and subsequently characterized. Generation of ADCs by antibody MMAE conjugation was conducted by two different approaches resulting in DARs of 2 and 2–8, respectively. Created with BioRender.com.

major diversity of the TCR repertoire.[23,24] Apart from healthy T lymphocytes, TCR expression is observed in mature T cell cancers including peripheral T cell lymphomas (PTCLs), adult T cell leukemia/lymphoma, and a substantial fraction of T-ALL.[25–29] Consequently, healthy T cells display a variety of different TCRs, whereas malignant T cells typically form clonal populations exclusively expressing one unique TCR.[30,31] This renders TCRs a highly promising target for cancer therapy offering the opportunity to selectively eradicate malignant T cells while sparing healthy T cells and thus preserving cellular immunity. Previous attempts to target tumor-specific TCRs involving anti-T cell receptor β chain constant domains 1 (TRBC1) as well as anti-TRBV8 and TRBV5 CAR T cells and bispecific antibodies targeting TRBV5-5 or TRBV12 in combination with CD3 have shown encouraging anti-tumor effects and significantly reduced T cell aplasia in preclinical models.[29,32,33] Beyond addressing specific TRBC or TRBV elements, it is feasible to address the TCR variable regions carrying unique antigenic determinants, referred to as idiotype.[34]

Here we describe the generation of TCR idiotype-directed ADCs for the treatment of T cell-derived cancers (Figure 1). To this end, it was necessary to identify and express a TCR, e.g., of a malignant T cell population. Subsequently, a chicken was immunized with the target TCR, followed by isolation of the genetic material and construction of a single-chain variable fragment (scFv) yeast surface display (YSD) library, which was screened by fluorescence-activated cell sorting (FACS) for TCR binders. The isolated TCR binders were tested toward off-target effects using polyclonal T lymphocytes derived from human healthy donor blood. The lead candidate, reformatted as full-length antibody, was further characterized regarding stability, aggregation behavior, affinity, cellular binding, and internalization properties. To ensure cytotoxicity of the molecule, the anti-TCR antibody was conjugated to the cytotoxin monomethyl auristatin E (MMAE) via two different approaches resulting in ADCs with drug-to-antibody ratios (DARs) of 2 and 2–8, respectively. The TCR idiotype-targeting ADCs effectively deplete cancerous T cells *in vitro* with varying potency depending on their drug load while sparing healthy T lymphocytes.

RESULTS

Library generation and screening for TCR idiotype-targeting antibodies

TCRs are present in all jawed vertebrates from lower vertebrates to mammals.[35] In addition to the diversification in overall structure and amino acid sequence, TCRs differ in their variable regions defined by six CDRs.[36] In order to obtain antibodies that target the variable region of a specific TCR, we conducted an animal immunization and subsequent screening campaign. As a proof of concept TCRA6, an αβ TCR specific for the T cell leukemia-associated human T cell lymphotropic virus type 1_{11-19} HTLV-1 peptide (A2-Tax) complexed with the human leukocyte antigen (HLA-A*0201) was used as target to generate TCR-specific antibodies.[37–39] Previous attempts involving immunization of chickens revealed high diversities of avian antibodies directed against human proteins.[40,41] Therefore, an adult laying hen was immunized with the soluble target TCRA6, which elicited a strong immune response (Figure S1). Based on the genetic material from chicken, an scFv YSD library consisting of 6×10^9 transformants was generated and screened using FACS. For library sorting, yeast cells were stained for scFv surface presentation using an anti-c-myc antibody fluorescein isothiocyanate (FITC) conjugate and antigen binding by DyLight650-labeled TCRA6. Over two consecutive rounds of

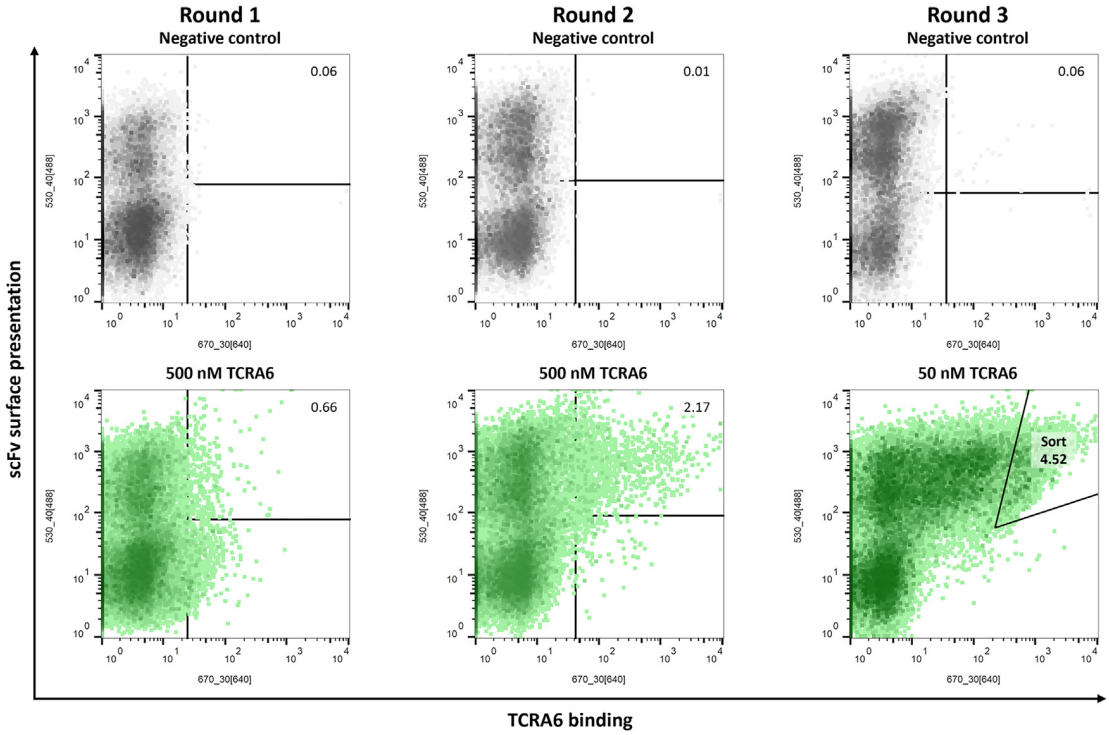

Figure 2. Screening of scFv immune library for TCRA6 binders by FACS

Sorting rounds 1–3 of the chicken-derived yeast surface-displayed scFv library are depicted in green with respective TCRA6 concentrations and percentages of cells in sorting gates. Negative controls without antigen incubation are shown in gray. Surface presentation was detected by anti-c-myc antibody FITC conjugate, and antigen binding was analyzed using DyLight650-labeled TCRA6. Density plots were created by FlowJo v10 Software.

screening using 500 nM antigen, we were able to enrich a yeast population binding to TCRA6 (Figure 2). In a third round, antigen concentration was reduced to 50 nM, and yeast cells demonstrating strong interaction with TCRA6 were sorted for further investigations.

Sequence analysis of four randomly selected scFv-displaying yeast single clones revealed four unique anti-TCRA6 (aTCRA6) scFv candidates (S1, S4, S7, and S10), which were heterogeneously expressed in *Escherichia coli*. To investigate, whether the scFvs specifically recognize TCRA6 via CDR binding, flow cytometric studies were performed by incubation of the respective scFvs with Jurkat wild-type (WT) T cells, a cell line derived from an acute T cell leukemia patient, which displays a cell-specific TCR differing from the target TCRA6.[42] Besides, on-target binding was verified using an engineered Jurkat T cell line exclusively expressing the target TCRA6, referred to as Jurkat TCRA6, which was generated by a successive approach of CRISPR-Cas9-based knockout of the inherent Jurkat αβ TCR and lentiviral transduction with the α and β chain of TCRA6. While two antibody single chains, aTCRA6 S4 and S7, revealed equal interaction with Jurkat TCRA6 target cells and Jurkat WT off-target cells, suggesting binding to constant portions of the TCR, S1 and S10, demonstrated 12- and 27-fold increased binding of target cells compared to off-target cells, respectively, indicating specificity for TCRA6 (Figure S2). The two best-performing scFvs were subsequently scrutinized in a biolayer interferometry (BLI) measurement that validated binding to immobilized TCRA6. Thereby, candidate aTCRA6 S1 showed superior binding properties compared to aTCRA6 S10 (Figure S3A). Affine binding was further demonstrated in cellular binding assays with Jurkat TCRA6 cells (Figure S3B). To exclude interaction with constant and off-target variable TCR regions, binding to polyclonal T lymphocytes derived from human healthy donor blood was investigated by flow cytometry (Figure S3C). The scFv aTCRA6 S1 was selected as the lead candidate due to its remarkable binding to TCRA6 on molecular and cellular level, while not targeting Jurkat WT cells as well as primary T lymphocytes from human blood, thus providing the desired anti-idiotypic properties.

Generation and functional characterization of anti-TCRA6 antibody

The scFv aTCRA6 S1 was reformatted as scFv-Fc fusion and as Fab-Fc full-length, chimeric chicken-human IgG antibody, expressed in Expi293F and purified via protein A affinity chromatography. Integrity, size, and purity of the proteins were initially confirmed using reducing SDS-PAGE (Figure S4A). Size exclusion chromatography (SEC) revealed favorable aggregation properties, with profiles displaying high uniformity and expected retention times of the analytes under native conditions (Figure S4B). Thermal stability, investigated via differential scanning fluorimetry, was determined by melting

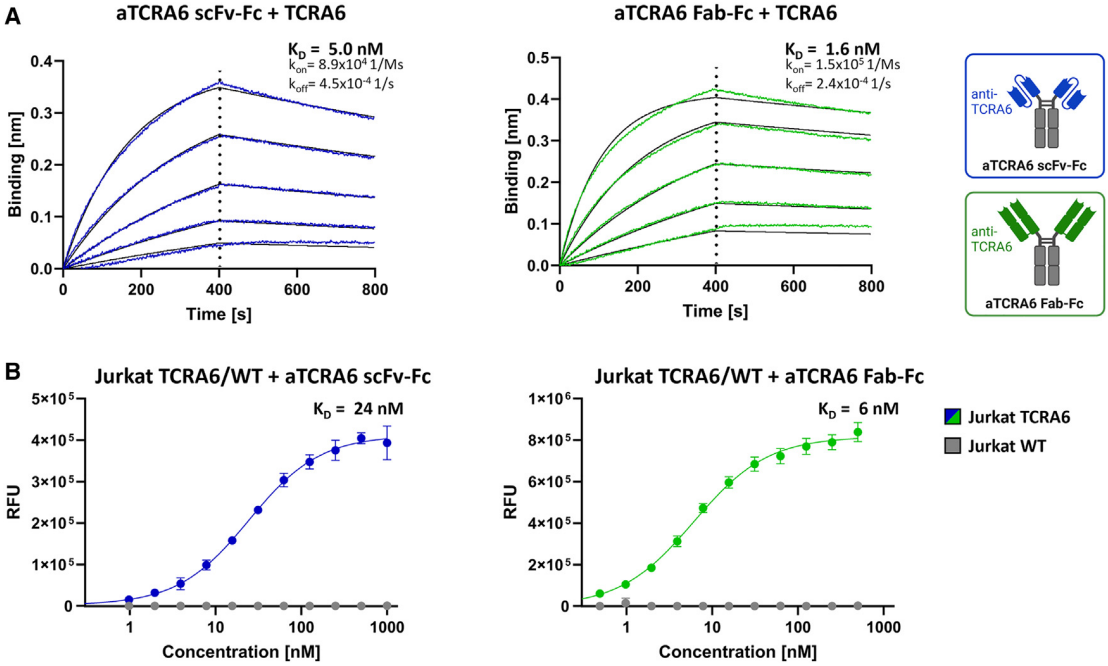

Figure 3. Binding properties of aTCRA6 scFv-Fc/Fab-Fc

(A) Binding kinetics. BLI measurement of aTCRA6 scFv-Fc (left) and aTCRA6 Fab-Fc (right) loaded onto AHC biosensor tips and associated with 3.9–62.5 nM TCRA6. Kinetic parameters were estimated using Savitzky-Golay filtering and 1:1 Langmuir modeling. (B) Cellular binding. Flow cytometry analysis of Jurkat TCRA6 target cells and Jurkat WT off-target T cells incubated with varying concentrations of aTCRA6 scFv-Fc (1–1,000 nM; left) or aTCRA6 Fab-Fc (0.5–500 nM; right) and stained via anti-human IgG Fc-PE secondary detection antibody. On-cell K_Ds were determined using variable slope four-parameter fit. Results are shown as mean RFU, and error bars represent standard deviation derived from experimental triplicates. Data are representative of three independent experiments.

temperatures of 60°C for both aTCRA6 scFv-Fc and aTCRA6 Fab-Fc (Figure S4C). In order to quantify binding kinetics, BLI measurements were conducted by loading the antibodies onto biosensors and subsequent association of TCRA6 in varying concentrations. Both formats of aTCRA6 showed excellent apparent affinities amounting to 5.0 nM (aTCRA6 scFv-Fc) and 1.6 nM (aTCRA6 Fab-Fc) and exhibited low off-rates, which indicated slow dissociation (Figure 3A). In line with molecular interactions, titration of aTCRA6 antibodies on Jurkat TCRA6 target cells resulted in curves demonstrating strong binding with estimated on-cell affinities of 24 nM (aTCRA6 scFv-Fc) and 6 nM (aTCRA6 Fab-Fc), while no off-target binding was observed on Jurkat WT T cells (Figure 3B). Idiotype specificity of aTCRA6 antibodies was further confirmed by 220-fold (aTCRA6 scFv-Fc) and 660-fold (aTCRA6 Fab-Fc) increased binding of target cells compared to off-target cells using saturating antibody concentrations, respectively. Taken together, the aTCRA6 scFv-Fc/Fab-Fc variants unveiled eminent biophysical properties combined with excellent antigen-binding abilities in molecular and cellular setups. Overall, the full-length aTCRA6 antibody in Fab format outperformed scFv-Fc fusion in terms of binding affinity.

Cytotoxicity of anti-TCRA6 ADCs

Engendering cytotoxic effects, we generated ADCs based on the identified aTCRA6 Fab-Fc antibody (sequence provided in Table S1). To this end, aTCRA6 was provided with either 2 or up to 8 (average DAR ~5) payload units consisting of PEG_4 linker, valine-citrulline dipeptide serving as cathepsin substrate, *p*-aminobenzyl alcohol self-immolative spacer, and the cytotoxin MMAE (Figure 4A). A DAR of 2 was obtained through a site-specific two-step approach of enzyme-mediated azide modification of the heavy chain's C terminus equipped with a recognition sequence for lipoate-protein ligase A and click chemistry using DBCO-modified payload.[40] ADCs armed with approximately 5 cytotoxins on average, referred to as $DAR5_{2\text{-}8}$, were generated via partial reduction of endogenous interchain cysteines and subsequent click reaction of thiols with maleimide-conjugated payload. Degree of conjugation was assessed by hydrophobic interaction chromatography (HIC), revealing successful payload attachment without remaining unconjugated fractions for both strategies (Figures S5B and S5C). By integration of signals, the average DAR for the cysteine-coupled aTCRA6 ADC was determined to be 4.9 (Figure S5C).

Since efficient internalization is a prerequisite for ADCs to properly exert their anti-proliferative effects, we first investigated internalization properties of aTCRA6. Therefore, the mAb was labeled with a pH-dependent dye exclusively exerting fluorescence under acidic conditions as given upon internalization and subsequent trafficking into endosomes and lysosomal vesicles.[43] Incubation of

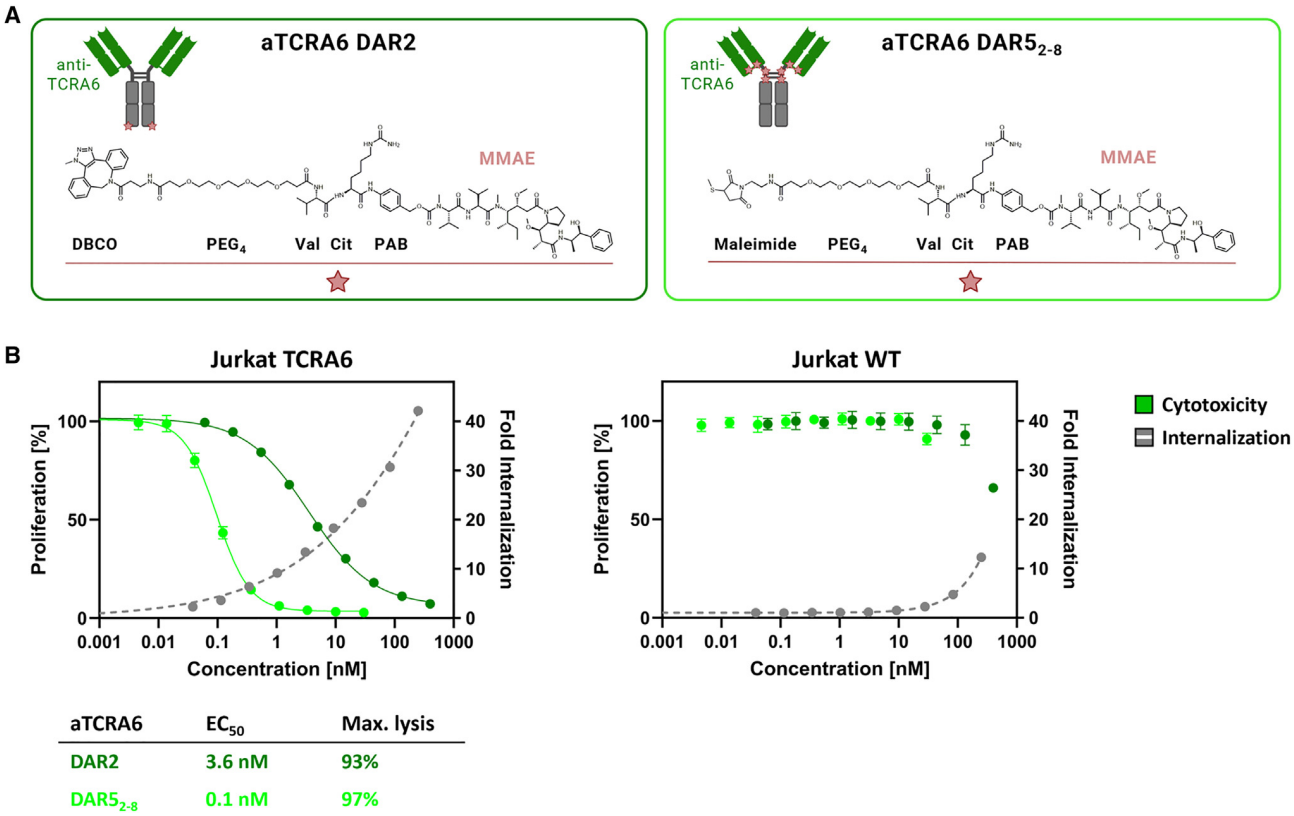

Figure 4. Internalization and cytotoxicity of aTCRA6 ADC variants

(A) Schematic representation of aTCRA6 ADCs. In aTCRA6 DAR2 (left), the anti-TCRA6 heavy chains are C-terminally modified with DBCO-PEG_4-Val-Cit-PAB-MMAE. In aTCRA6 $DAR5_{2-8}$ (right), the interchain cysteines of anti-TCRA6 mAb are conjugated to maleimide-PEG_4-Val-Cit-PAB-MMAE. DBCO, dibenzocyclooctyne; PEG, polyethylene glycol; Val, valine, Cit, citrulline; PAB, *p*-aminobenzyl alcohol; MMAE, monomethyl auristatin E. (B) Cytotoxicity was assessed by exposition of Jurkat TCRA6 target cells and Jurkat WT off-target cells to aTCRA6 DAR2 (0.06–400 nM) and aTCRA6 $DAR5_{2-8}$ (0.005–30 nM) for 72 h. Cell proliferation was normalized to untreated control cells (0 nM). Internalization was studied by application of pHAb-conjugated aTCRA6 antibody in varying concentrations (0.04–250 nM) to Jurkat TCRA6 target cells and Jurkat WT off-target cells and incubation overnight. Fold internalization was calculated by the ratio of relative fluorescence units (RFU) of the respective antibody sample and the untreated sample without antibody (0 nM). EC_{50}s were determined using variable slope four-parameter fit. Results are shown as mean, and error bars represent standard deviation derived from experimental triplicates. Data are representative of at least two independent experiments.

pH-dye-conjugated aTCRA6 with Jurkat TCRA6 target and Jurkat WT off-target cells was conducted overnight, followed by flow cytometric analysis. The fraction of endocytosed aTCRA6 increased in a concentration-dependent manner for Jurkat TCRA6 cells (Figure 4B). However, internalization in Jurkat WT cells was significantly lower, overall indicating potent and specific receptor-mediated uptake.

In order to evaluate *in vitro* cytotoxicity of the generated ADCs, Jurkat TCRA6 target cells and Jurkat WT off-target cells were exposed to the DAR2 and $DAR5_{2-8}$ ADCs for 72 h. Both ADCs exerted a robust concentration-dependent anti-proliferative effect on target T cells (Figure 4B). As expected, higher antibody drug load of aTCRA6 resulted in augmented cytotoxicity with the DAR2 ADC revealing an EC_{50} of 3.6 nM and 93% maximal killing and the $DAR5_{2-8}$ ADC exhibiting an EC_{50} of 0.1 nM and 97% maximal killing. Surprisingly, the half maximal effective concentration was decreased by a factor of 30 for the higher DAR ADC variant, indicating a markedly more potent drug delivery and intracellular MMAE release. Jurkat WT cells, serving as negative control, remained almost unaffected by ADC treatment. Application of ADCs at concentrations exceeding 100 nM presumably caused death of off-target cells due to unspecific ADC uptake.

To further scrutinize the cytotoxic properties of the generated ADCs, we measured induction of apoptosis in TCRA6-expressing target cells compared to Jurkat WT cells. Therefore, cells were exposed to ADCs at concentrations triggering maximal killing for a period of 72 h, stained with annexin V-FITC/propidium iodide (PI), and evaluated in microscopic and flow cytometric analysis. Treatment of target cells with both 300 nM aTCRA6 DAR2 and 30 nM aTCRA6 $DAR5_{2-8}$, resulted in significantly higher proportions of early apoptotic cells, as indicated by annexin V binding to phosphatidylserines exposed on the outer side of the cell membrane, as well as late apoptotic/necrotic cells with completely compromised cell membranes, as suggested by

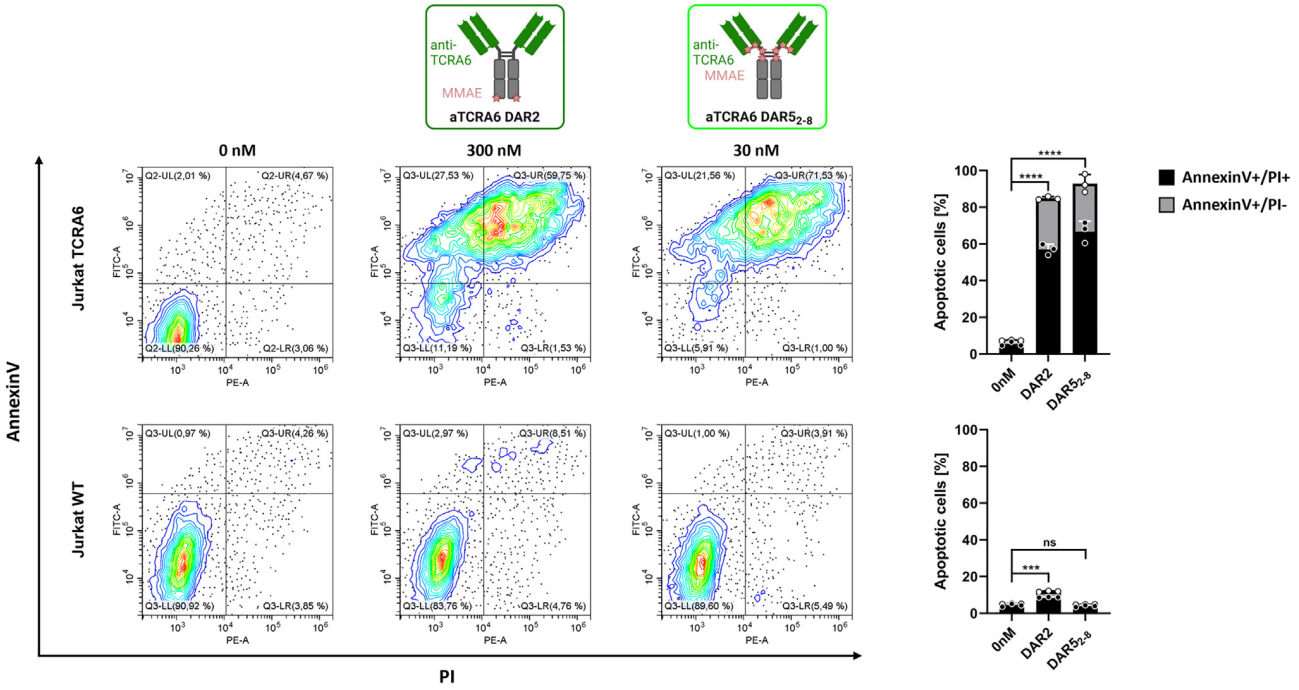

Figure 5. Apoptosis induction of aTCRA6 ADC variants

Jurkat TCRA6 target cells and Jurkat WT off-target cells were exposed to 300 nM aTCRA6 DAR2 and 30 nM aTCRA6 DAR$5_{2\text{-}8}$ for 72 h. Cells were stained with annexin V-FITC and propidium iodide (PI) and analyzed by flow cytometry. Percentage of annexin V-FITC+/PI+ and annexin V-FITC+/PI− (apoptotic cells) is depicted in right bar chart. Significant differences ($p < 0.05$) between ADCs and 0 nM control were determined using an unpaired, two-tailed t test and are depicted by * (0.1234 (ns), 0.0332 (*), 0.0021 (**), 0.0002 (***), and <0.0001 (****)). Results are shown as mean, and error bars represent standard deviation derived from experimental triplicates. Data are representative of two independent experiments.

PI staining of cellular DNA (Figures 5 and S7). Compared to untreated controls (0 nM), the aTCRA6 DAR2 and DAR$5_{2\text{-}8}$ ADCs provoked 11- and 13-fold increase of overall annexin V positivity in Jurkat TCRA6 cells, respectively (Figure 6). Morphologically, the cells displayed strong apoptotic signs post ADC regimen, which can be attributed to the anti-mitotic agent MMAE delivered by the antibody, which is described to cause cell-cycle arrest in G2/M phase and subsequent induction of apoptosis (Figure S7).[44,45] In TCRA6-negative

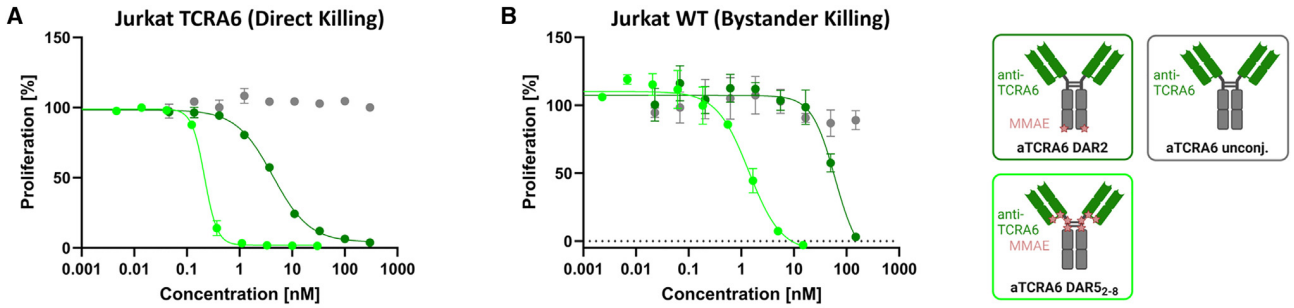

aTCRA6	EC_{50}	Max. lysis
DAR2	4.3 nM	96%
DAR$5_{2\text{-}8}$	0.2 nM	99%

aTCRA6	EC_{50}	Max. lysis
DAR2	60.4 nM	97%
DAR$5_{2\text{-}8}$	1.4 nM	100%

Figure 6. Bystander activity of aTCRA6 ADC variants

(A) Direct killing was determined by exposition of Jurkat TCRA6 target cells to aTCRA6 DAR2 (0.05–300 nM) and aTCRA6 DAR$5_{2\text{-}8}$ (0.005–30 nM) for 96 h. (B) Supernatants of pre-treated Jurkat TCRA6 target cells were transferred to freshly seeded Jurkat WT off-target cells in a ratio of 1:1 and incubated for 96 h. Results are shown as mean, and error bars represent standard deviation derived from experimental duplicates. Data are representative of at least two independent experiments.

Jurkat WT cells, induction of apoptosis by ADC administration was observed in a minor section for DAR2 (12%) and was barely detectable for $DAR5_{2\text{-}8}$ (5%). Consistent with the observed cytotoxic properties, the $DAR5_{2\text{-}8}$ ADC demonstrated superior total cell death induction, defined by effective concentration, maximal killing, and off-target effect, compared to the DAR2 ADC. This renders aTCRA6 $DAR5_{2\text{-}8}$ an ideal, promising molecule to combat T cell cancer, offering a wide therapeutic window by high tumor selectivity through anti-idiotypic properties and high potency via effective drug load.

Bystander effect of anti-TCRA6 ADCs

Depending on the developmental stage of the T cell upon malignant transformation, oligoclonal patterns have been observed in lymphoma cell populations.[1] While leukemias arrest at a certain stage of development and mature T cell-derived cancers have completed TCR rearrangement and form monoclonal lymphomas/leukemias, immature lymphoid precursor cells progress through sequential rearrangements that result in a clonotypic heterogeneous pool of lymphoma cells.[28,46,47] Moreover, downregulation of TCR expression has been observed in cancer cells.[18,29] Circumventing such tumor escape mechanisms, an ADC is capable to mediate bystander effects, (mainly) by internalization and degradation in target cells and subsequent permeation and diffusion of free payload, leading to the death of surrounding cells. Investigating the *in vitro* bystander activity of our aTCRA6 DAR2 and aTCRA6 $DAR5_{2\text{-}8}$ ADCs, direct cell killing was measured using Jurkat TCRA6 target cells, and bystander killing was analyzed by transfer of respective cell culture supernatants to Jurkat WT off-target cells. Consistent with our preliminary cytotoxicity data, direct killing of TCRA6-positive Jurkat cells was potently induced by the ADCs post 96 h (Figure 6A). Subsequently, cell culture supernatants of aTCRA6 ADC- and mAb-treated target cells were applied to TCRA6-negative Jurkat WT cells and incubated for an additional 96 h. Although target-negative Jurkat WT cells alone are sensitive to MMAE, but insensitive to aTCRA6 ADCs, supernatant transfer triggered cell death in a dose-dependent manner (Figures 4, S6, and 6B). Compared to half maximal effective doses for direct killing of target cells, EC_{50}s for bystander killing of target-negative cells are 7- to 14-fold increased, reflecting the effect of released MMAE on surrounding cells. While the primary mechanism of action of aTCRA6 ADCs is targeted delivery of MMAE to TCRA6 idiotype-expressing tumor cells, the cytotoxicity may be augmented by the bystander activity on target-positive as well as target-negative cells located in the tumor microenvironment.[48]

DISCUSSION

In contrast to the tremendous progress that has been made in the treatment of B cell lymphomas, the development of therapies for T cell-derived cancers remains challenging. Current investigational immunotherapies focus primarily on CAR T cells targeting pan-T cell antigens such as CD4, CD5, and CD7.[49–51] However, the success in clinical applications is severely hampered by fratricide, T cell aplasia, and product contamination with malignant cells.[18,49,52] To overcome the first two hurdles in adopting CAR technology for application in T cell malignancies, antigens with limited expression on normal cells, e.g., CD30, CD37, and CD1a, are addressed.[53–55] Following this concept, targeting of tumor-specific TCR constant domains has become more popular, ensuring selective eradication of tumor cells. Maciocia et al. made use of the fact that T cells mutually exclusively express the TCR β chain constant domains 1 or 2 (TRBC1 and TRBC2). Thus, TRBC1-based targeting in a CAR T cell setup unveiled compelling *in vitro* and *in vivo* anti-tumor effects under preservation of approximately half of the normal T cell population.[29] In addition to the issue of product contamination in the case of T cell malignancies, manufacturing of CAR T cells is a logistically time- and resource-intensive process due to the autologous nature of the personalized therapy approach. In the particular case of TRBC1-directed CAR T cells, CAR T cell efficacy may be further hampered by limited persistence due to TCR cross-linking on healthy T lymphocytes and CAR T cell cytolysis. Therefore, alternative strategies have been explored, including bispecific antibodies against distinct variable chains of the TCR β chain, which have proven effective in harnessing the host immune system's T cells to mediate cytotoxicity via CD3 recruitment in mouse models of human T cell cancers.[32] Another appealing antibody-based therapy class is represented by ADCs, which completely exclude bidirectional T cell killing while precisely inflicting chemotherapeutic damage on tumor cells.

In this study, we developed anti-TCR idiotype ADCs for specific elimination of T cell malignancies. Starting with the identification of an anti-idiotypic scFv derived from a chicken immune library, we reformatted the binder as full-length antibody, which was further conjugated to the cytotoxic payload MMAE (via a cleavable linker) under generation of aTCRA6 ADCs with DARs of 2 and 5 on average. Besides the remarkable single-digit nanomolar affinity of the aTCRA6 antibody on molecular and cellular levels, aTCRA6 ADCs demonstrated precise and potent *in vitro* anti-tumor activity, predominantly based on the induction of apoptotic cell death. Following release of the anti-mitotic agent MMAE, anti-proliferative bystander effects were observed in off-target cells further contributing to aTCRA6 ADCs' tumoricidal properties.

ADCs share a common architecture including a mAb component covalently bound to a cytotoxic payload via a synthetic linker. However, ADCs based on the same mAb carrier may exhibit different potencies, safeties, and pharmacokinetics due to independently modifiable key parameters such as linker technology, drug properties, as well as stoichiometry and placement of warheads.[56] Our aTCRA6 ADCs share mAb, protease-labile linker and payload, but they differ in their bioconjugation method, resulting in distinct antibody-payload linkages and DARs (Figure 4A). While chemoenzymatic payload coupling for generation of the DAR2 variant occurred site specifically at the antibody's C terminus under formation of a triazole, reaction of the reduced interchain cysteines with maleimide-modified payload results in thio-succinimide linkages and a heterogeneous drug load distribution varying from 2 to 8 entities per antibody. By further optimization of the conjugation conditions, a DAR of up to 8 is reportedly achievable.[57,58] Expectedly, comparing our two aTCRA6 ADC variants, the ADC with higher payload outperformed the DAR2 ADC

in terms of cytotoxicity and associated (absence of) off-target effects. It is common practice to increase the number of drugs per antibody in order to augment the potency of an ADC *in vitro*, albeit *in vivo* studies have revealed that excessive hydrophobic drug loading resulted in decreased efficacy due to reduced tumor exposure as they clear faster from circulation.[59–61] Previous investigations using anti-CD30 antibody brentuximab (or cAC10) in interchain cysteine conjugation-based MMAE ADCs containing DARs of 2, 4, and 8 determined the highest therapeutic index for DAR4 ADCs in xenograft-bearing immunodeficient mice.[62] Encouraging cancer treatment outcomes with cAC10-Val-Cit-PABC-MMAE, known as brentuximab vedotin, which consists of an average of four molecules of MMAE attached to the interchain cysteine residues, led to the first FDA approval of an ADC in 2011, for therapy of relapsed Hodgkin lymphoma and relapsed systemic anaplastic large cell lymphoma (ALCL).[63] Since tumors with a low percentage of CD30-positive cells can exhibit a comparable clinical response to brentuximab vedotin as high-CD30-expressing disease, bystander killing mechanisms likely contribute to ADC-mediated anti-tumor activity.[64,65] Linker design and drug chemistry dictate the ability of the cytotoxin to diffuse into surrounding cells and exert bystander effects, enabling the elimination of heterogeneous target-expressing populations.[59,66] Bystander activity may also be valuable for TCR targeting, as cancerous T cells often downregulate expression of the TCR or form oligoclonal populations in case of transformed lymphoid precursors undergoing TCR rearrangement.[1,18,29] However, in PTCL, malignant transformation mostly occurs after TCR rearrangement, resulting in monoclonality and over 95% TCR expression.[1,25] In leukemias (e.g., T-ALL), T cells become arrested at a certain stage of development. Consequently, in one-third of leukemia cases where TCRs are displayed, the cancerous populations are of monoclonal nature.[5,67] While pioneering approaches of Levy and Stevenson specifically addressing the clonally rearranged cell surface receptor in B cell lymphomas were superseded by pan-B cell targeting immunotherapies with demonstrable safety profiles, this concept may be rational in the context of T cell-derived cancers.[68,69] By precise targeting of malignant T cells, the relative T cell repertoire integrity is maintained, circumventing immunodeficiency and T cell aplasia.

An anthracycline-based treatment has been considered the standard frontline regimen for most types of PTCL, despite the fact that in most cases, results are suboptimal.[70,71] We propose an individualized strategy of tumor eradication feasible through TCR sequencing in order to identify the disease-causing T cell clone, providing a novel T cell lymphoma/leukemia therapy.[72] Thus, patients newly diagnosed with T cell diseases may receive chemotherapeutic first-line treatment to control tumor burden, and in case of relapse, TCR sequencing could be performed followed by generation of anti-TCR idiotype antibodies as exemplary demonstrated by chicken immunization. However, the anti-idiotype approach necessitates the production of a custom-made antibody for each individual patient. At present, implementation of personalized therapies is not as advanced, since time and resources required to manufacture and obtain regulatory approval frequently exceed therapeutic value. Nevertheless, individualized immunotherapy promises to broaden the responder patient population by highly specific targeting of tumor cells.[73] Attempts utilizing patient-tailored antibodies have primarily focused on hematologic cancers, achieving promising results, e.g., in multiple myeloma patients.[74–78] However, as an additional technical hurdle, humanization of the avian-derived molecule is imperative to produce a non-immunogenic antibody variant for therapeutic applications, which can be implemented by a straightforward method of chicken CDR grafting onto a human germline framework based on Vernier residue randomization, as previously described by our group.[79,80] Regarding drug resistance, patients may experience TCR-negative relapses following TCR-directed therapy, as frequently observed in previous clinical applications of single-antigen targeting biologics.[81–83] In addition, administration of ADCs for therapeutic purposes is often hampered by dose-limiting toxicities.[84,85] Ultimately, preclinical and early clinical studies are warranted to evaluate the feasibility and toxicity of anti-TCR idiotype-targeting ADCs for treatment of T cell malignancies.

In summary, we have demonstrated a unique approach to combat malignant T cells without inducing systemic immunosuppression derived from ablation of the entire T cell subset. With the development of anti-TCR idiotype ADCs, we provide proof of concept for precise tumor targeting by recognizing the clonally rearranged T lymphocyte receptor, potent anti-tumor activity based on the highly cytotoxic payload, and a favorable safety profile due to the exclusion of off-target effects. Our study may contribute to the future lymphoma/leukemia management by delivering a novel targeted immunotherapeutic starting point urgently needed in the setting of T cell-driven pathologies.

MATERIALS AND METHODS

Immunization of chicken and construction of yeast library

Chicken immunization and scFv YSD library construction were performed as reported previously.[41,86] Briefly, a pathogen-free adult laying hen (*Gallus gallus domesticus*) was immunized with TCRA6 (produced in-house) in combination with immune adjuvant AddaVax (InvivoGen, Toulouse, France) on days 1, 14, 28, 35, and 56.[37] The animal was sacrificed on day 63 for spleen resection and subsequent isolation of RNA. Additionally, antibody serum titer against TCRA6 was determined by ELISA. The immunization procedure as well as RNA extraction were executed at Davids Biotechnologie (Regensburg, Germany). Ethical approval for animal immunization was granted to Davids Biotechnologie (Regensburg, Germany). The experimental procedures and the care of the animals complied with EU animal welfare laws and regulations. For library generation, cDNA was synthesized from total splenic RNA. Subsequently, genes encoding VH and VL were amplified, randomly combined into scFv gene strings, and transferred into a linearized YSD vector (pCT) via homologous recombination in *Saccharomyces cerevisiae* strain EBY100 (MATa URA3-52 trp1 leu2Δ1 his3Δ200 pep4:HIS3 prb1Δ1.6R can1 GAL [pIU211:URA3]) (Thermo Fisher Scientific, Waltham, Massachusetts, USA). Library generation in

EBY100 cells was conducted according to the yeast transformation protocol published by Benatuil et al.[87]

Yeast library screening

Induction of scFv expression and surface presentation were accomplished by inoculation of yeast cells in synthetic galactose minimal medium with casein amino acids (SG-CAA) and incubation overnight at 30°C and 180 rpm. For library sorting, cells were harvested by centrifugation and washed once with PBS+0.1% (w/v) BSA (PBS-B). Antigen staining was conducted with DyLight650-labeled TCRA6 conjugated beforehand using 5-fold excess of DyLight650 NHS Ester (Thermo Fisher Scientific, Waltham, Massachusetts, USA). Simultaneously, staining for surface presentation using anti-c-myc antibody FITC conjugate (Miltenyi Biotec, Bergisch Gladbach, Germany; diluted 1:50) was performed for 30 min on ice. After washing three times with PBS-B, the yeast library was screened using BD Influx cell sorter with corresponding BD FACS Software v1.0 (BD, California, USA). During the sorting process collected yeast cells were plated on synthetic dextrose minimal medium with casein amino acids (SD-CAA) agar plates and incubated for 48 h at 30°C. General handling of yeast cells and scFv YSD library screening by FACS are described elsewhere.[86]

Expression and purification of scFv, scFv-Fc, and Fab-Fc constructs

Reformatting, expression, and purification of scFvs were performed as described previously.[88] In brief, isolated yeast vectors were sequenced, and scFv-encoding genes were cloned into a pET30 plasmid using golden gate assembly (GGA), followed by recombinant expression in *Escherichia coli* SHuffle T7 Express (New England Biolabs, Ipswich, Massachusetts, USA). A two-step affinity purification was conducted including IMAC and Strep-TactinXT purification, followed by buffer exchange against PBS. Production of Fc-fused scFvs and full-length antibodies (Fab-Fc) was performed by transfection of Expi293F cells with pTT5-derived GGA vectors and ExpiFectamine 293 Transfection Kit (Thermo Fisher Scientific, Waltham, Massachusetts, USA). For purification of Fc-containing antibody constructs, cell culture supernatants were collected 5 days after transfection, sterile filtered, and applied to a HiTrap protein An HP column (GE Healthcare, Piscataway, New Jersey, USA) using an ÄKTA pure chromatography system (GE Healthcare, Piscataway, New Jersey, USA). Buffer exchange against PBS was performed using a HiTrap Desalting column (GE Healthcare, Piscataway, New Jersey, USA).

Generation of Jurkat TCRA6 cell line

Engineered Jurkat cells exclusively expressing the TCRA6 were generated in succession by CRISPR-Cas9-based knockout of the individual Jurkat αβ TCR chains, enrichment by FACS, and lentiviral transduction of the respective TCRA6 α and β chains.

To this end, knockout of the endogenous Jurkat αβ TCR chains was performed as described in the Amaxa 4D-Nucleofector protocol by nucleofection of 3×10^5 Jurkat WT cells using the 4D-Nucleofector, the SE Cell Line Kit, and the CK-116 nucleofection program (Lonza, Switzerland). A Cas9/gRNA ribonucleoprotein complex (PNA Bio, Newbury Park, California, USA; 20 pmol) with chemically modified sgRNAs (Synthego Menlo Park, California, USA; 100 pmol) targeting the TRAC locus (5′-AGAGUCUCUCAGCUGGUACA-3′, targeting exon 1) and TRBC1 locus (5′-CUUUCCAGAGGACCUGAACA-3′, targeting exon 1) were utilized to achieve optimal nucleofection efficiency.[89] Following nucleofection and 1-week expansion, engineered Jurkat cells were washed with PBS both before and after incubation with an anti-αβ TCR BUV737-conjugated antibody (BD Horizon, Becton Dickinson, New Jersey, USA; diluted 1:40) for 30 min at 4°C to confirm the absence of αβ TCR surface expression using the FACS Celesta Cell Analyzer (BD, California, USA). Subsequently TCR-negative Jurkat cells were enriched using the FACS Aria Fusion (BD, California, USA).

For further engineering of the TCR-negative Jurkat cells, the encoding DNA sequence for TCRA6 α/β chain was cloned into a modified version of the pSLCAR-CD19-28z lentiviral transfer plasmid (Addgene plasmid #135991) generated by Scott McComb and colleagues.[90] Production of lentiviral particles with the generated TCRA6 vectors was conducted using a 3rd generation plasmid system as described recently, with minor modifications of the protocol.[91] Afterward 1×10^5 TCR-negative Jurkat cells were transduced by spinfection (32°C, 800 × *g*, 90 min) with a multiplicity of infection of 3–5, expanded for 2 weeks, and enriched for αβ TCR-positive surface expression as described using the FACS Aria Fusion (BD, California, USA).

Cell lines

T cells including Jurkat WT (Clone E6-1, DSMZ ACC 282) and Jurkat TCRA6 cells were cultured at 37°C and 5% CO_2. Jurkat WT cells were maintained in RPMI-1640 supplemented with 10% FBS and 1% penicillin-streptomycin. Jurkat TCRA6 cells were maintained in RPMI-1640 supplemented with 20% FBS, 10 mM HEPES, and 1% penicillin-streptomycin. Cells were sub-cultured every 2–3 days. Expi293F cells were cultured in Expi293 Expression Medium (Thermo Fisher Scientific, Waltham, Massachusetts, USA), sub-cultured every 3–4 days, and incubated at 37°C and 8% CO_2.

Thermal shift assay

Thermal stability was analyzed by differential scanning fluorimetry using a CFX Connect Real-Time PCR Detection System (Bio-Rad, California, USA) with a temperature gradient from 20°C to 95°C and 0.5°C/10 s. The derivatives of the melt curves were calculated with the corresponding Bio-Rad CFX Maestro software to determine the melt temperatures (Tm). All reactions were performed in PBS in presence of 1 mg/mL protein and SYPRO Orange (Thermo Fisher Scientific, Waltham, Massachusetts, USA; diluted 1:00).

Biolayer interferometry

For biolayer interferometric measurements, the Octet RED96 system (ForteBio, Sartorius, Göttingen, Germany) was used. Therefore, respective biosensor tips were soaked in PBS (pH 7.4) for at least 10 min before start of the assay.

For testing of two chicken-derived scFvs aTCRA6 S1 and S10, High Precision Streptavidin biosensors (SAX; Sartorius, Sartorius, Göttingen, Germany) were loaded with biotinylated TCRA6. All following steps were performed using kinetics buffer (KB; Sartorius, Göttingen, Germany). Association was measured for 200 s with 500 nM of respective scFvs followed by dissociation for 200 s.

Kinetics measurements were conducted for affinity determination of aTCRA6 scFv-Fc and aTCRA6 Fab-Fc. Anti-human IgG Fc capture biosensors (AHC; Sartorius Sartorius, Göttingen, Germany) were used to immobilize the antibodies. After a quenching step in KB (Sartorius, Göttingen, Germany), an association step using TCRA6 (produced in-house) with concentrations ranging from 3.9–62.5 nM was performed followed by a dissociation step in KB (400 s/step). Association in KB served as reference and was subtracted prior to evaluation steps. Data analysis was performed using ForteBio data analysis software 9.0. Binding kinetics including the equilibrium constant K_D were determined using Savitzky-Golay filtering and 1:1 Langmuir model.

Isolation of primary T cells from human healthy donor blood

Peripheral blood mononuclear cells (PBMCs) and subsequently primary T cells were isolated from buffy coats of fresh blood of healthy donors supplied by the German Red Cross Blood Donation Service (DRK-Blutspendedienst Baden-Württemberg-Hessen, Frankfurt, Germany). This study was approved by the Ethics Committee of the Goethe University Frankfurt, Germany (approval no. 329/10). All participants gave written informed consent in accordance with the Declaration of Helsinki.

Briefly, PBMCs were isolated by density gradient centrifugation using Biocoll (Biochrom, Cambridge, United Kingdom), followed by CD3-positive enrichment of primary T cells using the EasySep Human CD3 Positive Selection Kit II (StemCell Technologies, Vancouver, Canada) according to the instructions provided by the manufacturer. Afterward, primary T cells were cultivated in RPMI-1640 supplemented with 10% human serum (DRK-Blutspendedienst Baden-Württemberg-Hessen, Frankfurt, Germany), 25 mM HEPES, 1% penicillin-streptomycin, and 50 IU/mL IL-2 (PROLEUKIN S, Novartis Pharma, Basel, Switzerland).[92]

Cellular binding assay

Cellular binding of the antibodies was determined by flow cytometry. Engineered Jurkat TCRA6 cells served as target cells. Primary T cells derived from human healthy donor blood or Jurkat WT cells were used as negative controls to analyze unspecific cell binding. To this end, cells (1.5×10^5 cells/well) were washed with PBS-B and subsequently incubated with the respective aTCRA6 antibody constructs in varying concentrations for 30 min on ice. Followed by another PBS-B washing step, anti-human IgG Fc PE-conjugated secondary antibody (Thermo Fisher Scientific, Waltham, Massachusetts, USA; diluted 1:50), anti-his AF647-conjugated secondary antibody (Thermo Fisher Scientific, Waltham, Massachusetts, USA; diluted 1:50), or mouse anti-his secondary antibody (Qiagen, Venlo, Netherlands; diluted 1:50) and anti-mouse IgG APC-conjugated tertiary antibody (Thermo Fisher Scientific, Waltham, Massachusetts, USA; diluted 1:50) were applied for 20 min on ice. After another washing step with PBS-B, flow cytometry was performed using CytoFLEX S System (Beckman Coulter, Minnesota, USA). In case of antibody affinity titration to cells, the mean fluorescence intensity was plotted against the respective logarithmic concentration. The resulting curves were fitted with a variable slope four-parameter fit using GraphPad Prism.

Internalization assay

Investigations toward receptor-mediated antibody internalization were performed using pHAb Amine Reactive dye (Promega, Wisconsin, USA) according to the manufacturer's instructions. In brief, aTCRA6 Fab-Fc was conjugated with pHAb dye and applied to Jurkat WT and Jurkat TCRA6 T cells (2×10^4 cells/well) in different concentrations (0.04–250 nM) in a 96-well plate. After incubation overnight, cells were washed once with PBS, and internalization was measured using flow cytometry. Fold internalization was calculated by the ratio of relative fluorescence units (RFU) of the respective antibody sample and the untreated sample without antibody (0 nM). The resulting curves were fitted with a variable slope four-parameter fit.

Generation of ADCs

ADCs with a DAR of 2 were generated via a two-step approach of enzymatic modification and click chemistry reaction for conjugation of MMAE to the Fc fragment. Therefore, the C terminus of the antibody heavy chain was genetically fused with a lipoic acid ligase 12 aa acceptor peptide (LAP), which serves as recognition sequence for lipoate-protein ligase A (LplA) from *Escherichia coli*.[93] Lipoic acid ligase reaction was conducted with 0.1 equivalents (eq.) of a mutant lipoic acid ligase A ($LplA^{W37V}$)[94] accepting various carboxylic acid derivatives in the presence of 5 mM ATP, 5 mM $Mg(Ac)_2$, and 10–20 eq. azide-bearing lipoic acid derivative (synthesized in-house) in PBS (pH 7.4) for 1 h at 37°C. Azide-functionalized antibody was loaded onto protein A resin (protein A HP SpinTrap; Cytiva, Massachusetts, USA), and strain-promoted azide-alkyne [3 + 2] cycloaddition with 5 eq. DBCO-PEG_4-Val-Cit-PAB-MMAE was performed overnight at 4°C. After acidic elution of ADC from protein A column, the buffer was exchanged to PBS (pH 7.4), and successful conjugation was confirmed by HIC.

ADCs with a DAR of 2–8 were generated via a two-step approach including partial reduction of interchain disulfide bonds and thiol-maleimide Michael addition click reaction for conjugation of MMAE to the endogenous cysteines. Reduction of cystines was achieved by 2 h, 37°C incubation with 10 eq. tris(2-carboxyethyl) phosphine hydrochloride (TCEP-HCl). Subsequent reaction with 16 eq. maleimide-PEG_4-Val-Cit-PAB-MMAE was performed for 2 h at room temperature, followed by quenching of conjugation reaction using 50 eq. N-acetylcysteine for 15 min at 37°C. The ADC was purified from the reaction mixture using protein A spin columns (protein A HP SpinTrap; Cytiva, Massachusetts, USA). After acidic

elution of ADC from protein A resin, the buffer was exchanged to PBS (pH 7.4), and conjugation including DAR distribution was analyzed by HIC.

Hydrophobic interaction chromatography

HIC was performed using TSKGel Butyl-NPR column (Tosoh Bioscience, Griesheim, Germany) in combination with 1260 Infinity chromatography system (Agilent Technologies, Waldbronn, Germany) to analyze successful antibody-MMAE conjugation as well degree of conjugation. Separation was obtained using Eluent A (1.5 M $(NH_4)_2SO_4$, 25 mM Tris [pH 7.5]) and Eluent B (25 mM Tris [pH 7.5]) in a linear gradient of 0%–100% Eluent B over 25 min at a flow rate of 0.9 mL/min. 30 µg of protein samples were injected at a concentration of 0.3 mg/mL, and protein elution was monitored by absorbance at 220 nm. The average DAR was determined by integration of the absorbance peak areas of the different species using the following equation: $= \frac{\sum_{n=0}^{8} n \times A(DARn)}{\sum_{n=0}^{8} A(DARn)}$, where n refers to the individual DAR value and $A(DARn)$ refers to the peak area of the respective DAR species.[95]

Size exclusion chromatography

Analytical SEC using TSKgel SuperSW3000 column (Tosoh Bioscience, Griesheim, Germany) in combination with 1260 Infinity chromatography system (Agilent Technologies, Waldbronn, Germany) was performed to assess aggregation behavior of antibodies and ADCs. Chromatography was run with 30 µg protein (0.3 mg/mL) at a flow rate of 0.35 mL/min with PBS for 20 min, and protein elution was detected by measuring absorbance at 220 nm.

Cytotoxicity assay

Cytotoxic effects of aTCRA6 DAR2 and aTCRA6 $DAR5_{2\text{-}8}$ ADCs were estimated by exposing Jurkat WT and Jurkat TCRA6 T cells to different ADC concentrations. Cell viability was analyzed 72 h post ADC addition by a fluorometric method using CellTiter-Blue Cell Viability Assay (Promega, Wisconsin, USA) according to the manufacturer's instructions. Briefly, cells were seeded in a 96-well plate (1×10^4 cells/well) with the desired ADC concentrations ranging from 0.06–400 nM (for DAR2 ADC) or 0.005–30 nM (for $DAR5_{2\text{-}8}$ ADC) in a serial dilution. After 72 h, redox dye (resazurin) was added to the cells, and the plate was incubated for 3–4 h. Fluorescence of resorufin ($560_{Ex}/590_{Em}$) was recorded using CLARIOstar plus microplate reader (BMG LABTECH, Offenburg, Germany). Cell proliferation was normalized to untreated control cell fluorescence values. The resulting curves were fitted with a variable slope four-parameter fit, and EC_{50}s were calculated using GraphPad Prism.

Apoptosis assay

To determine induction of apoptosis of aTCRA6 DAR2 and aTCRA6 $DAR5_{2\text{-}8}$ ADCs in Jurkat WT and Jurkat TCRA6 cells, annexin V/PI staining was conducted. Therefore, cells were seeded in a 24-well plate (5×10^4 cells/well) and incubated with 300 nM (DAR2 ADC) or 30 nM ($DAR5_{2\text{-}8}$ ADC) ADCs for 72 h. Annexin V-FITC/PI staining ROTITEST Annexin V (Carl Roth & Co. KG, Karlsruhe, Germany) was applied for apoptosis detection of T cells according to the manufacturer's instructions. The analysis was performed using CytoFLEX S System (Beckman Coulter, Minnesota, USA) and the fluorescence microscope Zeiss Axio V.A1 with Axio Cam ICM1 and AxioVision 1.0.1.0 software (Carl Zeiss AG, Jena, Germany).

Bystander killing assay

To investigate bystander activity of ADCs, target Jurkat TCRA6 cells were exposed to ADCs for 4 days, and subsequent supernatant was transferred to off-target Jurkat WT cells, and cell viability was determined after 4 days of incubation. Therefore, Jurkat TCRA6 cells were seeded in a 96-well plate (2×10^4 cells/well) with the desired ADC concentrations ranging from 0.05–300 nM (DAR2 ADC) or 0.005–30 nM ($DAR5_{2\text{-}8}$ ADC) in a serial dilution. For direct killing, Jurkat TCRA6 cells were seeded at a density of 1×10^4 cells/well. After 96 h, viability readout for direct cell killing was measured using CellTiter-Blue Cell Viability Assay (Promega, Wisconsin, USA). For bystander effect analysis, target-negative Jurkat WT cells were seeded at a density of 1×10^4 cells/well after 96 h of initial ADC incubation. Centrifuged cell culture supernatant of the ADC-treated target-positive Jurkat TCRA6 cells was transferred to the seeded Jurkat WT cells and incubated for 96 h at 37°C with 5% CO_2. Cell viability was determined using the CellTiter-Blue Cell Viability Assay (Promega, Wisconsin, USA) and CLARIOstar plus microplate reader (BMG LABTECH, Offenburg, Germany), with the detailed protocol described in section cytotoxicity assay. Cell proliferation was normalized to untreated control cell fluorescence values. The resulting curves were fitted with a variable slope four-parameter fit, and EC_{50}s were calculated using GraphPad Prism.

DATA AND CODE AVAILABILITY

The raw data supporting the conclusions of this article will be made available by the authors, without undue reservation.

SUPPLEMENTAL INFORMATION

Supplemental information can be found online at https://doi.org/10.1016/j.omton.2024.200850.

ACKNOWLEDGMENTS

The authors would like to thank Peter Bitsch for synthesis of azide-modified lipoic acid as well as technical support in bioconjugation analytics. We acknowledge support by the German Research Foundation (grant KO1390/14-1) and the Open Access Publishing Fund of Technical University of Darmstadt.

AUTHOR CONTRIBUTIONS

K.S.: conceptualization, investigation, data curation, and writing – original draft. J. Habermann: conceptualization, investigation, and writing – review & editing. P.W.: conceptualization, investigation, and writing – review & editing. J. Harwardt: investigation and writing – review & editing. E.U.: conceptualization and writing - review & editing. H.K.: conceptualization, project administration, and writing – original draft.

DECLARATION OF INTERESTS

The authors declare no competing interests.

REFERENCES

1. Iyer, A., Hennessey, D., and Gniadecki, R. (2022). Clonotype pattern in T-cell lymphomas map the cell of origin to immature lymphoid precursors. Blood Adv. *6*, 2334–2345.
2. Belver, L., and Ferrando, A. (2016). The genetics and mechanisms of T cell acute lymphoblastic leukaemia. Nat. Rev. Cancer *16*, 494–507.
3. Malcolm, T.I.M., Hodson, D.J., Macintyre, E.A., and Turner, S.D. (2016). Challenging perspectives on the cellular origins of lymphoma. Open Biol. *6*, 160232.
4. (1997). The Non-Hodgkin's Lymphoma Classification Project; A Clinical Evaluation of the International Lymphoma Study Group Classification of Non-Hodgkin's Lymphoma. Blood *89*, 3909–3918.
5. Pui, C.-H., Robison, L.L., and Look, A.T. (2008). Acute lymphoblastic leukaemia. Lancet (London, England) *371*, 1030–1043.
6. Bhansali, R.S., and Barta, S.K. (2023). SOHO State of the Art Updates and Next Questions | Challenging Cases in Rare T-Cell Lymphomas. Clin. Lymphoma Myeloma Leuk. *23*, 642–650.
7. Asselin, B.L., Devidas, M., Wang, C., Pullen, J., Borowitz, M.J., Hutchison, R., Lipshultz, S.E., and Camitta, B.M. (2011). Effectiveness of high-dose methotrexate in T-cell lymphoblastic leukemia and advanced-stage lymphoblastic lymphoma: a randomized study by the Children's Oncology Group (POG 9404). Blood *118*, 874–883.
8. Mak, V., Hamm, J., Chhanabhai, M., Shenkier, T., Klasa, R., Sehn, L.H., Villa, D., Gascoyne, R.D., Connors, J.M., and Savage, K.J. (2013). Survival of patients with peripheral T-cell lymphoma after first relapse or progression: spectrum of disease and rare long-term survivors. J. Clin. Oncol. *31*, 1970–1976.
9. Schmitz, N., Lenz, G., and Stelljes, M. (2018). Allogeneic hematopoietic stem cell transplantation for T-cell lymphomas. Blood *132*, 245–253.
10. Teachey, D.T., and Pui, C.-H. (2019). Comparative features and outcomes between paediatric T-cell and B-cell acute lymphoblastic leukaemia. Lancet Oncol. *20*, e142–e154.
11. Bock, A.M., Nowakowski, G.S., and Wang, Y. (2022). Bispecific Antibodies for Non-Hodgkin Lymphoma Treatment. Curr. Treat. Options Oncol. *23*, 155–170.
12. Bellei, M., Foss, F.M., Shustov, A.R., Horwitz, S.M., Marcheselli, L., Kim, W.S., Cabrera, M.E., Dlouhy, I., Nagler, A., Advani, R.H., et al. (2018). The outcome of peripheral T-cell lymphoma patients failing first-line therapy: a report from the prospective, International T-Cell Project. Haematologica *103*, 1191–1197.
13. Raetz, E.A., and Teachey, D.T. (2016). T-cell acute lymphoblastic leukemia. Hematology *2016*, 580–588.
14. Maude, S.L., Teachey, D.T., Porter, D.L., and Grupp, S.A. (2015). CD19-targeted chimeric antigen receptor T-cell therapy for acute lymphoblastic leukemia. Blood *125*, 4017–4023.
15. Cappell, K.M., and Kochenderfer, J.N. (2023). Long-term outcomes following CAR T cell therapy: what we know so far. Nat. Rev. Clin. Oncol. *20*, 359–371.
16. Klein, C., Jamois, C., and Nielsen, T. (2021). Anti-CD20 treatment for B-cell malignancies: current status and future directions. Expert Opin. Biol. Ther. *21*, 161–181.
17. Zinzani, P.L., and Minotti, G. (2022). Anti-CD19 monoclonal antibodies for the treatment of relapsed or refractory B-cell malignancies: a narrative review with focus on diffuse large B-cell lymphoma. J. Cancer Res. Clin. Oncol. *148*, 177–190.
18. Fleischer, L.C., Spencer, H.T., and Raikar, S.S. (2019). Targeting T cell malignancies using CAR-based immunotherapy: challenges and potential solutions. J. Hematol. Oncol. *12*, 141.
19. Iżykowska, K., Rassek, K., Korsak, D., and Przybylski, G.K. (2020). Novel targeted therapies of T cell lymphomas. J. Hematol. Oncol. *13*, 176.
20. Makita, S., and Tobinai, K. (2017). Mogamulizumab for the treatment of T-cell lymphoma. Expert Opin. Biol. Ther. *17*, 1145–1153.
21. Richardson, N.C., Kasamon, Y.L., Chen, H., Claro, R.A. de, Ye, J., Blumenthal, G.M., Farrell, A.T., and Pazdur, R. (2019). FDA Approval Summary: Brentuximab Vedotin in First-Line Treatment of Peripheral T-Cell Lymphoma. Oncologist *24*, e180–e187.
22. Davis, M.M., and Bjorkman, P.J. (1988). T-cell antigen receptor genes and T-cell recognition. Nature *334*, 395–402.
23. Robins, H.S., Campregher, P.V., Srivastava, S.K., Wacher, A., Turtle, C.J., Kahsai, O., Riddell, S.R., Warren, E.H., and Carlson, C.S. (2009). Comprehensive assessment of T-cell receptor beta-chain diversity in alphabeta T cells. Blood *114*, 4099–4107.
24. Rudolph, M.G., Stanfield, R.L., and Wilson, I.A. (2006). How TCRs bind MHCs, peptides, and coreceptors. Annu. Rev. Immunol. *24*, 419–466.
25. Went, P., Agostinelli, C., Gallamini, A., Piccaluga, P.P., Ascani, S., Sabattini, E., Bacci, F., Falini, B., Motta, T., Paulli, M., et al. (2006). Marker expression in peripheral T-cell lymphoma: a proposed clinical-pathologic prognostic score. J. Clin. Oncol. *24*, 2472–2479.
26. Jamal, S., Picker, L.J., Aquino, D.B., McKenna, R.W., Dawson, D.B., and Kroft, S.H. (2001). Immunophenotypic analysis of peripheral T-cell neoplasms. A multiparameter flow cytometric approach. Am. J. Clin. Pathol. *116*, 512–526.
27. Foucar, K. (2007). Mature T-cell leukemias including T-prolymphocytic leukemia, adult T-cell leukemia/lymphoma, and Sézary syndrome. Am. J. Clin. Pathol. *127*, 496–510.
28. Asnafi, V., Beldjord, K., Boulanger, E., Comba, B., Le Tutour, P., Estienne, M.-H., Davi, F., Landman-Parker, J., Quartier, P., Buzyn, A., et al. (2003). Analysis of TCR, pT alpha, and RAG-1 in T-acute lymphoblastic leukemias improves understanding of early human T-lymphoid lineage commitment. Blood *101*, 2693–2703.
29. Maciocia, P.M., Wawrzyniecka, P.A., Philip, B., Ricciardelli, I., Akarca, A.U., Onuoha, S.C., Legut, M., Cole, D.K., Sewell, A.K., Gritti, G., et al. (2017). Targeting the T cell receptor β-chain constant region for immunotherapy of T cell malignancies. Nat. Med. *23*, 1416–1423.
30. Kim, H., Kim, I.S., Chang, C.L., Kong, S.Y., Lim, Y.T., Kong, S.G., Cho, E.H., Lee, E.Y., Shin, H.J., Park, H.J., et al. (2019). T-Cell Receptor Rearrangements Determined Using Fragment Analysis in Patients With T-Acute Lymphoblastic Leukemia. Ann. Lab. Med. *39*, 125–132.
31. Oon, M.L., Lim, J.Q., Lee, B., Leong, S.M., Soon, G.S.-T., Wong, Z.W., Lim, E.H., Li, Z., Yeoh, A.E.J., Chen, S., et al. (2021). T-Cell Lymphoma Clonality by Copy Number Variation Analysis of T-Cell Receptor Genes. Cancers *13*, 340.
32. Paul, S., Pearlman, A.H., Douglass, J., Mog, B.J., Hsiue, E.H.-C., Hwang, M.S., DiNapoli, S.R., Konig, M.F., Brown, P.A., Wright, K.M., et al. (2021). TCR β chain-directed bispecific antibodies for the treatment of T cell cancers. Sci. Transl. Med. *13*, eabd3595.
33. Li, F., Zhang, H., Wang, W., Yang, P., Huang, Y., Zhang, J., Yan, Y., Wang, Y., Ding, X., Liang, J., et al. (2022). T cell receptor β-chain-targeting chimeric antigen receptor T cells against T cell malignancies. Nat. Commun. *13*, 4334.
34. Bona, C.A. (1997). Idiotypes in Medicine: Autoimmunity, Infection and Cancer (Anti-idiotypes (Elsevier)).
35. Antonacci, R., Massari, S., Linguiti, G., Caputi Jambrenghi, A., Giannico, F., Lefranc, M.-P., and Ciccarese, S. (2020). Evolution of the T-Cell Receptor (TR) Loci in the Adaptive Immune Response: The Tale of the TRG Locus in Mammals. Genes *11*, 624.
36. Wong, W.K., Leem, J., and Deane, C.M. (2019). Comparative Analysis of the CDR Loops of Antigen Receptors. Front. Immunol. *10*, 2454.
37. Sádio, F., Stadlmayr, G., Stadlbauer, K., Gräf, M., Scharrer, A., Rüker, F., and Wozniak-Knopp, G. (2020). Stabilization of soluble high-affinity T-cell receptor with de novo disulfide bonds. FEBS Lett. *594*, 477–490.
38. Cole, D.K., Sami, M., Scott, D.R., Rizkallah, P.J., Borbulevych, O.Y., Todorov, P.T., Moysey, R.K., Jakobsen, B.K., Boulter, J.M., Baker, B.M., and Yi, L. (2013). Increased Peptide Contacts Govern High Affinity Binding of a Modified TCR Whilst Maintaining a Native pMHC Docking Mode. Front. Immunol. *4*, 168.
39. Furukawa, Y., Fujisawa, J., Osame, M., Toita, M., Sonoda, S., Kubota, R., Ijichi, S., and Yoshida, M. (1992). Frequent clonal proliferation of human T-cell leukemia virus type 1 (HTLV-1)-infected T cells in HTLV-1-associated myelopathy (HAM-TSP). Blood *80*, 1012–1016.
40. Schoenfeld, K., Harwardt, J., Habermann, J., Elter, A., and Kolmar, H. (2023). Conditional activation of an anti-IgM antibody-drug conjugate for precise B cell lymphoma targeting. Front. Immunol. *14*, 1258700.
41. Grzeschik, J., Yanakieva, D., Roth, L., Krah, S., Hinz, S.C., Elter, A., Zollmann, T., Schwall, G., Zielonka, S., and Kolmar, H. (2019). Yeast Surface Display in

Combination with Fluorescence-activated Cell Sorting Enables the Rapid Isolation of Antibody Fragments Derived from Immunized Chickens. Biotechnol. J. *14*, e1800466.

42. Gioia, L., Siddique, A., Head, S.R., Salomon, D.R., and Su, A.I. (2018). A genome-wide survey of mutations in the Jurkat cell line. BMC Genom. *19*, 334.
43. Li, Z., Wang, M., Yao, X., Li, H., Li, S., Liu, L., Yu, D., Li, X., Fang, J., and Huang, C. (2018). Development of novel anti-CD19 antibody-drug conjugates for B-cell lymphoma treatment. Int. Immunopharmacol. *62*, 299–308.
44. Cunningham, D., Parajuli, K.R., Zhang, C., Wang, G., Mei, J., Zhang, Q., Liu, S., and You, Z. (2016). Monomethyl Auristatin E Phosphate Inhibits Human Prostate Cancer Growth. Prostate *76*, 1420–1430.
45. Best, R.L., LaPointe, N.E., Azarenko, O., Miller, H., Genualdi, C., Chih, S., Shen, B.-Q., Jordan, M.A., Wilson, L., Feinstein, S.C., and Stagg, N.J. (2021). Microtubule and tubulin binding and regulation of microtubule dynamics by the antibody drug conjugate (ADC) payload, monomethyl auristatin E (MMAE): Mechanistic insights into MMAE ADC peripheral neuropathy. Toxicol. Appl. Pharmacol. *421*, 115534.
46. Yoneda, N., Tatsumi, E., Kawano, S., Matsuo, Y., Minowada, J., and Yamaguchi, N. (1993). Human recombination activating gene-1 in leukemia/lymphoma cells: expression depends on stage of lymphoid differentiation defined by phenotype and genotype. Blood *82*, 207–216.
47. Iyer, A., Hennessey, D., O'Keefe, S., Patterson, J., Wang, W., Wong, G.K.-S., and Gniadecki, R. (2020). Branched evolution and genomic intratumor heterogeneity in the pathogenesis of cutaneous T-cell lymphoma. Blood Adv. *4*, 2489–2500.
48. Kovtun, Y.V., Audette, C.A., Ye, Y., Xie, H., Ruberti, M.F., Phinney, S.J., Leece, B.A., Chittenden, T., Blättler, W.A., and Goldmacher, V.S. (2006). Antibody-drug conjugates designed to eradicate tumors with homogeneous and heterogeneous expression of the target antigen. Cancer Res. *66*, 3214–3221.
49. Raikar, S.S., Fleischer, L.C., Moot, R., Fedanov, A., Paik, N.Y., Knight, K.A., Doering, C.B., and Spencer, H.T. (2018). Development of chimeric antigen receptors targeting T-cell malignancies using two structurally different anti-CD5 antigen binding domains in NK and CRISPR-edited T cell lines. OncoImmunology *7*, e1407898.
50. Gomes-Silva, D., Srinivasan, M., Sharma, S., Lee, C.M., Wagner, D.L., Davis, T.H., Rouce, R.H., Bao, G., Brenner, M.K., and Mamonkin, M. (2017). CD7-edited T cells expressing a CD7-specific CAR for the therapy of T-cell malignancies. Blood *130*, 285–296.
51. Ma, G., Shen, J., Pinz, K., Wada, M., Park, J., Kim, S., Togano, T., and Tse, W. (2019). Targeting T Cell Malignancies Using CD4CAR T-Cells and Implementing a Natural Safety Switch. Stem Cell Rev. Rep. *15*, 443–447.
52. Cooper, M.L., Choi, J., Staser, K., Ritchey, J.K., Devenport, J.M., Eckardt, K., Rettig, M.P., Wang, B., Eissenberg, L.G., Ghobadi, A., et al. (2018). An "off-the-shelf" fratricide-resistant CAR-T for the treatment of T cell hematologic malignancies. Leukemia *32*, 1970–1983.
53. Ramos, C.A., Ballard, B., Zhang, H., Dakhova, O., Gee, A.P., Mei, Z., Bilgi, M., Wu, M.-F., Liu, H., Grilley, B., et al. (2017). Clinical and immunological responses after CD30-specific chimeric antigen receptor-redirected lymphocytes. J. Clin. Invest. *127*, 3462–3471.
54. Scarfò, I., Ormhøj, M., Frigault, M.J., Castano, A.P., Lorrey, S., Bouffard, A.A., van Scoyk, A., Rodig, S.J., Shay, A.J., Aster, J.C., et al. (2018). Anti-CD37 chimeric antigen receptor T cells are active against B- and T-cell lymphomas. Blood *132*, 1495–1506.
55. Sánchez-Martínez, D., Baroni, M.L., Gutierrez-Agüera, F., Roca-Ho, H., Blanch-Lombarte, O., González-García, S., Torrebadell, M., Junca, J., Ramírez-Orellana, M., Velasco-Hernández, T., et al. (2019). Fratricide-resistant CD1a-specific CAR T cells for the treatment of cortical T-cell acute lymphoblastic leukemia. Blood *133*, 2291–2304.
56. Sochaj, A.M., Świderska, K.W., and Otlewski, J. (2015). Current methods for the synthesis of homogeneous antibody-drug conjugates. Biotechnol. Adv. *33*, 775–784.
57. Walsh, S.J., Bargh, J.D., Dannheim, F.M., Hanby, A.R., Seki, H., Counsell, A.J., Ou, X., Fowler, E., Ashman, N., Takada, Y., et al. (2021). Site-selective modification strategies in antibody-drug conjugates. Chem. Soc. Rev. *50*, 1305–1353.
58. Lyon, R.P., Bovee, T.D., Doronina, S.O., Burke, P.J., Hunter, J.H., Neff-LaFord, H.D., Jonas, M., Anderson, M.E., Setter, J.R., and Senter, P.D. (2015). Reducing hydrophobicity of homogeneous antibody-drug conjugates improves pharmacokinetics and therapeutic index. Nat. Biotechnol. *33*, 733–735.
59. Matikonda, S.S., McLaughlin, R., Shrestha, P., Lipshultz, C., and Schnermann, M.J. (2022). Structure-Activity Relationships of Antibody-Drug Conjugates: A Systematic Review of Chemistry on the Trastuzumab Scaffold. Bioconjug. Chem. *33*, 1241–1253.
60. Bryant, P., Pabst, M., Badescu, G., Bird, M., McDowell, W., Jamieson, E., Swierkosz, J., Jurlewicz, K., Tommasi, R., Henseleit, K., et al. (2015). In Vitro and In Vivo Evaluation of Cysteine Rebridged Trastuzumab-MMAE Antibody Drug Conjugates with Defined Drug-to-Antibody Ratios. Mol. Pharm. *12*, 1872–1879.
61. Adem, Y.T., Schwarz, K.A., Duenas, E., Patapoff, T.W., Galush, W.J., and Esue, O. (2014). Auristatin antibody drug conjugate physical instability and the role of drug payload. Bioconjug. Chem. *25*, 656–664.
62. Hamblett, K.J., Senter, P.D., Chace, D.F., Sun, M.M.C., Lenox, J., Cerveny, C.G., Kissler, K.M., Bernhardt, S.X., Kopcha, A.K., Zabinski, R.F., et al. (2004). Effects of drug loading on the antitumor activity of a monoclonal antibody drug conjugate. Clin. Cancer Res. *10*, 7063–7070.
63. Senter, P.D., and Sievers, E.L. (2012). The discovery and development of brentuximab vedotin for use in relapsed Hodgkin lymphoma and systemic anaplastic large cell lymphoma. Nat. Biotechnol. *30*, 631–637.
64. Brown, M.P., and Staudacher, A.H. (2014). Could bystander killing contribute significantly to the antitumor activity of brentuximab vedotin given with standard first-line chemotherapy for Hodgkin lymphoma? Immunotherapy *6*, 371–375.
65. Masuda, S., Miyagawa, S., Sougawa, N., and Sawa, Y. (2015). CD30-targeting immunoconjugates and bystander effects. Nat. Rev. Clin. Oncol. *12*, 245.
66. Staudacher, A.H., and Brown, M.P. (2017). Antibody drug conjugates and bystander killing: is antigen-dependent internalisation required? Br. J. Cancer *117*, 1736–1742.
67. Campana, D., van Dongen, J.J., Mehta, A., Coustan-Smith, E., Wolvers-Tettero, I.L., Ganeshaguru, K., and Janossy, G. (1991). Stages of T-cell receptor protein expression in T-cell acute lymphoblastic leukemia. Blood *77*, 1546–1554.
68. Hamblin, T.J., Cattan, A.R., Glennie, M.J., Stevenson, G.T., Stevenson, F.K., Watts, H.F., and Stevenson, G.T. (1987). Initial experience in treating human lymphoma with a chimeric univalent derivative of monoclonal anti-idiotype antibody. Blood *69*, 790–797.
69. Miller, R.A., Maloney, D.G., Warnke, R., and Levy, R. (1982). Treatment of B-cell lymphoma with monoclonal anti-idiotype antibody. N. Engl. J. Med. *306*, 517–522.
70. Armitage, J.O. (2017). The aggressive peripheral T-cell lymphomas: 2017. Am. J. Hematol. *92*, 706–715.
71. Sibon, D. (2022). Peripheral T-Cell Lymphomas: Therapeutic Approaches. Cancers *14*, 2332.
72. Simone, M. de, Rossetti, G., and Pagani, M. (2018). Single Cell T Cell Receptor Sequencing: Techniques and Future Challenges. Front. Immunol. *9*, 1638.
73. Scheetz, L., Park, K.S., Li, Q., Lowenstein, P.R., Castro, M.G., Schwendeman, A., and Moon, J.J. (2019). Engineering patient-specific cancer immunotherapies. Nat. Biomed. Eng. *3*, 768–782.
74. Meeker, T.C., Lowder, J., Maloney, D.G., Miller, R.A., Thielemans, K., Warnke, R., and Levy, R. (1985). A clinical trial of anti-idiotype therapy for B cell malignancy. Blood *65*, 1349–1363.
75. Santos, C.F., Chen, I., States, D.J., Darwech, I., and McCord, A. (2019). PRECLINICAL ANTI-TUMOR ACTIVITY OF A RAPIDLY-SYNTHESIZED MONOCLONAL ANTIBODY TARGETING B-CELL RECEPTOR POSITIVE LYMPHOMA. Hematol. Oncol. *37*, 515–517.
76. Ott, P.A., Hu, Z., Keskin, D.B., Shukla, S.A., Sun, J., Bozym, D.J., Zhang, W., Luoma, A., Giobbie-Hurder, A., Peter, L., et al. (2017). An immunogenic personal neoantigen vaccine for patients with melanoma. Nature *547*, 217–221.
77. Pawlyn, C., and Davies, F.E. (2019). Toward personalized treatment in multiple myeloma based on molecular characteristics. Blood *133*, 660–675.
78. Puttemans, J., Stijlemans, B., Keyaerts, M., Vander Meeren, S., Renmans, W., Fostier, K., Debie, P., Hanssens, H., Rodak, M., Pruszynski, M., et al. (2022). The Road to Personalized Myeloma Medicine: Patient-specific Single-domain Antibodies for Anti-idiotypic Radionuclide Therapy. Mol. Cancer Ther. *21*, 159–169.
79. Bogen, J.P., Elter, A., Grzeschik, J., Hock, B., and Kolmar, H. (2022). Humanization of Chicken-Derived Antibodies by Yeast Surface Display. Methods Mol. Biol. *2491*, 335–360.

80. Elter, A., Bogen, J.P., Hinz, S.C., Fiebig, D., Macarrón Palacios, A., Grzeschik, J., Hock, B., and Kolmar, H. (2021). Humanization of Chicken-Derived scFv Using Yeast Surface Display and NGS Data Mining. Biotechnol. J. *16*, e2000231.

81. Charette, M. de, and Houot, R. (2018). Hide or defend, the two strategies of lymphoma immune evasion: potential implications for immunotherapy. Haematologica *103*, 1256–1268.

82. Kaimi, Y., Takahashi, Y., Taniguchi, H., Ochi, T., Makino, H., Makita, S., Iwaki, N., Fukuhara, S., Munakata, W., Ogawa, C., et al. (2024). Loss of or decrease in CD30 expression in four patients with anaplastic large cell lymphoma after brentuximab vedotin-containing therapy. Virchows Arch. *43*, 1161–1166.

83. Schoenfeld, K., Harwardt, J., and Kolmar, H. (2024). Better safe than sorry: dual targeting antibodies for cancer immunotherapy. Biol. Chem. *405*, 443–459.

84. Connors, J.M., Jurczak, W., Straus, D.J., Ansell, S.M., Kim, W.S., Gallamini, A., Younes, A., Alekseev, S., Illés, Á., Picardi, M., et al. (2018). Brentuximab Vedotin with Chemotherapy for Stage III or IV Hodgkin's Lymphoma. N. Engl. J. Med. *378*, 331–344.

85. Wadleigh, M., Richardson, P.G., Zahrieh, D., Lee, S.J., Cutler, C., Ho, V., Alyea, E.P., Antin, J.H., Stone, R.M., Soiffer, R.J., and DeAngelo, D.J. (2003). Prior gemtuzumab ozogamicin exposure significantly increases the risk of veno-occlusive disease in patients who undergo myeloablative allogeneic stem cell transplantation. Blood *102*, 1578–1582.

86. Bogen, J.P., Grzeschik, J., Krah, S., Zielonka, S., and Kolmar, H. (2020). Rapid Generation of Chicken Immune Libraries for Yeast Surface Display. Methods Mol. Biol. *2070*, 289–302.

87. Benatuil, L., Perez, J.M., Belk, J., and Hsieh, C.-M. (2010). An improved yeast transformation method for the generation of very large human antibody libraries. Protein Eng. Des. Sel. *23*, 155–159.

88. Hinz, S.C., Elter, A., Rammo, O., Schwämmle, A., Ali, A., Zielonka, S., Herget, T., and Kolmar, H. (2020). A Generic Procedure for the Isolation of pH- and Magnesium-Responsive Chicken scFvs for Downstream Purification of Human Antibodies. Front. Bioeng. Biotechnol. *8*, 688.

89. Hendel, A., Bak, R.O., Clark, J.T., Kennedy, A.B., Ryan, D.E., Roy, S., Steinfeld, I., Lunstad, B.D., Kaiser, R.J., Wilkens, A.B., et al. (2015). Chemically modified guide RNAs enhance CRISPR-Cas genome editing in human primary cells. Nat. Biotechnol. *33*, 985–989.

90. Bloemberg, D., Nguyen, T., MacLean, S., Zafer, A., Gadoury, C., Gurnani, K., Chattopadhyay, A., Ash, J., Lippens, J., Harcus, D., et al. (2020). A High-Throughput Method for Characterizing Novel Chimeric Antigen Receptors in Jurkat Cells. Mol. Ther. Methods Clin. Dev. *16*, 238–254.

91. Müller, S., Bexte, T., Gebel, V., Kalensee, F., Stolzenberg, E., Hartmann, J., Koehl, U., Schambach, A., Wels, W.S., Modlich, U., and Ullrich, E. (2019). High Cytotoxic Efficiency of Lentivirally and Alpharetrovirally Engineered CD19-Specific Chimeric Antigen Receptor Natural Killer Cells Against Acute Lymphoblastic Leukemia. Front. Immunol. *10*, 3123.

92. Prommersberger, S., Hudecek, M., and Nerreter, T. (2020). Antibody-Based CAR T Cells Produced by Lentiviral Transduction. Curr. Protoc. Immunol. *128*, e93.

93. Puthenveetil, S., Liu, D.S., White, K.A., Thompson, S., and Ting, A.Y. (2009). Yeast display evolution of a kinetically efficient 13-amino acid substrate for lipoic acid ligase. J. Am. Chem. Soc. *131*, 16430–16438.

94. Baruah, H., Puthenveetil, S., Choi, Y.-A., Shah, S., and Ting, A.Y. (2008). An engineered aryl azide ligase for site-specific mapping of protein-protein interactions through photo-cross-linking. Angew. Chem. *47*, 7018–7021.

95. Singh, A.P., Sharma, S., and Shah, D.K. (2016). Quantitative characterization of in vitro bystander effect of antibody-drug conjugates. J. Pharmacokinet. Pharmacodyn. *43*, 567–582.

OMTON, Volume *32*

Supplemental information

T cell receptor-directed antibody-drug conjugates for the treatment of T cell-derived cancers

Katrin Schoenfeld, Jan Habermann, Philipp Wendel, Julia Harwardt, Evelyn Ullrich, and Harald Kolmar

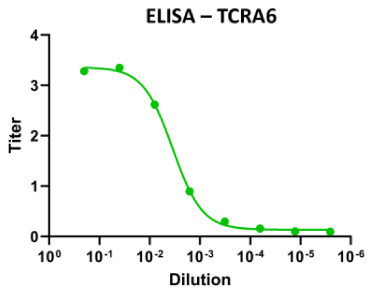

Figure S1 Chicken immune response against TCRA6. Enzyme-linked immunosorbent assay (ELISA) for determination of final antibody titer in serum of immunized chickens. Experiment was conducted by Davids Biotechnologie GmbH (Regensburg, Germany).

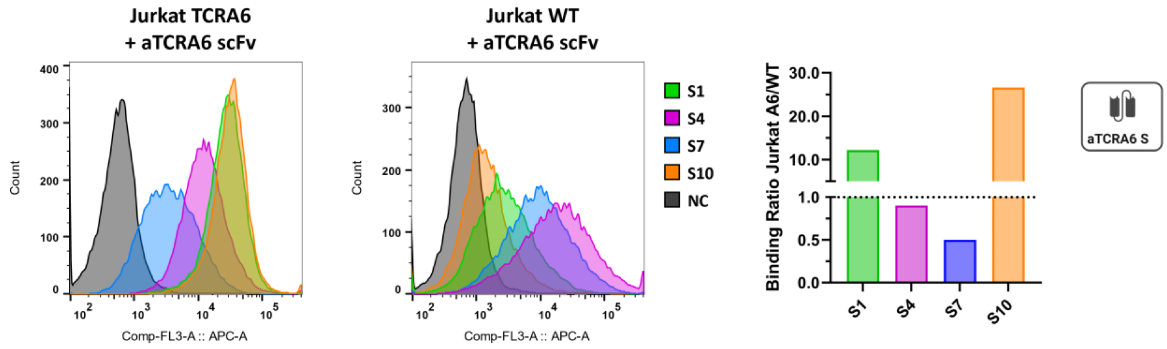

Figure S2 Cellular binding of aTCRA6 scFvs. Flow cytometry analysis of Jurkat TCRA6 target and Jurkat WT off-target T cells incubated with 1000 nM of aTCRA6 scFv candidates S1, S4, S7, and S10, respectively. Negative controls without scFv incubation are shown in black. Staining was conducted *via* anti-his AF647-conjugated secondary detection antibody. Binding ratios of Jurkat TCRA6 to Jurkat WT cells were calculated by division of by normalized mean fluorescence values.

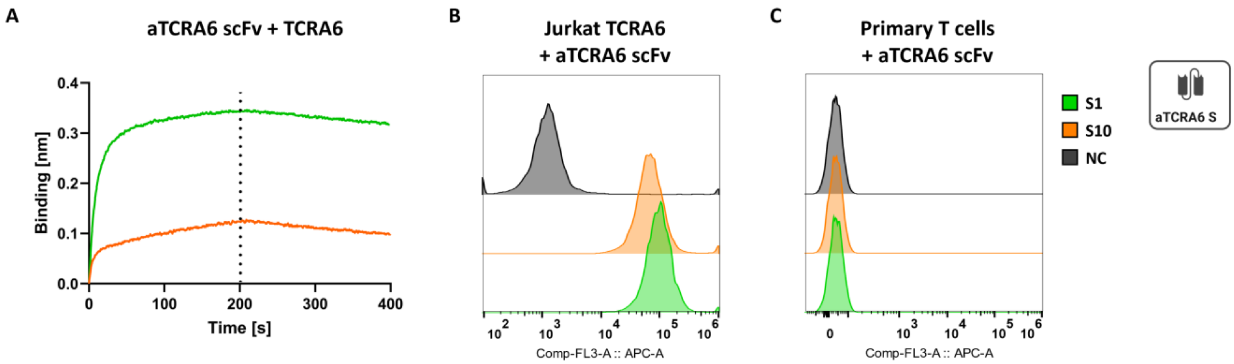

Figure S3 Binding properties of aTCRA6 scFvs S1 and S10. (A) BLI measurement. Biotinylated TCRA6 was loaded onto SAX biosensor tips and associated with 500 nM aTCRA6 S1 and S10, respectively. (B) Target cell binding. Flow cytometry analysis of Jurkat TCRA6 target cells incubated with 1000 nM aTCRA6 S1 and S10, respectively. Staining was conducted using anti-his AF647-conjugated secondary detection antibody. (C) Off-target cell binding. Flow cytometry analysis of primary T cells isolated from human donor blood incubated with 1000 nM aTCRA6 S1 and S10, respectively. Staining was performed using mouse anti-his secondary antibody and anti-mouse IgG APC tertiary antibody for detection.

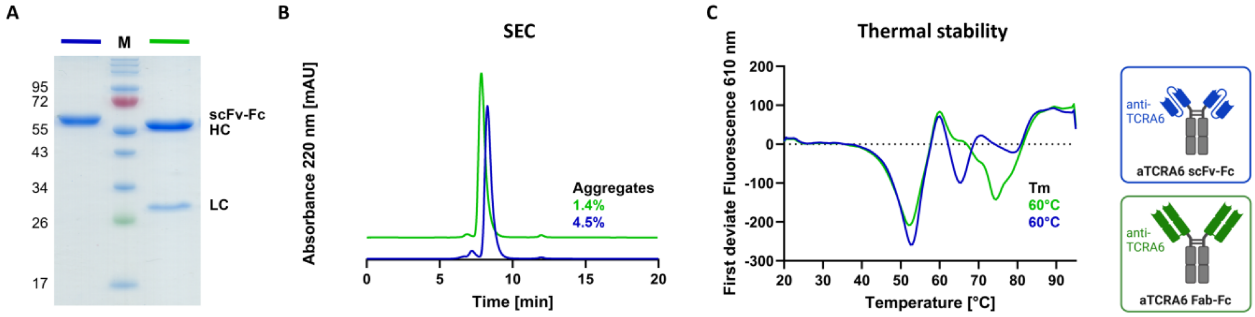

Figure S4 Biophysical characterization of aTCRA6 scFv-Fc/Fab-Fc. (A) Reducing SDS-PAGE of depicted aTCRA6 antibodies. (B) Size exclusion chromatography. The percentages of aggregation were determined by integration of the absorbance peak areas. (C) Thermal shift assay. Thermal stability was analyzed using differential scanning fluorimetry with SYPRO Orange dye. Derivatives of melt curves and melting temperatures (Tm) were assessed using the BioRad CFX Maestro software.

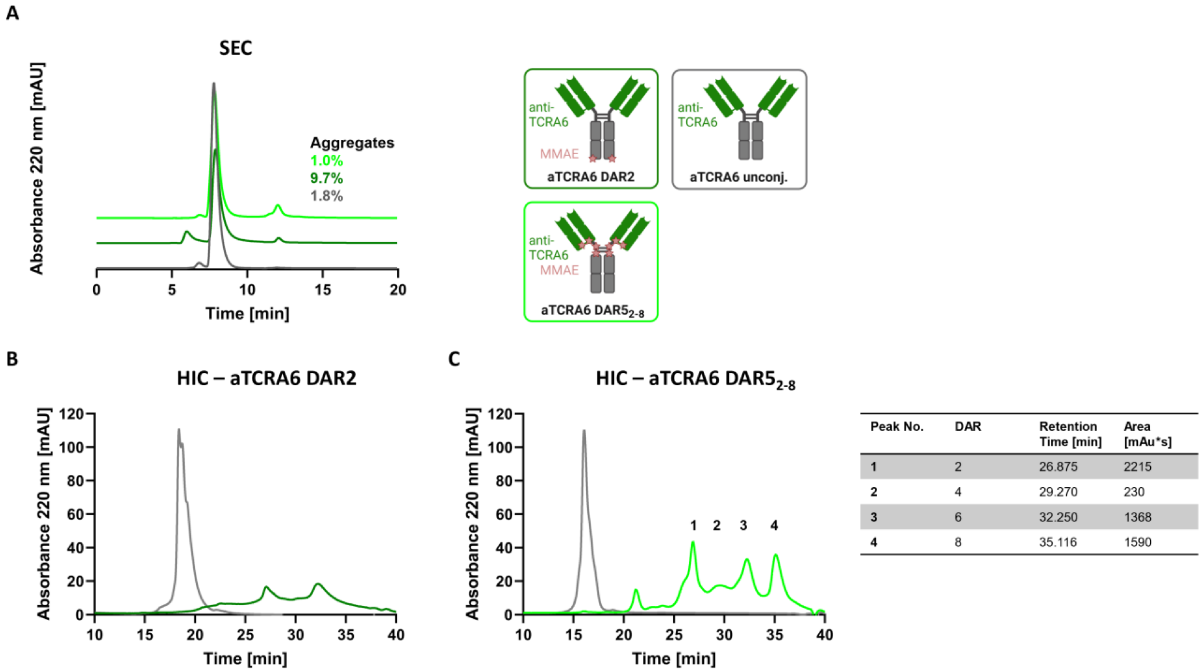

Peak No.	DAR	Retention Time [min]	Area [mAu*s]
1	2	26.875	2215
2	4	29.270	230
3	6	32.250	1368
4	8	35.116	1590

Figure S5 Biophysical characterization of aTCRA6 DAR2 and DAR5$_{2-8}$ ADCs. (A) Size exclusion chromatography. The percentages of aggregation were determined by integration of the absorbance peak areas. (B) Hydrophobic interaction chromatography of aTCRA6 DAR2. (C) Hydrophobic interaction chromatography of aTCRA6 DAR5$_{2-8}$. The absorbance peak areas of the different species, labelled as 1-4, are depicted in the table.

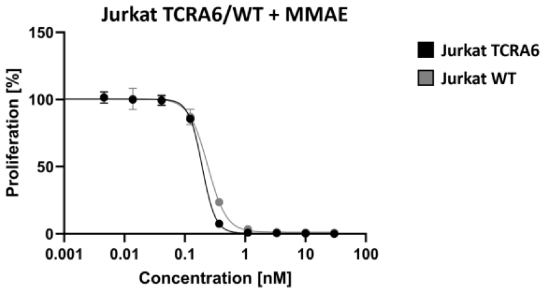

Cell line	EC_{50}	Max. lysis
Jurkat TCRA6	0.19 nM	100%
Jurkat WT	0.24 nM	99%

Figure S6 Cytotoxicity of MMAE on Jurkat TCRA6 and Jurkat WT cells. Cytotoxicity was assessed by exposition of Jurkat TCRA6 target cells and Jurkat WT off-target cells to 0.005-30 nM MMAE for 72 h. Cell proliferation was normalized to untreated control cells (0 nM). EC_{50}s were determined using variable slope four-parameter fit. Results are shown as mean, error bars represent standard deviation derived from experimental triplicates. Data is representative of three independent experiments.

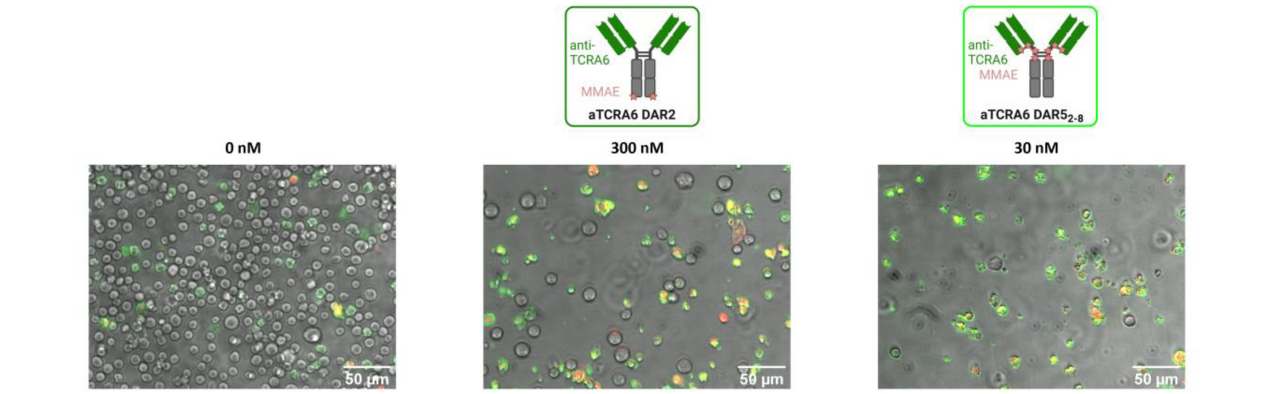

Figure S7 Microscopic images of apoptosis induction in Jurkat TCRA6 by aTCRA6 ADC variants. Jurkat TCRA6 target cells were exposed to 300 nM aTCRA6 DAR2 and 30 nM aTCRA6 DAR5$_{2-8}$ for 72 h. Cells were stained with Annexin V-FITC (green) and propidium iodide (red) and analyzed by fluorescence microscopy. Merges of bright field and fluorescence images are depicted.

Table S1 Amino acid sequences in one-letter code of the chimeric chicken-human aTCRA6S1 light and heavy chain. CDRs are highlighted in bold, the LAP-tag is underlined.

aTCRA6S1 LC	ALTQPSSVSANLGGTVEITCS**GSSGNYYG**WYQQKSPGSAPVTVIY**YND KRPS**NIPSRFSGSKSGSTATLTITGVQAEDEAVYYCG**GFDSNYVGI**FGA GTTLTVLGQPKAAPSVTLFPPSSEELQANKATLVCLISDFYPGAVTVAW KADSSPVKAGVETTTPSKQSNNKYAASSYLSLTPEQWKSHKSYSCQVT HEGSTVEKTVAPTECS
aTCRA6S1 HC	AVTLDESGGGLQTPGGTLSLVCKAS**GFDFSSYLMF**WVRQAPGKGLEFI AS**ISSNDALSTDYGAAVKG**RATISRDNGQSTLRLQLNNLRAEDTGNYY CAK**SAGGWTYGHAGSIDA**WGHGTEVIVSSASTKGPSVFPLAPSSKSTS GGTAALGCLVKDYFPEPVTVSWNSGALTSGVHTFPAVLQSSGLYSLSS VVTVPSSSLGTQTYICNVNHKPSNTKVDKKVEPKSCDKTHTCPPCPAPE LLGGPSVFLFPPKPKDTLMISRTPEVTCVVVDVSHEDPEVKFNWYVDG VEVHNAKTKPREEQYNSTYRVVSVLTVLHQDWLNGKEYKCKVSNKAL PAPIEKTISKAKGQPREPQVYTLPPSRDELTKNQVSLTCLVKGFYPSDIA VEWESNGQPENNYKTTPPVLDSDGSFFLYSKLTVDKSRWQQGNVFSCS VMHEALHNHYTQKSLSLSPGK<u>GFEIDKVWYDLDA</u>

4.4 Bispecific killer cell engagers employing species cross-reactive NKG2D binders redirect human and murine lymphocytes to ErbB2/HER2-positive malignancies

Title:

Bispecific killer cell engagers employing species cross-reactive NKG2D binders redirect human and murine lymphocytes to ErbB2/HER2-positive malignancies

Authors:

Jordi Pfeifer Serrahima*, Katrin Schoenfeld*, Ines Kühnel, Julia Harwardt, Arturo Macarrón Palacios, Maren Prüfer, Margareta Kolaric, Pranav Oberoi, Harald Kolmar and Winfried S. Wels

*shared first authorship

Bibliographic data:

Frontiers in Immunology

Volume 15 - 2024, Section Cancer Immunity and Immunotherapy

Article first published: 29th August 2024

DOI: 10.3389/fimmu.2024.1457887

Contributions by Katrin Schoenfeld:

- Planning of the project with Jordi Pfeifer Serrahima
- Generation and screening of the scFv library for human/murine cross-reactive NKG2D binders
- Production and characterization of scFvs and scFv-Fc antibodies
- Writing of the manuscript and generation of figures with Jordi Pfeifer Serrahima

frontiers | Frontiers in Immunology

TYPE Original Research
PUBLISHED 29 August 2024
DOI 10.3389/fimmu.2024.1457887

OPEN ACCESS

EDITED BY
Stefan B. Eichmüller,
German Cancer Research Center (DKFZ), Germany

REVIEWED BY
Frank Momburg,
German Cancer Research Center (DKFZ), Germany
Dafne Müller,
University of Stuttgart, Germany

*CORRESPONDENCE
Winfried S. Wels
wels@gsh.uni-frankfurt.de
Harald Kolmar
harald.kolmar@tu-darmstadt.de

†These authors have contributed equally to this work and share first authorship

‡These authors have contributed equally to this work and share last authorship

RECEIVED 01 July 2024
ACCEPTED 08 August 2024
PUBLISHED 29 August 2024

CITATION
Pfeifer Serrahima J, Schoenfeld K, Kühnel I, Harwardt J, Macarrón Palacios A, Prüfer M, Kolaric M, Oberoi P, Kolmar H and Wels WS (2024) Bispecific killer cell engagers employing species cross-reactive NKG2D binders redirect human and murine lymphocytes to ErbB2/HER2-positive malignancies. *Front. Immunol.* 15:1457887. doi: 10.3389/fimmu.2024.1457887

Bispecific killer cell engagers employing species cross-reactive NKG2D binders redirect human and murine lymphocytes to ErbB2/HER2-positive malignancies

Jordi Pfeifer Serrahima[1,2†], Katrin Schoenfeld[3†], Ines Kühnel[1], Julia Harwardt[3], Arturo Macarrón Palacios[3], Maren Prüfer[1], Margareta Kolaric[1], Pranav Oberoi[1], Harald Kolmar[3,4*‡] and Winfried S. Wels[1,2,5*‡]

[1]Georg-Speyer-Haus, Institute for Tumor Biology and Experimental Therapy, Frankfurt, Germany, [2]Frankfurt Cancer Institute, Goethe University, Frankfurt, Germany, [3]Institute for Organic Chemistry and Biochemistry, Technical University of Darmstadt, Darmstadt, Germany, [4]Centre for Synthetic Biology, Technical University of Darmstadt, Darmstadt, Germany, [5]German Cancer Consortium (DKTK), Partner Site Frankfurt/Mainz, Frankfurt, Germany

NKG2D is an activating receptor expressed by natural killer (NK) cells and other cytotoxic lymphocytes that plays a pivotal role in the elimination of neoplastic cells through recognition of different stress-induced cell surface ligands (NKG2DL). To employ this mechanism for cancer immunotherapy, we generated NKG2D-engaging bispecific antibodies that selectively redirect immune effector cells to cancer cells expressing the tumor-associated antigen ErbB2 (HER2). NKG2D-specific single chain fragment variable (scFv) antibodies cross-reactive toward the human and murine receptors were derived by consecutive immunization of chicken with the human and murine antigens, followed by stringent screening of a yeast surface display immune library. Four distinct species cross-reactive (sc) scFv domains were selected, and reformatted into a bispecific engager format by linking them via an IgG4 Fc domain to a second scFv fragment specific for ErbB2. The resulting molecules (termed scNKAB-ErbB2) were expressed as disulfide-linked homodimers, and demonstrated efficient binding to ErbB2-positive cancer cells as well as NKG2D-expressing primary human and murine lymphocytes, and NK-92 cells engineered with chimeric antigen receptors derived from human and murine NKG2D (termed hNKAR and mNKAR). Two of the scNKAB-ErbB2 molecules were found to compete with the natural NKG2D ligand MICA, while the other two engagers interacted with an epitope outside of the ligand binding site. Nevertheless, all four tested scNKAB-ErbB2 antibodies were similarly effective

in redirecting the cytotoxic activity of primary human and murine lymphocytes as well as hNKAR-NK-92 and mNKAR-NK-92 cells to ErbB2-expressing targets, suggesting that further development of these species cross-reactive engager molecules for cancer immunotherapy is warranted.

KEYWORDS

bispecific killer cell engager, BiKE, NKG2D, ErbB2, HER2, natural killer cells, NK-92, chimeric antigen receptor

1 Introduction

Bispecific antibodies that crosslink activating receptors on cytotoxic lymphocytes with tumor-associated surface antigens hold enormous potential for targeted cancer immunotherapy. While bispecific T-cell engagers (BiTEs) such as blinatumomab selectively redirect T lymphocytes to cancer cells via binding to CD3 (1), bispecific and trispecific killer cell engagers (BiKEs, TriKEs) which interact with the IgG-binding receptor CD16a (FcγRIIIa), natural cytotoxicity receptors (NCRs), or the C-type lectin-like protein Natural Killer Group 2D (NKG2D) predominantly recruit innate killer cells to the tumor (2–4). With respect to the latter, most progress has been made with bispecific antibodies that activate CD16a-positive natural killer (NK) cells, and several such molecules are currently evaluated in clinical trials for the treatment of lymphoma, advanced solid cancers, multiple myeloma (MM) or acute myeloid leukemia (AML) (5). In a different approach, Gaulthier and colleagues designed TriKEs with further enhanced activating potential by combining an IgG1 Fc region for engagement of CD16a with an antibody fragment specific for NKp46, a natural cytotoxicity receptor almost exclusively expressed on NK cells, and a tumor-targeting domain recognizing antigens like CD123 on AML cells (6). Similar to NCRs, NKG2D represents a promising activating receptor for engager-mediated redirection of cytotoxic lymphocytes to cancer cells, with different NKG2D-targeted approaches being under active development (2, 7).

NKG2D is not only expressed by NK cells, but also NKT cells, $CD8^+$ T cells, and subpopulations of $CD4^+$ and $\gamma\delta$ T cells, and is critically involved in the immunosurveillance of malignancies and pathogens (8, 9). In humans, NKG2D recognizes eight stress-induced cell surface ligands (NKG2DL) that are expressed by almost all cancer types, and include the MHC class I-related molecules MICA and MICB, as well as the six UL16-binding proteins ULBP1 to ULBP6 (10, 11). Nevertheless, low or absent NKG2DL expression by leukemia-initiating cells (12), and removal of NKG2DL from the cell surface by proteolytic shedding can still result in escape of cancer cells from NKG2D-mediated immune surveillance (13–15). Bispecific NKG2D engagers circumvent this dependency on NKG2DL expression, and redirect NKG2D-positive effector lymphocytes to tumor cells irrespective of the presence of natural ligands. For NKG2D binding, such recombinant molecules employ NKG2D-specific single chain fragment variable (scFv) antibodies or nanobodies (16–20), or domains derived from natural NKG2D ligands like ULBP2 or MICA (21–24). These NKG2D-engaging units are linked to a second binding domain targeting surface antigens expressed by hematological malignancies or solid tumors.

Like all engagers of this architecture, bispecific NKG2D antibodies depend on the quality and effectiveness of the cytotoxic lymphocytes they recruit to the tumor. However, in cancer patients endogenous NK cells are often functionally compromised. Therefore, *ex vivo* expanded NK cells from healthy donors are typically employed for adoptive NK cell immunotherapies (25, 26). Also the continuously expanding human NK cell line NK-92 and chimeric antigen receptor (CAR)-engineered derivatives thereof are being developed for clinical applications (27–30). Unlike allogeneic T lymphocytes, unrelated donor NK cells do not induce graft-*versus*-host disease (GvHD), even if applied in an HLA-unmatched setting (25). This makes them ideal candidates for the development of safe and cost-effective off-the-shelf therapeutics. Consequently, to enhance the efficacy of bispecific killer cell engagers that interact with CD16a or NKG2D, strategies have been devised to combine them with adoptive transfer of CD16a-positive donor NK cells (31), or allogeneic NK or T cells engineered with an NKG2D-derived CAR (18, 20).

To expand the armamentarium of NKG2D binders suitable for engineering effective engager molecules, here we immunized chicken with human and murine NKG2D, generated a yeast surface display immune library and selected a panel of four novel avian scFv antibody fragments, which in contrast to current molecules not only activate human NKG2D but also its murine homolog. The species cross-reactive (sc) binding domains were then employed to derive bispecific NKG2D-activating antibodies (termed NKABs) by fusing them via an IgG4 Fc region to a second scFv fragment which targets the tumor-associated antigen ErbB2 (HER2). Utilizing NKG2D-positive primary human and murine lymphocytes as well as established NK-92 cells engineered to express NKG2D-derived CARs (termed NKARs) either based on

human or murine NKG2D, we investigated binding of the resulting scNKAB-ErbB2 molecules to human and murine NKG2D receptors, competition with the natural NKG2D ligand MICA and redirection of the effector lymphocytes to ErbB2-expressing cancer cells in comparison to reference NKAB-ErbB2 molecules that interact only with human or murine NKG2D.

2 Materials and methods

2.1 Cells and culture conditions

MDA-MB-453 and MDA-MB-468 breast carcinoma, and EL-4 T-cell lymphoma cells (all ATCC, Manassas, VA) were cultured in DMEM (Gibco, Thermo Fisher Scientific, Darmstadt, Germany), A20 B-cell lymphoma and K562 erythroleukemia cells (both ATCC), and CEM.NKR and RMA/neo T lymphoblastoid cells (kindly provided by Alexander Steinle, Goethe University, Frankfurt, Germany) in RPMI 1640 medium (Gibco, Thermo Fisher Scientific). All media were supplemented with 10% heat-inactivated FBS (Capricorn Scientific, Ebsdorfergrund, Germany), 2 mM L-glutamine, 100 U/mL penicillin and 100 µg/mL streptomycin (all Gibco), and 50 µM β-mercaptoethanol (Sigma-Aldrich, Merck, Darmstadt, Germany) for A20 cells. Expi293F embryonic kidney cells were cultured in Expi293 expression medium (both Gibco, Thermo Fisher Scientific). NK-92 cells (32) (kindly provided by NantKwest, Inc., Culver City, CA) and genetically engineered derivatives thereof were grown in X-VIVO 10 medium (Lonza, Cologne, Germany) supplemented with 5% heat-inactivated human AB plasma (German Red Cross Blood Donation Service Baden-Württemberg-Hessen, Frankfurt, Germany) and 100 IU/mL IL-2 (Proleukin; Novartis Pharma, Nürnberg, Germany). Peripheral blood mononuclear cells (PBMCs) were isolated from commercially obtained buffy coats of anonymous blood donors (German Red Cross Blood Donation Service Baden-Württemberg-Hessen) by Ficoll-Hypaque density gradient centrifugation, and cultured in X-VIVO 10 medium supplemented with 5% heat-inactivated human AB plasma, 500 IU/mL IL-2 and 50 ng/mL hIL-15 (Peprotech, Hamburg, Germany). Murine NK cells were isolated from splenocytes derived from C57BL/6 mice by MACS separation using the NK Cell Isolation Kit (Miltenyi Biotec, Bergisch Gladbach, Germany). Splenocytes and murine NK cells were kept in RPMI 1640 medium supplemented with 50 µM β-mercaptoethanol and 20 ng/mL mIL-15 (Miltenyi Biotec).

2.2 Generation of recombinant NKG2D proteins and immunization of chicken

Constructs for expression of NKG2D-Fc fusion proteins were generated by assembling sequences encoding an immunoglobulin heavy chain signal peptide, the extracellular domain of human NKG2D (hNKG2D; UniProtKB: P26718, amino acid residues 82-216) or murine NKG2D (mNKG2D; UniProtKB: Q2TJJ6, amino acid residues 98-232), and either hinge, CH2 and CH3 domains of human IgG4 in plasmid pcDNA3, or a Strep-Tag II, a 6xHis-Tag, a Tobacco Etch Virus (TEV) cleavage site and hinge, CH2 and CH3 domains of human IgG1 in plasmid pTT5. Expi293F cells were then transiently transfected with the resulting vectors using the ExpiFectamine 293 Transfection Kit according to the manufacturer's recommendations (Gibco, Thermo Fisher Scientific). Recombinant proteins were purified from culture supernatants by affinity chromatography employing a Protein G column (Pierce, Thermo Fisher Scientific) with an ÄKTA FPLC system (GE Healthcare Europe, Freiburg, Germany) for IgG4 fusion proteins, and a Protein A column (Cytiva, Dreieich, Germany) with an ÄKTA Pure Protein Purification System (GE Healthcare) for IgG1 fusion proteins.

For immunizations, the Fc domains of IgG1-based hNKG2D-Fc and mNKG2D-Fc fusion proteins were removed by cleavage with TEV protease, processed Fc domains and unprocessed full-length proteins were removed by passing the reaction mixtures through a Protein A column, and remaining hNKG2D-His and mNKG2D-His fragments were purified using an immobilized metal affinity chromatography column (Cytiva) and a Strep-Tactin column (IBA Lifesciences, Göttingen, Germany). Immunization of a pathogen-free adult laying hen (*Gallus gallus domesticus*) was performed at Davids Biotechnologie GmbH (Regensburg, Germany), with 3 intramuscular injections of purified hNKG2D-His protein with AddaVax adjuvant (InvivoGen, Toulouse, France) at days 1, 14 and 28, followed by 2 booster injections with a 1:1 mix of hNKG2D-His and mNKG2D-His proteins at days 42 and 56. Peripheral blood was collected to confirm serum antibody reactivity with hNKG2D and mNKG2D by ELISA, and the animal was sacrificed at day 63 for spleen resection and subsequent RNA extraction.

2.3 Screening for NKG2D-binding scFv antibody fragments

An scFv yeast surface display (YSD) library was generated as described previously (33–35). Briefly, cDNA was synthesized from total splenic RNA, and VH and VL sequences were amplified in separate PCR reactions. Complete scFv sequences were then assembled from VH, $(G_4S)_3$ linker and VL fragments in a subsequent fusion PCR, and transferred into linearized YSD vector (pCT) via a homologous recombination-based process in *Saccharomyces cerevisiae* strain EBY100 (Thermo Fisher Scientific), following the yeast transformation protocol of Benatuil and colleagues for library generation (36). Prior to cell sorting, scFv expression and surface presentation was induced by inoculation of yeast cells in Synthetic Galactose minimal medium with Casein Amino Acids (SG-CAA) and incubation overnight at 30°C and 180 rpm.

General procedures for handling of yeast cells and library screening were described previously (34). Specifically, for screening of NKG2D binders, yeast cells were harvested by centrifugation, washed with PBS containing 0.1% (w/v) BSA (PBS-B), and incubated with human or murine NKG2D-Fc or NKG2D-His fusion proteins for 30 min on ice. After washing with PBS-B, surface display of the Myc-tag containing scFv

antibodies and binding to recombinant NKG2D was detected simultaneously by incubation with a FITC-conjugated Myc-tag specific antibody (SH1-26E7.1.3; Miltenyi Biotec), and PE-conjugated anti-human IgG Fc (polyclonal) or AF647-conjugated His-tag-specific antibodies (4E3D10H2/E3) (both Thermo Fisher Scientific) for 20 min on ice in the dark. Then, cells were washed with PBS-B, and screened by flow cytometric cell sorting using a Sony SH800S device. Collected yeast cells were plated onto Synthetic Dextrose minimal medium with Casein Amino Acids (SD-CAA) agar plates and propagated for subsequent analysis or screening rounds by incubation at 30°C.

Four individual scFv antibody domains species cross-reactive with human and murine NKG2D (termed sc1, sc2, sc4 and sc7) were selected from the output of the library screening, and for subsequent analysis were linked to hinge, CH2 and CH3 domains of human IgG1 (UniProtKB: P01857-1, amino acid residues 99-330), expressed as Fc fusion proteins in Expi293F cells, and purified from culture supernatants via Protein A affinity chromatography as described above.

2.4 Design, expression and purification of bispecific killer cell engagers

Generation of a prototypic bispecific molecule (here termed hNKAB-ErbB2) consisting of an N-terminal scFv domain derived from human NKG2D-specific KYK-2.0 antibody, linked via a human IgG4 Fc region to a C-terminal scFv sequence specific for ErbB2 was described previously (18). For interaction with murine NKG2D, a similar mNKAB-ErbB2 molecule was generated by fusing the extracellular domain of murine NKG2D ligand MULT-1 (UniProtKB: D2CKI9, amino acid residues 26-211) to hinge, CH2 and CH3 domains of murine IgG1 (UniProtKB: P01868, amino acid residues 98-324, with the cysteine at position 102 replaced by a serine), followed by a $(G_4S)_2$ linker and the ErbB2-specific scFv (FRP5) antibody domain (37). Likewise, bispecific killer cell engagers employing the NKG2D-specific scFv antibody domains derived from the yeast display library screens were generated by replacing the KYK-2.0 scFv domain of hNKAB-ErbB2 with sc1, sc2, sc4 and sc7 sequences, yielding scNKAB-ErbB2(1), scNKAB-ErbB2(2), scNKAB-ErbB2(4) and scNKAB-ErbB2(7). All NKAB sequences were complemented by an N-terminal immunoglobulin heavy chain signal peptide, assembled *in silico*, *de novo* synthesized (GeneArt, Thermo Fisher Scientific), and inserted into mammalian expression vector pcDNA3. Expi293F cells were transiently transfected with the resulting plasmids, and recombinant molecules were purified from culture supernatants by affinity chromatography using either a Protein G column (hNKAB-ErbB2 and scNKAB-ErbB2 molecules) or a Protein A column (mNKAB-ErbB2) with an ÄKTA FPLC system as described above. Purity of recombinant NKAB molecules was confirmed by SDS-PAGE followed by Coomassie staining. NKAB-containing elution fractions were combined and dialyzed against DPBS. Protein concentrations were determined using a Nanodrop 1000 spectrophotometer (Thermo Fisher Scientific) considering molecular mass and extinction coefficient of the individual proteins.

2.5 Generation of NKG2D-CAR expressing NK cells and ErbB2-expressing tumor cells

The generation of established human NK-92 cells expressing an NKG2D-based chimeric antigen receptor that encompasses an immunoglobulin heavy chain signal peptide, the extracellular domain of human NKG2D, a $(G_4S)_2$ linker, a Myc-tag, a modified CD8α hinge region and transmembrane and intracellular signaling domains of human CD3ζ (hNKG2D.z, here termed hNKAR) was described previously (18, 20). A similar CAR based on murine NKG2D (mNKG2D.z, termed mNKAR) was designed by replacing the extracellular domain of human NKG2D with the corresponding murine sequence (UniProtKB: Q2TJJ6, amino acid residues 98-232, with the cysteine at position 99 replaced by a serine). The complete mNKAR sequence was then inserted into lentiviral transfer plasmid pHR'SIN-cPPT-SIRW upstream of IRES and near-infrared fluorescent protein (iRFP) sequences (38), resulting in vector pS-mNKAR-IRW. VSV-G pseudotyped vector particles were produced in HEK293T cells, and NK-92 cells were transduced as described previously (39). mNKAR-expressing NK-92 cells were enriched by sorting of iRFP-positive cells using a FACSAria Fusion Flow Cytometer (BD Biosciences, Heidelberg, Germany). Surface expression of NKG2D-CARs on hNKAR-NK-92 and mNKAR-NK-92 cells was confirmed by flow cytometry using an AF647-conjugated Myc-tag-specific antibody (9E10; BioLegend, Koblenz, Germany), and PE-conjugated antibodies specific for human NKG2D (BAT221; Miltenyi Biotec) or murine NKG2D (CX5; BioLegend). All flow cytometric measurements were performed with an LSRFortessa Cell Analyzer (BD Biosciences). Data were processed using FlowJo software (version 10.6.0; BD Biosciences). ErbB2-expressing CEM.NKR/ErbB2 and RMA/neo/ErbB2 cells were generated by transduction with VSV-G pseudotyped lentiviral vector encoding full-length human ErbB2 (20), followed by flow cytometric cell sorting using Alexa Fluor 647-conjugated anti-human ErbB2 antibody (24D2; BioLegend).

2.6 Degranulation of NK cells

Degranulation of NKAR-NK-92 cells upon exposure to immobilized anti-NKG2D scFv-Fc fusion proteins was analyzed by detecting surface expression of lysosomal-associated membrane protein 1 (LAMP-1, CD107a). The wells of a 96-well flat-bottom microtiter plate were coated overnight with 100 µl DPBS containing 500 ng of the respective protein. After washing the plate with DPBS and blocking unspecific binding sites with DPBS supplemented with 10% FCS for 20 min at room temperature, hNKAR-NK-92 and mNKAR-NK-92 cells were plated at $5x10^5$ cells/well in the presence of GolgiStop (BD Biosciences) and PE-conjugated CD107a-specific antibody (H4A3; BioLegend). NK cells kept in medium in the absence of scFv-Fc fusion proteins or stimulated with 50 ng/mL phorbol 12-myristate 13-acetate (PMA) and 500 ng/mL ionomycin (both Sigma-Aldrich) served as controls. After 4 hours of incubation at 37°C, the cells were washed with DPBS and analyzed by flow cytometry.

2.7 Binding assays

Binding of NKG2D-Fc or NKAB fusion proteins to tumor cells expressing ErbB2 or human or murine NKG2D ligands, as well as binding of NKAB molecules to NKAR-expressing NK-92 cells was investigated by flow cytometry. Cells were incubated with 12.5 nM of hNKG2D-Fc, mNKG2D-Fc or NKAB proteins followed by staining with APC-conjugated human or murine IgG-specific detection antibodies (both Jackson ImmunoResearch, Cambridgeshire, UK). Competition of soluble MICA by NKAB antibodies was analyzed by incubating hNKAR-NK-92 cells with 20 nM of recombinant His-tag-conjugated extracellular domain of MICA (SinoBiological, Eschborn, Germany) in the absence or presence of 5, 10 or 20 nM of a respective NKAB molecule. Remaining MICA bound to hNKAR-NK-92 cells was detected with APC-conjugated His-tag-specific antibody (J095G46; BioLegend). Simultaneous binding of NKAB antibodies to *ex vivo* expanded primary effector cells and the target antigen ErbB2 was analyzed by incubation of the cells with NKAB molecules, followed by staining with PE-conjugated recombinant extracellular domain of ErbB2 (AcroBiosystems, Basel, Switzerland). To discriminate different lymphocyte subsets, human cells were in addition stained with BV421-conjugated anti-CD56 (NCAM16.2; BD Biosciences), FITC-conjugated anti-CD3 (OKT3; BioLegend) and APC-conjugated anti-CD8 (BW135/80; Miltenyi Biotec) antibodies, and murine cells with BV421-conjugated anti-CD19 (6D5; BioLegend), APC-conjugated anti-NK1.1 (PK136; Miltenyi Biotec) and PE/Cyanine7-conjugated anti-CD3 (500A2; BioLegend) antibodies. NKG2D surface expression was investigated using PE-conjugated antibodies specific for human (BAT221; Miltenyi Biotec) or murine NKG2D (CX5; BioLegend). Dead cells were excluded by staining with fixable viability dye eFluor780 (eBioscience, Thermo Fisher Scientific). In all experiments, cells were blocked with human (Fc1; BD Biosciences) or murine (93; BioLegend) Fc receptor blocking agent prior to antibody staining.

2.8 Cytotoxicity assays

Cytotoxicity of NKAR-NK-92 cells and NKG2D-expressing primary human and murine lymphocytes was analyzed in flow cytometry-based assays as described previously (39). Briefly, tumor cells were labeled with Calcein Violet AM (CV) or Far Red (FR) (CellTrace; Invitrogen, Thermo Fisher Scientific) and incubated with effector cells at different effector to target cell (E/T) ratios for 3 hours (NKAR-NK-92 cells and human PBMCs) or 4 hours (murine splenocytes) at 37°C in the presence or absence of bispecific NKAB antibodies. Dead target cells were identified by staining with propidium iodide (PI) or 4',6-diamidino-2-phenylindole (DAPI) followed by flow cytometric quantification of CV/PI, FR/PI or FR/DAPI double-positive cells with an LSRFortessa Cell Analyzer. Spontaneous target cell lysis was subtracted to calculate specific cytotoxicity. Data were analyzed using FlowJo software.

2.9 Statistical analysis

Unless stated otherwise, quantitative data are represented as mean with standard deviation (SD). Statistical significance (P value < 0.05) was determined using unpaired t-test. All statistical analyses were performed with Prism 10 (Version 10.1.1.323; GraphPad Software, Boston, MA).

3 Results

3.1 Generation of NKG2D-specific scFv antibodies

Human and murine NKG2D share about 70% amino acid sequence identity in their extracellular domains. Hence, to ensure a sufficient immune response and generate antibodies reactive with human and murine receptors, we chose chicken for immunization as a phylogenetically distant species. Previous studies have demonstrated a satisfactory diversity of avian antibodies directed against epitopes conserved across mammalian species (33–35, 40). His-tagged recombinant proteins encompassing the extracellular domains of human (hNKG2D) and murine NKG2D (mNKG2D) were generated as described in Materials and Methods, and used for immunization of a pathogen-free adult laying hen with 3 intramuscular injections of hNKG2D-His at days 1, 14 and 28, followed by 2 booster injections with a 1:1 mixture of hNKG2D-His and mNKG2D-His proteins at days 42 and 56 (schematically shown in Figure 1A). Then, serum antibody reactivity with hNKG2D and mNKG2D was confirmed by ELISA (data not shown). The animal was sacrificed at day 63, and the spleen was resected for RNA extraction and cDNA preparation. Sequences encoding the variable domains of antibody heavy (VH) and light chains (VL) were amplified in separate PCR reactions, and randomly assembled into scFv antibodies with a $(G_4S)_3$ linker sequence connecting VH and VL domains following previously established procedures (33–35).

For screening of NKG2D binders, scFv sequences were then used to generate a yeast surface display (YSD) antibody library (34), comprising approximately 5 x 10^8 transformants. To enrich for high affinity antibodies, the library was screened by 4 consecutive rounds of flow cytometric cell sorting with decreasing antigen concentrations, using recombinant hNKG2D-Fc fusion protein in rounds 1 (1000 nM) and 2 (500 nM), followed by screening with hNKG2D-His in round 3 (500 nM) and mNKG2D-His in round 4 (100 nM) (Figure 1B). This resulted in a yeast population with surface-displayed scFv molecules that demonstrated strong binding to the extracellular domains of both, human and murine NKG2D (Output Round 4). Ten single yeast cell clones were randomly selected, and analyzed by flow cytometry for binding of human and murine NKG2D, with four distinct clones displaying superior species cross-reactive (sc) binding to the human and murine receptors (clones sc1, sc2, sc4 and sc7) (Figure 1C).

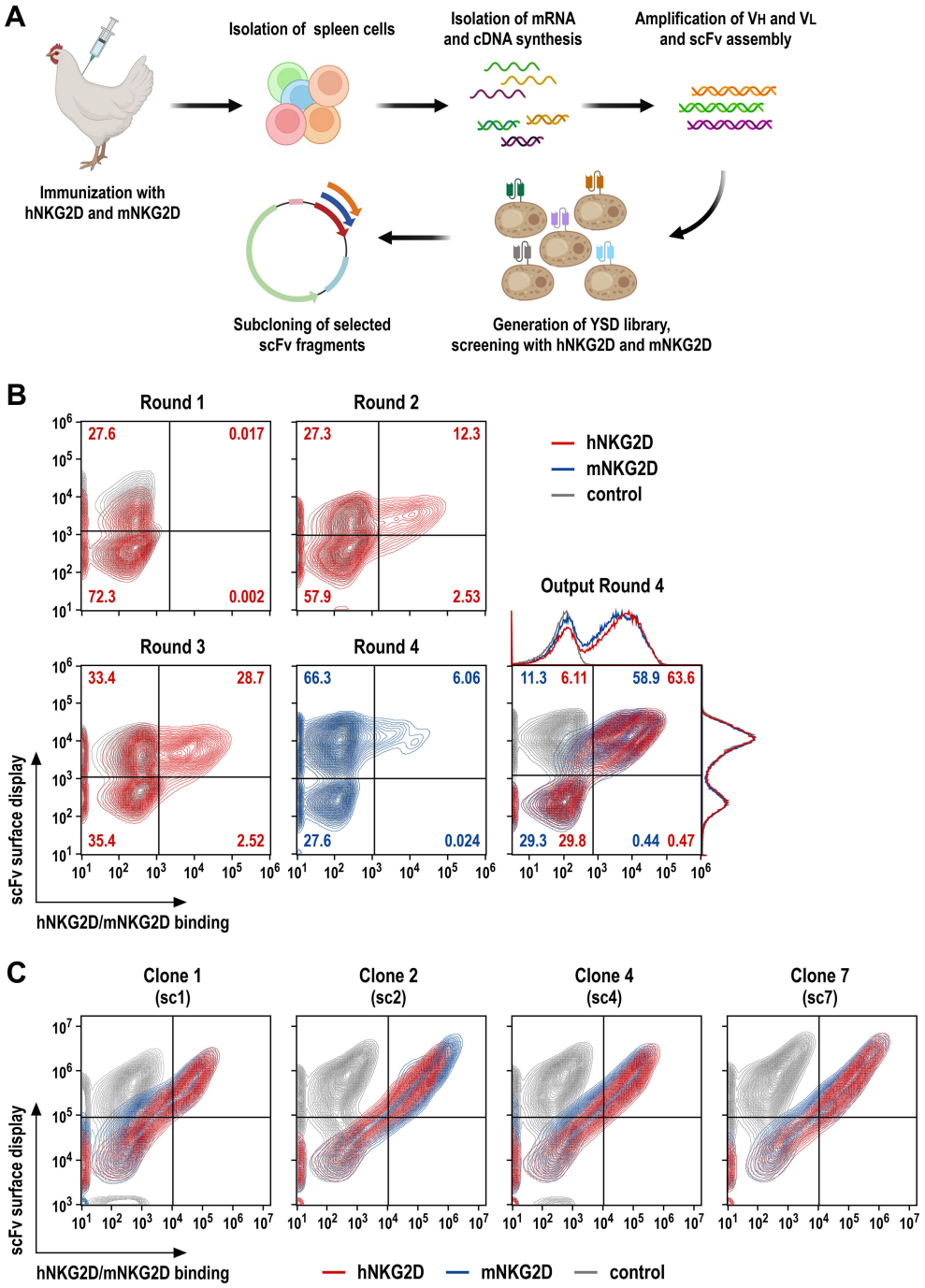

FIGURE 1
Screening of NKG2D-binding scFv antibody fragments by yeast surface display. **(A)** A laying hen was immunized with purified hNKG2D-His protein at days 1, 14 and 28, followed by booster injections with a 1:1 mix of hNKG2D-His and mNKG2D-His proteins at days 42 and 56. The spleen was resected at day 63 for RNA extraction and cDNA synthesis. VH and VL antibody sequences were amplified in separate PCR reactions, scFv sequences were assembled from VH, $(G_4S)_3$ linker and VL fragments in a fusion PCR, and transferred into a yeast surface display vector. **(B)** Yeast cells displaying NKG2D-binding scFv antibodies were identified by incubation with human NKG2D-Fc (screening rounds 1 and 2; red), or human (round 3; red) or murine NKG2D-His fusion proteins (round 4; blue), followed by PE-conjugated anti-human IgG Fc or AF647-conjugated His-tag-specific antibodies, respectively. ScFv surface display was confirmed by simultaneous staining with a FITC-conjugated antibody recognizing a C-terminal Myc-tag fused to the scFv sequences. In each case, yeast cells displaying NKG2D-binding scFv antibodies were enriched by flow cytometric cell sorting, expanded and subjected to a subsequent screening round. Cross-reactivity of displayed scFv antibodies of the yeast library obtained after the final screening round 4 was confirmed using hNKG2D-His and mNKG2D-His proteins. **(C)** Four individual yeast clones displaying species cross-reactive (sc) scFv antibodies (termed sc1, sc2, sc4 and sc7) binding to human and murine NKG2D as confirmed by staining with hNKG2D-His (red) and mNKG2D-His (blue) proteins were selected from the library screens for subsequent experiments. Yeast cells only incubated with Myc-tag-specific and secondary antibodies served as controls (gray).

3.2 Binding of NKG2D-specific scFv antibodies to NKG2D-CAR engineered NK cells

To functionally characterize the selected scFv antibodies, we employed derivatives of the clinically used human NK cell line NK-92 that were engineered to express NKG2D-based chimeric antigen receptors, either encompassing the extracellular domain of human or murine NKG2D, fused to a Myc-tag, a CD8α hinge region, and transmembrane and intracellular domains of CD3ζ (termed hNKAR and mNKAR, respectively) (Figure 2A). NK-92 cells expressing the human NKAR were previously shown to specifically recognize and kill human tumor cells which endogenously express NKG2D ligands, but not to target on their own murine cells only harboring murine NKG2DL (18, 20). To generate the similar mNKAR-NK-92 cells, a corresponding NKG2D-CD3ζ sequence employing the extracellular domain of murine NKG2D (amino acid residues 98-232, with an unpaired cysteine at position 99 replaced by a serine) was derived. Upon transduction with the respective lentiviral vector, NK-92 cells stably expressing the murine NKAR and an iRFP marker gene were

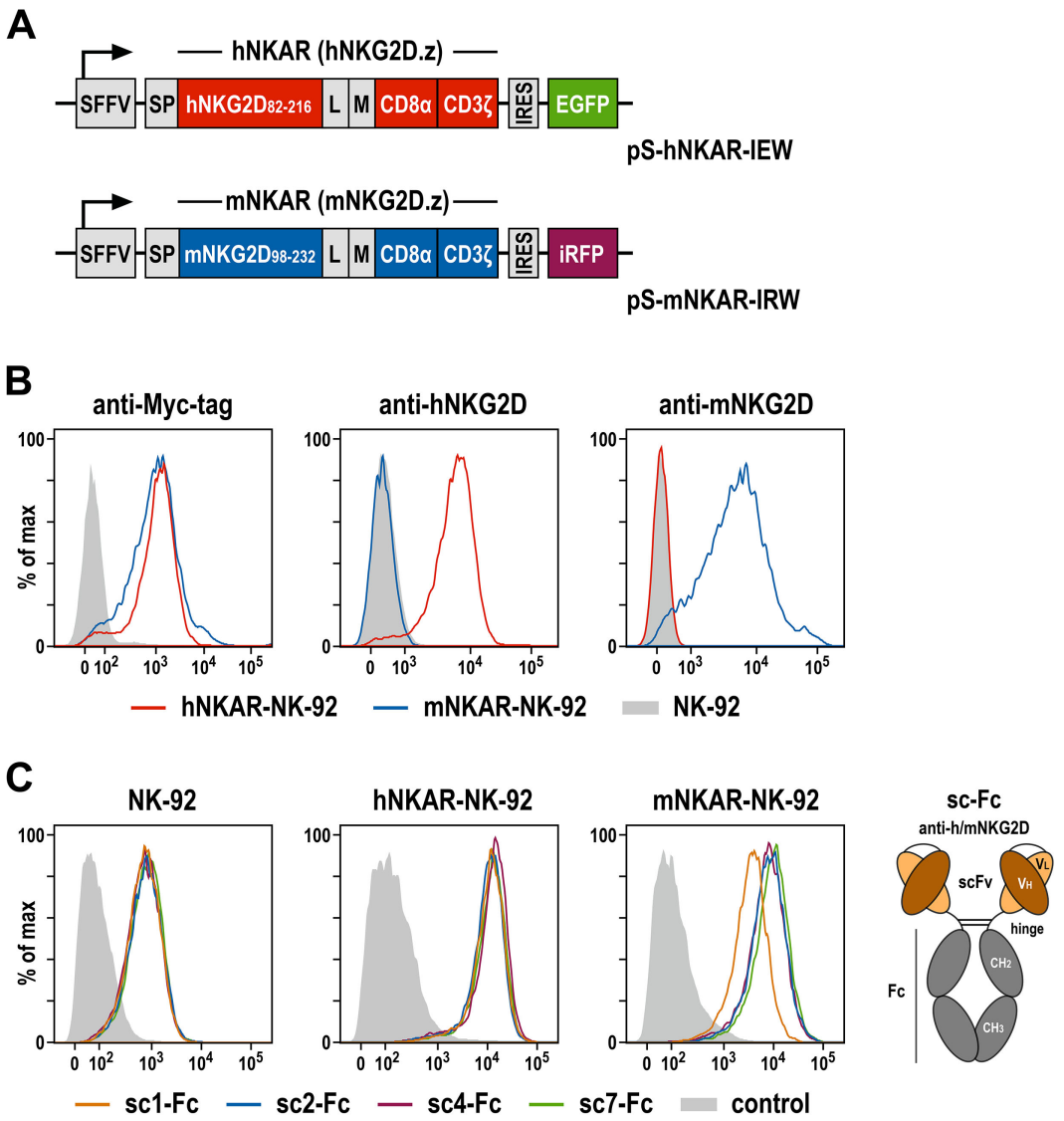

FIGURE 2
NKG2D-CAR expressing NK-92 cells as a model system to analyze NKG2D-binding antibodies. **(A)** Lentiviral transfer plasmids encoding NKG2D-based CARs under control of the Spleen Focus Forming Virus promoter (SFFV). hNKAR and mNKAR sequences consist of an immunoglobulin heavy chain signal peptide (SP), the extracellular domain of either human or murine NKG2D, a flexible $(G_4S)_2$ linker (L), a Myc-tag (M), a CD8α hinge region, and transmembrane and intracellular domains of CD3ζ. hNKAR and mNKAR sequences are followed by an internal ribosome entry site (IRES) and enhanced green fluorescent protein (EGFP) or near-infrared fluorescent protein (iRFP) cDNA, respectively. **(B)** Expression of NKG2D-CARs on the surface of sorted hNKAR-NK-92 and mNKAR-NK-92 cells was analyzed by flow cytometry as indicated using fluorochrome-labeled antibodies specific for the Myc-tag, human NKG2D or murine NKG2D. Parental NK-92 cells served as control. **(C)** Binding of scFv antibodies from the yeast surface display library screens to NKG2D and NKG2D-CAR expressing cells. The selected scFv antibodies sc1, sc2, sc4 and sc7 were expressed as scFv-Fc fusion proteins (sc-Fc; schematically shown on the right), and binding of the recombinant molecules to parental NK-92, hNKAR-NK-92 and mNKAR-NK-92 cells was analyzed by flow cytometry as indicated using an anti-human IgG antibody. Cells only stained with secondary antibody served as controls.

enriched by flow cytometric cell sorting. Surface expression of hNKAR and mNKAR by the NK-92 derivatives was confirmed by staining with antibodies recognizing the Myc-tag contained in both CAR sequences, or selectively interacting with human or murine NKG2D (Figure 2B). As expected, hNKAR-NK-92 cells were unable to lyse murine A20 B-cell lymphoma and EL-4 T-cell lymphoma cells. Conversely, mNKAR-NK-92 cells effectively killed A20 cells which express murine NKG2DL, but not mNKG2DL-negative EL-4 cells, confirming functionality of the murine NKAR (see Supplementary Figure 1).

To analyze binding of the selected scFv antibodies derived from the immune library, recombinant scFv-Fc fusion proteins of clones sc1, sc2, sc4 and sc7 were generated and tested by flow cytometry using parental NK-92 cells and the hNKAR- or mNKAR-expressing derivatives (Figure 2C). Thereby all four antibodies displayed specific binding to NK-92 cells attributed to the moderate expression of endogenous NKG2D (18, 20), but markedly enhanced binding to hNKAR-NK-92 and mNKAR-NK-92 cells. This confirms specific and species cross-reactive interaction of the selected scFv antibodies with human and murine NKG2D presented on the surface of cytotoxic lymphocytes. Furthermore, if immobilized on plastic, the NKG2D-specific scFv-Fc fusion proteins also triggered degranulation of hNKAR-NK-92 and mNKAR-NK-92 cells, demonstrating their ability to activate human and murine NKG2D receptors (see Supplementary Figure 2).

3.3 Design of bispecific killer cell engagers recognizing NKG2D and the tumor-associated antigen ErbB2

Previously, we generated a prototypic bispecific antibody able to simultaneously interact with human NKG2D and the cellular proto-oncogene ErbB2 (HER2), which is overexpressed by a subtype of breast carcinomas and many other cancers of epithelial origin (41). This molecule, here termed hNKAB-ErbB2, consists of an N-terminal scFv moiety derived from antibody KYK-2.0 specific for human NKG2D (42), linked via the hinge, CH2 and CH3 regions of human IgG4 to a second, ErbB2-specific scFv domain derived from antibody FRP5 at the C-terminus (schematically shown in Figure 3A, left) (18, 37). Produced as a disulfide-linked homodimer, the hNKAB-ErbB2 molecule specifically redirected human lymphocytes endogenously expressing NKG2D or engineered with an NKG2D-based CAR to ErbB2-positive target cells irrespective of NKG2DL expression. Applying the same protein design, here we generated four similar bispecific killer cell engagers (termed scNKAB-ErbB2) that employ the selected sc1, sc2, sc4 and sc7 scFv moieties for NKG2D binding, but retain the IgG4 Fc domain and ErbB2-specific antibody fragment of the original hNKAB-ErbB2 molecule (Figure 3A, right). As a control protein, we also designed an mNKAB-ErbB2 molecule (Figure 3A, middle), which carries the extracellular domain of murine NKG2D ligand MULT-1 for selective binding to murine NKG2D, followed by hinge, CH2 and CH3 domains of murine IgG1, and the ErbB2-specific scFv fragment shared with the other NKAB molecules.

The NKAB antibodies were expressed as secreted proteins in transiently transfected Expi293F cells and purified from culture supernatants by Protein G (hNKAB-ErbB2, scNKAB-ErbB2 proteins) or Protein A (mNKAB-ErbB2) affinity chromatography. Elution fractions containing high amounts of recombinant proteins were combined and analyzed by SDS-PAGE under reducing and non-reducing conditions, followed by Coomassie staining to confirm integrity and purity of the recombinant proteins (Figure 3B). Thereby, purified hNKAB-ErbB2, mNKAB-ErbB2 and scNKAB-ErbB2 proteins predominantly consisted of intact disulfide-linked dimers (Figure 3B, right), which were separated into monomers under reducing conditions (Figure 3B, left). With a calculated molecular mass in monomeric form of 74 to 78 kDa, similar mobility of the NKAB proteins was expected in SDS gels under reducing conditions. Nevertheless, Coomassie staining revealed more pronounced differences in the apparent mass of the scNKAB-ErbB2 molecules, suggestive of different compactness of their tertiary structures. The murine reference molecule mNKAB-ErbB2 (calculated mass of the monomer: 74 kDa) even showed a major band at an apparent molecular mass of >100 kDa, most likely due to more pronounced N-linked glycosylation compared to the other NKAB proteins, as suggested by analysis with an N-linked glycosylation site prediction tool (43).

3.4 Binding of bispecific NKAB molecules to NKAR-expressing NK cells and ErbB2-positive tumor cells

Bispecific binding of the scNKAB-ErbB2 molecules was analyzed by flow cytometry using hNKAR-NK-92 and mNKAR-NK-92 cells, which as lymphocytes are negative for ErbB2, as well as ErbB2-overexpressing MDA-MB-453 and ErbB2-negative MDA-MB-468 breast carcinoma cells. hNKAB-ErbB2 and mNKAB-ErbB2 proteins were included for comparison. The results are shown in Figure 3C. NK-92 cells expressing the human NKG2D-CAR were strongly bound by hNKAB-ErbB2 and the four scNKAB-ErbB2 clones, but with the scNKAB-ErbB2 molecules displaying an approximately two-fold increase in median fluorescence intensity (MFI) when compared to the former, and scNKAB-ErbB2(7) showing the strongest binding (see Supplementary Table 1). As expected, mNKAB-ErbB2 did not bind to hNKAR-NK-92 cells, but via its MULT-1 ligand domain strongly interacted with the murine NKG2D-CAR of mNKAR-NK-92 cells. Due to the moderate endogenous expression of human NKG2D by NK-92 cells, prototypic hNKAB-ErbB2 also displayed limited binding to mNKAR-NK-92 cells. In contrast, confirming specific recognition of the murine NKG2D-CAR seen with the respective scFv-Fc fusion proteins, the species cross-reactive scNKAB-ErbB2 molecules interacted more strongly with mNKAR-NK-92 cells, with scNKAB-ErbB2(7) again displaying the most pronounced NKG2D interaction of the four clones (see Supplementary Table 1). scNKAB-ErbB2 molecules as well as hNKAB-ErbB2 and mNKAB-ErbB2 proteins showed comparable and very strong binding to ErbB2-positive MDA-MB-453 cells, but not to ErbB2-negative MDA-MB-468 cells, confirming that the ErbB2-specific FRP5 antibody domain shared by all NKAB molecules was functional to the same extent.

To test whether the epitopes of the generated scNKAB-ErbB2 molecules within NKG2D overlap with the binding site of a natural

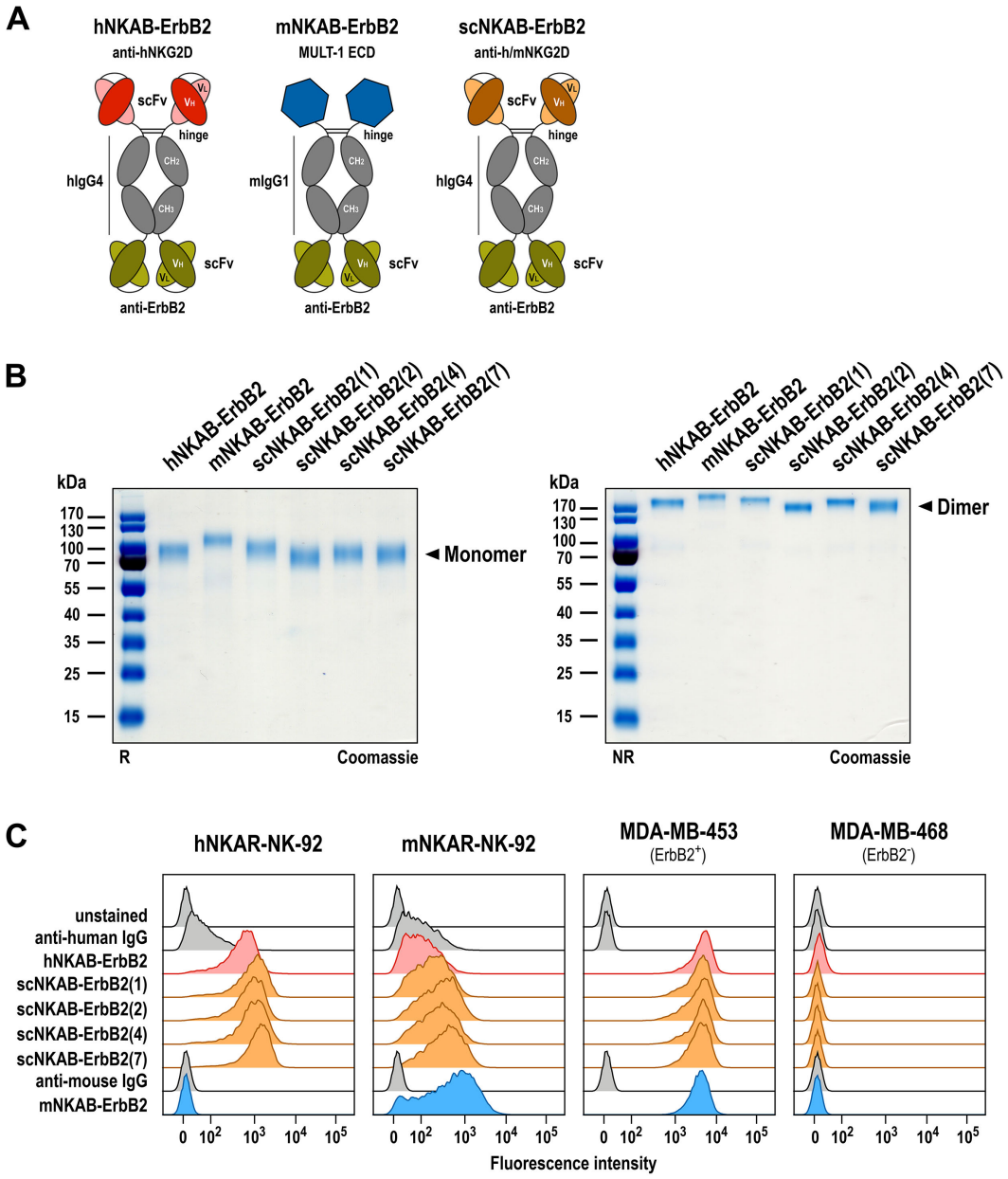

FIGURE 3
Generation of bispecific killer cell engagers. **(A)** Schematic representation of prototypic hNKAB-ErbB2 (left) and species cross-reactive scNKAB-ErbB2 molecules (right) that consist of an N-terminal scFv antibody fragment binding to NKG2D, followed by hinge, CH2 and CH3 domains of human IgG4 (hIgG4), a $(G_4S)_2$ linker, and an ErbB2-specific C-terminal scFv antibody fragment. mNKAB-ErbB2 (middle) carries the extracellular domain (ECD) of murine NKG2D ligand MULT-1 at the N-terminus, followed by hinge, CH2 and CH3 domains of murine IgG1 (mIgG1), a $(G_4S)_2$ linker, and an ErbB2-specific C-terminal scFv antibody fragment. Disulfide bridges facilitating formation of homodimers are indicated by lines.
(B) Analysis of purified NKAB antibodies by SDS-PAGE under reducing (R, left) and non-reducing (NR, right) conditions and Coomassie staining. NKAB monomers and dimers are indicated by arrowheads. **(C)** Binding of purified NKAB molecules at a concentration of 12.5 nM to NK-92 cells expressing human (hNKAR-NK-92) or murine (mNKAR-NK-92) NKG2D-CARs, and ErbB2-positive MDA-MB-453 and ErbB2-negative MDA-MB-468 breast carcinoma cells was investigated by flow cytometry as indicated. Unstained cells and cells only incubated with secondary antibody served as controls.

NKG2D ligand, we analyzed binding of 20 nM of recombinant soluble MICA (sMICA) to its cognate NKG2D and hNKAR receptors on hNKAR-NK-92 cells in the absence or presence of increasing concentrations of NKAB proteins ranging from 5 to 20 nM. In the absence of competitor, sMICA readily bound to hNKAR-NK-92 cells (Figure 4A). This was prevented by addition of prototypic hNKAB-ErbB2 known to compete with sMICA for NKG2D binding (18), but not by the mNKAB-ErbB2 control protein unable to interact with human NKG2D (Figure 4B). Similar to hNKAB-ErbB2, also species cross-reactive scNKAB-ErbB2(2) and scNKAB-ErbB2(7) molecules markedly inhibited sMICA binding, while scNKAB-ErbB2(1) did not compete sMICA, and scNKAB-ErbB2(4) only slightly reduced ligand binding to hNKAR-NK-92 cells at the highest concentration applied (Figure 4C), possibly caused by steric hindrance. Accordingly, the scFv antibody domains from clones sc2 and sc7

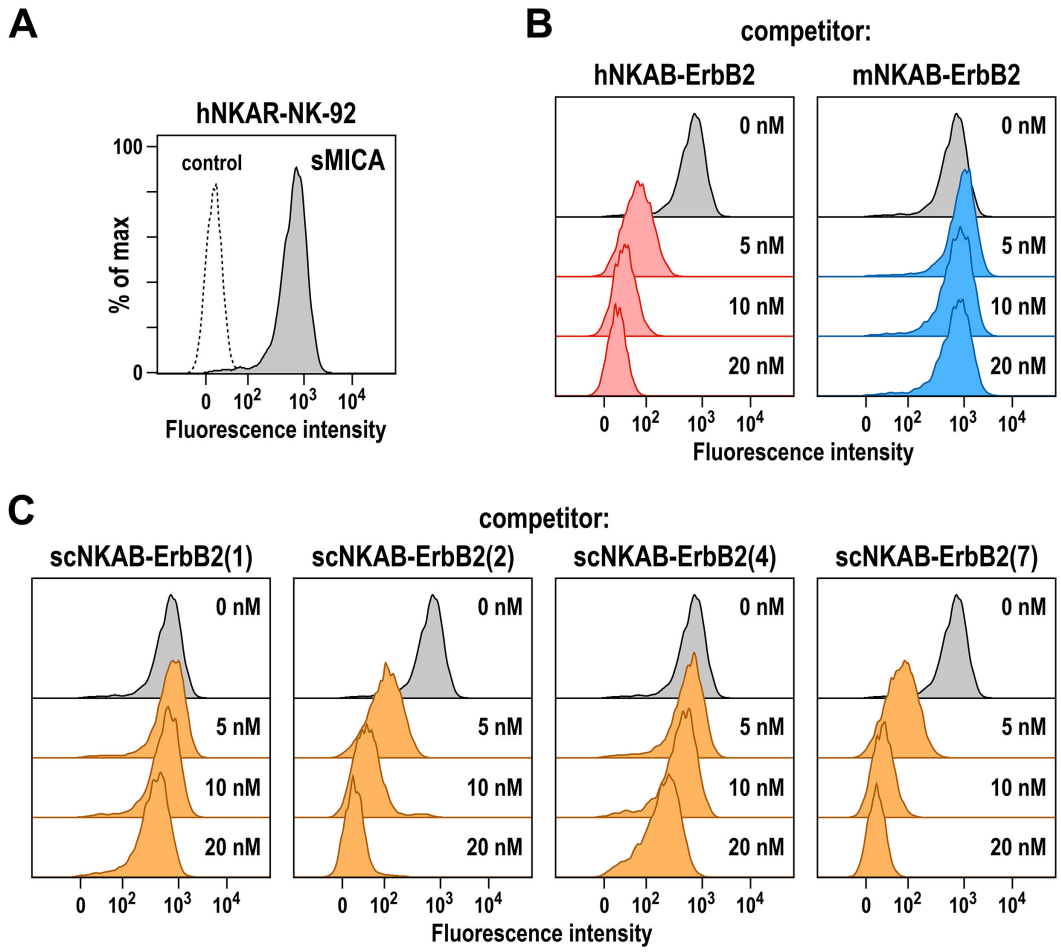

FIGURE 4
Competition of MICA binding by bispecific killer cell engagers. **(A)** Binding of His-tagged soluble MICA (sMICA) (20 nM) to hNKAR-NK-92 cells in the absence of NKAB molecules (gray area) was determined by flow cytometry with APC-conjugated anti-His-tag antibody. Control cells were only stained with secondary antibody (dashed line). **(B)** Competition of sMICA binding by prototypic hNKAB-ErbB2 was confirmed by incubation of cells with 20 nM of sMICA in the absence (gray area) or presence of increasing concentrations of hNKAB-ErbB2 (left). mNKAB-ErbB2 which is unable to interact with human NKG2D was included as negative control (right). **(C)** The ability of species cross-reactive NKAB antibodies to compete binding of sMICA to NKAR-NK-92 cells was investigated in similar experiments with purified scNKAB-ErbB2 proteins as indicated.

are competitive binders that can prevent access of soluble MICA, while scFv domains from clones sc1 and sc4 apparently bind to NKG2D regions distinct from the ligand binding site.

3.5 Simultaneous binding of NKAB molecules to NKG2D-positive primary lymphocytes and the ErbB2 target antigen

Next, we performed binding assays to test whether the species cross-reactive scNKAB-ErbB2 proteins in addition to the artificial hNKAR and mNKAR receptors on NK-92 cells can also interact with primary human and murine lymphocytes endogenously expressing NKG2D in its native form. For human cells, freshly isolated PBMCs from three healthy donors were incubated with antibodies specific for CD3, CD56 and CD8 to differentiate between NK ($CD3^-$ $CD56^+$), NKT-like ($CD3^+$ $CD56^+$) and CD8-positive T cells ($CD3^+$ $CD8^+$ $CD56^-$). In addition, cells were either incubated with an NKG2D-specific antibody to confirm NKG2D surface expression, or the different NKAB molecules to analyze their simultaneous interaction with NKG2D and the target antigen ErbB2. For this, binding of the NKAB proteins was detected with a PE-conjugated recombinant ErbB2 protein. As exemplarily shown for a representative donor in Figure 5A, left panels, gated NK, NKT-like and $CD8^+$ T cell subpopulations were all strongly positive for NKG2D, with $CD8^+$ T cells expressing even more elevated levels of the receptor than NK and NKT-like cells. Prototypic hNKAB-ErbB2 protein as well as all tested scNKAB-ErbB2 molecules readily bound to both, the NKG2D-positive primary lymphocytes and recombinant ErbB2, while mNKAB-ErbB2 as expected did not interact with the human cells (Figure 5A, middle). Thereby, in accordance with their enhanced NKG2D expression, $CD8^+$ T cells were stained more strongly by the bispecific engagers. As indicated by the respective MFI values, prototypic hNKAB-ErbB2, scNKAB-ErbB2(2) and scNKAB-ErbB2(7) displayed most efficient binding to the NKG2D-positive human lymphocytes and recombinant ErbB2, with less pronounced signals obtained with scNKAB-ErbB2(1) and scNKAB-ErbB2(4) (Figure 5A, right).

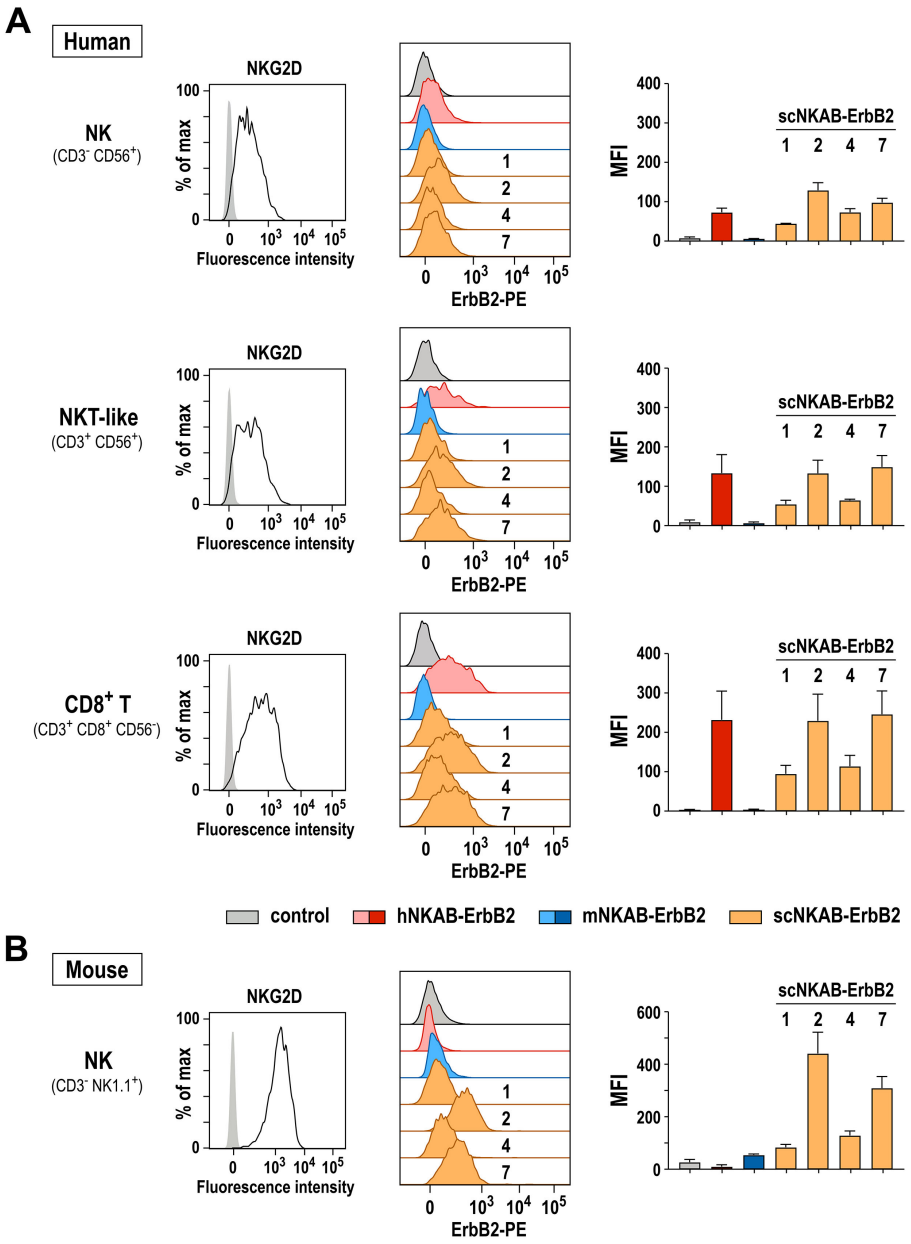

FIGURE 5
Bispecific binding of NKAB molecules to NKG2D-positive primary lymphocytes and ErbB2. Binding of purified scNKAB-ErbB2 proteins (orange), hNKAB-ErbB2 (red) and mNKAB-ErbB2 (blue) to gated NK, NKT-like and CD8$^+$ T cell subpopulations of human PBMCs **(A)**, as well as *ex vivo* expanded murine NK cells **(B)** was analyzed by flow cytometry, detecting bound NKAB molecules with recombinant PE-conjugated ErbB2 extracellular domain to confirm simultaneous interaction with NKG2D and ErbB2. Cells stained with ErbB2-PE in the absence of an NKAB molecule (gray) served as controls. Middle panels show representative histograms of cells from one donor and one animal, respectively. Panels on the right display median fluorescence intensities (MFI). Mean values ± SD are shown; n=3 individual donors in **(A)** and n=2 individual animals in **(B)**. NKG2D surface expression by human NK, NKT-like and CD8$^+$ T cell subpopulations and murine NK cells was confirmed by flow cytometry with NKG2D-specific antibodies (left panels).

Binding to murine lymphocytes endogenously expressing NKG2D was analyzed in similar experiments using *ex vivo* expanded murine NK cells obtained from two C57BL/6 mice (Figure 5B). Also in this case, scNKAB-ErbB2(2) and scNKAB-ErbB2(7) displayed the most efficient interaction with the NKG2D-positive cells and simultaneous binding to the ErbB2 target antigen. Specific signals obtained with mNKAB-ErbB2, scNKAB-ErbB2(1) and scNKAB-ErbB2(4) were much less pronounced, while hNKAB-ErbB2 in agreement with its selectivity for human NKG2D showed no binding to the murine cells.

3.6 NKAB-mediated redirection of primary lymphocytes to ErbB2-positive tumor cells

To investigate the influence of scNKAB-ErbB2 molecules on the antitumoral activity of primary human and murine lymphocytes, as

model systems we first generated by lentiviral transduction and flow cytometric cell sorting stably ErbB2-expressing derivatives of the human and murine T lymphoblastic cell lines CEM.NKR and RMA/neo, which have both been described as largely resistant to the natural cytotoxicity of human and murine NK cells, respectively (44, 45). Specific binding of the four scNKAB-ErbB2 engagers and the hNKAB-ErbB2 and mNKAB-ErbB2 control molecules to the resulting CEM.NKR/ErbB2 and RMA/neo/ErbB2 cells was confirmed by flow cytometry, while no binding to the ErbB2-negative parental cell lines was detected (see Supplementary Figure 3).

NKAB-mediated redirection of human lymphocytes to CEM.NKR/ErbB2 cells was then analyzed in cytotoxicity assays with PBMCs from three additional healthy donors, with gated NK, NKT-like and $CD8^+$ T cell subpopulations consistently displaying high level expression of endogenous NKG2D (see Supplementary Figure 4). As expected, irrespective of the presence of NKAB-ErbB2 molecules, ErbB2-negative but NK-sensitive K562 erythroleukemia cells included as a positive control were readily killed by innate effector cells within the PBMCs (Figure 6A, left). In contrast, CEM.NKR/ErbB2 cells remained largely unaffected by PBMCs after 3 hours of co-incubation at an effector to target (E/T) ratio of 10:1, which was also the case in the presence of 0.64 nM of a scFv-Fc fusion protein (FRP5-Fc) containing the same ErbB2-specific scFv fragment and human IgG4 Fc domain as the scNKAB-ErbB2 molecules (46), but lacking NKG2D-specific binding (Figure 6A, right). Conversely, cytolytic activity of the PBMCs against the ErbB2-positive targets was enhanced by addition of the ErbB2-specific antibody trastuzumab, which in contrast to FRP5-Fc is of human IgG1 isotype and capable of inducing antibody-dependent cellular cytotoxicity (ADCC) by triggering FcγRIIIa (CD16a) on NK cells. However, most potent and significantly enhanced killing of CEM.NKR/ErbB2 by the PBMCs was observed in the presence of 0.64 nM of the prototypic hNKAB-ErbB2 protein and the four species cross-reactive scNKAB-ErbB2 engagers, while addition of these molecules had no effect on the low basal activity of PBMCs against ErbB2-negative CEM.NKR cells (Figure 6A, middle).

The influence of the scNKAB-ErbB2 molecules on cytotoxicity of primary murine lymphocytes was investigated using splenocytes from three C57BL/6 mice as effectors. Thereby, all cells of the gated NK and most cells of the NKT-like subpopulations displayed high level expression of endogenous NKG2D, while in contrast to human $CD8^+$ T cells, only a small proportion of murine $CD8^+$ T cells were NKG2D-positive (see Supplementary Figure 5). BALB/c-derived A20 B-cell lymphoma cells included as a positive control were readily killed by the C57BL/6 splenocytes after 4 hours of co-incubation at an E/T ratio of 20:1, without the presence of scNKAB-ErbB2 or mNKAB-ErbB2 engagers further enhancing cytotoxicity (Figure 6B, left). While ErbB2-negative RMA/neo cells with around 40% of specific lysis proved more sensitive toward the murine splenocytes than expected, also in this case addition of the scNKAB-ErbB2 or mNKAB-ErbB2 molecules had no significant effect on cell killing (Figure 6B, middle). This was different for RMA/neo/ErbB2 cells, which were more potently killed by splenocytes in the presence of 0.64 nM of the four scNKAB-ErbB2 engagers and mNKAB-ErbB2, while the FRP5-Fc isotype control molecule had no effect (Figure 6B, right).

3.7 Targeted cytotoxicity of NKG2D-CAR engineered effectors mediated by scNKAB-ErbB2 engagers

To analyze the antitumoral activity of the scNKAB-ErbB2 molecules in combination with the NKG2D-CAR engineered effector cell lines hNKAR-NK-92 and mNKAR-NK-92, we employed human MDA-MB-453 breast cancer cells as targets which endogenously express different NKG2D ligands, but also high levels of ErbB2 (18). ErbB2-negative K562 erythroleukemia and MDA-MB-468 breast carcinoma cells were included as controls. After co-incubation for 3 hours at an E/T ratio of 5:1, NK-sensitive K562 cells were lysed effectively by hNKAR-NK-92 and mNKAR-NK-92 cells, which was not affected by the scNKAB-ErbB2 engagers, hNKAB-ErbB2 or mNKAB-ErbB2 (Figure 7A, top). While under the chosen conditions around 20% of ErbB2-positive MDA-MB-453 cells were already killed by hNKAR-NK-92 cells in the absence of NKAB antibodies, specific lysis was markedly enhanced to more than 50% by addition of 0.64 nM of each of the scNKAB-ErbB2 molecules (Figure 7A, middle). Also the prototypic hNKAB-ErbB2 molecule but not mNKAB-ErbB2 significantly increased cytotoxicity of NK-92 cells expressing the human NKG2D-CAR. In the case of mNKAR-NK-92 cells, the scNKAB-ErbB2 engagers were most potent in enhancing targeted cytotoxicity against MDA-MB-453 cells, with specific lysis even more pronounced than when combined with hNKAR-NK-92 cells. Likewise, mNKAB-ErbB2 significantly triggered the murine NKG2D-CAR against the ErbB2-positive target cells. Also moderate but statistically significant activity of hNKAB-ErbB2 was detected, which cannot engage the mNKAR, but the endogenous human NKG2D of mNKAR-NK-92 cells. In the case of MDA-MB-468 breast carcinoma cells which are negative for ErbB2, basal cytotoxic activity of hNKAR-NK-92 and mNKAR-NK-92 cells was not affected by any of the ErbB2-specific NKAB molecules (Figure 7A, bottom).

For hNKAB-ErbB2, concentrations between 0.16 and 0.64 nM were previously established as optimal to trigger effective cytotoxicity of NKG2D-positive primary lymphocytes and hNKAR-NK-92 cells. Concentrations lower than that were insufficient to fully activate the effector cells, and higher engager concentrations led to competition of productive interactions with the target receptors by free protein, both resulting in gradually reduced cytotoxicity (18). To test whether this is also the case for the newly developed scNKAB-ErbB2 molecules, in the next set of experiments hNKAR-NK-92 and mNKAR-NK-92 cells were co-incubated with ErbB2-positive MDA-MB-453 target cells at an E/T ratio of 2:1 in the presence of increasing concentrations of the different engagers, ranging from 0.006 to 16 nM (Figure 7B). Under these conditions, prototypic hNKAB-ErbB2 was most active at a concentration of 0.16 nM in reducing the number of viable target cells by hNKAR-NK-92, and triggered by endogenous human NKG2D, by mNKAR-NK-92 cells. The mNKAB-ErbB2 control protein had most pronounced activity in combination with mNKAR-NK-92 cells at concentrations of 0.16 and 0.64 nM, but confirming the results described above, was inactive in combination with hNKAR-NK-92 cells. The four scNKAB-ErbB2 engagers again

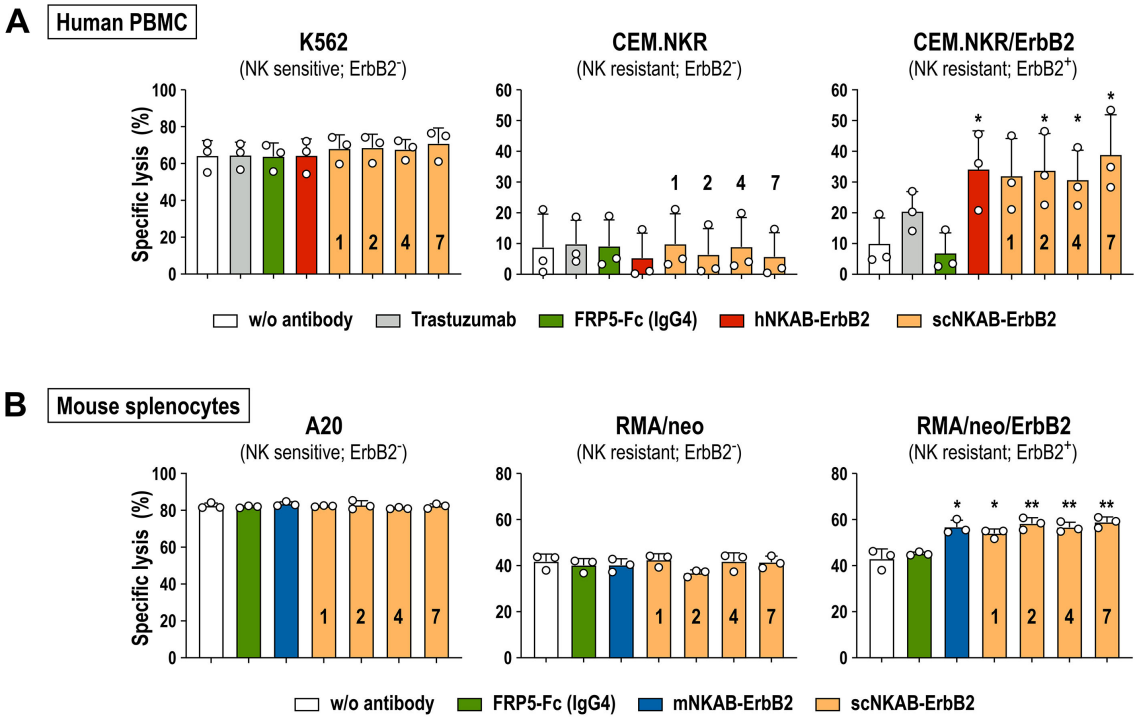

FIGURE 6
NKAB-mediated redirection of primary human and murine lymphocytes endogenously expressing NKG2D to ErbB2-expressing tumor cells. **(A)** Cytotoxicity of human PBMCs in the absence or presence of 0.64 nM of the indicated ErbB2-specific NKAB molecules against human K562 erythroleukemia, and CEM.NKR or CEM.NKR/ErbB2 T lymphoblastic cells was determined after 3 hours of co-incubation at an E/T ratio of 10:1. Samples kept in the absence of an antibody or incubated with 0.64 nM of trastuzumab or an ErbB2-specific scFv fusion protein containing a human IgG4 Fc domain (FRP5-Fc) were included as controls. **(B)** Cytotoxicity of murine splenocytes in the absence or presence of 0.64 nM of the indicated ErbB2-specific NKAB molecules against murine A20 B-cell lymphoma, and RMA/neo or RMA/neo/ErbB2 T lymphoblastic cells was determined after 4 hours of co-incubation at an E/T ratio of 20:1. Samples kept in the absence of an antibody or incubated with 0.64 nM of FRP5-Fc (IgG4) were included as controls. Mean values ± SD are shown; n=3 independent donors or animals. **, $p < 0.01$; *, $p < 0.05$. Statistical significance is indicated for differences in comparison to samples without antibody.

showed much more pronounced activity in combination with hNKAR-NK-92 and mNKAR-NK-92 cells than hNKAB-ErbB2 and mNKAB-ErbB2, with 0.16 and 0.64 nM identified as optimal antibody concentrations. Importantly, even under suboptimal conditions, the species cross-reactive molecules retained higher activity than hNKAB-ErbB2 and mNKAB-ErbB2 at their optimal concentrations, suggesting more stable and productive immunological synapse formation over a wide range of scNKAB-ErbB2 concentrations.

4 Discussion

The activating receptor NKG2D and its ligands represent an important system to sense cellular stress upon malignant transformation or infection by pathogens, and enable innate lymphocytes and subsets of T cells to selectively and efficiently eliminate the affected target cells (8, 9). Different approaches have been developed to employ this mechanism for cancer immunotherapy, which include boosting NKG2DL-induced activation of effector lymphocytes with NKG2D-based CARs, pharmacological enhancement of NKG2DL expression on cancer cells, preventing proteolytic ligand shedding, and designing BiKE molecules that redirect cytotoxic effectors to tumor cells independent from NKG2DL recognition (2, 7, 12, 47, 48). In our study, we generated four novel bispecific killer cell engagers that displayed cross-reactive binding to human and murine NKG2D receptors, and selectively and efficiently redirected NKG2D-positive primary human and murine lymphocytes as well as NK cells engineered with human or murine NKG2D-CARs to cancer cells expressing the clinically highly relevant tumor-associated antigen ErbB2 (HER2).

Formation of species cross-reactive NKG2D antibodies was induced by consecutive immunization of a chicken with recombinant human and murine NKG2D proteins, and the most effective binders were then selected by screening of a scFv antibody yeast surface display library using decreasing concentrations of the human and murine antigens (33–35, 40). Binding and degranulation experiments with recombinant scFv-Fc fusion proteins and NK-92 cells expressing NKG2D-CARs derived from human (hNKAR) or murine NKG2D (mNKAR) confirmed specificity of the selected antibody clones sc1, sc2, sc4 and sc7, and demonstrated their ability to activate both, human and murine NKG2D receptors (see Supplementary Figure 2). Following the validated design of an ErbB2-specific NKG2D engager that exclusively interacts with human NKG2D (here termed hNKAB-ErbB2) (18, 42), we generated four similar scNKAB-ErbB2

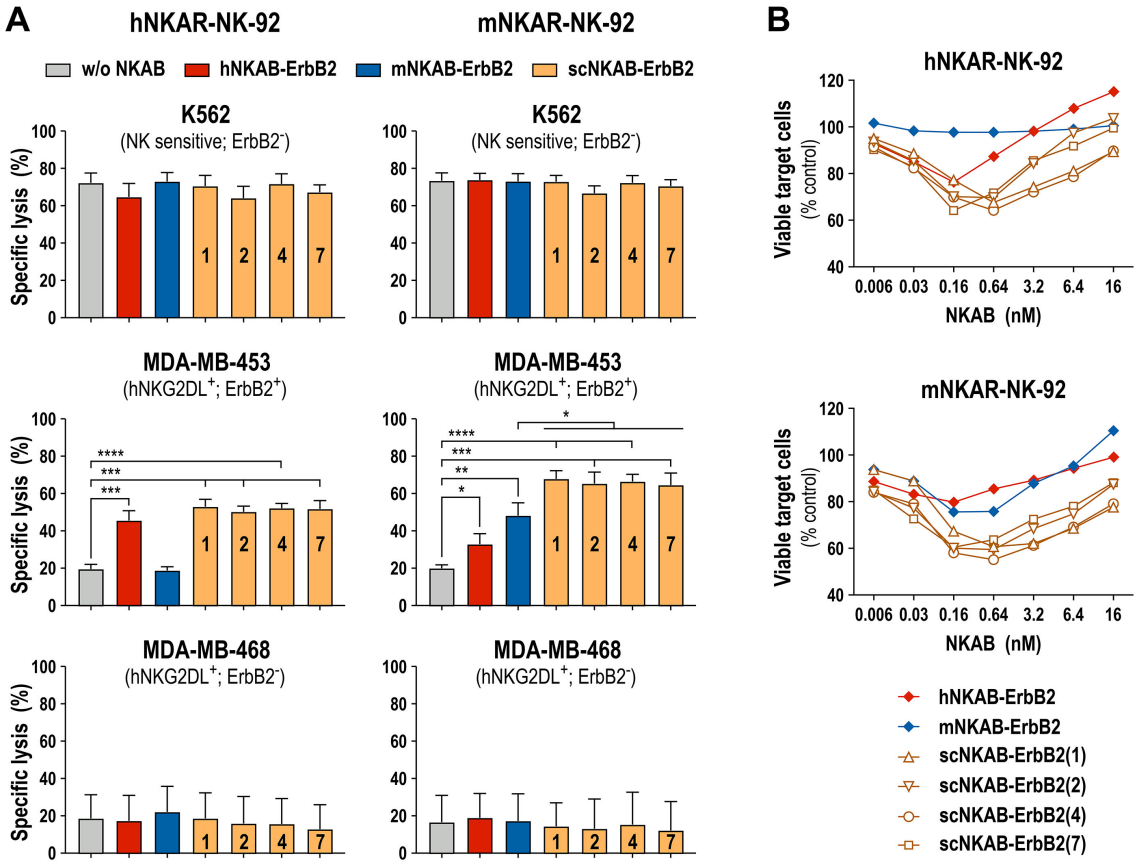

FIGURE 7
Redirection of NKG2D-CAR engineered NK-92 cells by ErbB2-targeted NKAB molecules. **(A)** NKAB-independent natural cytotoxicity of hNKAR-NK-92 (left panels) and mNKAR-NK-92 cells (right panels) against NK-sensitive K562 erythroleukemia cells (top) and NKAB-mediated killing of ErbB2-positive MDA-MB-453 breast carcinoma cells (middle) in the absence or presence of 0.64 nM of the indicated NKAB-ErbB2 molecules was determined after 3 hours of co-incubation at an E/T ratio of 5:1. ErbB2-negative MDA-MB-468 breast carcinoma cells (bottom) were included as control. Mean values ± SD are shown; n=3 independent experiments. ****, $p < 0.0001$; ***, $p < 0.001$; **, $p < 0.01$; *, $p < 0.05$. **(B)** Cytotoxic activity of hNKAR-NK-92 (top) or mNKAR-NK-92 cells (bottom) against MDA-MB-453 cells in the presence of increasing concentrations of the indicated NKAB-ErbB2 molecules was determined after 3 hours of co-incubation at an E/T ratio of 2:1. Data points represent mean values of the percentage of viable tumor cells normalized to values obtained after co-incubation of effector and target cells in the absence of NKAB antibodies. n=3 independent experiments.

molecules which all carry an N-terminal NKG2D-binding domain, connected by a human IgG Fc region to the ErbB2-binding domain at the C-terminus. While NKAB molecules based on the structure of ADCC-inducing IgG1 are functional (18), here we chose IgG4 to limit simultaneous interaction with CD16a and to clearly attribute the observed effects to NKG2D engagement (49). Facilitated by disulfide bridges within the IgG hinge region, the scNKAB-ErbB2 molecules were expressed as tetravalent homodimers, which readily interacted with hNKAR-NK-92 and mNKAR-NK-92 cells as well as ErbB2-expressing breast carcinoma cells. Thereby, all four scNKAB-ErbB2 molecules bound more effectively to the human NKG2D receptor than the prototypic hNKAB-ErbB2 molecule, with scNKAB-ErbB2(7) displaying the strongest interaction (see Supplementary Table 1).

In competition assays with an excess of soluble MICA, scNKAB-ErbB2(2) and scNKAB-ErbB2(7) proteins effectively prevented binding of the natural ligand to NKG2D, while scNKAB-ErbB2(1) and scNKAB-ErbB2(4) did not compete with sMICA. This is indicative of the epitopes of the latter being distinct from the ligand binding site. Although we only investigated blockade of MICA, this likely extends to other human NKG2DL, which share a similar binding surface on NKG2D (50, 51). Interestingly, when simultaneous interaction with NKG2D-expressing PBMC subpopulations and the ErbB2 target antigen was investigated by detecting bound NKAB molecules with recombinant ErbB2, prototypic hNKAB-ErbB2 as well as scNKAB-ErbB2(2) and scNKAB-ErbB2(7), which all compete with MICA, resulted in stronger signals. Likewise, scNKAB-ErbB2 (2) and scNKAB-ErbB2(7) displayed more pronounced bispecific binding to NKG2D-positive murine NK cells and recombinant ErbB2. Since this differential binding did not affect lymphocyte activation in cytotoxicity assays with tumor cells, it may reflect different accessibility of the ErbB2-specific scFv domain of NKG2D-bound NKAB molecules for soluble ErbB2 monomers, without obvious impact on the higher avidity interactions of the homodimeric NKAB molecules with naturally expressed ErbB2 that is anchored in the target cell membrane.

Proteolytic shedding of NKG2D ligands has been described as a mechanism of tumor cells to evade NKG2D-mediated immune surveillance, with the released soluble NKG2DL not only reducing

ligand density on the target cell surface, but also impairing immune responses by blockade and downregulation of NKG2D on cytolytic effector cells (13, 14). While non-competing BiKE molecules similar to scNKAB-ErbB2(1) and scNKAB-ErbB2(4) were shown to remain functional in the presence of NKG2D ligands (17), the same was demonstrated for MICA-competing prototypic hNKAB-ErbB2 (18). Enhanced by avidity effects of the bivalent NKG2D binder, hNKAB-ErbB2 prevented occupation of NKG2D by soluble MICA even at high concentrations, and restored NKG2D-dependent effector cell activity (18). This could also be expected for the NKG2DL-competing molecules scNKAB-ErbB2(2) and scNKAB-ErbB2(7). Indeed, despite quantitative differences in their binding to NKG2D (see Supplementary Table 1), ligand-competing and non-competing scNKAB-ErbB2 molecules were equally effective in redirecting primary lymphocytes and NKG2D-CAR expressing NK cells to ErbB2-positive tumor targets.

With a structure and molecular mass similar to an intact IgG antibody, Fc-containing scNKAB-ErbB2 molecules are expected to have a longer serum half-life than small tandem scFv-scFv fusions like blinatumomab, which requires continuous infusion in patients to achieve relevant concentrations in the blood (52). Furthermore, bivalent binding of the homodimeric NKAB proteins to both of their targets, ErbB2 and NKG2D, is likely important for formation of a more stable immunological synapse and effective tumor cell killing, as indicated by data from our previous study with prototypic hNKAB-ErbB2. When dimer formation of hNKAB-ErbB2 was prevented by removal of disulfide bridges within the antibody hinge region, the resulting monomer was less efficient in triggering activation of NKG2D-CAR expressing NK cells against ErbB2-positive cancer cells (18). Likewise, in the case of nanobody-based bispecific NKG2DxErbB2 antibodies, bivalent binders displayed a 20- to 60-fold increase in affinity when compared to their monovalent counterparts (17). When tested at a fixed protein concentration of 0.64 nM in combination with primary human and murine lymphocytes as effectors, the species cross-reactive scNKAB-ErbB2 molecules showed similar antitumoral activity as hNKAB-ErbB2 and mNKAB-ErbB2, respectively. Nevertheless, more detailed analysis with hNKAR-NK-92 and mNKAR-NK-92 cells carrying CARs based on human and murine NKG2D, despite a similar optimum at 0.16 to 0.64 nM, revealed marked scNKAB-ErbB2 activity over a broader concentration range than hNKAB-ErbB2 and mNKAB-ErbB2. In particular scNKAB-ErbB2(1) and scNKAB-ErbB2(4) showed less pronounced reduction of effector cell activity at higher NKAB concentrations due to competition with free protein, suggesting more stable cell-cell contacts mediated by these molecules.

To the best of our knowledge, this is the first report on bispecific killer cell engagers that recruit both, human and murine lymphocytes. We devised a strategy for immunization and screening, which despite differences in the amino acid sequences of the human and murine antigens, facilitated the generation of species cross-reactive NKG2D binders. Similar to studies with antibodies that target immune checkpoint molecules like PD-1, CTLA-4 and TIGIT (53–55), this could aid further preclinical development of the bispecific killer cell engagers by allowing testing in immunocompetent mouse tumor models. Thereby, investigating their interaction with endogenous immune cells *in vivo* as done here with isolated murine splenocytes *ex vivo*, and evaluating potential adverse effects may provide insights not possible in more artificial tumor xenograft models in immunodeficient mice. The ErbB2-specific FRP5 antibody domain used in our study does not react with the murine ErbB2 homolog (56). Nevertheless, the high degree of sequence identity between the human and murine antigens still allows the evaluation of ErbB2-targeted immunotherapies with murine tumor cells modified to express human ErbB2 in immunocompetent BALB/c and C57BL/6 mouse models (18, 57). Our data demonstrate enhanced functionality of the newly generated scNKAB-ErbB2 engagers compared to the previously described species-restricted hNKAB-ErbB2 molecule. Thereby, the bispecific scNKAB antibodies proved effective in specifically redirecting the cytotoxic activity of primary lymphocytes as well as NKG2D-CAR engineered NK cells to ErbB2-positive cancer targets. Due to their modular design, these molecules could easily be adapted to interact with CD16a in addition to NKG2D and to target other tumor-associated surface antigens by exchanging their respective Fc and scFv domains (18, 20). At present, the generated NKG2D-binding moieties are still of avian origin. Hence, an important next step for further development will be the humanization of their sequences following established procedures (58).

Data availability statement

The original contributions presented in the study are included in the article/Supplementary Material. Further inquiries can be directed to the corresponding authors.

Ethics statement

Ethical approval was not required for the studies on humans in accordance with the local legislation and institutional requirements because only commercially available materials and established cell lines were used. Ethical approval was not required for the studies on animals in accordance with the local legislation and institutional requirements because only isolated tissues and established cell lines were used.

Author contributions

JP: Conceptualization, Formal analysis, Investigation, Methodology, Visualization, Writing – original draft, Writing – review & editing. KS: Conceptualization, Formal analysis, Investigation, Methodology, Visualization, Writing – original draft, Writing – review & editing. IK: Formal analysis, Investigation, Methodology, Writing – review & editing. JH: Formal analysis, Investigation, Methodology, Writing – review & editing. AM: Investigation, Methodology, Writing – review & editing.

MP: Investigation, Methodology, Writing – review & editing. MK: Investigation, Methodology, Writing – review & editing. PO: Investigation, Methodology, Writing – review & editing. HK: Conceptualization, Project administration, Supervision, Writing – review & editing. WW: Conceptualization, Formal analysis, Project administration, Supervision, Visualization, Writing – original draft, Writing – review & editing.

Funding

The author(s) declare financial support was received for the research, authorship, and/or publication of this article. This work was supported in part by grants from Deutsche Forschungsgemeinschaft (DFG) (WE 2589/6-1), LOEWE Center Frankfurt Cancer Institute (FCI) (HMWK III L 5-519/03/03.001-0015), and institutional funds of Georg-Speyer-Haus. Georg-Speyer-Haus is funded jointly by the German Federal Ministry of Health and the Hessian Ministry of Higher Education, Research, Science and the Arts.

Acknowledgments

We thank Annette Trzmiel and Stefan Stein for flow cytometric cell sorting, and Barbara Uherek and Thorsten Geyer for excellent technical assistance.

Conflict of interest

KS, JH, AM, PO, HK and WW are named as inventors on patents and patent applications in the field of cancer immunotherapy owned by their respective academic institutions.

The remaining authors declare that the research was conducted in the absence of any commercial or financial relationships that could be construed as a potential conflict of interest.

Publisher's note

Supplementary material

The Supplementary Material for this article can be found online at: https://www.frontiersin.org/articles/10.3389/fimmu.2024.1457887/full#supplementary-material

References

1. Goebeler ME, Bargou RC. T cell-engaging therapies - BiTEs and beyond. *Nat Rev Clin Oncol*. (2020) 17:418–34. doi: 10.1038/s41571-020-0347-5

2. Peipp M, Klausz K, Boje AS, Zeller T, Zielonka S, Kellner C. Immunotherapeutic targeting of activating natural killer cell receptors and their ligands in cancer. *Clin Exp Immunol*. (2022) 209:22–32. doi: 10.1093/cei/uxac028

3. Klein C, Brinkmann U, Reichert JM, Kontermann RE. The present and future of bispecific antibodies for cancer therapy. *Nat Rev Drug Discovery*. (2024) 23:301–19. doi: 10.1038/s41573-024-00896-6

4. Fenis A, Demaria O, Gauthier L, Vivier E, Narni-Mancinelli E. New immune cell engagers for cancer immunotherapy. *Nat Rev Immunol*. (2024) 7:471–86. doi: 10.1038/s41577-023-00982-7

5. Rolin C, Zimmer J, Seguin-Devaux C. Bridging the gap with multispecific immune cell engagers in cancer and infectious diseases. *Cell Mol Immunol*. (2024) 21:643–61. doi: 10.1038/s41423-024-01176-4

6. Gauthier L, Virone-Oddos A, Beninga J, Rossi B, Nicolazzi C, Amara C, et al. Control of acute myeloid leukemia by a trifunctional NKp46-CD16a-NK cell engager targeting CD123. *Nat Biotechnol*. (2023) 41:1296–306. doi: 10.1038/s41587-022-01626-2

7. Lazarova M, Wels WS, Steinle A. Arming cytotoxic lymphocytes for cancer immunotherapy by means of the NKG2D/NKG2D-ligand system. *Expert Opin Biol Ther*. (2020) 20:1491–501. doi: 10.1080/14712598.2020.1803273

8. Stojanovic A, Correia MP, Cerwenka A. The NKG2D/NKG2DL axis in the crosstalk between lymphoid and myeloid cells in health and disease. *Front Immunol*. (2018) 9:827. doi: 10.3389/fimmu.2018.00827

9. Wensveen FM, Jelenčić V, Polić B. NKG2D: A master regulator of immune cell responsiveness. *Front Immunol*. (2018) 9:441. doi: 10.3389/fimmu.2018.00441

10. Cerwenka A, Lanier LL. NKG2D ligands: unconventional MHC class I-like molecules exploited by viruses and cancer. *Tissue Antigens*. (2003) 61:335–43. doi: 10.1034/j.1399-0039.2003.00070.x

11. Raulet DH, Gasser S, Gowen BG, Deng W, Jung H. Regulation of ligands for the NKG2D activating receptor. *Annu Rev Immunol*. (2013) 31:413–41. doi: 10.1146/annurev-immunol-032712-095951

12. Paczulla AM, Rothfelder K, Raffel S, Konantz M, Steinbacher J, Wang H, et al. Absence of NKG2D ligands defines leukaemia stem cells and mediates their immune evasion. *Nature*. (2019) 572:254–9. doi: 10.1038/s41586-019-1410-1

13. Salih HR, Rammensee HG, Steinle A. Cutting edge: down-regulation of MICA on human tumors by proteolytic shedding. *J Immunol*. (2002) 169:4098–102. doi: 10.4049/jimmunol.169.8.4098

14. Groh V, Wu J, Yee C, Spies T. Tumour-derived soluble MIC ligands impair expression of NKG2D and T-cell activation. *Nature*. (2002) 419:734–8. doi: 10.1038/nature01112

15. Song H, Kim J, Cosman D, Choi I. Soluble ULBP suppresses natural killer cell activity via down-regulating NKG2D expression. *Cell Immunol*. (2006) 239:22–30. doi: 10.1016/j.cellimm.2006.03.002

16. Chan WK, Kang S, Youssef Y, Glankler EN, Barrett ER, Carter AM, et al. A CS1-NKG2D bispecific antibody collectively activates cytolytic immune cells against multiple myeloma. *Cancer Immunol Res*. (2018) 6:776–87. doi: 10.1158/2326-6066.CIR-17-0649

17. Raynaud A, Desrumeaux K, Vidard L, Termine E, Baty D, Chames P, et al. Anti-NKG2D single domain-based antibodies for the modulation of anti-tumor immune response. *Oncoimmunology*. (2020) 10:1854529. doi: 10.1080/2162402X.2020.1854529

18. Zhang C, Röder J, Scherer A, Bodden M, Pfeifer Serrahima J, Bhatti A, et al. Bispecific antibody-mediated redirection of NKG2D-CAR natural killer cells facilitates dual targeting and enhances antitumor activity. *J Immunother Cancer*. (2021) 9:e002980. doi: 10.1136/jitc-2021-002980

19. Lutz S, Klausz K, Albici AM, Ebinger L, Sellmer L, Teipel H, et al. Novel NKG2D-directed bispecific antibodies enhance antibody-mediated killing of Malignant B cells by NK cells and T cells. *Front Immunol*. (2023) 14:1227572. doi: 10.3389/fimmu.2023.1227572

20. Kiefer A, Prüfer M, Röder J, Pfeifer Serrahima J, Bodden M, Kühnel I, et al. Dual targeting of glioblastoma cells with bispecific killer cell engagers directed to EGFR and ErbB2 (HER2) facilitates effective elimination by NKG2D-CAR-engineered NK cells. *Cells*. (2024) 13:246. doi: 10.3390/cells13030246

21. von Strandmann EP, Hansen HP, Reiners KS, Schnell R, Borchmann P, Merkert S, et al. A novel bispecific protein (ULBP2-BB4) targeting the NKG2D receptor on natural killer (NK) cells and CD138 activates NK cells and has potent antitumor activity against human multiple myeloma *in vitro* and *in vivo*. *Blood*. (2006) 107:1955–62. doi: 10.1182/blood-2005-05-2177

22. Rothe A, Jachimowicz RD, Borchmann S, Madlener M, Keßler J, Reiners KS, et al. The bispecific immunoligand ULBP2-aCEA redirects natural killer cells to tumor

cells and reveals potent anti-tumor activity against colon carcinoma. *Int J Cancer*. (2014) 134:2829–40. doi: 10.1002/ijc.28609

23. Kellner C, Günther A, Humpe A, Repp R, Klausz K, Derer S, et al. Enhancing natural killer cell-mediated lysis of lymphoma cells by combining therapeutic antibodies with CD20-specific immunoligands engaging NKG2D or NKp30. *Oncoimmunology*. (2016) 5:e1058459. doi: 10.1080/2162402X.2015.1058459

24. Pan M, Wang F, Nan L, Yang S, Qi J, Xie J, et al. αVEGFR2-MICA fusion antibodies enhance immunotherapy effect and synergize with PD-1 blockade. *Cancer Immunol Immunother*. (2023) 72:969–84. doi: 10.1007/s00262-022-03306-1

25. Miller JS, Lanier LL. Natural killer cells in cancer immunotherapy. *Annu Rev Cancer Biol*. (2019) 3:77–103. doi: 10.1146/annurev-cancerbio-030518-055653

26. Maskalenko NA, Zhigarev D, Campbell KS. Harnessing natural killer cells for cancer immunotherapy: dispatching the first responders. *Nat Rev Drug Discovery*. (2022) 21:559–77. doi: 10.1038/s41573-022-00413-7

27. Arai S, Meagher R, Swearingen M, Myint H, Rich E, Martinson J, et al. Infusion of the allogeneic cell line NK-92 in patients with advanced renal cell cancer or melanoma: a phase I trial. *Cytotherapy*. (2008) 10:625–32. doi: 10.1080/14653240802301872

28. Tonn T, Schwabe D, Klingemann HG, Becker S, Esser R, Koehl U, et al. Treatment of patients with advanced cancer with the natural killer cell line NK-92. *Cytotherapy*. (2013) 15:1563–70. doi: 10.1016/j.jcyt.2013.06.017

29. Tang X, Yang L, Li Z, Nalin AP, Dai H, Xu T, et al. First-in-man clinical trial of CAR NK-92 cells: safety test of CD33-CAR NK-92 cells in patients with relapsed and refractory acute myeloid leukemia. *Am J Cancer Res*. (2018) 8:1083–9.

30. Burger MC, Forster MT, Romanski A, Straßheimer F, Macas J, Zeiner PS, et al. Intracranial injection of natural killer cells engineered with a HER2-targeted chimeric antigen receptor in patients with recurrent glioblastoma. *Neuro Oncol*. (2023) 25:2058–71. doi: 10.1093/neuonc/noad087

31. Kerbauy LN, Marin ND, Kaplan M, Banerjee PP, Berrien-Elliott MM, Becker-Hapak M, et al. Combining AFM13, a bispecific CD30/CD16 antibody, with cytokine-activated blood and cord blood-derived NK cells facilitates CAR-like responses against CD30(+) Malignancies. *Clin Cancer Res*. (2021) 27:3744–56. doi: 10.1158/1078-0432.CCR-21-0164

32. Gong JH, Maki G, Klingemann HG. Characterization of a human cell line (NK-92) with phenotypical and functional characteristics of activated natural killer cells. *Leukemia*. (1994) 8:652–8.

33. Grzeschik J, Yanakieva D, Roth L, Krah S, Hinz SC, Elter A, et al. Yeast surface display in combination with fluorescence-activated cell sorting enables the rapid isolation of antibody fragments derived from immunized chickens. *Biotechnol J*. (2019) 14:e1800466. doi: 10.1002/biot.201800466

34. Bogen JP, Grzeschik J, Krah S, Zielonka S, Kolmar H. Rapid generation of chicken immune libraries for yeast surface display. *Methods Mol Biol*. (2020) 2070:289–302. doi: 10.1007/978-1-4939-9853-1_16

35. Schoenfeld K, Harwardt J, Habermann J, Elter A, Kolmar H. Conditional activation of an anti-IgM antibody-drug conjugate for precise B cell lymphoma targeting. *Front Immunol*. (2023) 14:1258700. doi: 10.3389/fimmu.2023.1258700

36. Benatuil L, Perez JM, Belk J, Hsieh CM. An improved yeast transformation method for the generation of very large human antibody libraries. *Protein Eng Des Sel*. (2010) 23:155–9. doi: 10.1093/protein/gzq002

37. Wels W, Harwerth IM, Zwickl M, Hardman N, Groner B, Hynes NE. Construction, bacterial expression and characterization of a bifunctional single-chain antibody-phosphatase fusion protein targeted to the human erbB-2 receptor. *Biotechnol (N Y)*. (1992) 10:1128–32. doi: 10.1038/nbt1092-1128

38. Oberoi P, Kamenjarin K, Ossa JFV, Uherek B, Bönig H, Wels WS. Directed differentiation of mobilized hematopoietic stem and progenitor cells into functional NK cells with enhanced antitumor activity. *Cells*. (2020) 9:811. doi: 10.3390/cells9040811

39. Schönfeld K, Sahm C, Zhang C, Naundorf S, Brendel C, Odendahl M, et al. Selective inhibition of tumor growth by clonal NK cells expressing an ErbB2/HER2-specific chimeric antigen receptor. *Mol Ther*. (2015) 23:330–8. doi: 10.1038/mt.2014.219

40. Hinz SC, Elter A, Rammo O, Schwämmle A, Ali A, Zielonka S, et al. A generic procedure for the isolation of pH- and magnesium-responsive chicken scFvs for downstream purification of human antibodies. *Front Bioeng Biotechnol*. (2020) 8:688. doi: 10.3389/fbioe.2020.00688

41. Oh DY, Bang YJ. HER2-targeted therapies - a role beyond breast cancer. *Nat Rev Clin Oncol*. (2020) 17:33–48. doi: 10.1038/s41571-019-0268-3

42. Kwong KY, Baskar S, Zhang H, Mackall CL, Rader C. Generation, affinity maturation, and characterization of a human anti-human NKG2D monoclonal antibody with dual antagonistic and agonistic activity. *J Mol Biol*. (2008) 384:1143–56. doi: 10.1016/j.jmb.2008.09.008

43. Gupta R, Brunak S. Prediction of glycosylation across the human proteome and the correlation to protein function. *Pac Symp Biocomput*. (2002) 7:310–22.

44. Howell DN, Andreotti PE, Dawson JR, Cresswell P. Natural killing target antigens as inducers of interferon: studies with an immunoselected, natural killing-resistant human T lymphoblastoid cell line. *J Immunol*. (1985) 134:971–6. doi: 10.4049/jimmunol.134.2.971

45. Kärre K, Ljunggren HG, Piontek G, Kiessling R. Selective rejection of H-2-deficient lymphoma variants suggests alternative immune defence strategy. *Nature*. (1986) 319:675–8. doi: 10.1038/319675a0

46. Pfeifer Serrahima J, Zhang C, Oberoi P, Bodden M, Röder J, Arndt C, et al. Multivalent adaptor proteins specifically target NK cells carrying a universal chimeric antigen receptor to ErbB2 (HER2)-expressing cancers. *Cancer Immunol Immunother*. (2023) 72:2905–18. doi: 10.1007/s00262-023-03374-x

47. Curio S, Jonsson G, Marinović S. A summary of current NKG2D-based CAR clinical trials. *Immunother Adv*. (2021) 1:ltab018. doi: 10.1093/immadv/ltab018

48. Ferrari de Andrade L, Tay RE, Pan D, Luoma AM, Ito Y, Badrinath S, et al. Antibody-mediated inhibition of MICA and MICB shedding promotes NK cell-driven tumor immunity. *Science*. (2018) 359:1537–42. doi: 10.1126/science.aao0505

49. Bruhns P, Iannascoli B, England P, Mancardi DA, Fernandez N, Jorieux S, et al. Specificity and affinity of human Fcgamma receptors and their polymorphic variants for human IgG subclasses. *Blood*. (2009) 113:3716–25. doi: 10.1182/blood-2008-09-179754

50. Radaev S, Kattah M, Zou Z, Colonna M, Sun PD. Making sense of the diverse ligand recognition by NKG2D. *J Immunol*. (2002) 169:6279–85. doi: 10.4049/jimmunol.169.11.6279

51. Fan J, Shi J, Zhang Y, Liu J, An C, Zhu H, et al. NKG2D discriminates diverse ligands through selectively mechano-regulated ligand conformational changes. *EMBO J*. (2022) 41:e107739. doi: 10.15252/embj.2021107739

52. Mocquot P, Mossazadeh Y, Lapierre L, Pineau F, Despas F. The pharmacology of blinatumomab: state of the art on pharmacodynamics, pharmacokinetics, adverse drug reactions and evaluation in clinical trials. *J Clin Pharm Ther*. (2022) 47:1337–51. doi: 10.1111/jcpt.13741

53. Gjetting T, Gad M, Fröhlich C, Lindsted T, Melander MC, Bhatia VK, et al. Sym021, a promising anti-PD1 clinical candidate antibody derived from a new chicken antibody discovery platform. *MAbs*. (2019) 11:666–80. doi: 10.1080/19420862.2019.1596514

54. Li D, Li J, Chu H, Wang Z. A functional antibody cross-reactive to both human and murine cytotoxic T-lymphocyte-associated protein 4 via binding to an N-glycosylation epitope. *MAbs*. (2020) 12:1725365. doi: 10.1080/19420862.2020.1725365

55. Yang F, Zhao L, Wei Z, Yang Y, Liu J, Li Y, et al. A cross-species reactive TIGIT-blocking antibody Fc dependently confers potent antitumor effects. *J Immunol*. (2020) 205:2156–68. doi: 10.4049/jimmunol.1901413

56. Harwerth IM, Wels W, Marte BM, Hynes NE. Monoclonal antibodies against the extracellular domain of the erbB-2 receptor function as partial ligand agonists. *J Biol Chem*. (1992) 267:15160–7. doi: 10.1016/S0021-9258(18)42160-6

57. Rohrbach F, Weth R, Kursar M, Sloots A, Mittrücker HW, Wels WS. Targeted delivery of the ErbB2/HER2 tumor antigen to professional APCs results in effective antitumor immunity. *J Immunol*. (2005) 174:5481–9. doi: 10.4049/jimmunol.174.9.5481

58. Bogen JP, Elter A, Grzeschik J, Hock B, Kolmar H. Humanization of chicken-derived antibodies by yeast surface display. *Methods Mol Biol*. (2022) 2491:335–60. doi: 10.1007/978-1-0716-2285-8_18

Supplementary Material

Bispecific killer cell engagers employing species cross-reactive NKG2D binders redirect human and murine lymphocytes to ErbB2/HER2-positive malignancies

Jordi Pfeifer Serrahima, Katrin Schoenfeld, Ines Kühnel, Julia Harwardt, Arturo Macarrón Palacios, Maren Prüfer, Margareta Kolaric, Pranav Oberoi, Harald Kolmar, Winfried S. Wels

1 Supplementary Table

Supplementary Table 1. Binding of NKAB antibodies to NK and tumor cells

Sample	hNKAR-NK-92	mNKAR-NK-92	MDA-MB-453	MDA-MB-468
anti-human IgG	58.5[a)]	84	10.9	10.3
hNKAB-ErbB2	559	99.1	4660	18.5
scNKAB-ErbB2(1)	972	187	3902	10.9
scNKAB-ErbB2(2)	849	290	3985	10.3
scNKAB-ErbB2(4)	962	250	4198	10.9
scNKAB-ErbB2(7)	1291	385	3933	10.9
anti-mouse IgG	10.3	14.5	10.9	10.9
mNKAB-ErbB2	10.3	522	3933	10.3

Binding of bispecific scNKAB-ErbB2 molecules and the indicated control proteins at a concentration of 12.5 nM to NKG2D-CAR expressing hNKAR-NK-92 and mNKAR-NK-92 cells, and ErbB2-positive MDA-MB-453 and ErbB2-negative MDA-MB-468 breast carcinoma cells was analyzed by flow cytometry. [a)]Data are indicated as median fluorescence intensity (MFI). Respective histograms are shown in Figure 3C.

2 Supplementary Figures

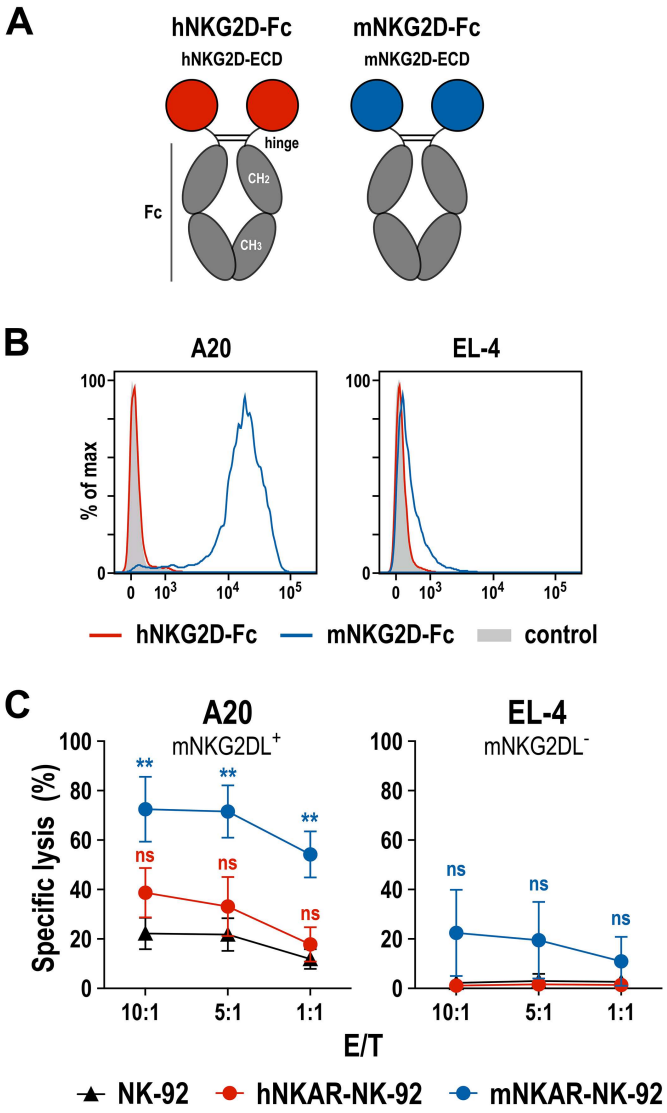

Supplementary Figure 1. Intrinsic activity of mNKAR-NK-92 cells against NKG2DL-positive tumor targets. (**A**) Schematic representation of recombinant hNKG2D-Fc and mNKG2D-Fc proteins, consisting of the extracellular domain of human (red) or murine (blue) NKG2D at the N-terminus, fused to hinge, CH2 and CH3 domains of human IgG4 (Fc). (**B**) Detection of NKG2DL expression on the surface of murine A20 B-cell lymphoma and EL-4 T-cell lymphoma cells by flow cytometry with purified hNKG2D-Fc (red) and mNKG2D-Fc (blue) proteins followed by APC-conjugated anti-human IgG antibody. Cells stained only with secondary antibody (gray areas) served as control. (**C**) Cytolytic activity of mNKAR-NK-92 (blue), hNKAR-NK-92 (red) and parental NK-92 cells (black) against murine A20 and EL-4 cells was determined after 3 hours of co-incubation at the indicated effector to target (E/T) ratios. Mean values ± SD are shown; n=3 independent experiments. **, $p < 0.01$; ns, $p > 0.05$ (not significant). Statistical significance is indicated for differences in comparison to parental NK-92 cells.

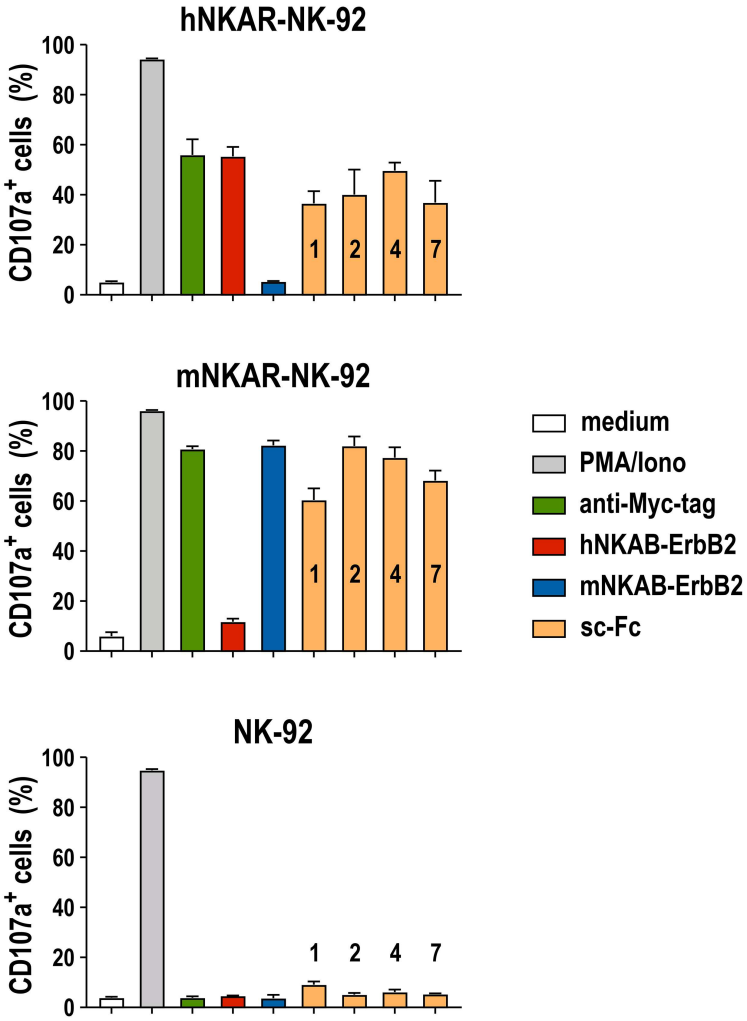

Supplementary Figure 2. Degranulation of NKG2D-CAR expressing NK-92 cells upon activation by species cross-reactive NKG2D binders. hNKAR-NK-92 (top) and mNKAR-NK-92 cells (middle) were stimulated for 4 hours with immobilized scFv-Fc fusion proteins derived from selected yeast display library clones sc1, sc2, sc4 and sc7. Control samples were stimulated with PMA and ionomycin, Myc-tag-specific antibody triggering the NKG2D-CARs in the absence of NKG2D binders, bispecific antibodies solely interacting with human (hNKAB-ErbB2) or murine NKG2D (mNKAB-ErbB2), or were kept in the absence of a stimulator (medium). Parental NK-92 cells were included for comparison (bottom). Mean values ± SD are shown; n=3 independent experiments.

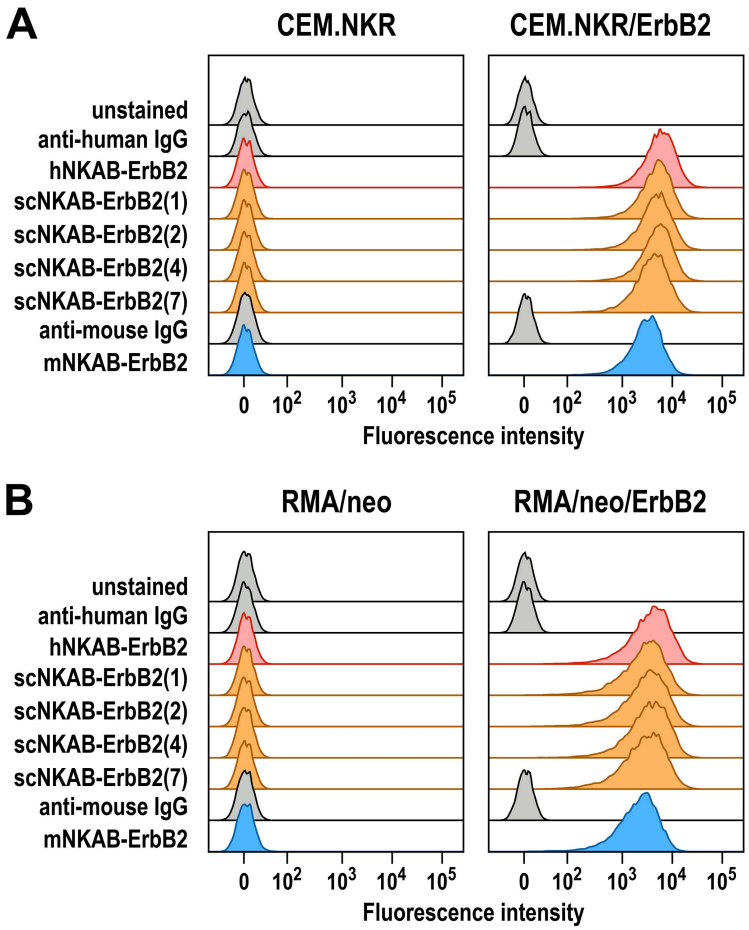

Supplementary Figure 3. Binding of NKAB molecules to ErbB2-expressing human and murine tumor cells. Binding of purified scNKAB-ErbB2, hNKAB-ErbB2 and mNKAB-ErbB2 proteins to human CEM.NKR/ErbB2 (**A**) and murine RMA/neo/ErbB2 T lymphoblastoid cells (**B**) generated by transduction with an ErbB2-encoding lentiviral vector was investigated by flow cytometry as indicated (right panels). Unstained cells and cells only incubated with secondary antibody served as controls. ErbB2-negative parental cells are included for comparison (left panels).

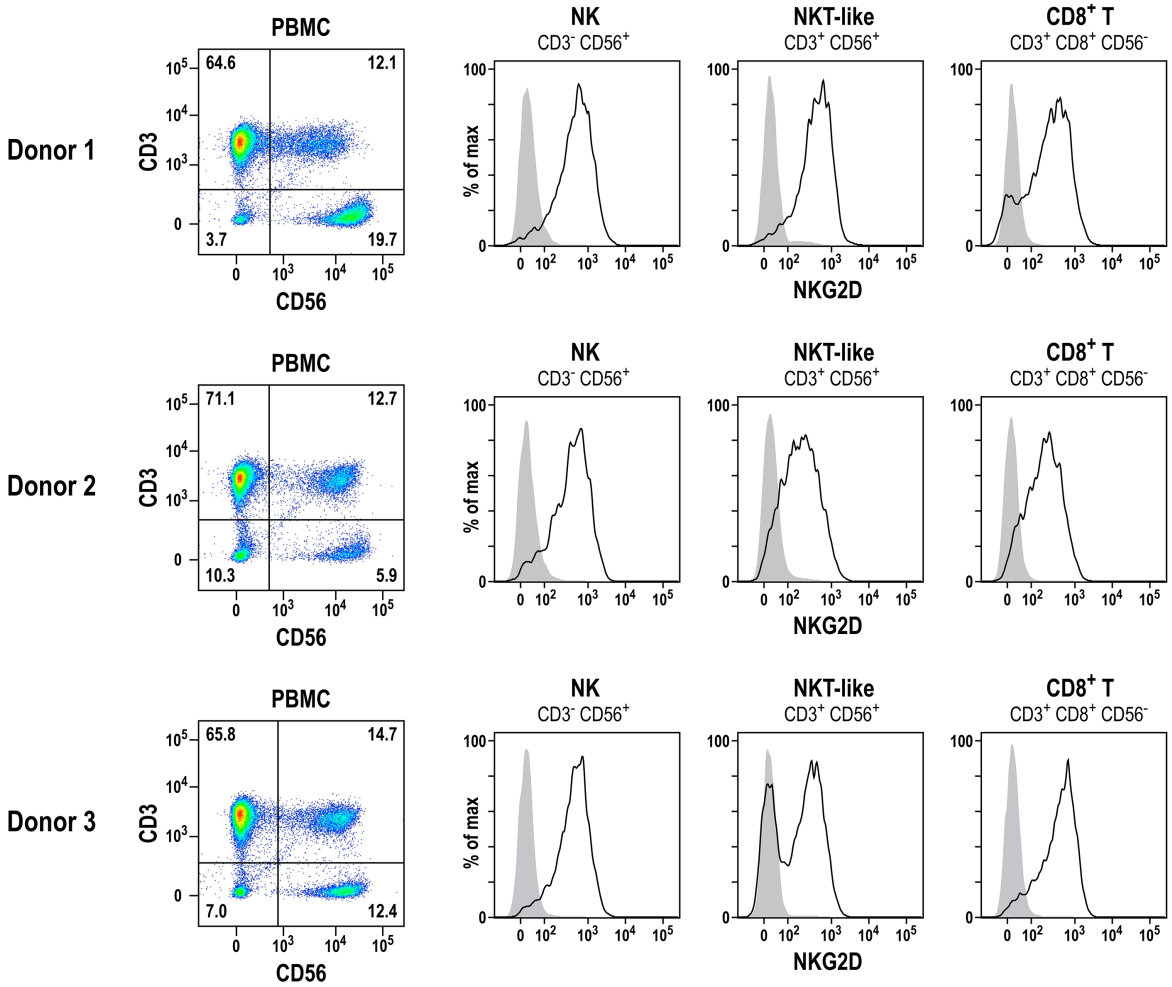

Supplementary Figure 4. Phenotypic characterization of human PBMCs used for the cell killing experiments shown in Figure 7A. PBMCs from three healthy donors were analyzed by multi-color flow cytometry to identify relative proportions of NK ($CD3^-$ $CD56^+$), NKT-like ($CD3^+$ $CD56^+$) and T cells ($CD3^+$ $CD56^-$), and NKG2D surface expression by gated NK, NKT-like and $CD8^+$ T cell subpopulations as indicated. Cells stained with the panel antibodies in the absence of anti-NKG2D served as control (gray areas).

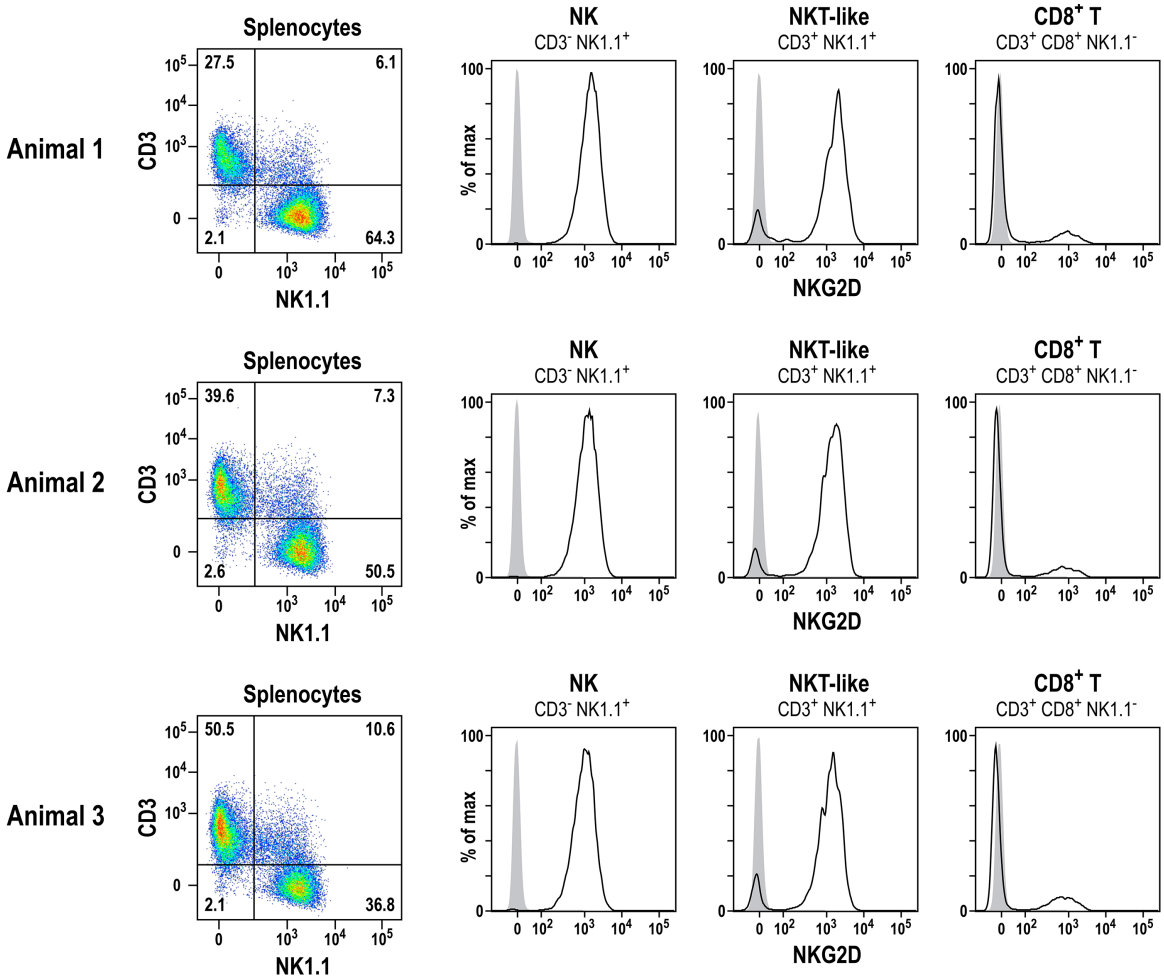

Supplementary Figure 5. Phenotypic characterization of murine splenocytes used for the cell killing experiments shown in Figure 7B. Splenocytes from three individual C57BL/6 mice were analyzed by multi-color flow cytometry to identify relative proportions of NK ($CD3^-$ $NK1.1^+$), NKT-like ($CD3^+$ $NK1.1^+$) and T cells ($CD3^+$ $NK1.1^-$), and NKG2D surface expression by gated NK, NKT-like and $CD8^+$ T cell subpopulations as indicated. Cells stained with the panel antibodies in the absence of anti-NKG2D served as control (gray areas).

5 Danksagung

An dieser Stelle möchte ich mich bei allen Personen, die mich während der Zeit meiner Promotion begleitet und unterstützt haben, herzlich bedanken!

In erster Linie möchte ich meinem Doktorvater **Prof. Dr. Harald Kolmar** danken. Danke für die Möglichkeit im Arbeitskreis Kolmar zu promovieren, die uneingeschränkte Unterstützung und das stets entgegengebrachte Vertrauen. Außerdem möchte ich mich für die produktiven Jahre bedanken, in denen ich die Möglichkeit hatte viele Dinge auszuprobieren und zu lernen. Das hat mir sowohl während meiner Promotion als auch im Hinblick auf meine Zukunft sehr geholfen!

Mein weiterer Dank gilt **PD Dr. Björn Hock**, für die Übernahme der Rolle des ersten Fachprüfers in meiner Disputationsprüfung und die Aufgaben und Hilfestellungen auch außerhalb des Unilabors, im Bereich der Lehre, als auch der biopharmazeutischen Industrie.

Prof. Dr. Evelyn Ullrich danke ich vielmals für die Übernahme des Korreferats, sowie für die produktive Zusammenarbeit in Kooperationsprojekten mit der Arbeitsgruppe Ullrich am Uniklinikum in Frankfurt.

Prof. Dr. Beatrix Süß danke ich für die freundliche Übernahme der zweiten Fachprüfung und die Möglichkeit meine erste wissenschaftliche Erfahrung im Rahmen der Bachelorarbeit in der Arbeitsgruppe Süß zu sammeln.

Bei **Julia Harwardt** und **Carolin Dombrowsky** möchte ich mich dafür bedanken, dass Ihr vom ersten Tag des Studiums bis zum Ende der Promotion als Laborpartnerinnen, Kolleginnen und Freundinnen an meiner Seite wart. Das gleiche Schicksal teilend, haben wir uns immer wieder gegenseitig motiviert und inspiriert. Ich danke Euch für unzählige Momente als *Triplikat* bei gemeinsamen Mittags- und Kaffeepausen, Krisensitzungen, Feiern und Konferenzen. Danke, dass Ihr dieses Kapitel unvergesslich gemacht habt!

Darüber hinaus danke ich **Dr. Sebastian Bitsch** und **Peter Bitsch**. Mit Euch wurde der Laboralltag nie langweilig, ob mit großartigen Liedern, Tischkickerspielen oder einfach eurer positiven Art, Ihr habt immer für Abwechslung und gute Laune gesorgt. Danke, nicht nur dafür, sondern auch für Eure Ratschläge und Hilfsbereitschaft.

Der *next generation*, **Felix Geyer**, **Felix Meiser** und **Adrian Bloch,** danke ich für die angenehme Zusammenarbeit und die Wiedereinführung des Feierabendbiers und der Grillevents. Ich wünsche Euch viel Erfolg für die restliche Promotion!

Außerdem bedanke ich mich bei **Dr. Arturo Macarrón Palacios** für die Unterstützung seit Beginn meiner Masterarbeit. Dank Deinem Zuspruch und Vertrauen habe ich schnell gelernt selbstständig an Projekten zu arbeiten und diese weiterzuentwickeln.

Ebenso möchte ich mich bei **Philipp Wendel** und **Jordi Pfeifer Serrahima** für die zuverlässige und erfolgreiche Zusammenarbeit sowie die gemeinsamen Publikationen in Kooperationsprojekten mit den Arbeitsgruppen von Prof. Dr. Evelyn Ullrich am Uniklinikum in Frankfurt, bzw. der Arbeitsgruppe von Prof. Dr. Winfried S. Wels am Georg-Speyer-Haus in Frankfurt bedanken.

Janine Becker und **Dana Schmidt** danke ich für die unermüdliche Hilfe sowohl im Labor als auch bei organisatorischen Angelegenheiten. Ich bedanke mich, dass Ihr jegliche Art von Informationen und Arbeitsmaterial immer parat hattet!

Danke, **Babara Diestelmann** und **Cecilia Gorus**, für die Hilfsbereitschaft bei bürokratischen und administrativen Aufgaben sowie die herzlichen Begrüßungen und netten Gespräche.

Sarah Hofmann, Ingo Bork, Alessandro Emmanuello, Dominic Happel, Michael Ulitzka, Dr. Jorge Lerma Romero, Dr. Stefania Cararra, Dr. Jan Habermann, Dr. Adrian Elter, Dr. Ataurehman Ali, und allen weiteren aktuellen und ehemaligen Mitgliedern des **Arbeitskreises Kolmar** danke ich für das stets angenehme Arbeitsklima und die unvergessliche Zeit im Labor, auf Konferenzen, dem ChemCup und im Kleinwalsertal.

Ein besonderer Dank gilt **meiner Familie** für die bedingungslose Unterstützung. Meinen Eltern Britta und Friedel, meinen Geschwistern Magnus, Marie und Artus, sowie meinem Freund Joshua möchte ich herzlich für den Rückhalt und Zuspruch in allen Belangen danken. Ohne Euch wäre das alles nicht möglich gewesen!

6 Affirmations

Erklärung laut Promotionsordnung

§8 Abs. 1 lit. c der Promotionsordnung der TU Darmstadt

Ich versichere hiermit, dass die elektronische Version meiner Dissertation mit der schriftlichen Version übereinstimmt und für die Durchführung des Promotionsverfahrens vorliegt.

§8 Abs. 1 lit. d der Promotionsordnung der TU Darmstadt

Ich versichere hiermit, dass zu einem vorherrigen Zeitpunkt noch keine Promotion versucht wurde und zu keinem früheren Zeitpunkt an einer in- oder ausländischen Hochschule eingereicht wurde. In diesem Fall sind nähere Angaben über Zeitpunkt, Hochschule, Dissertationsthema und Ergebnis dieses Versuchs mitzuteilen.

§9 Abs. 1 der Promotionsordnung der TU Darmstadt

Ich versichere hiermit, dass die vorliegende Dissertation selbstständig und nur unter Verwendung der angegebenen Quellen verfasst wurde.

§9 Abs. 2 der Promotionsordnung der TU Darmstadt

Die Arbeit hat bisher noch nicht zu Prüfungszwecken gedient.

Darmstadt, 27. August 2024

_____

Katrin Schoenfeld

TECHNISCHE UNIVERSITÄT DARMSTADT

Erklärung zum Eigenanteil an den Veröffentlichungen der kumulativen Dissertation

Im Folgenden ist aufgelistet, mit welchem Anteil ich an den Veröffentlichungen beteiligt war.

Mein Anteil an der folgenden Veröffentlichung beträgt 80%

1] **Schoenfeld K**, Harwardt J, Habermann J, Elter A and Kolmar H (2023) Conditional activation of an anti-IgM antibody-drug conjugate for precise B cell lymphoma targeting. *Frontiers in immunology*

Mein Anteil an der folgenden Veröffentlichung beträgt 45%

2] **Schoenfeld K***, Harwardt J*, Kolmar H (2024) Better safe than sorry: dual targeting antibodies for cancer immunotherapy. *Biological chemistry*

Mein Anteil an der folgenden Veröffentlichung beträgt 80%

3] **Schoenfeld K**, Habermann J, Wendel P, Harwardt J, Ullrich E, Kolmar H (2024) T cell receptor-directed antibody-drug conjugates for the treatment of T cell-derived cancers. *Molecular Therapy Oncology*

Mein Anteil an der folgenden Veröffentlichung beträgt 40%

4] Pfeifer Serrahima J*, **Schoenfeld K***, Kühnel I, Harwardt J, Macarrón Palacios A, Prüfer M, Kolaric M, Oberoi P, Kolmar H, Wels WS (2024) Bispecific killer cell engagers employing species cross-reactive NKG2D binders redirect human and murine lymphocytes to ErbB2/HER2-positive malignancies. *Frontiers in immunology (under review)*

*geteilte Erstautorenschaft

Darmstadt, 23. Juli 2024

Katrin Schoenfeld

Erklärung zur Begutachtung der Veröffentlichung

TECHNISCHE UNIVERSITÄT DARMSTADT

Prof. Dr. Harald Kolmar

Referent*in

Prof. Dr. Evelyn Ullrich

Co-Referent*in

23. Juli 2024

Datum

Weder Referent (Prof. Dr. Harald Kolmar) noch Co-Referentin (Prof. Dr. Evelyn Ullrich) der vorliegenden kumulativen Doktorarbeit waren an der Begutachtung nachstehender Veröffentlichungen beteiligt:

1] **Schoenfeld K**, Harwardt J, Habermann J, Elter A and Kolmar H (2023) Conditional activation of an anti-IgM antibody-drug conjugate for precise B cell lymphoma targeting. *Frontiers in immunology*

2] **Schoenfeld K***, Harwardt J*, Kolmar H (2024) Better safe than sorry: dual targeting antibodies for cancer immunotherapy. *Biological chemistry*

3] **Schoenfeld K**, Habermann J, Wendel P, Harwardt J, Ullrich E, Kolmar H (2024) T cell receptor-directed antibody-drug conjugates for the treatment of T cell-derived cancers. *Molecular Therapy Oncology*

4] Pfeifer Serrahima J*, **Schoenfeld K***, Kühnel I, Harwardt J, Macarrón Palacios A, Prüfer M, Kolaric M, Oberoi P, Kolmar H, Wels WS (2024) Bispecific killer cell engagers employing species cross-reactive NKG2D binders redirect human and murine lymphocytes to ErbB2/HER2-positive malignancies. *Frontiers in immunology (under review)*

*geteilte Erstautorenschaft

Darmstadt, 23. Juli 2024

Referent
Prof. Dr. Harald Kolmar

Co-Referentin
Prof. Dr. Evelyn Ullrich